Exploring and expanding the natural chemical space of bacterial diterpenes

Wei *et al.*

Supplementary Method 1. VCD calculations

An arbitrary enantiomer of each diterpene was constructed using ComputeVOA (BioTools, inc., Jupiter, FL). In cases where relative stereochemistry or carbon skeleton was ambiguous, diastereomers or alternate structures were also constructed. A thorough conformational search was performed at the MM level using the MMF94 force field in a 7–8 kcal mol^{-1} energy window for all structures. All conformers of each structure were subjected to DFT level optimization and frequency calculation with Gaussian '09 (Wallingford, CT)[1] using the B3PW91 / 6-31G(d) method. The resulting lowest energy unique conformations were reoptimized using the B3PW91 / cc-pVTZ method (max ~20 conformers), and the IR and VCD frequencies recalculated at this level. The resulting spectra from both methods were Boltzmann averaged (using both Free Energy and Electronic Energy), plotted at 5 cm^{-1} resolution and then x-axis scaled (range of 0.968–0.985 - values obtained using CompareVOA and varied with basis set and functional) for comparison to the experimental IR and VCD spectra. The two different weighing methods (Free Energy and Electronic Energy) gave consistent results for stereochemistry, so in each case the method which better reproduced the experimental data was ultimately used for similarity values and plots. In each case, the B3PW91 / 6-31G(d) calculations gave reasonable results and were used to determine the absolute configuration of each diterpene. The higher-level calculations (B3PW91 / cc-pVTZ) in each case gave improved results as compared to the 6-31G(d) calculations – this was essential for the more difficult assignments of relative configuration or carbon skeleton in the cases where NMR data proved ambiguous. Quantitative comparisons of the experimental and DFT spectra resulted in high similarity (S_{fg}) and enantiomeric similarity index (ESI) values and very high confidence level (CompareVOA, BioTools, Inc., Jupiter, FL) assignments[2,3]. When determining the relative configuration or carbon skeleton, multiple instances of CompareVOA were used – one for each distinct structure calculated. The matches consistently had confidence levels of 97–100, while mismatched structures were much lower, typically not more than 85 and often much lower than that.

Supplementary Method 2. Cloning design for protein production

Primers (Supplementary Table 31) were designed for T5 exonuclease-dependent assembly (TEDA)[4]. PCR was conducted with Q5 DNA polymerase using the synthesized plasmids containing individual TS genes as templates. The PCR products were purified by gel extraction and cloned into the pET28a(+) vector, which was linearized with *Bam*HI and *Hin*dIII, and transformed into NEB Turbo *E. coli* competent cells. The sequences of plasmids containing TS genes with N-terminal His_6 tags were confirmed by Genewiz Sanger sequencing.

Supplementary Method 3. Protein production and purification

For protein production, plasmids harboring each TS gene were individually transformed into *E. coli* BL21 Star. *E. coli* strains were grown in LB containing 50 mg mL^{-1} kanamycin for antibiotic selection. Each strain was grown in 3 × 1 L of LB at 37 °C with shaking at 200 rpm until an OD_{600} of 0.6 was reached. After addition of 0.3 mM (final concentration) isopropyl β-D-1-thiogalactopyranoside (IPTG) for gene expression, the cells were incubated at 16 °C with shaking for approximately 18 h. Cells were harvested by centrifugation at 5000 *g* for 10 min at 25 °C and the pellet was resuspended in cold lysis buffer (50 mM Tris-HCl, pH 8.0, containing 150 mM NaCl). Cells were lysed by sonication (Sonic Dismembrator Model 500) and the lysates were centrifuged at 40,000 *g* for 30 min at 4 °C. Target proteins from the supernatant

were loaded onto a nickel-affinity chromatography column packed with HisPur™ Ni-NTA Resin (Thermo Scientific). The resin was successively washed with lysis buffer containing 20 mM imidazole with the same volume of supernatant and eluted with 3 mL of elution buffer (lysis buffer containing 500 mM imidazole). The target protein was immediately desalted using a PD-10 column (GE Healthcare Biosciences) and concentrated using an Amicon Ultra-15 concentrator (Millipore) in 50 mM Tris-HCl, pH 8.0, containing 150 mM NaCl. Protein purities were detected by SDS-PAGE analysis, and concentration was determined by the Bradford assay[5]. Individual aliquots of each protein were flash-frozen in liquid nitrogen and stored at –80 °C for use.

Supplementary Note 1. Structural elucidation of 1–5

Tetraisoquinene (1)

The NMR spectra of **1** (Supplementary Table 1, Supplementary Fig. 5–11) revealed a single alkene with no olefinic protons, as well as five methyl groups, six methylene carbons, five methine carbons, and two sp^3 quaternary carbons; thus, **1** was tetracyclic. ^{1}H-^{1}H COSY analysis revealed three spin systems connecting C-14-C-1(C-20)-C-2-C-3, C-6-C-7-C-8, and C-10-(C-15-C-16/C-17)-C-11-C-12. Several key correlations from the ^{1}H-^{13}C HMBC spectra connected these fragments into an angular tetraquinane skeleton: H_3-18 to C-8, C-9, C-10, and C-13; H_2-12 to C-9, C-13, and C-14; H-6 to C-4, C-5, C-9, C-13, and C-14; H_3-19 to C-3, C-4, C-5, and C-6; and H-14 to C-3, C-4, C-5, C-6, C-9, and C-13. The relative configuration of **1** was determined by NOESY correlations from H-14 to H_3-18 and H_α-8, H_β-8 to H_3-20, and H_β-12 to H-6, H-10, and H_3-20. We used VCD to determine the absolute configuration of **1** to be 1*S*,6*S*,9*S*,10*S*,13*S*,14*S* (Supplementary Fig. 12).

Salbirenol (2)

The GC-MS of **2** showed a molecular ion peak at, supporting a molecular formula of $C_{20}H_{34}O$ and a diterpene with four degrees of unsaturation (Supplementary Fig. 13). The NMR spectra of **2** (Supplementary Table 2, Supplementary Fig. 14–20) revealed a single alkene with one olefinic proton, as well as five methyl groups, six methylene carbons, five methine carbons, one of which was oxygenated, and two sp^3 quaternary carbons. ^{1}H-^{1}H COSY correlations supported fragments of C-20-C-2-C-3-C-4, C-6-C-7-C-8-C-9, C-10-C-11, and C-16-C-15-C-17. Extensive ^{1}H-^{13}C HMBC correlations supported a 7/5/6 skeleton: H-13 to C-8, C-11, C-12, and C-14; H-1 to C-2, C-3, C-5, C-13, and C-14; H_3-20 to C-1, C-2, and C-3; H_3-19 to C-4, C-5, C-6, and C-14; H_3-18 to C-8, C-9, and C-10; and H-15 to C-11, C-12, and C-13. Although several NOESY correlations were detected for **2**, due to peak overlap we could not assign the relative configuration of **2** by NMR. Using VCD in comparison with the calculated spectra of nearly all 32 possible stereoisomers, the absolute configuration of **2** was determined to be 1*S*,2*S*,5*R*,8*R*,9*S*,14*S* (Supplementary Fig. 21).

Chitino-2,5(6),9(10)-triene (3)

The GC-MS of **3** showed a molecular ion peak at *m/z* 272.2498 (Supplementary Fig. 22), supporting a molecular formula of $C_{20}H_{32}$ and a diterpene with five degrees of unsaturation. The NMR spectra of **3** (Supplementary Table 3, Supplementary Fig. 23–29) revealed three double bonds with four olefinic protons, as well as five methyl groups, five methylene carbons, three methine carbons, two sp^2 and one sp^3 quaternary carbons. ^{1}H-^{1}H COSY analysis revealed connected fragments of C-2-C-3-C-4, C-7-C-8, and C-10-C-11-C-12(C-18-C-19/C-20)-C-13-C-14. Key correlations from the ^{1}H-^{13}C HMBC spectra connected these fragments into a bicyclic skeleton: H-2 to C-1; H_2-14 to C-1; H_3-15 to C-1, C-2 and C-14; H-18 to C-11 and C-13; H_3-16 to C-4, C-5 and C-6; and H_3-17 to C-8, C-9, and C-10. The relative configuration of **3** was determined by NOESY correlations from H-11 to H_3-15, H-11 to H_3-20, and H_3-15 to H_3-19. The absolute configuration of **3** was determined to be 1*R*,11*S*,12*R* by VCD (Supplementary Fig. 30–31).

Peysonnosene (4)

The GC-MS of **4** showed a molecular ion peak at *m/z* 272.2498 (Supplementary Fig. 32), supporting a molecular formula of $C_{20}H_{32}$ and a diterpene with five degrees of unsaturation. De novo structural elucidation by 1D and 2D NMR (Supplementary Table 4, Supplementary Fig. 33–39) revealed four rings consisting of five methyl groups, six methylene carbons, five methine carbons, and four quaternary carbons. ^{1}H-^{1}H COSY correlations supported connected fragments of C-1-C-2, C-4-C-5, C-19-C-7-C-8-C-9, and C-12-C-13-C-14-C-15-C-16/C-17. ^{1}H-^{13}C HMBC correlations from H_3-20 to C-2, C-3, and C-4, as well as from H-1 to C-3, C-6, C-10, C-11, and C-12 built the C/D ring system. Additional HMBC correlations from H-18 to C-9, C-10, C-11, and C-14 and from H-19 to C-6, C-7, and C-8 confirmed the 5/6/3/6 planar structure of **4**. The relative configuration of **4**, which was supported by limited NOESY correlations, was proposed to be the same as that of the peyssonnosides. We confirmed its absolute configuration, 1*S*,6*S*,7*R*,10*S*,11*S*,14*S*, by VCD (Supplementary Fig. 40).

Clavulara-1(15),17-diene (5)

The GC-MS of **5** showed a molecular ion peak at *m/z* 272.2502 (Supplementary Fig. 41), supporting a molecular formula of $C_{20}H_{32}$ and a diterpene with five degrees of unsaturation. The NMR spectra of **5** (Supplementary Table 5, Supplementary Fig. 42–49) revealed two double bonds with four olefinic protons, as well as three methyl groups, eight methylene carbons, three methine carbons, two sp^2 and two sp^3 quaternary carbons. ^{1}H-^{1}H COSY analysis revealed three spin systems connecting C-2-C-3-C-4, C-13-C-14, and C-7-C-8-C-9-C-10-C-11. Key correlations from the ^{1}H-^{13}C HMBC spectra connected these fragments into a tricyclic skeleton: H_2-7 to C-12; H-9 to C-12; H_3-19 to C-9; H_2-18 to C-9; H_3-16 to C-8, C-11, C-12, and C-13; H_3-15 to C-1, C-2, and C-14; and H_3-20 to C-4, C-5, C-6, and C-14. The relative configuration of **5** was determined by NOESY correlations from H_3-16 to H_3-19, H-14 to H_3-16, and H-8 to H_3-20. The absolute configuration of **5** was determined to be 5*R*,8*R*,9*R* 12*S*,14*S* by VCD (Supplementary Fig. 50).

Supplementary Note 2. Isolated yields of diterpenes 1–28

1, 70 mg from 6 L; **2**, 50 mg from 12 L; **3**, 3 mg from 12 L; **4**, 2 mg from 12 L; **5**, 10 mg from 12 L; **6**, 2 mg from 12 L of *Ps*VS; **6**, 10 mg from 6 L of *Od*VS; **7**, 2 mg from 12 L; **8**, 10 mg from 12 L; **9**, 45 mg from 12 L; **10**, 250 mg from 12 L; **11**, 15 mg from 12 L; **12**, 40 mg from 12 L; **13**, 1 mg from 12 L; **14**, 2 mg from 12 L; **15**, 4 mg from 12 L; **16**, 10 mg from 12 L; **17**, 10 mg from 12 L; **18**, 20 mg from 12 L; **19**, 10 mg from 12 L of *N*Bnd4; **19**, 15 mg from 12 L of *Ma*Bnd4; **20**, 2 mg from 12 L of *S*PhpS; **20**, 4 mg from 12 L of *Cp*PhpS; **21**, 930 mg from 12 L of *Mp*McS; **21**, 5 mg from 12 L of *Mb*McS; **21**, 4 mg from 12 L of *S*McS; **22**, 10 mg from 12 L of *Bp*CAS; **22**, 3 mg from 12 L of *Mp*McS; **22**, 5 mg from 12 L of *Ml*McS; **22**, 4 mg from 12 L of *Mb*McS; **23**, 20 mg from 12 L; **24**, 6 mg from 12 L; **25**, 31 mg from 12 L; **26**, 2 mg from 12 L; **27**, 6 mg from 12 L; **28**, 30 mg from 12 L.

Supplementary Note 3. Spectroscopic data of isolated compounds

Tetraisoquinene (**1**): colorless oil; *RI* = 1924; $[\alpha]_D^{21}$ = +121.4 (*c* = 1, CH_2Cl_2); ^1H and ^{13}C NMR data, see Supplementary Table 1 and Supplementary Fig. 5–11; UV (acetonitrile:water = 9:1) λ_{max} = 210 nm; IR (film) ν_{max} 2952, 2905, 1452, 1369 cm^{-1}.

Salbirenol (**2**): colorless oil; R_f = *RI* = 2024; $[\alpha]_D^{21}$ = -2.72 (c = 1, CH_2Cl_2); ^1H and ^{13}C NMR data, see Supplementary Table 2 and Supplementary Fig. 14–20; UV (acetonitrile:water = 9:1) λ_{max} = 210 nm; IR (film) ν_{max} 3483, 2950, 2918, 2889, 1457, 1382, 956, 943 cm^{-1}.

Chitino-2,5(6),9(10)-triene (**3**): colorless oil; *RI* = 1907; $[\alpha]_D^{21}$ = +29.9 (c = 0.1, CH_2Cl_2); ^1H and ^{13}C NMR data, see Supplementary Table 3 and Supplementary Fig. 23–29; UV (acetonitrile:water = 9:1) λ_{max} = 210 nm; IR (film) ν_{max} 2953, 2863, 1455, 1383, 1264, 895, 712 cm^{-1}.

Peysonnosene (**4**): colorless oil; *RI* = 1947; $[\alpha]_D^{21}$ = -12.4 (c = 0.1, CH_2Cl_2); ^1H and ^{13}C NMR data, see Supplementary Table 4 and Supplementary Fig. 33–39; UV (acetonitrile:water = 9:1) λ_{max} = 210 nm; IR (film) ν_{max} 2929, 2857, 1445, 1381, 893 cm^{-1}.

Clavulara-1(15),17-diene (**5**): colorless oil; *RI* = 2072; $[\alpha]_D^{21}$ = +61.6 (c = 1, CH_2Cl_2); ^1H and ^{13}C NMR data, see Supplementary Table 5 and Supplementary Fig. 42–48; UV (acetonitrile:water = 9:1) λ_{max} = 210 nm; IR (film) ν_{max} 2929, 2876, 1648, 1386, 893 cm^{-1}.

Variediene (**6**): colorless oil; *RI* = 1842; $[\alpha]_D^{21}$ = -65.8 (c = 1, CH_2Cl_2); ^1H and ^{13}C NMR data, see Supplementary Table 6 and Supplementary Fig. 52–56; UV (acetonitrile:water = 9:1) λ_{max} = 210 nm.

1*S*-Verticilla-3,7,11(12)-triene (**7**): colorless oil; *RI* = 2056; $[\alpha]_D^{21}$ = +96.8 (c = 0.1, CH_2Cl_2); ^1H and ^{13}C NMR data, see Supplementary Table 7 and Supplementary Fig. 59–64; UV (acetonitrile:water = 9:1) λ_{max} = 210 nm.

1*S*-Verticilla-3,8(19),11(12)-triene (**8**): colorless oil; *RI* = 2026; $[\alpha]_D^{21}$ = +166.4 (c = 0.5, CH_2Cl_2); ^1H and ^{13}C NMR data, see Supplementary Table 8 and Supplementary Fig. 67–72; UV (acetonitrile:water = 9:1) λ_{max} = 210 nm.

(-)-Sandaracopimaradiene (**9**): colorless oil; *RI* = 1996; ^1H and ^{13}C NMR data, see Supplementary Table 9 and Supplementary Fig. 75–79; UV (acetonitrile:water = 9:1) λ_{max} = 210 nm.

Venezuelaene A (**10**): colorless oil; *RI* = 2041; $[\alpha]_D^{21}$ = -31.4 (c 1.0, CH_2Cl_2); ^1H and ^{13}C NMR data, see Supplementary Table 10 and Supplementary Fig. 82–83; UV (acetonitrile:water = 9:1) λ_{max} = 210 nm.

Venezuelaene A2 (**11**): colorless oil; *RI* = 1936; $[\alpha]_D^{21}$ = +5.5 (c = 0.1, CH_2Cl_2); ^1H and ^{13}C NMR data, see Supplementary Table 11 and Supplementary Fig. 86–92; UV (acetonitrile:water = 9:1) λ_{max} = 210 nm.

Odyverdiene B2 (**12**): colorless oil; *RI* = 1971; $[\alpha]_D^{21}$ = -32.4 (c = 1, CH_2Cl_2); ^1H and ^{13}C NMR data, see Supplementary Table 12 and Supplementary Fig. 96–102; UV (acetonitrile:water = 9:1) λ_{max} = 210 nm.

1*S*,3*E*,7*E*,11*R*,12*S*-dolabella-3,7,18-triene (**13**): colorless oil; *RI* = 1961; $[\alpha]_D^{21}$ = -25.6 (c 0.04, CH_2Cl_2); ^1H and ^{13}C NMR data, see Supplementary Table 13 and Supplementary Fig. 106–107; UV (acetonitrile:water = 9:1) λ_{max} = 210 nm.

1*R**,3*E*,7*E*,11*S**,12*S**-dolabella-3,7,18-triene (**14**): colorless oil; *RI* = 2003; $[\alpha]_D^{21}$ = +30.6 (c 0.1, CH_2Cl_2); ^1H and ^{13}C NMR data, see Supplementary Table 14 and Supplementary Fig. 109–115; UV (acetonitrile:water = 9:1) λ_{max} = 210 nm.

1*R*,7*E*,10*E*,12*R*-dolabella-4(16),7,10-triene (**15**): colorless oil; *RI* = 1989; $[\alpha]_D^{21}$ = +105.2 (c = 1.0, CH_2Cl_2); ^1H and ^{13}C NMR data, see Supplementary Table 15 and Supplementary Fig. 117–122; UV (acetonitrile:water = 9:1) λ_{max} = 210 nm.

(+)-2*S*,3*S*,6*R*,7*Z*,10*Z*,11*R*-cyclooctat-7(8),10(14)-diene (**16**): colorless oil; *RI* = 1890; $[\alpha]_D^{21}$ = +85.6 (c = 1.0, CH_2Cl_2); ^1H and ^{13}C NMR data, see Supplementary Table 16 and Supplementary Fig. 126–132; UV (acetonitrile:water = 9:1) λ_{max} = 210 nm.

(–)-2*R*,3*S*,6*R*,7*Z*,10*Z*,11*S*-cyclooctat-7(8),10(14)-diene (**17**): colorless oil; *RI* = 1836; $[\alpha]_D^{21}$ = -34.9 (c = 1.0, CH_2Cl_2); ^1H and ^{13}C NMR data, see Supplementary Table 17 and Supplementary Fig. 136–141; UV (acetonitrile:water = 9:1) λ_{max} = 210 nm.

Monoprenyl-β-curcumene (**18**): colorless oil; *RI* = 2361; $[\alpha]_D^{21}$ = +25.8 (c = 1.0, CH_2Cl_2); ^1H and ^{13}C NMR data, see Supplementary Table 18 and Supplementary Fig. 145–149; UV (acetonitrile:water = 9:1) λ_{max} = 210 nm.

Benditerpetriene (**19**): colorless oil; *RI* = 1918; $[\alpha]_D^{21}$ = +41.0 (c = 1.0, CH_2Cl_2); ^1H and ^{13}C NMR data, see Supplementary Table 19 and Supplementary Fig. 152–153; UV (acetonitrile:water = 9:1) λ_{max} = 210 nm.

Prehydropyrene (**20**): colorless oil; *RI* = 1968; $[\alpha]_D^{21}$ = +17.7 (c = 2.0, CH_2Cl_2); ^1H and ^{13}C NMR data, see Supplementary Table 20 and Supplementary Fig. 155–159; UV (acetonitrile:water = 9:1) λ_{max} = 210 nm.

Micromonocyclol (**21**): colorless oil; *RI* = 2085; $[\alpha]_D^{21}$ = +21.9 (c = 1.0, CH_2Cl_2); ^1H and ^{13}C NMR data, see Supplementary Table 21 and Supplementary Fig. 162–166; UV (acetonitrile:water = 9:1) λ_{max} = 210 nm.

Cembrene A (**22**): colorless oil; *RI* = 1989; $[\alpha]_D^{21}$ = -9.5 (c = 0.1, CH_2Cl_2); ^1H and ^{13}C NMR data, see Supplementary Table 22 and Supplementary Fig. 168–173; UV (acetonitrile:water = 9:1) λ_{max} = 210 nm.

(*S*)-Nephthenol (**23**): colorless oil; *RI* = 2361; $[\alpha]_D^{21}$ = +13.5 (c = 1.0, CH_2Cl_2); ^1H and ^{13}C NMR data, see Supplementary Table 23 and Supplementary Fig. 175–176; UV (acetonitrile:water = 9:1) λ_{max} = 210 nm.

Iso-cembrene C (**24**): colorless oil; *RI* = 1989; ^1H and ^{13}C NMR data, see Supplementary Table 24 and Supplementary Fig. 178–182; UV (acetonitrile:water = 9:1) λ_{max} = 210 nm.

Spiroviolene (**25**): colorless oil; *RI* = 1727; ^1H and ^{13}C NMR data, see Supplementary Table 25 and Supplementary Fig. 184–188; UV (acetonitrile:water = 9:1) λ_{max} = 210 nm.

Spata-13,17-diene (**26**): colorless oil; *RI* = 1910; ^1H and ^{13}C NMR data, see Supplementary Table 26 and Supplementary Fig. 191–192; UV (acetonitrile:water = 9:1) λ_{max} = 210 nm.

Cneorubin Y (**27**): colorless oil; *RI* = 1975; ^1H and ^{13}C NMR data, see Supplementary Table 27 and Supplementary Fig. 194; UV (acetonitrile:water = 9:1) λ_{max} = 210 nm.

β-springene (**28**): colorless oil; *RI* = 1924; ^1H and ^{13}C NMR data, see Supplementary Table 28 and Supplementary Fig. 196–200; UV (acetonitrile:water = 9:1) λ_{max} = 210 nm.

Supplementary Table 1. ^{13}C NMR (150 MHz) and ^{1}H NMR (600 MHz) spectroscopic data for tetraisoquinene (**1**) isolated from TiqS (d in ppm, *J* in Hz).[a] The raw NMR data of **1** was deposited to np-mrd.org under accession number: NP0341974.

	1	
No.	δ_C	δ_H
1	34.00, CH	1.95 (m, 1H)*
2	37.2, CH_2	1.94 (m, 1H)*
		1.48 (m, 1H)*
3	20.1, CH_2	2.05 (m, 1H)
		1.94 (m, 1H)*
4	140.3, qC	-
5	129.8, qC	-
6	67.1, CH	2.60 (d, *J* = 8.7, 1H)
7	27.7, CH_2	1.90 (m, 1H)*
		1.51 (m, 1H)*
8	37.8, CH_2	1.85 (m, 1H)*
		1.44 (td, *J* = 12.2, 7.8, 1H)
9	65.1, qC	-
10	51.9, CH	1.36 (ddd, *J* = 10.8, 9.2, 7.9, 1H)
11	29.2, CH_2	1.82 (m, 1H)*
		1.23 (m, 1H)
12	33.0, CH_2	1.88 (m, 1H)*
		1.59 (m, 1H)*
13	55.1, qC	-
14	60.2, CH	2.87 (dq, *J* = 4.7, 2.8, 1H)
15	30.5, CH	1.51 (m, 1H)*
16	22.8, CH_3	1.01 (d, *J* = 6.6, 3H)
17	23.0, CH_3	0.93 (d, *J* = 6.6, 3H)
18	17.4, CH_3	0.92 (s, 3H)
19	12.9, CH_3	1.58 (s, 3H)
20	15.6, CH_3	0.84 (d, *J* = 7.3, 3H)

[a] Assignments are based on 1D and 2D NMR experiments in C_6D_6

* Signals are overlapped

Supplementary Table 2. ^{13}C NMR (150 MHz) and ^{1}H NMR (600 MHz) spectroscopic data for salbirenol (**2**) isolated from SalS (d in ppm, *J* in Hz).[a] The raw NMR data of **2** was deposited to np-mrd.org under accession number: NP0342000.

	2	
No.	δ_C	δ_H
1	77.4, CH	3.40 (s, 1H)
2	34.1, CH	1.56 (m, 1H)
3	23.6, CH_2	1.70 (m, 1H)*
		1.13 (m, 1H)*
4	34.4, CH_2	1.52 (ddd, *J* = 14.0, 4.0, 2.7, 1H)
		1.42 (td, *J* = 13.8, 4.4, 1H)
5	44.0, qC	-
6	35.2, CH_2	2.41 (td, *J* = 11.2, 8.8, 1H)
		1.04 (dd, *J* = 11.5, 8.2, 1H)
7	27.6, CH_2	1.84 (m, 1H)
		1.77 (m, 1H)*
8	48.0, CH	1.91 (td, *J* = 10.3, 6.4, 1H)
9	33.8, CH	1.76 (m, 1H)*
10	36.5, CH_2	1.64 (m, 1H)
		1.13 (m, 1H)*
11	24.8, CH_2	2.27 (tdd, *J* = 13.3, 6.8, 1.9, 1H)
		1.70 (m, 1H)*
12	142.5, qC	-
13	125.0, CH	5.15 (d, *J* = 1.8, 1H)
14	55.1, qC	-
15	36.9, CH	2.19 (p, *J* = 6.8, 1H)
16	21.7, CH_3	0.98 (d, *J* = 6.8, 3H)
17	21.1, CH_3	0.97 (d, *J* = 6.8, 3H)
18	20.1, CH_3	0.95 (d, *J* = 6.6, 3H)
19	27.0, CH_3	0.86 (s, 3H)
20	19.2, CH_3	0.89 (d, *J* = 6.8, 3H)

[a] Assignments are based on 1D and 2D NMR experiments in C_6D_6

* Signals are overlapped

Supplementary Table 3. ^{13}C NMR (150 MHz) and ^{1}H NMR (600 MHz) spectroscopic data for chitin-2,5(6),9(10)-triene (**3**) isolated from ChtS (d in ppm, *J* in Hz).[a] The raw NMR data of **3** was deposited to np-mrd.org under accession number: NP0342001.

	3	
No.	δ_C	δ_H
1	49.2, qC	-
2	143.6, CH	5.51 (d, *J*= 15.7, 1H)
3	126.1, CH	5.64 (ddd, *J* = 15.7, 8.7, 5.3, 1H)
4	43.3, CH_2	2.72 (dd, *J* = 12.0, 8.6, 1H)
		2.46 (dd, *J* = 12.0, 5.3, 1H)
5	139.2, qH	-
6	126.5, CH	5.03 (m, 1H)
7	25.2, CH_2	2.19 (m, 1H)*
		1.98 (m, 1H)*
8	41.0, CH_2	2.12 (m, 1H)*
		1.98 (m, 1H)*
9	131.9, qC	-
10	134.3, CH	4.79 (dt, *J* = 10.4, 1.4, 1H)
11	56.5, CH	2.14 (m, 1H)*
12	56.7, CH	1.41 (m, 1H)*
13	30.7, CH_2	1.73 (m, 1H)
		1.40 (m, 1H)*
14	40.2, CH_2	1.60 (m, 1H)
		1.48 (m, 1H)*
15	27.4, CH_3	1.10 (s, 3H)
16	18.0, CH_3	1.57 (s, 3H)
17	16.0, CH_3	1.35 (s, 3H)
18	34.5, CH	1.48 (m, 1H)*
19	21.7, CH_3	0.90 (d, *J* = 6.6, 3H)
20	22.9, CH_3	0.93 (d, *J* = 6.6, 3H)

[a] Assignments are based on 1D and 2D NMR experiments in C_6D_6

* Signals are overlapped

Supplementary Table 4. ^{13}C NMR (150 MHz) and ^{1}H NMR (600 MHz) spectroscopic data for peysonnosene (**4**) isolated from PeyS (d in ppm, *J* in Hz).[a] The raw NMR data of **4** was deposited to np-mrd.org under accession number: NP0342002.

	4	
No.	δ_C	δ_H
1	20.7, CH	0.97 (m, 1H)*
2	121.1, CH	5.64 (dt, *J* = 3.5, 1.8, 1H)
3	133.0, qC	-
4	29.3, CH_2	1.92 (m, 1H)
		1.53 (m, 1H)*
5	24.4, CH_2	1.73 (m, 1H)*
		1.52 (m, 1H)*
6	29.4, qC	-
7	36.1, CH	1.52 (m, 1H)*
8	27.9, CH_2	1.25 (td, *J* = 4.8, 2.7, 1H)
		0.79 (m, 1H)*
9	39.9, CH_2	1.56 (m, 1H)*
		0.96 (m, 1H)*
10	42.8, qC	-
11	47.0, qC	-
12	27.6, CH_2	1.37 (m, 2H)*
13	29.2, CH_2	1.72 (m, 1H)*
		1.29 (m, 1H)
14	62.9, CH	1.21 (ddd, *J* = 12.9, 8.1, 5.1, 1H)
15	29.7, CH	1.60 (m, 1H)
16	24.1, CH_3	0.96 (d, *J* = 6.6, 3H)
17	23.8, CH_3	0.93 (d, *J* = 6.6, 3H)
18	19.7, CH_3	0.79 (s, 3H)
19	19.8, CH_3	0.98 (d, *J* = 6.3, 3H)
20	24.2, CH_3	1.65 (s, 3H)

[a] Assignments are based on 1D and 2D NMR experiments in C_6D_6

* Signals are overlapped

Supplementary Table 5. ^{13}C NMR (150 MHz) and ^{1}H NMR (600 MHz) spectroscopic data for clavulara-1(15),17-diene (**5**) isolated from CvdS (d in ppm, *J* in Hz).[a] The raw NMR data of **5** was deposited to np-mrd.org under accession number: NP0342003.

	5	
No.	δ_C	δ_H
1	152.0, qC	-
2	38.6, CH_2	2.30 (ddt, *J* = 12.5, 4.1, 2.1, 1H)
		1.92 (td, *J* = 12.5, 5.8, 1H)
3	24.4, CH_2	1.69 (m, 1H)*
		1.50 (m, 1H)*
4	44.8, CH_2	1.22 (m, 2H)
5	40.1, qC	-
6	41.2, CH_2	1.60 (m, 1H)
		1.36 (m, 1H)*
7	23.6, CH_2	1.50 (m, 2H)*
8	48.3, CH	2.04 (td, *J* = 11.9, 7.8, 1H)
9	49.9, CH	2.78 (dt, *J* = 11.5, 9.2, 1H)
10	28.8, CH_2	1.82 (m, 1H)*
		1.73 (m, 1H)
11	44.8, CH_2	1.36 (m, 1H)*
		1.26 (td, *J* = 12.5, 4.9, 1H)
12	44.8, qC	-
13	45.2, CH_2	1.80 (dd, *J* = 13.8, 3.6, 1H)*
		1.36 (m, 1H)*
14	48.9, CH	1.97 (m, 1H)
15	107.1, CH_2	4.90 (q, *J* = 1.5, 1H)
		4.71 (br s, 1H)
16	19.1, CH_3	0.94 (s, 3H)
17	147.5, qC	-
18	112.3, CH_2	4.97 (p, *J* = 1.5, 1H)
		4.89 (p, *J* = 1.5, 1H)
19	24.4, CH_3	1.69 (s, 3H)
20	15.9, CH_3	0.85 (s, 3H)

[a] Assignments are based on 1D and 2D NMR experiments in C_6D_6

* Signals are overlapped

Supplementary Table 6. ^{13}C NMR (150 MHz) and ^{1}H NMR (600 MHz) spectroscopic data for variediene (**6**) isolated from *Od*VS and *Ps*VS (d in ppm, *J* in Hz).[a] The raw NMR data of **6** was deposited to np-mrd.org under accession number: NP0342004.

	6		**6**[b]
No.	δ_C	δ_H	δ_C
1	44.9, CH_2	2.17 (m, 1H)*	44.99
		2.14 (m, 1H)*	
2	144.0, qC	-	144.08
3	121.0, qC	-	121.01
4	38.0, CH_2	1.95 (m, 2H)*	38.10
5	25.0, CH_2	1.98 (m, 1H)*	25.09
		1.93 (m, 1H)*	
6	127.0, CH	5.21 (dd, *J* = 11.0, 4.3, 1H)	127.02
7	138.9, qC	-	139.00
8	40.7, CH_2	2.12 (m, 1H)*	40.76
		2.08 (m, 1H)*	
9	41.3, CH_2	2.22 (dtd, *J* = 13.7, 11.8, 5.7, 1H)	41.38
		1.56 (m, 1H)*	
10	44.7, CH	2.30 (d, *J* = 11.2, 1H)	44.72
11	48.7, qC	-	48.79
12	41.8, CH_2	1.48 (m, 1H)	41.88
		1.40 (m, 1H)	
13	41.3, CH_2	1.24 (m, 1H)	41.40
14	68.5, CH	1.29 (s, 1H)	68.52
15	43.2, qC	-	43.21
16	21.5, CH_3	1.59 (s, 3H)	21.59
17	16.2, CH_3	1.36 (s, 3H)	16.28
18	31.5, CH_3	1.22 (s, 3H)	31.55
19	32.1, CH_3	0.95 (s, 3H)	32.18
20	24.6, CH_3	0.78 (s, 3H)	24.61

[a] Assignments are based on 1D and 2D NMR experiments in $CDCl_3$

[b] The NMR matches that of previously reported[6]

* Signals are overlapped

Supplementary Table 7. ^{13}C NMR (150 MHz) and ^{1}H NMR (600 MHz) spectroscopic data for 1*S*-verticilla-2,6,10(11)-triene (**7**) isolated from *Cn*VrtS (d in ppm, *J* in Hz).[a] The raw NMR data of **7** was deposited to np-mrd.org under accession number: NP0342005.

	7		**7**[b]
No.	δ_C	δ_H	δ_C
1	43.2, CH	1.53 (m, 1H)*	42.9
2	34.6, CH_2	2.67 (dddd, *J* = 14.1, 12.0, 6.6, 1.8, 1H) 1.90 (m, 1H)*	34.2
3	127.2, CH	5.27 (br d, *J* = 12.1, 1H)	126.8
4	131.5, qC	-	131.5
5	40.6, CH_2	2.02 (m, 1H) 1.93 (m, 1H)*	40.2
6	26.4, CH_2	2.16 (m, 1H)* 1.94 (m, 1H)*	26.0
7	129.0, CH	4.80 (br d, *J* = 10.7, 1H)	128.6
8	132.7, qC	-	132.8
9	38.9, CH_2	2.55 (td, *J* = 13.0, 5.1, 1H) 1.94(m, 1H)*	38.5
10	26.5, CH_2	2.16 (m,2H)*	26.1
11	136.4, qC	-	136.1
12	126.5, qC	-	126.3
13	31.8, CH_2	2.31 (m, 1H) 1.81 (dd, *J* = 17.5, 7.1, 1H)	31.5
14	27.9, CH_2	1.54 (m, 2H)*	27.5
15	37.3, qC	-	37.0
16	24.7, CH_3	0.87 (s, 3H)	24.6
17	33.1, CH_3	1.03 (s, 3H)	32.9
18	21.9, CH_3	1.64 (s, 3H)	21.7
19	16.8, CH_3	1.52 (s, 3H)	26.6
20	15.6, CH_3	1.50 (s, 3H)	15.4

[a] Assignments are based on 1D and 2D NMR experiments in C_6D_6

[b] The NMR matches that of previously reported[7]

* Signals are overlapped

Supplementary Table 8. ^{13}C NMR (150 MHz) and ^{1}H NMR (600 MHz) spectroscopic data for 1*S*-verticilla-2,7(19),10(11)-triene (**8**) isolated from *S*VrtS (d in ppm, *J* in Hz).[a] The raw NMR data of **8** was deposited to np-mrd.org under accession number: NP0342006.

	8	
No.	δ_C	δ_H
1	43.64, CH	1.52 (m, 1H)*
2	34.70, CH_2	2.65 (m, 1H)
		2.01 (m, 1H)*
3	125.80, CH	5.37 (ddd, *J* = 10.7, 5.2, 1.0, 1H)
4	132.62, qC	-
5	39.52, CH_2	1.92 (dd, *J* = 13.6, 5.9, 1H)
		1.68 (td, *J* = 13.1, 12.8, 1.4, 1H)
6	26.30, CH_2	1.54 (m, 1H)*
		1.24 (dddt, *J* = 13.8, 12.0, 10.4, 1.5, 1H)
7	35.43, CH_2	2.39 (ddt, *J* = 12.8, 10.3, 1.4, 1H)
		2.02 (m, 1H)*
8	154.54, qC	-
9	34.19, CH_2	2.12 (m, 2H)*
10	31.15, CH_2	2.48 (m, 1H)
		2.18 (m, 1H)*
11	137.10, qC	-
12	129.19, qC	-
13	31.49, CH_2	2.12 (m, 1H)*
		1.85 (dd, *J* = 17.7, 7.7, 1H)
14	27.54, CH_2	2.16 (m, 1H)*
		1.52 (m, 1H)*
15	37.77, qC	-
16	33.50, CH_3	1.04 (s, 3H)
17	25.50, CH_3	1.06 (s, 3H)
18	21.86, CH_3	1.62 (s, 3H)
19	111.50, CH_2	4.84 (dt, *J* = 2.6, 0.7, 1H)
		4.82 (dd, *J* = 2.9, 1.2, 1H)
20	17.16, CH_3	1.56 (s, 3H)

[a] Assignments are based on 1D and 2D NMR experiments in C_6D_6

* Signals are overlapped

Supplementary Table 9. ^{13}C NMR (150 MHz) and ^{1}H NMR (600 MHz) spectroscopic data for (−)-sandaracopimaradiene (**9**) isolated from *Chj*DCS (d in ppm, *J* in Hz).[a]

	9		**9**[b]
No.	δ_C	δ_H	δ_C
1	39.4, CH_2	1.72 (m, H_b)* 1.02 (m, H_a)*	39.4
2	18.9, CH_2	1.53 (m, H_a)* 1.45 (m, H_b)*	18.8
3	42.2, CH_2	1.41 (m, H_b) 1.18 (td, *J* = 13.4, 3.8, H_a)	42.2
4	33.3, qC	-	33.3
5	54.8, CH	1.03 (m, H_a)*	54.8
6	22.6, CH_2	1.58 (m, H_a)* 1.30 (qd, *J* = 13.0, 4.5, H_b)	22.6
7	36.1, CH_2	2.26 (ddd, *J* = 14.1, 4.6, 2.1, H_a) 2.07 (dddd, *J* = 13.9, 12.0, 5.8, 2.0, H_b)	36.0
8	137.4, qC	-	137.3
9	50.7, CH	1.71 (m, H_a)*	50.6
10	38.3, qC	-	38.3
11	18.8, CH_2	1.59 (m, H_b)* 1.51 (m, H_a)*	19.0
12	34.7, CH_2	1.47 (m, H_a)* 1.35 (m, H_b)*	34.6
13	37.4, qC	-	37.4
14	128.5, CH	5.21 (q, *J* = 1.8, 1H)	128.5
15	149.2, CH	5.78 (dd, *J* = 17.4, 10.6, 1H)	149.1
16	109.9, CH_2	4.91 (dd, *J* = 24.3, 1.5, 1H) 4.89 (dd, *J* = 17.4, 1.5, 1H)	110.0
17	25.9, CH_3	1.04 (s, 3H)	26.0
18	34.1, CH_3	0.88 (s, 3H)	33.8
19	22.1, CH_3	0.85 (s, 3H)	22.1
20	15.0, CH_3	0.80 (s, 3H)	15.0

[a] Assignments are based on 1D and 2D NMR experiments in $CDCl_3$

[b] The NMR matches that of previously reported[8]

* Signals are overlapped

Supplementary Table 10. ^{13}C NMR (150 MHz) and ^{1}H NMR (600 MHz) spectroscopic data for venezuelaene A (**10**) isolated from *Sa*VenA (d in ppm, *J* in Hz).[a] The raw NMR data of **10** was deposited to np-mrd.org under accession number: NP0342007.

	10		**10**[b]
No.	δ_C	δ_H	δ_C
1	45.2, CH	1.20 (m, 1H)*	45.2
2	61.9, CH	2.36 (dq, *J* = 12.1, 3.2, 1H)	61.9
3	55.5, C	-	55.5
4	30.5, CH_2	1.39 (dddd, *J* = 11.5, 10.4, 8.5, 1.0, 1H) 1.22 (m, 1H)*	30.5
5	35.2, CH_2	2.68 (m, 1H) 2.50 (ddtd, *J* = 16.7, 8.6, 2.1, 1.1, 1H)	35.2
6	133.9, C	-	133.9
7	126.6, C	-	126.6
8	37.5, CH_2	2.18 (dddd, *J* = 17.0, 4.8, 2.9, 0.9, 1H) 2.08 (m, 1H)	37.5
9	33.0, CH_2	1.88 (dddd, *J* = 13.2, 5.0, 3.7, 1.4, 1H) 0.86 (m, 1H)*	33.0
10	45.1, CH	0.82 (m, 1H)*	45.1
11	31.6, CH	1.23 (m, 1H)*	31.6
12	32.4, CH_2	1.65 (m, 1H) 1.28 (m, 1H)*	32.3
13	20.5, CH_2	1.28 (m, 1H)*	20.5
14	53.2, CH	1.97 (ddd, *J* = 13.0, 10.3, 5.2, 1H)	53.2
15	41.0, C	-	40.9
16	26.2, CH_3	0.95 (s, 3H)	26.2
17	21.6, CH_3	0.85 (s, 3H)	21.6
18	21.0, CH_3	0.89 (d, *J* = 6.6, 3H)	21.0
19	21.8, CH_3	1.57 (s, 3H)	21.8
20	18.2, CH_3	0.81 (d, *J* = 1.1, 3H)	18.2

[a] Assignments are based on 1D NMR experiments in $CDCl_3$

[b] The NMR matches that of previously reported[9]

* Signals are overlapped

Supplementary Table 11. ^{13}C NMR (200 MHz) and ^{1}H NMR (800 MHz) spectroscopic data for venezuelaene A2 (**11**) isolated from *Ss*VenA (d in ppm, *J* in Hz).[a] The raw NMR data of **11** was deposited to np-mrd.org under accession number: NP0342008.

	11	
No.	δ_C	δ_H
1	38.5, CH	2.23 (m, 1H)
2	153.1, qC	-
3	61.7, qC	-
4	32.2, CH_2	1.85 (m, 1H)*
		1.25 (ddd, *J* = 12.2, 7.4, 1.0, 1H)
5	37.5, CH_2	2.75 (ddddd, *J* = 15.0, 9.6, 7.4, 3.8, 1.4, 1H)
		2.18 (m, 1H)*
6	135.8, qC	-
7	33.7, CH	2.16 (m, 1H)*
8	34.0, CH_2	1.73 (dddd, *J* = 13.8, 11.7, 9.4, 4.41, 1H)
		1.51 (m, 1H)*
9	32.94, CH_2	1.86 (m, 1H)*
		1.21 (ddt, *J* = 13.7, 10.1, 4.6, 1H)
10	47.0, CH	0.96 (m, 1H)*
11	37.1, CH	1.01 (m, 1H)
12	32.95, CH_2	1.41 (dq, *J* = 13.5, 4.6, 1H)
		1.10 (m, 1H)
13	22.4, CH_2	1.57 (m, 1H)
		1.50 (m, 1H)*
14	48.6, CH	2.33 (ddd, *J* = 10.2, 8.0, 3.5, 1H)
15	42.4, qC	-
16	23.5, CH_3	0.82 (s, 3H)
17	23.4, CH_3	0.74 (s, 3H)
18	20.4, CH_3	0.86 (d, *J* = 6.3, 3H)
19	20.9, CH_3	0.92 (d, *J* = 7.1, 3H)
20	21.4, CH_3	0.98 (s, 3H)

[a] Assignments are based on 1D and 2D NMR experiments in $CDCl_3$

* Signals are overlapped

Supplementary Table 12. ^{13}C NMR (150 MHz) and ^{1}H NMR (600 MHz) spectroscopic data for odyverdiene B2 (**12**) isolated from *Salk*S (d in ppm, *J* in Hz).[a] The raw NMR data of **12** was deposited to np-mrd.org under accession number: NP0342009.

	12	
No.	δ_C	δ_H
1	43.3, CH	1.45 (m, 1H)*
2	54.7, CH	1.84 (q, *J* = 7.2, 1H)
3[%]	34.88, CH	2.01 (m, 1H)*
4	32.1, CH_2	1.92 (m, 1H)*
		1.38 (m, 1H)*
5	30.3, CH_2	1.93 (m, 1H)*
		1.57 (dtd, *J* = 13.0, 10.1, 7.1, 1H)
6	45.8, CH	2.60 (t, *J* = 6.9, 1H)
7	154.5, qC	-
8	40.0, CH_2	2.44 (m, 1H)
		2.03 (m, 1H)*
9[%]	34.80, CH_2	1.68 (m, 1H)*
		1.04 (m, 1H)
10	47.9, CH	1.06 (m, 1H)
11	38.4, CH	1.12 (m, 1H)*
12[%]	34.91, CH_2	1.99 (m, 1H)
		1.11 (m, 1H)*
13	31.5, CH_2	1.48 (m, 2H)*
14	56.2, CH	1.78 (ddd, *J* = 11.4, 9.7, 3.3, 1H)
15	150.3, qC	-
16	110.8, CH_2	4.71 (m, 1H)*
		4.65 (br s, 1H)
17	19.56, CH_3	1.65 (s, 3H)
18	21.7, CH_3	0.96 (d, *J* = 6.1, 3H)
19	108.5, CH_2	4.71 (m, 2H)*
20	19.54, CH_3	0.91 (d, *J* = 7.3, 3H)

[a] Assignments are based on 1D and 2D NMR experiments in $CDCl_3$

* Signals are overlapped

[%] ^{13}C signals for 3, 9, and 12 are indistinguishable in HSQC

Supplementary Table 13. ^{13}C NMR (150 MHz) and ^{1}H NMR (600 MHz) spectroscopic data for 1*S*,3*E*,7*E*,11*R*,12*S*-dolabella-3,7,18-triene (**13**) isolated from *Sa*VenA (d in ppm, *J* in Hz).[a] The raw NMR data of **13** was deposited to np-mrd.org under accession number: NP0342010.

	13		**13**[b]
No.	δ_C	δ_H	δ_C
1	44.9, C	-	44.9
2	40.5, CH_2	2.13 (m, 1H)*	40.5
		1.80 (m, 1H)	
3	124.3, CH	4.98 (t, *J* = 7.4, 1H)	124.3
4	133.8, C	-	133.9
5	39.6, CH_2	2.10 (m, 2H)*	39.6
6	24.8, CH_2	2.15 (m, 1H)*	24.8
		2.10 (m, 1H)*	
7	125.0, CH	4.86, (t, *J* = 7.6, 1H)	125.0
8	136.0, C	-	136.0
9	37.3, CH_2	2.01 (m, 1H)*	37.3
		1.81 (m, 1H)	
10	30.8, CH_2	1.43 (m, 1H)	30.7
		1.26 (m, 1H)*	
11	44.4 CH	1.49 (m, 1H)	44.4
12	57.9, CH	2.24 (td, *J* = 9.8, 7.5 1H)	57.9
13	28.9, CH_2	1.60 (m, 1H)*	28.9
		1.50 (m, 1H)	
14	41.5, CH_2	1.60 (m, 1H)*	41.5
		1.38 (m, 1H)	
15	23.2, CH_3	0.92 (s, 3H)	23.2
16	16.0, CH_3	1.53 (s, 3H)	16.0
17	17.4, CH_3	1.52 (s, 3H)	17.4
18	148.6, C	-	148.6
19	19.0, CH_3	1.74 (s, 3H)	19.0
20	110.9, CH_2	4.78 (d, *J* = 2.6, 1H)	110.9
		4.66 (dd, *J* = 2.7, 1.4, 1H)	

[a] Assignments are based on 1D NMR experiments in $CDCl_3$

[b] The NMR matches that of previously reported[10]

* Signals are overlapped

Supplementary Table 14. ^{13}C NMR (150 MHz) and ^{1}H NMR (600 MHz) spectroscopic data for 1*R**,3*E*,7*E*,11*S**,12*S**-dolabella-3,7,18-triene (**14**) isolated from *Cb*DS (d in ppm, *J* in Hz).[a] The raw NMR data of **14** was deposited to np-mrd.org under accession number: NP0342011.

	14		**14**[b]
No.	δ_C	δ_C	δ_C
1	46.7, qC	-	46.5
2	43.5, CH_2	2.23 (m, 1H)* 1.70 (dd, *J* = 7.0, 4.1)	43.4
3	125.9, CH	5.15 (dd, *J* = 11.5, 4.7, 1H)	125.8
4	134.7, qC	-	134.5
5	40.0, CH_2	2.21 (m, 1H)* 2.07 (m, 1H)*	39.9
6	24.6, CH_2	2.30 (m, 1H) 2.06 (m, 1H)*	24.4
7	127.5, CH	4.86 (m, 1H)	127.3
8	134.1, qC	-	133.9
9	37.9, CH_2	2.14 (ddd, 1H, *J* = 14.2, 9.8, 5.1) 1.89 (dt, 1H, *J* = 12.5, 5.8)	37.7
10	24.5, CH_2	1.34 (ddt, 1H, *J* = 14.7, 9.9, 5.1) 1.24 (m, 1H)	24.4
11	41.9, CH	1.75 (dt, 1H, *J* = 8.1, 4.0)	41.8
12	51.2, CH	2.63 (dt, 1H, *J* = 10.4, 6.7)	51.0
13	28.6, CH_2	1.64 (m, 1H)* 1.58 (m, 1H)*	28.5
14	42.2, CH_2	1.53 (m, 1H) 1.43 (ddd, *J* = 12.7, 9.5, 7.5, 1H)	42.1
15	24.5, CH_3	1.07 (s, 3H)	24.3
16	15.8, CH_3	1.531 (s, 3H)	15.6
17	16.8, CH_3	1.525 (s, 3H)	16.7
18	147.0, qC	-	146.9
19	23.7, CH_3	1.72 (s, 3H)	23.5
20	111.3, CH_2	4.83 (t, 1H, *J* = 1.8) 4.66 (dd, 1H, *J* = 2.2, 1.2)	111.2

[a] Assignments are based on 1D and 2D NMR experiments in $CDCl_3$

[b] The NMR matches that of previously reported[11]

* Signals are overlapped

Supplementary Table 15. ^{13}C NMR (150 MHz) and ^{1}H NMR (600 MHz) spectroscopic data for 1*R*,7*E*,10*E*,12*R*-dolabella-4(16),7,10-triene (**15**) isolated from *Sh*DS (d in ppm, *J* in Hz).[a] The raw NMR data of **15** was deposited to np-mrd.org under accession number: NP0342012.

	15	
No.	δ_C	δ_H
1	46.6, qC	-
2	39.0, CH_2	1.50 (m, 2H)*
3	33.0, CH_2	2.00 (m, 1H)
		1.74 (m, 1H)*
4	153.2, qC	-
5	38.3, CH_2	2.23 (m, 1H)*
		1.76 (m, 1H)*
6	30.5, CH_2	2.24 (m, 1H)*
		2.10 (m, 1H)
7	126.2, CH	5.13 (m, 1H)
8	135.9, qC	-
9	39.5, CH_2	2.96 (t, *J* = 12.3, 1H)
		2.43 (dd, *J* = 12.7, 3.5, 1H)
10	122.3, CH	5.21 (ddd, *J* = 11.8, 3.6, 2.4, 1H)
11	149.7, qC	-
12	49.4, CH	2.64, (dddd, *J* = 6.0, 4.8, 2.8, 1.4, 1H)
13	25.0, CH_2	1.57, (m, 2H)*
14	43.5, CH_2	1.64, (m, 1H)*
		1.47, (m, 1H)*
15	27.8, CH_3	1.12, (s, 3H)
16	109.6, CH_2	4.87, (t, *J* = 2.1, 1H)
		4.77, (br s, 1H)
17	17.4, CH_3	1.60, (s, 3H)
18	32.6, CH	1.85, (td, *J* = 6.8, 5.4, 1H)
19	21.9, CH_3	0.95, (d, *J* = 6.9, 3H)
20	18.6, CH_3	0.86, (d, *J* = 6.8, 3H)

[a] Assignments are based on 1D and 2D NMR experiments in C_6D_6

* Signals are overlapped

Supplementary Table 16. ^{13}C NMR (150 MHz) and ^{1}H NMR (600 MHz) spectroscopic data for (+)-2*S*,3*S*,6*R*,7*Z*,10*Z*,11*R*-cyclooctat-7(8),10(14)-diene (**16**) isolated from *Kp*CdS (d in ppm, *J* in Hz).[a] The raw NMR data of **16** was deposited to np-mrd.org under accession number: NP0342013.

	16	
No.	δ_C	δ_H
1	40.4, CH_2	1.54 (m, 1H)*
		1.28 (d, *J* = 13.7, 1H)
2	45.0, CH	2.02 (m, 1H)*
3	37.0, CH	2.03 (m, 1H)*
4	34.2, CH_2	1.80 (m, 1H)*
		1.32 (qd, *J* = 7.3, 2.8, 1H)
5	27.8, CH_2	1.54 (m, 1H)*
		1.80 (m, 1H)*
6	41.1, CH	3.19 (td, *J* = 8.0, 3.6, 1H)
7	137.1, qC	-
8	123.8, CH	5.43 (ddd, *J* = 7.1, 3.4, 1.7, 1H)
9	26.2, CH_2	3.09 (dt, *J* = 18.4, 3.4, 1H)
		2.48 (ddt, *J* = 18.4, 6.9, 3.1)
10	139.1, qC	-
11	51.6, qC	-
12	36.9, CH_2	1.72 (ddd, *J* = 12.9, 9.4, 6.2, 1H)
		1.54 (m, 1H)*
13	28.5, CH_2	2.20 (m, 2H)
14	139.7, qC	-
15	27.3, CH	2.72 (p, *J* = 6.8, 1H)
16	21.2, CH_3	0.93 (d, *J* = 7.0, 3H)
17	20.6, CH_3	0.97 (d, *J* = 7.0, 3H)
18	17.2, CH_3	0.75 (d, *J* = 6.7, 3H)
19	22.9, CH_3	1.68 (s, 3H)
20	28.6, CH_3	1.04 (s, 3H)

[a] Assignments are based on 1D and 2D NMR experiments in $CDCl_3$

* Signals are overlapped

Supplementary Table 17. ^{13}C NMR (150 MHz) and ^{1}H NMR (600 MHz) spectroscopic data for (–)-2*R*,3*S*,6*R*,7*Z*,10*Z*,11*S*-cyclooctat-7(8),10(14)-diene (**17**) isolated from *Sl*CdS (*slt18_1078*) (d in ppm, *J* in Hz).[a] The raw NMR data of **17** was deposited to np-mrd.org under accession number: NP0342014.

	17		**17**[b]
No.	δ_C	δ_H	δ_C
1	48.4, CH_2	1.74 (m, 1H)* 1.62 (m, 1H)*	48.2
2	53.7, CH	0.91 (m, 1H)*	53.5
3	43.2, CH	1.37 (tt, *J* = 10.3, 6.1, 1H)	43.0
4	36.1, CH_2	1.71 (m, 1H)* 1.07 (m, 1H)	35.9
5	28.0, CH_2	1.80 (ddt, *J* = 13.0, 7.8, 2.5, 1H) 1.58 (m, 1H)*	29.7
6	49.3, CH	2.75 (br t, *J* = 8.1, H)	49.1
7	139.8, qC	-	139.6
8	124.0, CH	5.45 (tt, *J* = 8.4, 1.6, 1H)	123.8
9	23.5, CH_2	2.52 (m, 2H)	23.4
10	142.0, qC	-	141.9
11	51.5, qC	-	51.3
12	37.5, CH_2	1.52 (dt, *J* = 11.8, 9.5, 1H) 1.43 (ddd, *J* = 11.9, 7.3, 1.3, 1H)	37.3
13	26.5, CH_2	2.10 (dddd, *J* = 15.3, 9.6, 7.3, 1.7, 1H) 2.02 (ddt, *J* = 15.4, 9.0, 1.5, 1H)	26.3
14	140.2, qC	-	140.0
15	28.0, CH	2.63 (hept, *J* = 6.8, 1H)	27.8
16	21.6, CH_3	0.91 (d, *J* = 6.8, 3H)	20.9
17	21.1, CH_3	0.97 (d, *J* = 6.9, 3H)	21.5
18	18.2, CH_3	0.94 (d, *J* = 6.5, 3H)	18.0
19	20.3, CH_3	1.65 (s, 3H)	20.6
20	26.2, CH_3	0.93 (s, 3H)	26.0

[a] Assignments are based on 1D and 2D NMR experiments in $CDCl_3$

[b] The NMR matches that of previously reported[12] with the exception of the assignment of the H-5 protons

* Signals are overlapped

Supplementary Table 18. ^{13}C NMR (150 MHz) and ^{1}H NMR (600 MHz) spectroscopic data for monoprenyl-β-curcumene (**18**) isolated from *St*MpcS (d in ppm, *J* in Hz).[a] The raw NMR data of **18** was deposited to np-mrd.org under accession number: NP0342015.

	18	
No.	δ_C	δ_H
1	27.0, CH_2	2.59 (m, 2H)*
2	119.3, CH	5.43 (p, *J* = 2.9, 1.6 1H)
3	131.1, qC	-
4	32.0, CH_2	2.53 (m, 2H)*
		1.68 (m, 1H)*
5	118.4, CH	5.46 (m, 1H)
6	139.1, qC	-
7	40.7, CH	2.15 (m, 1H)*
8	35.5, CH_2	1.50 (dtd, *J* = 13.3, 8.2, 6.8, 1H)
		1.35 (m, 1H)*
9	26.5, CH_2	2.04 (q, *J* = 7.5, 2H)
10	125.3, CH	5.27 (tq, J = 6.9, 1.3, 1H)*
11	134.9, qC	-
12	40.3, CH_2	2.10 (q, *J* = 7.3, 2H)*
13	27.2, CH_2	2.18 (m, 2H)*
14	125.0, CH	5.24 (tdt, *J* = 7.0, 3.0, 1.4, 1H)
15	131.2, qC	-
16	25.9, CH_3	1.68 (d, *J* = 1.4, 3H)
17	19.9, CH_3	1.56 (s, 3H)
18	16.1, CH_3	1.59 (br s, 3H)
19	17.8, CH_3	1.01 (d, *J* = 6.9, 3H)
20	23.2, CH_3	1.60 (br s, 3H)

[a] Assignments are based on 1D and 2D NMR experiments in C_6D_6

* Signals are overlapped

Supplementary Table 19. ^{13}C NMR (150 MHz) and ^{1}H NMR (600 MHz) spectroscopic data for benditerpetriene (**19**) isolated from *N*Bnd4 and *Ma*Bnd4 (d in ppm, *J* in Hz).[a] The raw NMR data of **19** was deposited to np-mrd.org under accession number: NP0342016.

	19		**19**[b]
No.	δ_C	δ_H	δ_C
1	35.1, CH	2.45 (m, 2H)	35.1
2	132.4, CH	4.66 (m, 1H)	132.4
2*	133.0, CH	4.77 (m,1H)	133.0
3	130.8, qC	-	130.8
4	37.6, CH_2	2.09 (m, 2H)	37.6
4*	39.2, CH_2	2.09 (m, 2H)	39.2
5	24.2, CH_2	2.30 (m, 1H) 2.06 (m, 1H)	24.2
5*	24.5, CH_2	2.30 (m, 1H) 2.06 (m, 1H)	24.5
6	121.7, CH	4.94 (m, 1H)	121.7
6*	128.6, CH	4.94 (m, 1H)	128.6
7	135.3, qC	-	135.3
7*	138.3, qC	-	138.3
8	41.8, CH_2	2.29 (m, 1H) 1.77 (m, 1H)	41.8
9	32.1, CH_2	1.72 (m, 1H) 1.26 (m, 1H)	32.1
9*	34.8, CH_2	2.29 (m, 1H) 1.54 (m, 1H)	34.8
10	43.8, CH	1.31 (m, 1H)	43.8
10*	45.9, CH	1.31 (m, 1H)	45.9
11	33.6, CH	1.69 (m, 1H)	33.6
11*	36.1, CH	1.69 (m, 1H)	36.1
12	26.9, CH_2	1.70 (m, 2H)	26.9
13	26.6, CH_2	1.33 (m, 1H) 1.35 (m, 1H)	26.6
13*	26.6, CH_2	1.50 (m, 1H) 1.52 (m, 1H)	26.6
14	46.5, CH	1.93 (m, 1H)	46.5
15	149.8, qC	-	149.8
16	110.2, CH_2	4.65 (br d, 1H) 4.64 (m, 1H)	110.2
17	19.0, CH_3	1.59 (s, 3H)	19.0
18	19.2, CH_3	1.10 (d, J = 7.3, 3H)	19.2
19	19.0, CH_3	1.59 (s, 3H)	19.0
20	15.6, CH_3	1.47 (d, J = 1.4, 3H)	15.6

[a] Assignments are based on 1D and 2D NMR experiments in C_6D_6

[b] The NMR matches that of previously reported[13]

* Multiple signals due to ring flipped conformers in solution.

Supplementary Table 20. ^{13}C NMR (150 MHz) and ^{1}H NMR (600 MHz) spectroscopic data for prehydropyrene (**20**) isolated from *S*PhpS and *Cp*PhpS (d in ppm, *J* in Hz).[a] The raw NMR data of **20** was deposited to np-mrd.org under accession number: NP0342017.

	20		**20**[b]
No.	δ_C	δ_H	δ_C
1	43.8, CH	2.43 (dt, *J* = 10.8, 3.3, 1H)	43.8
2	128.6, CH	4.64 (d, *J* = 10.8, 1H)	128.5
3	131.1, qC	-	131.1
4	41.1, CH_2	2.15 (m, 1H)* 1.88 (m, 1H)*	41.1
5	27.1, CH_2	2.16 (m, 1H)* 2.03 (m, 1H)*	27.1
6	127.6, CH	4.73 (m, 1H)	127.6
7	138.0, qC	-	138.0
8	35.3, CH_2	2.16 (m, 1H)* 2.10 (m, 1H)	35.3
9	29.2, CH_2	1.90 (m, 1H)* 1.44 (m, 1H)*	29.2
10	49.9, CH	1.35 (m, 1H)*	49.9
11	27.8, CH	1.72 (m, 1H)*	27.8
12	37.0, CH_2	1.77 (m, 1H)* 1.00 (m, 1H)*	37.0
13	26.1, CH_2	1.58 (qd, *J* = 13.2, 3.9, 1H) 1.40 (m, 1H)*	26.1
14	51.8, CH	2.05 (m, 1H)*	51.8
15	148.5, qC	-	148.5
16	110.1, CH_2	4.86 (t, *J* = 1.8, 1H) 4.70 (br s, 1H)	110.1
17	23.0, CH_3	1.76 (s, 3H)	23.0
18	20.7, CH_3	0.87 (d, *J* = 6.3, 3H)	20.7
19	16.5, CH_3	1.35 (s, 3H)	16.4
20	17.2, CH_3	1.42 (d, *J* = 1.5, 3H)	17.2

[a] Assignments are based on 1D and 2D NMR experiments in C_6D_6

[b] The NMR matches that of previously reported[14]

* Multiple signals due to ring flipped conformers in solution.

Supplementary Table 21. ^{13}C NMR (150 MHz) and ^{1}H NMR (600 MHz) spectroscopic data for micromonocyclol (**21**) isolated from *Mp*McS, *Mb*McS, and *S*McS (d in ppm, *J* in Hz).[a]

	21		**21**[b]
No.	δ_C	δ_H	δ_C
1	138.2, CH	5.56 (d, *J* = 16.1, 1H)	138.2
2	133.4, CH	5.44 (d, *J* = 16.1, 1H)	133.4
3	73.1, qC	-	73.0
4	43.9, CH_2	1.72 (ddd, *J* = 13.8, 7.7, 6.1, 1H) 1.55 (m, 1H)*	43.9
5	22.8, CH_2	2.12 (m, 1H)* 2.05 (m, 1H)*	22.7
6	128.3, CH	5.03 (m, 1H)*	128.3
7	132.8, qC	-	132.8
8	39.9, CH_2	2.08 (m, 2H)*	39.9
9	25.1, CH_2	2.10 (m, 2H)*	25.1
10	125.1, CH	5.04 (m, 1H)*	125.1
11	135.3, qC	-	135.3
12	40.5, CH_2	1.92 (m, 2H)	40.5
13	24.4, CH_2	1.20 (m, 2H)*	24.4
14	42.3, CH	1.22 (m, 1H)*	42.3
15	35.5, qC	-	35.5
16	26.9, CH_3	0.98 (s, 3H)	26.9
17	27.8, CH_3	0.99 (s, 3H)	27.9
18	16.3, CH_3	1.54 (d, 3H, *J* = 1.4)	16.2
19	15.4, CH_3	1.48 (q, 3H, *J* = 1.3)	15.4
20	29.8, CH_3	1.20 (s, 3H)	29.8

[a] Assignments are based on 1D and 2D NMR experiments in C_6D_6

[b] The NMR matches that of previously reported[15]

* Multiple signals due to ring flipped conformers in solution.

Supplementary Table 22. ^{13}C NMR (150 MHz) and ^{1}H NMR (600 MHz) spectroscopic data for cembrene A (**22**) isolated from *Mp*McS, *Mb*McS, *Ml*CAS, and *Bp*CAS (d in ppm, *J* in Hz).[a] The raw NMR data of **22** was deposited to np-mrd.org under accession number: NP0350556.

	22		**22**[b]
No.	δ_C	δ_H	δ_C
1	46.0, CH	2.05 (m, 1H)*	45.9
2	32.4, CH_2	2.02 (m, 1H)* 1.98 (m, 1H)*	32.4
3	121.9, CH	5.06 (m, 1H)	121.7
4	133.9, qC	-	133.8
5	39.0, CH_2	2.20 (m, 1H)* 2.15 (m, 1H)*	38.9
6	24.9, CH_2	2.29 (m, 1H) 2.20 (m, 1H)*	24.8
7	124.0, CH	5.19 (m, 1H)	124.0
8	134.8, qC	-	134.7
9	39.4, CH_2	2.08 (m, 2H)*	39.4
10	23.8, CH_2	2.15 (m, 2H)*	23.7
11	125.9, CH	4.98 (m, 1H)	125.9
12	133.4, qC	-	133.4
13	34.0, CH_2	1.96 (m, 1H)* 1.78 (ddd, *J* = 14.6, 9.4, 3.7, 1H)	33.9
14	28.2, CH_2	1.69 (m, 1H)* 1.38 (dddd, *J* = 13.7, 9.4, 6.8, 3.8)	28.1
15	149.3, qC	-	149.2
16	110.1, CH_2	4.71 (dt, *J* = 3.1, 1.7, 1H) 4.65 (m, 1H)	110.1
17	19.3, CH_3	1.68 (q, 3H, *J* = 1.5, 1.0)	19.2
18	18.0, CH_3	1.58 (s, 3H)	18.0
19	15.5, CH_3	1.60 (s, 3H)	15.5
20	15.3, CH_3	1.60 (s, 3H)	15.2

[a] Assignments are based on 1D and 2D NMR experiments in $CDCl_3$

[b] The NMR matches that of previously reported[16]

* Signals are overlapped

Supplementary Table 23. ^{13}C NMR (150 MHz) and ^{1}H NMR (600 MHz) spectroscopic data for nephthenol (**23**) isolated from *Bp*CAS (d in ppm, *J* in Hz).[a] The raw NMR data of **23** was deposited to np-mrd.org under accession number: NP0080347.

	23		**23**[b]
No.	δ_C	δ_H	δ_C
1	28.6, CH_2	2.10 (m, 1H)* 1.89 (dt, *J* = 15.2, 7.6, 1H)	29.0
2	126.1, CH	5.10 (m, 1H)	126.9
3	133.5, qC	-	133.0
4	39.0, CH_2	2.10 (m, 2H)*	39.3
5	24.8, CH_2	2.20 (m, 1H) 2.10 (m, 1H)*	25.2
6	125.9, CH	4.94 (m, 1H)	126.3
7	133.2, qC	-	133.0
8	39.6, CH_2	2.10 (m, 1H)* 2.00 (m, 1H)*	39.9
9	24.2, CH_2	2.10 (m, 2H)*	24.5
10	125.2, CH	5.00 (m, 1H)	125.3
11	134.2, qC	-	134.3
12	37.9, CH_2	2.10 (m, 1H)* 2.02 (m, 1H)*	38.2
13	28.4, CH_2	1.65 (dddd, *J* = 13.6, 10.0, 6.3, 3.8, 1H) 1.28 (m, 1H)	28.8
14	48.6, CH	1.33 (tt, *J* = 7.7, 4.0)	48.8
15	74.1, qC	-	73.2
16	27.7, CH_3	1.20, (s, 3H)*	27.9
17	27.8, CH_3	1.20, (s, 3H)*	27.9
18	15.7, CH_3	1.57 (s, 3H)*	15.8
19	15.5, CH_3	1.57 (s, 3H)*	15.5
20	15.7, CH_2	1.57 (s, 3H)*	15.7

[a] Assignments are based on 1D and 2D NMR experiments in $CDCl_3$

[b] The NMR matches that of previously reported in C_6D_6[17]

* Signals are overlapped

Supplementary Table 24. ^{13}C NMR (150 MHz) and ^{1}H NMR (600 MHz) spectroscopic data for *iso*-cembrene C (**24**) isolated from *Ny*ICS (d in ppm, *J* in Hz).[a]

	24		**24**[b]
No.	δ_C	δ_H	δ_C
1	133.7,qC	-	133.7
2	38.9, CH_2	2.13 (m, 2H)	39.0
3	24.9, CH_2	2.17 (m, 2H)*	24.9
4	126.3, CH	4.93 (t, *J* = 6.7, 1H)	126.3
5	133.0, qC	-	133.1
6	39.9, CH_2	2.02 (m, 2H)	40.0
7	23.8, CH_2	2.06 (m, 2H)	23.8
8	124.0, CH	5.00 (t, *J* = 7.3, 1H)	124.1
9	134.9, qC	-	135.0
10	37.4, CH_2	1.94 (t, *J* = 7.6, 1H)	37.4
11	31.4, CH_2	2.17 (m, 2H)*	31.4
12	131.2, qC	-	131.2
13	30.5, CH_2	2.80 (d, *J* = 7.0, 2H)	30.5
14	124.7, CH	5.04 (t, *J* = 7.0, 1H)	124.8
15	15.9, CH_3	1.59 (s, 3H)	15.9
16	14.9, CH_3	1.56 (s, 3H)	15.0
17	15.2, CH_3	1.58 (s, 3H)	15.3
18	124.7, qC	-	124.7
19	20.5, CH_3	1.64 (s, 3H)	20.5
20	20.7, CH_3	1.67 (s, 3H)	20.7

[a] Assignments are based on 1D and 2D NMR experiments in $CDCl_3$

[b] The NMR matches that of previously reported[18]

* Signals are overlapped

Supplementary Table 25. ^{13}C NMR (150 MHz) and ^{1}H NMR (600 MHz) spectroscopic data for spiroviolene (**25**) isolated from *S130*SvS (d in ppm, *J* in Hz).[a] The raw NMR data of **25** was deposited to np-mrd.org under accession number: NP0016132.

	25		**25**[b]
No.	δ_C	δ_H	δ_C
1	128.5, CH	4.77 (dd, *J* = 2.9, 0.6, 1H)	128.7
2	148.5, qC	-	148.7
3	44.4, CH	1.65 (m, 1H)	44.5
4	30.9, CH_2	1.74 (m, 1H)* 1.27 (m, 1H)*	31.0
5	30.3, CH_2	1.74 (m, 1H)* 1.26 (m, 1H)*	30.4
6	46.3, CH	1.85 (ddq, *J* = 10.5, 8.8, 6.7, 1H)	46.4
7	53.4, qC	-	53.5
8	39.1, CH_2	1.93 (td, *J* = 12.7, 7.0, 1H) 1.68 (m, 1H)	39.3
9	32.6, CH_2	1.68 (m, 1H) 1.02 (m, 1H)*	32.8
10	58.9, CH	2.68 (dtd, *J* = 12.6, 6.5, 2.9, 1H)	59.1
11	63.3, qC	-	63.5
12	38.2, CH_2	1.67 (m, 1H) 1.55 (m, 1H)	38.4
13	40.4, CH_2	1.55 (m, 1H) 1.39 (m, 1H)	40.5
14	65.7, CH	1.53 (m, 1H)	65.9
15	41.1, qC	-	41.2
16	28.9, CH_3	1.02 (s, 3H)	29.1
17	25.9, CH_3	0.99 (s, 3H)	26.0
18	32.2, CH_3	1.29 (s, 3H)	32.3
19	14.8, CH_3	0.88 (d, *J* = 6.8, 3H)	15.0
20	14.8, CH_3	0.86 (d, *J* = 6.7, 3H)	15.0

[a] Assignments are based on 1D and 2D NMR experiments in $CDCl_3$

[b] The NMR matches that of previously reported[19]

* Signals are overlapped

Supplementary Table 26. ^{13}C NMR (150 MHz) and ^{1}H NMR (600 MHz) spectroscopic data for spata-13,17-diene (**26**) isolated from SpS (d in ppm, *J* in Hz).[a]

	26		**26**[b]
No.	δ_C	δ_H	δ_C
1	44.1, CH	1.76 (tq, *J* = 13.2, 6.2, 1H)	44.1
2	38.6, CH	1.98 (m, 1H)*	38.6
3	37.1, CH	1.77 (dq, *J* = 12.8, 6.5, 1H)	37.1
4	34.9, CH_2	1.69 (m, 1H)* 1.28 (m, 1H)*	34.9
5	28.3, CH_2	1.42 (m, 1H)* 1.67 (m, 1H)*	28.3
6	45.4, CH	2.03 (m, 1H)*	45.4
7	42.2, qC	-	42.2
8	41.8, CH_2	1.40 (m, 1H)* 1.56 (m, 1H)*	41.8
9	28.4, CH_2	1.67 (m, 1H)* 1.98 (m, 1H)*	28.4
10	48.9, CH	2.48 (dt, *J* = 11.8, 5.5, 1H)	48.9
11	149.2, qC	-	149.2
12	36.6, CH_2	1.96 (m, 2H)*	36.6
13	26.7, CH_2	2.05 (m, 1H)* 2.16 (td, *J* = 14.6, 6.3, 1H)	26.7
14	124.6, CH	5.11 (dddt, *J* = 7.0, 2.9, 1.4, 1H)	124.6
15	131.5, qC	-	131.5
16	25.8, CH_3	1.68 (s, 3H)	25.8
17	17.8, CH_3	1.60 (s, 3H)	17.8
18	108.3, CH_2	4.80 (d, *J* = 16.8, 2H)	108.2
19	20.5, CH_3	0.93 (s, 3H)	20.5
20	14.4, CH_3	0.84 (d, *J* = 6.8, 1.8, 3H)	14.4

[a] Assignments are based on 1D NMR experiments in $CDCl_3$

[b] The NMR matches that of previously reported[20]

* Signals are overlapped

Supplementary Table 27. ^{13}C NMR (150 MHz) and ^{1}H NMR (600 MHz) spectroscopic data for cneorubin Y (**27**) isolated from SpS (d in ppm, *J* in Hz).[a]

	27	**27**[b]
No.	δ_H	δ_H
1	1.29 (m, 1H)*	1.29
2	4.36 (d, *J* = 11.5, 1H)	4.36
3	-	-
4	2.21 (dt, *J* = 12.0, 3.4, 1H)	2.21
	1.85 (m, 1H)*	1.85
5	2.02 (m, 1H)*	2.02
	2.11 (m, 1H)*	2.11
6	4.83 (dd, *J* = 11.2, 5.1, 1H)	2.73
7	-	-
8	2.42 (dd, *J* = 13.0, 4.1, 1H)	2.42
	1.71 (m, 1H)	1.71
9	1.87 (m, 1H)*	1.87
	1.23 (m, 1H)*	1.23
10	0.60 (ddd, *J* = 11.9, 8.7, 2.9, 1H)	0.60
11	-	-
12	1.32 (m, 1H)*	1.32
	1.20 (m, 1H)*	1.20
13	2.05 (m, 2H)*	2.05
14	5.11 (m, 1H)	5.11
15	-	-
16	1.67 (s, 3H)	1.67
17	1.61 (s, 3H)	1.61
18	1.02 (s, 3H)	1.02
19	1.48 (s, 3H)	1.48
20	1.66 (s, 3H)	1.66

[a] Assignments are based on 1D NMR experiments in $CDCl_3$

[b] The NMR matches that of previously reported[20]

* Signals are overlapped

Supplementary Table 28. ^{13}C NMR (150 MHz) and ^{1}H NMR (600 MHz) spectroscopic data for β-springene (**28**) isolated from StSS (d in ppm, *J* in Hz)[a]

	28		**28**[b]
No.	δ_C	δ_H	δ_C
1	115.8, CH_2	5.03 (dd, *J* = 10.4, 1.7, 2H)	115.6
2	139.0, CH	6.38 (dd, *J* = 17.6, 10.8, 1H)	139.1
3	146.2, qC	-	146.2
4	31.5, CH_2	2.25 (m, 2H)	31.5
5	26.7, CH_2	2.21 (m, 2H)	26.7
6	124.1, CH	5.19 (tq, *J* = 6.9, 1.4, 1H)	124.1
7	135.0, qC	-	134.9
8	39.8, CH_2	2.01 (m, 2H)*	39.8
9	26.7, CH_2	2.09 (m, 2H)*	26.7
10	124.3, CH	5.13 (m, 1H)*	124.3
11	135.5, qC	-	135.4
12	39.8, CH_2	2.01 (m, 2H)*	39.8
13	26.8, CH_2	2.09 (m, 2H)*	26.8
14	124.4, CH	5.13 (m, 1H)*	124.5
15	131.3, qC	-	131.2
16	25.7, CH_3	1.70 (s, 3H)	25.7
17	17.7, CH_3	1.62 (s, 3H)*	17.7
18	16.1, CH_3	1.63 (s, 3H)*	16.0
19	16.1, CH_3	1.63 (s, 3H)*	16.0
20	113.1, CH_2	5.27 (d, *J* = 17.6, 1H) 5.08 (d, *J* = 10.8, 1H)	113.0

[a] Assignments are based on 1D and 2D NMR experiments in $CDCl_3$

[b] The NMR matches that of previously reported[21]

* Signals are overlapped

Supplementary Table 29. Strains used in this study.

Strain	Description	Source
E. coli NEB Turbo	Host for general cloning	New England Biolabs
E. coli BL21 Star (DE3)	Host for high-level protein production	Invitrogen

Supplementary Table 30. Plasmids used in this study.

Plasmid	Description*	Source/Reference
pET28a	Plasmid for heterologous expression in *E. coli*	Novagen
pJR1064b	pCDF-MKI4: pCDF harboring kinases *Ec-Th*iM and *At-IPK*, *Ec-idi*, and GGPP synthase (*bnd3*). Ribosome binding sites were inserted before each gene.	[22]
pJR4001	pET28a harboring *tiqS* (TS76)	This study
pJR4002	pET28a harboring *salS* (TS32)	This study
pJR4003	pET28a harboring *chtS* (TS170)	This study
pJR4004	pET28a harboring *peyS* (TS247)	This study
pJR4005	pET28a harboring *cvdsS* (TS86)	This study
pJR4006	pET28a harboring *odvS* (TS280)	This study
pJR4007	pET28a harboring *psvS* (TS297)	This study
pJR4008	pET28a harboring *cnvrtS* (TS80)	This study
pJR4009	pET28a harboring *svrtS* (TS248)	This study
pJR4010	pET28a harboring *chjdcs* (TS261)	This study
pJR4011	pET28a harboring *savenA* (TS44)	This study
pJR4012	pET28a harboring *ssvenA* (TS197)	This study
pJR4013	pET28a harboring *salkS* (TS113)	This study
pJR4014	pET28a harboring *cbdS* (TS211)	This study
pJR4015	pET28a harboring *shdS* (TS79)	This study
pJR4016	pET28a harboring *kpcdS* (TS324)	This study
pJR4017	pET28a harboring *slcdS* (TS7)	This study
pJR4018	pET28a harboring *stmpcS* (TS189)	This study
pJR4019	pET28a harboring *nbnd4* (TS304)	This study
pJR4020	pET28a harboring *mabnd4* (TS305)	This study
pJR4021	pET28a harboring *sphpS* (TS95)	This study
pJR4022	pET28a harboring *cphpsS* (TS253)	This study
pJR4023	pET28a harboring *mpmcsS* (TS362)	This study
pJR4024	pET28a harboring *mbmcsS* (TS363)	This study
pJR4025	pET28a harboring *smcS* (TS364)	This study
pJR4026	pET28a harboring *mlcaS* (TS213)	This study
pJR4027	pET28a harboring *bpcaS* (TS270)	This study
pJR4028	pET28a harboring *nylcS* (TS160)	This study
pJR4029	pET28a harboring *s130svS* (TS419)	This study
pJR4030	pET28a harboring *spS* (TS369)	This study
pJR4031	pET28a harboring *stss* (TS159)	This study

* TS ID designates Rudolf lab TS library

Supplementary Table 31. Primers used in this study.

Name	Sequence (5´–3´)	Purpose
Tetraisoquinenes _F	GTGGACAGCAAATGGGTCGCGGATCCATGATAACCAGTCAACGT	Subclone *tiqS* for protein production and purification in *E. coli*
Tetraisoquinenes _R	TCGAGTGCGGCCGCAAGCTTTCATCTCTCGGTCTGTACCCGGG	
Salbirenol _F	GGACAGCAAATGGGTCGCGGATCCATGCGCAAACTTTCAGATATTGTACTGC	Subclone *salS* for protein production and purification in *E. coli*
Salbireno _R	GTGCGGCCGCAAGCTTTTATGACAGCCGAAGCGTGTGCCC	
Peysonnosene _F	AATGGGTCGCGGATCCATGGTTCAGTCTGGTCTGTTAA	Subclone *peyS* for protein production and purification in *E. coli*
Peysonnosene _R	AGTGCGGCCGCAAGCTTTTATAACAAATGTTTCAGTTCACT	
Odyverdiene B2 _F	AAATGGGTCGCGGATCCATGTCTCATACGACCACCGT	Subclone *salkS* for protein production and purification in *E. coli*
Odyverdiene B2 _R	TCGAGTGCGGCCGCAAGCTTTTATGAGGGCAGACCATTA	
Variediene _F	ATGGGTCGCGGATCCATGAAGAAAATCTTTCAACAAATCCAG	Subclone *odvS* for protein production and purification in *E. coli*
Variediene _R	TGCGGCCGCAAGCTTCTATGTAAGCAGCTTCTCCATAA	
Prehydropyrene _F	ATGGGTCGCGGATCCATGGTTGAGTTTCACGTGC	Subclone *sphpS* for protein production and purification in *E. coli*
Prehydropyrene _R	CTCGAGTGCGGCCGCAAGCTTTTACAGGTGATCC	

Supplementary Table 32. 16S rRNA used for phylogenetic tree in Fig. 1A.

Phylum	Strain	16S rRNA accession number from NCBI
Acidobacteriota	*Acidobacterium capsulatum* ATCC 51196	NR_074106.1
Actinomycetota	*Actinomyces trachealis*	NR_181378.1
Aquificota	*Aquifex aeolicus*	NR_075056.2
Armatimonadota	*Armatimonas rosea*	NR_113009.1
Atribacterota	*Atribacter laminatus*	NR_179389.1
Bacillota	*Bacillus stercoris*	NR_181952.1
Bacteroidota	*Bacteroides propionicigenes*	NR_181731.1
Balneolota	*Balneola alkaliphila*	NR_044367.1
Bdellovibrionota	*Bdellovibrio bacteriovorus*	NR_027553.1
Caldisericota	*Caldisericum exile*	NR_075015.2
Calditrichota	*Calditrix palaeochoryensis*	NR_116885.1
Campylobacterota	*Campylobacter californiensis*	NR_197757.1
Chlamydiota	*Chlamydia gallinacea* 08-1274/3	NR_136425.1
Chlorobiota	*Chlorobium ferrooxidans* DSM 13031	NR_119288.2
Chloroflexota	*Chloroflexus islandicus*	NR_148571.2
Chrysiogenota	*Chrysiogenes arsenatis*	NR_029283.1
Coprothermobacterota	*Coprothermobacter proteolyticus*	NR_074653.1
Cyanobacteriota	*Neolyngbya regalis* BLCC-M54	NR_197633.1
Deferribacterota	*Deferribacter desulfuricans* SSM1	NR_075025.2
Deinococcota	*Deinococcus arenicola*	NR_197655.1
Dictyoglomota	*Dictyoglomus thermophilum* H-6-12	NR_118360.1
Elusimicrobiota	*Elusimicrobium minutum*	NR_115046.1
Fibrobacterota	*Fibrobacter succinogenes* subsp. succinogenes S85	NR_118361.1
Fusobacteriota	*Fusobacterium massiliense*	NR_179530.1
Gemmatimonadota	*Gemmatimonas phototrophica*	NR_136770.1
Ignavibacteriota	*Ignavibacterium album* JCM 16511	NR_112875.1
Kiritimatiellota	*Kiritimatiella glycovorans*	NR_146840.1
Lentisphaerota	*Lentisphaera profundi*	NR_145667.1
Mycoplasmatota	*Mycoplasma enhydrae*	NR_181978.1
Myxococcota	*Myxococcus stipitatus*	NR_102512.2
Nitrososphaerota	*Nitrososphaera viennensis*	NR_134097.1
Nitrospinota	*Nitrospina watsonii*	NR_178548.1
Nitrospirota	*Nitrospira lenta*	NR_148573.1
Planctomycetota	*Rhodopirellula islandica*	NR_181990.1
Pseudomonadota	*Pseudomonas svalbardensis*	NR_197749.1
Rhodothermota	*Rhodothermus bifroesti*	NR_181695.1
Spirochaetota	*Spirochaeta lutea*	NR_136451.1
Synergistota	*Synergistes jonesii*	NR_044616.1
Thermodesulfobacteriota	*Thermodesulfobacterium geofontis* OPF15	NR_118457.1
Thermomicrobiota	*Thermomicrobium carboxidum*	NR_134218.1
Thermoproteota	*Thermoproteus uzoniensis*	NR_177322.1
Thermotogota	*Thermotoga petrophila* RKU-10	NR_042374.2
Verrucomicrobiota	*Verrucomicrobium spinosum* DSM 4136	NR_026266.1

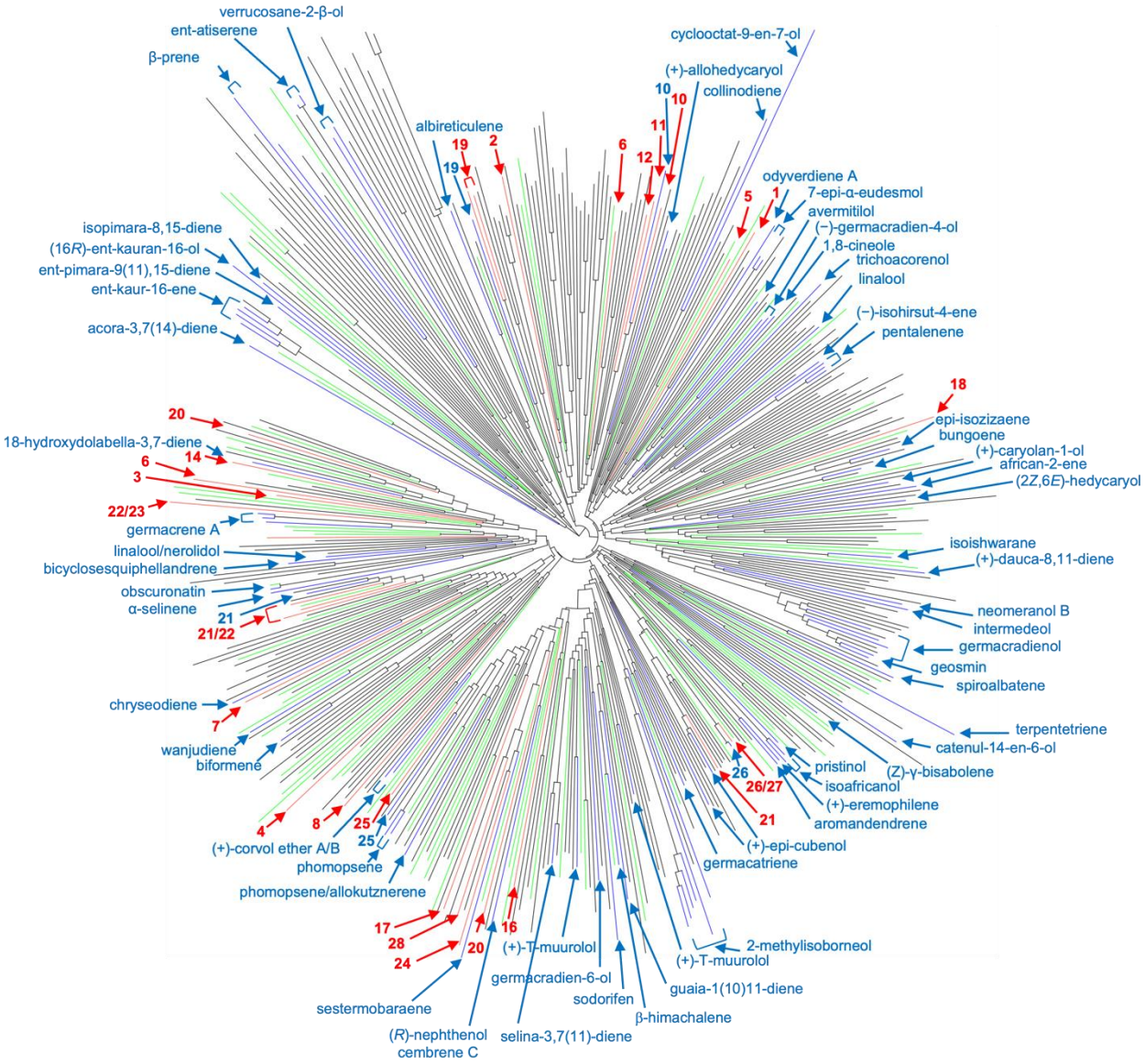

Supplementary Fig. 1. Phylogenetic analysis of 475 type I TSs from bacteria shown broad distribution of di-TSs. This is the same tree as shown in Fig. 1, enlarged for clarity. The blue lines represented previously characterized TSs, red lines are the 31 TSs characterized in this study, green lines are the other 94 TSs that showed di-TS activity but not studied here, and black lines are the remaining 209 TSs in our bacterial TS library. Phylogenetic trees were constructed in MEGA11 [23] with the Neighbor-Joining algorithm, bootstrap analysis with 1000 replicates, and visualized and annotated using iTOL[24].

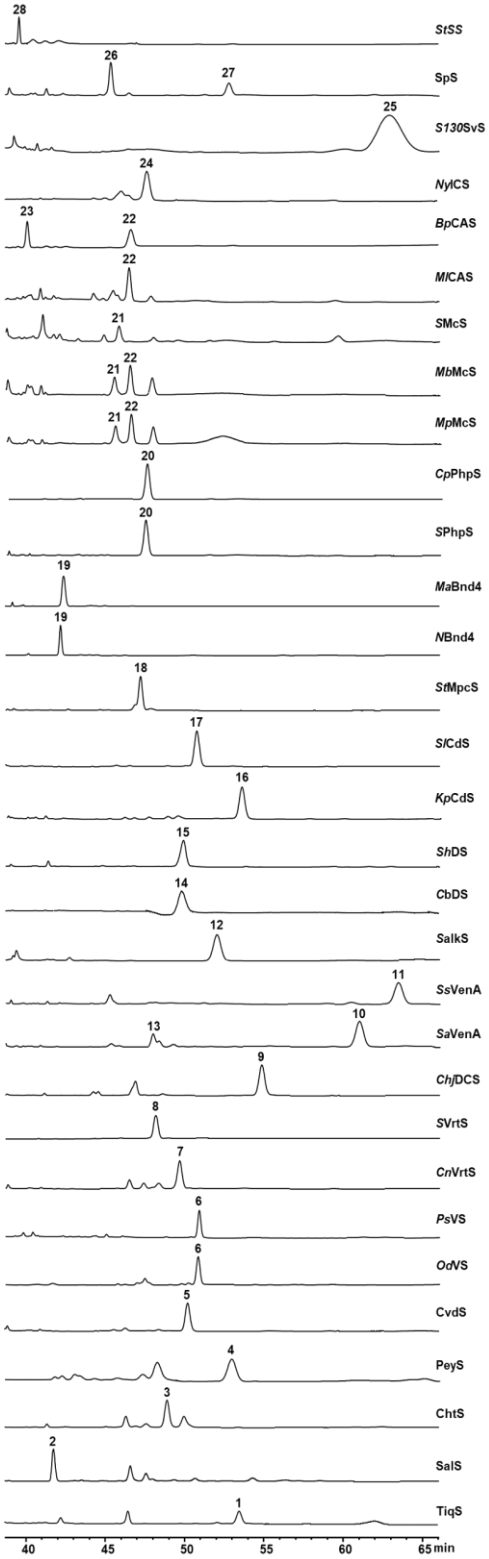

Supplementary Fig. 2. HPLC-UV analysis of diterpenes produced by the 31 TSs screened in *E. coli*. Absorbance was detected at 210 nm.

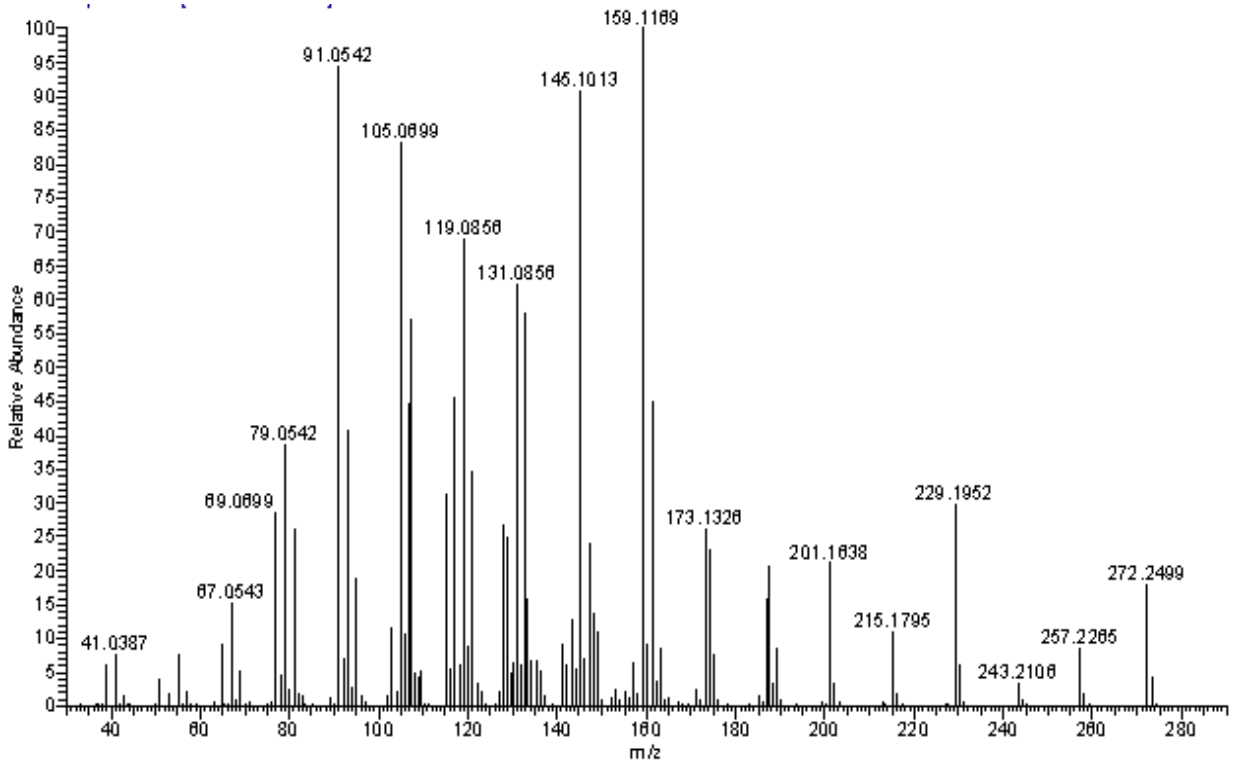

Supplementary Fig. 3. EIMS of tetraisoquinene **(1)**.

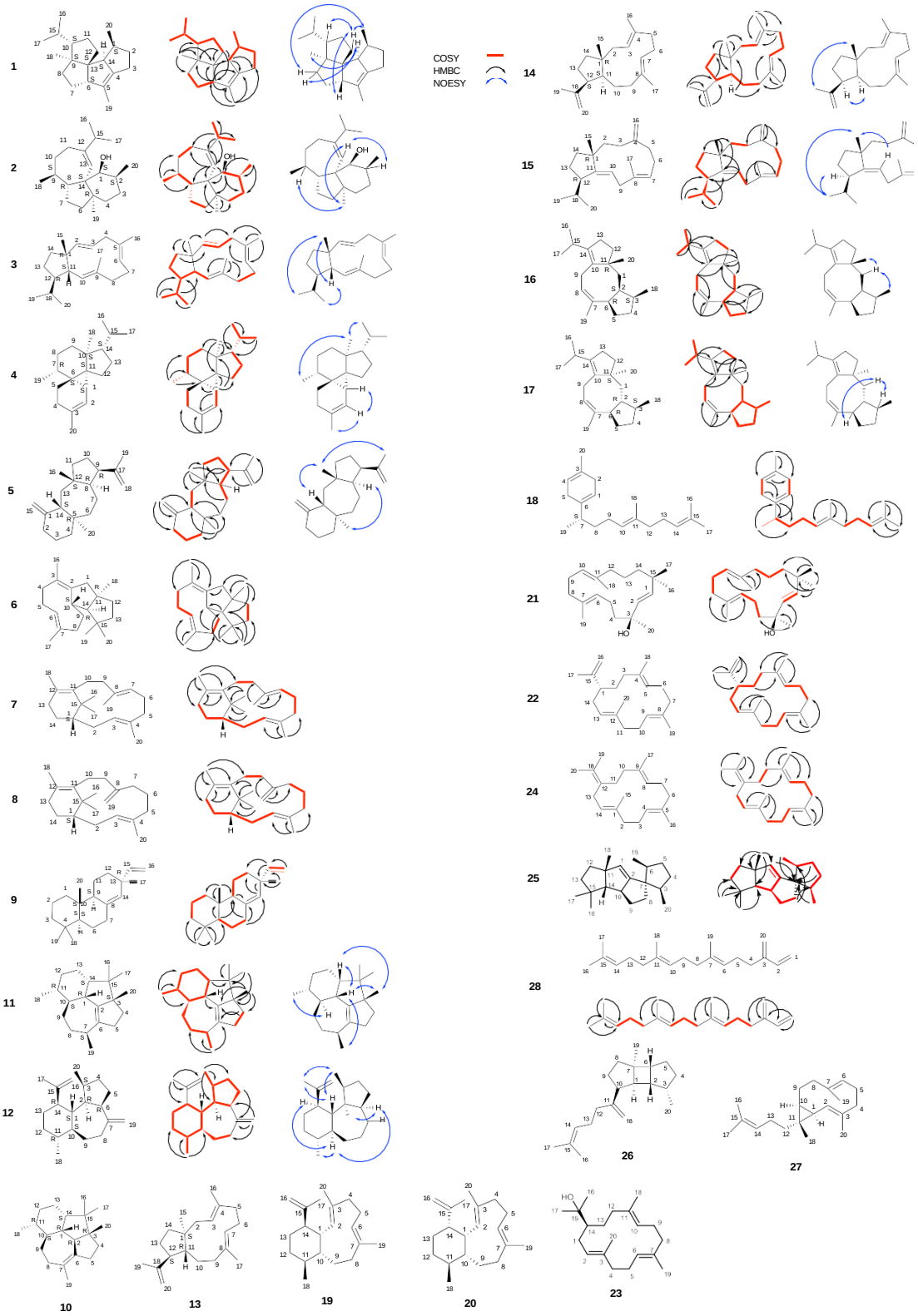

Supplementary Fig. 4. The structures and key 2D NMR correlations for diterpenes **1**–**28**.

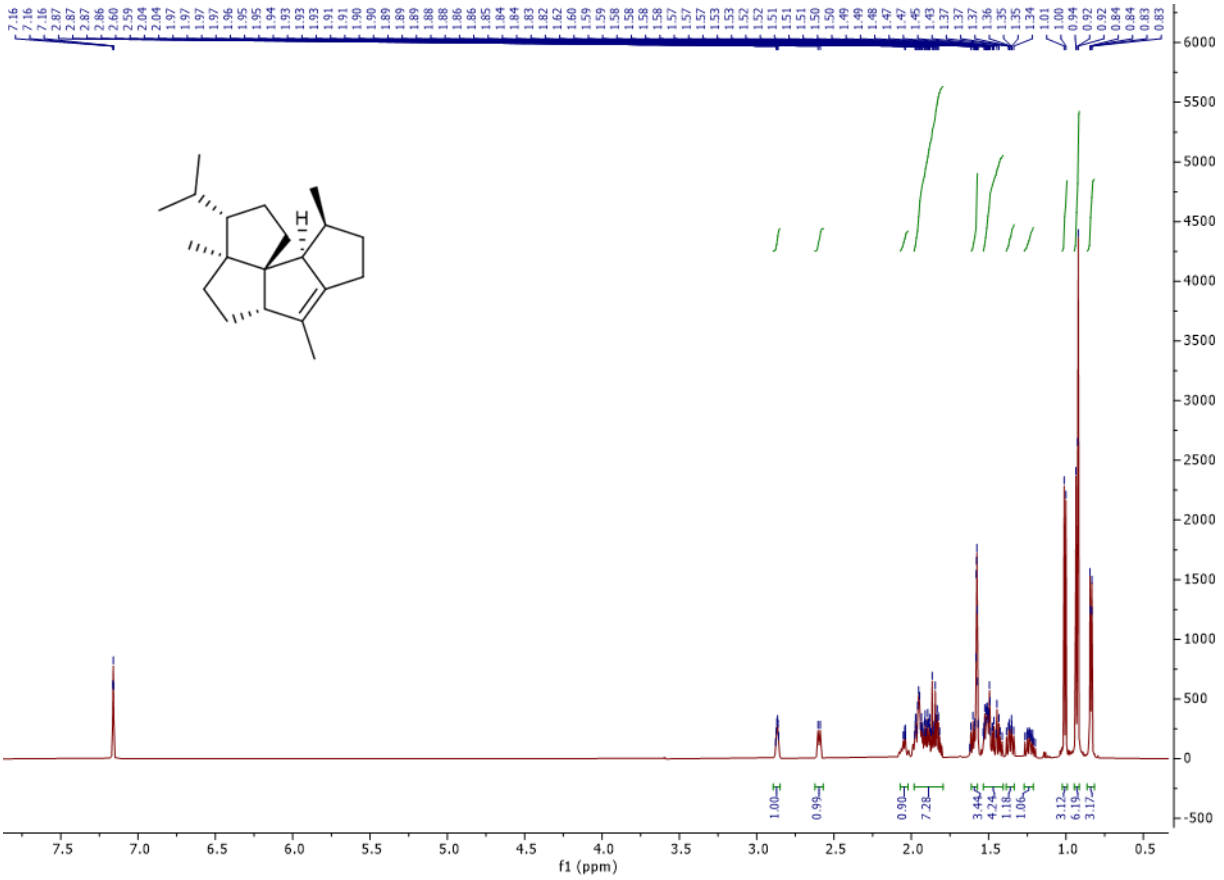

Supplementary Fig. 5. ^{1}H NMR spectrum of tetraisoquinene **(1)** in C_6D_6 (600 MHz).

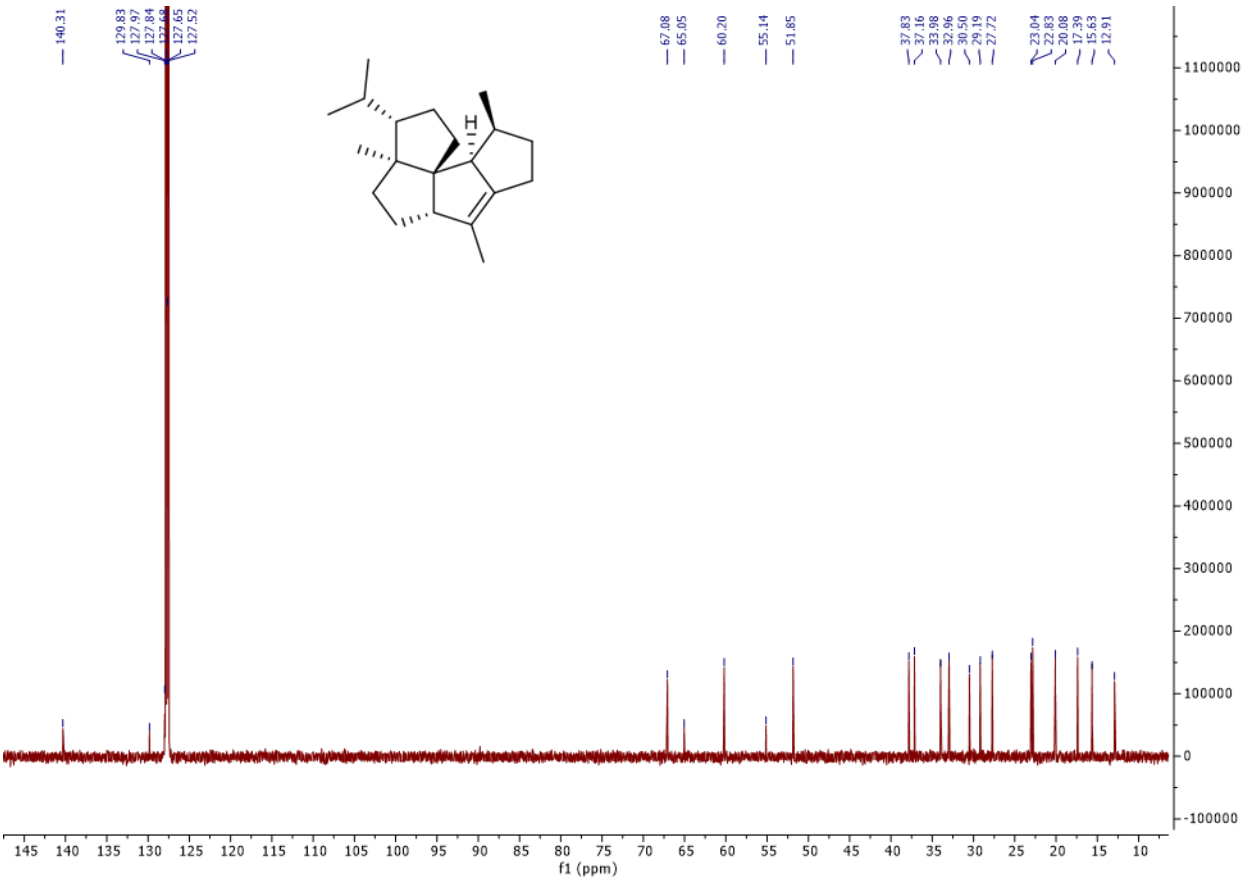

Supplementary Fig. 6. ^{13}C NMR spectrum of tetraisoquinene **(1)** in C_6D_6 (151 MHz).

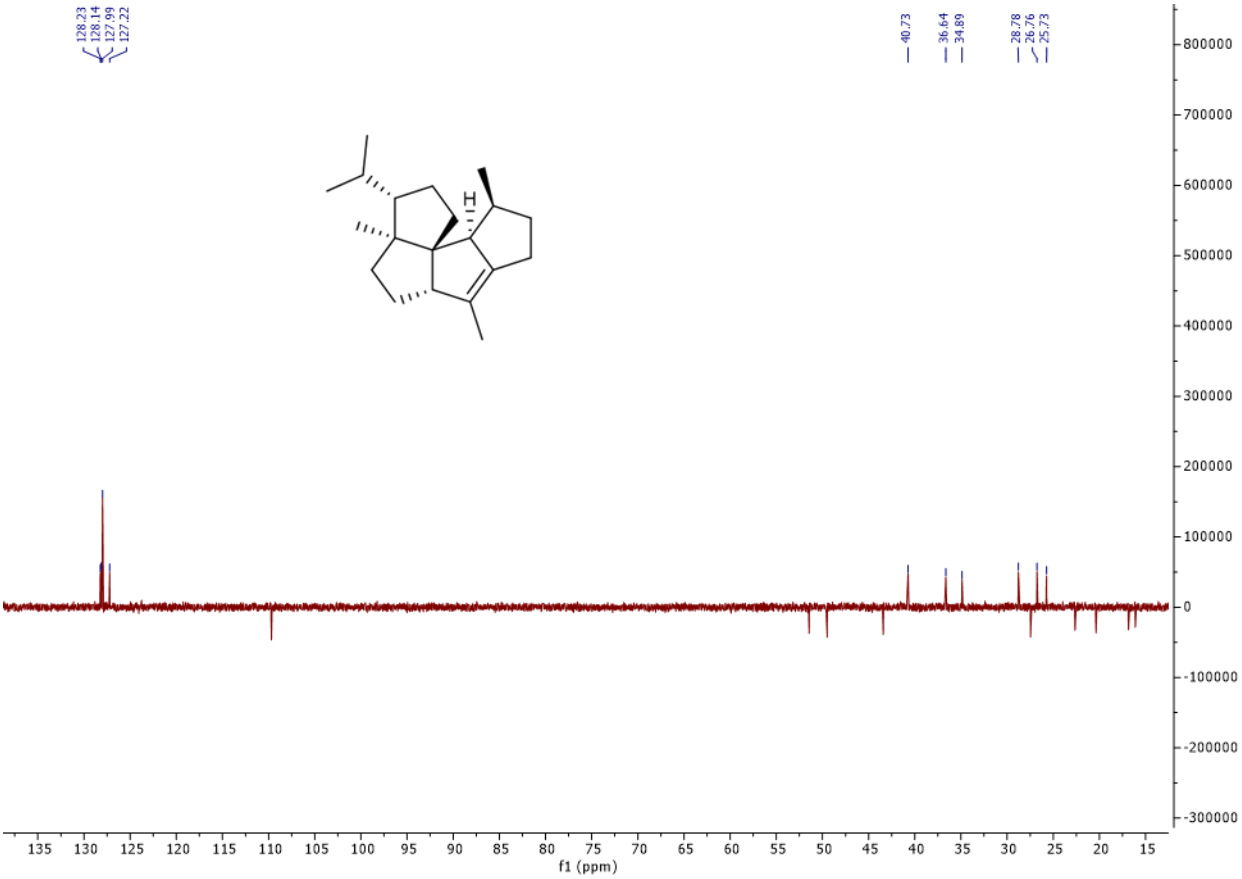

Supplementary Fig. 7. DEPT 135 spectrum of tetraisoquinene **(1)** in C_6D_6 (151 MHz).

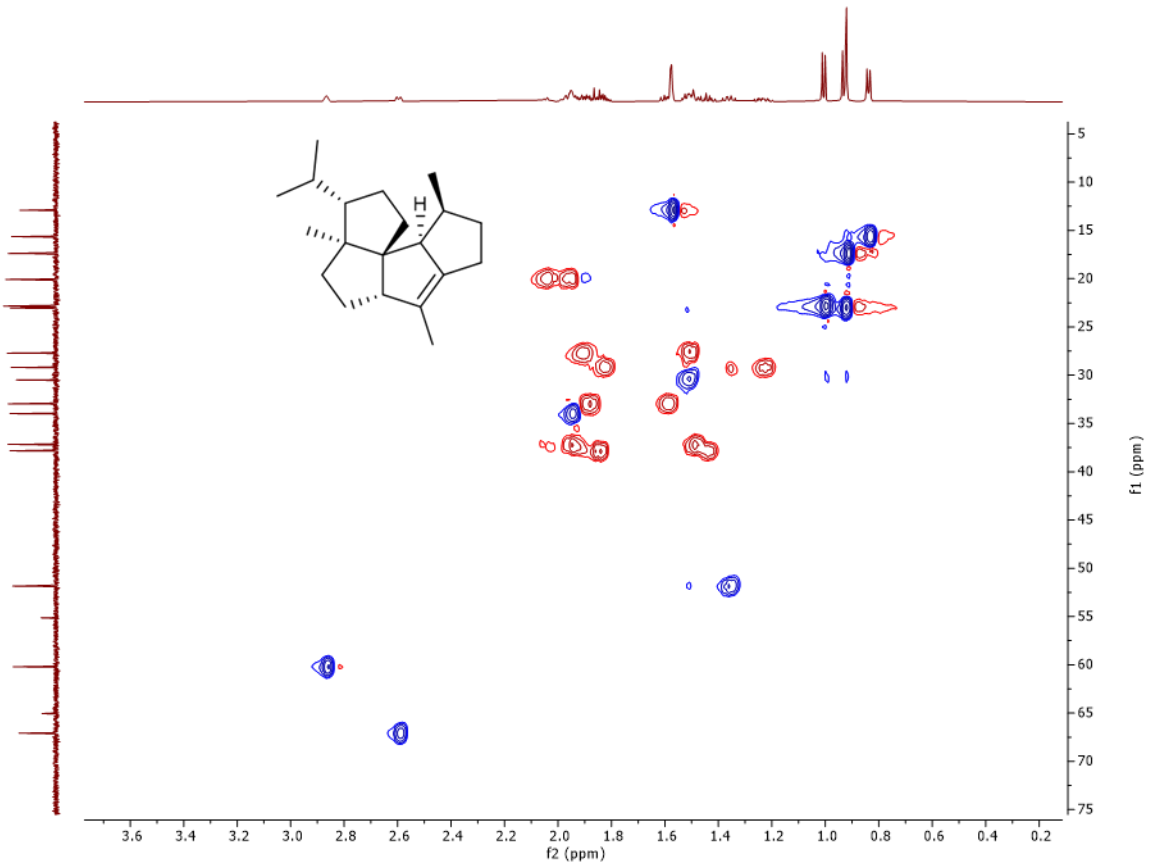

Supplementary Fig. 8. HSQC spectrum of tetraisoquinene **(1)** in C_6D_6

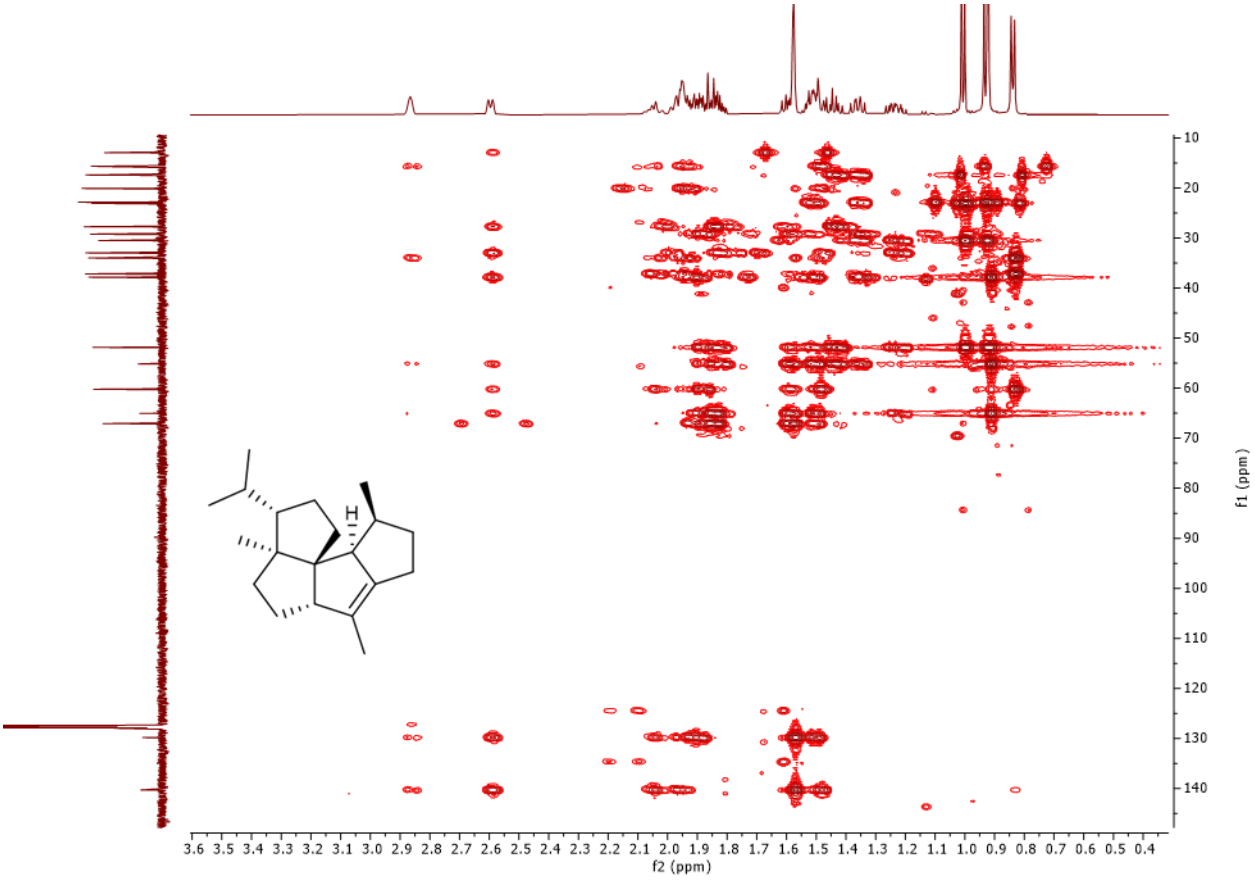

Supplementary Fig. 9. HMBC spectrum of tetraisoquinene **(1)** in C_6D_6.

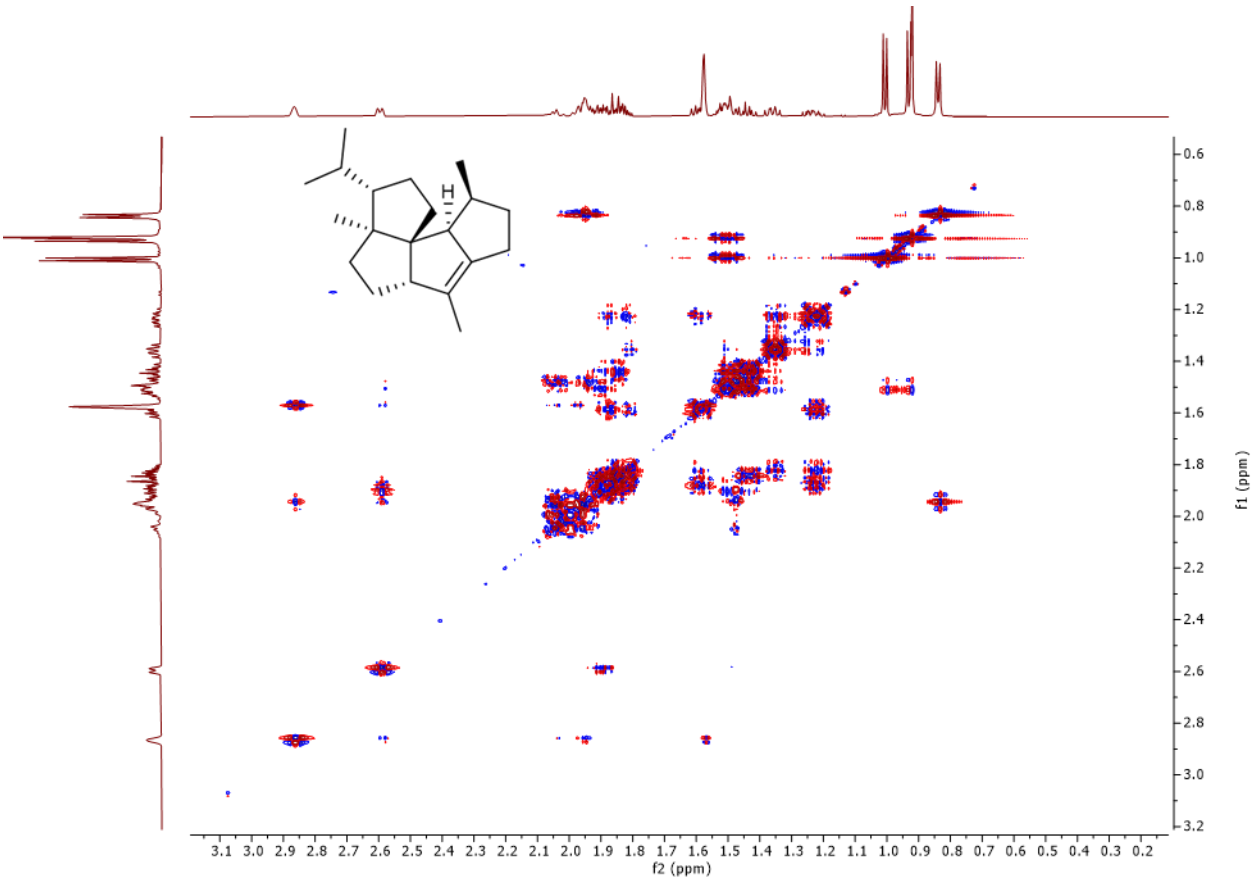

Supplementary Fig. 10. COSY spectrum of tetraisoquinene **(1)** in C_6D_6.

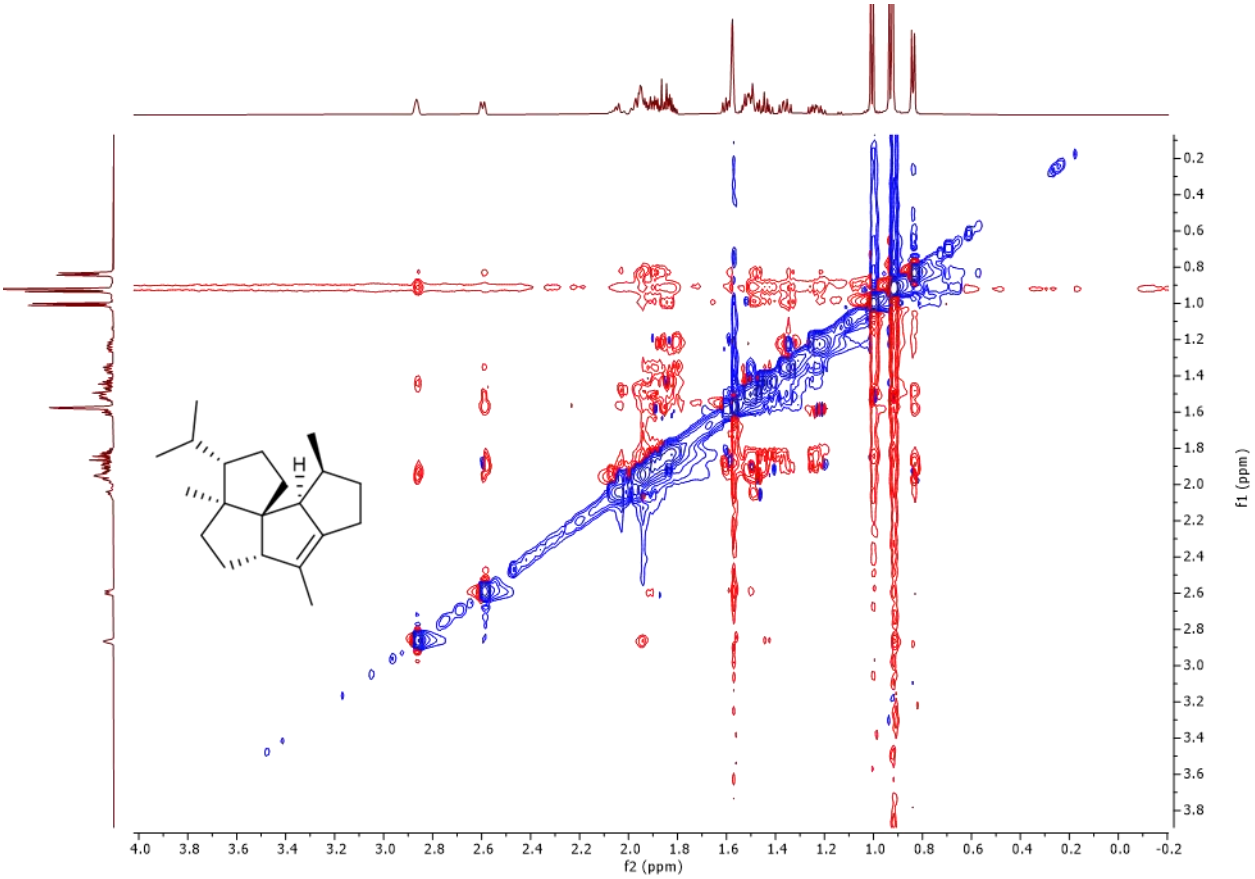

Supplementary Fig. 11. NOESY spectrum of tetraisoquinene **(1)** in C_6D_6.

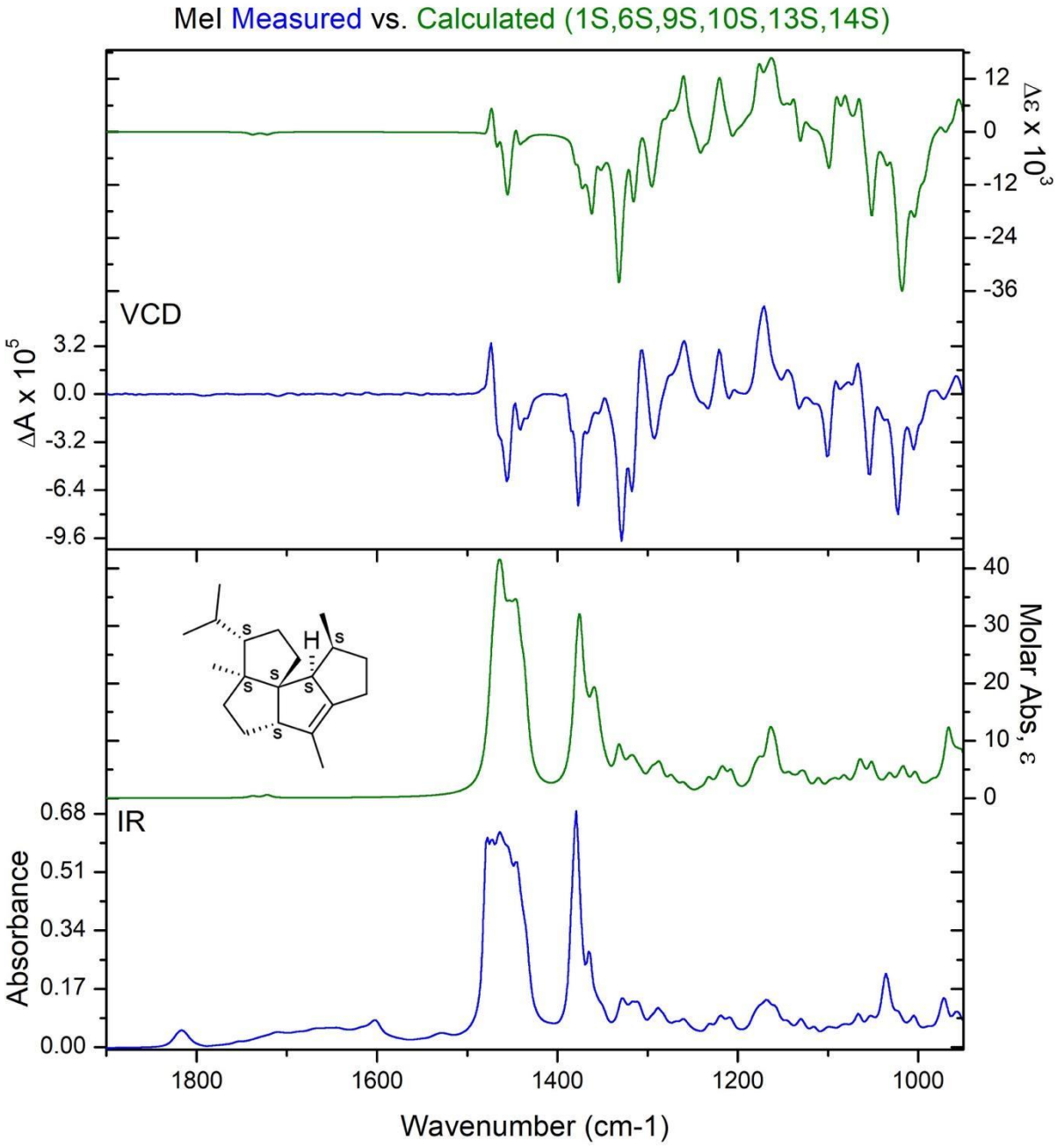

Supplementary Fig. 12. DFT calculated (green) and experimental (blue) VCD and IR spectra of tetraisoquinene **(1)**.

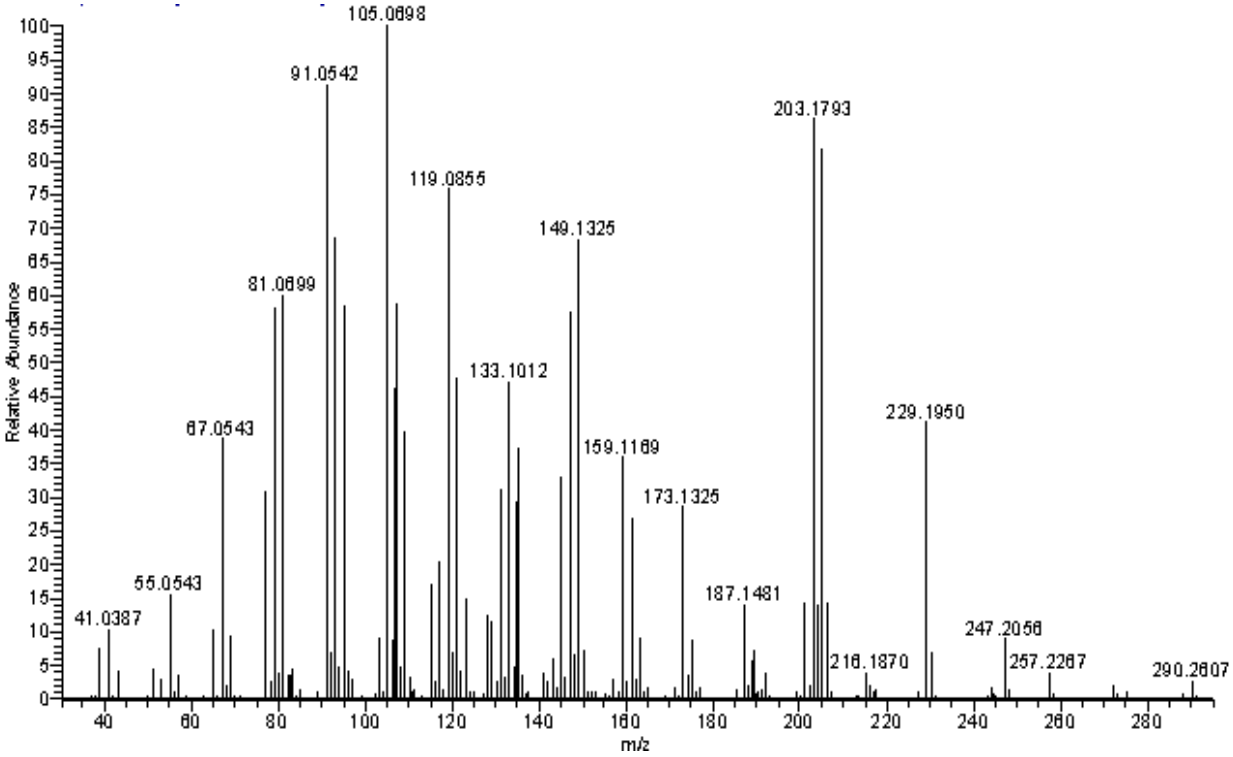

Supplementary Fig. 13. EIMS of salbirenol (**2**).

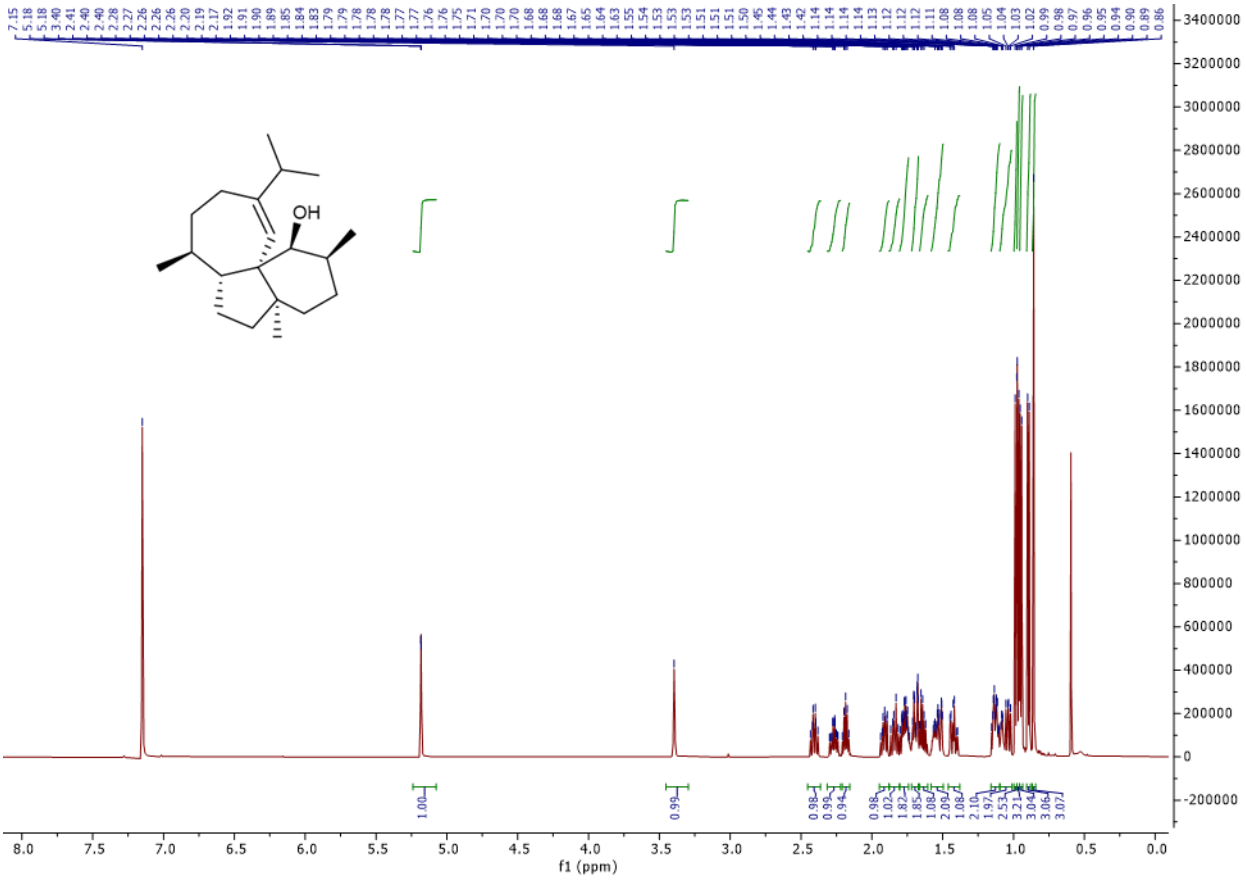

Supplementary Fig. 14. ^{1}H NMR spectrum of salbirenol (**2**) in C_6D_6 (600 MHz).

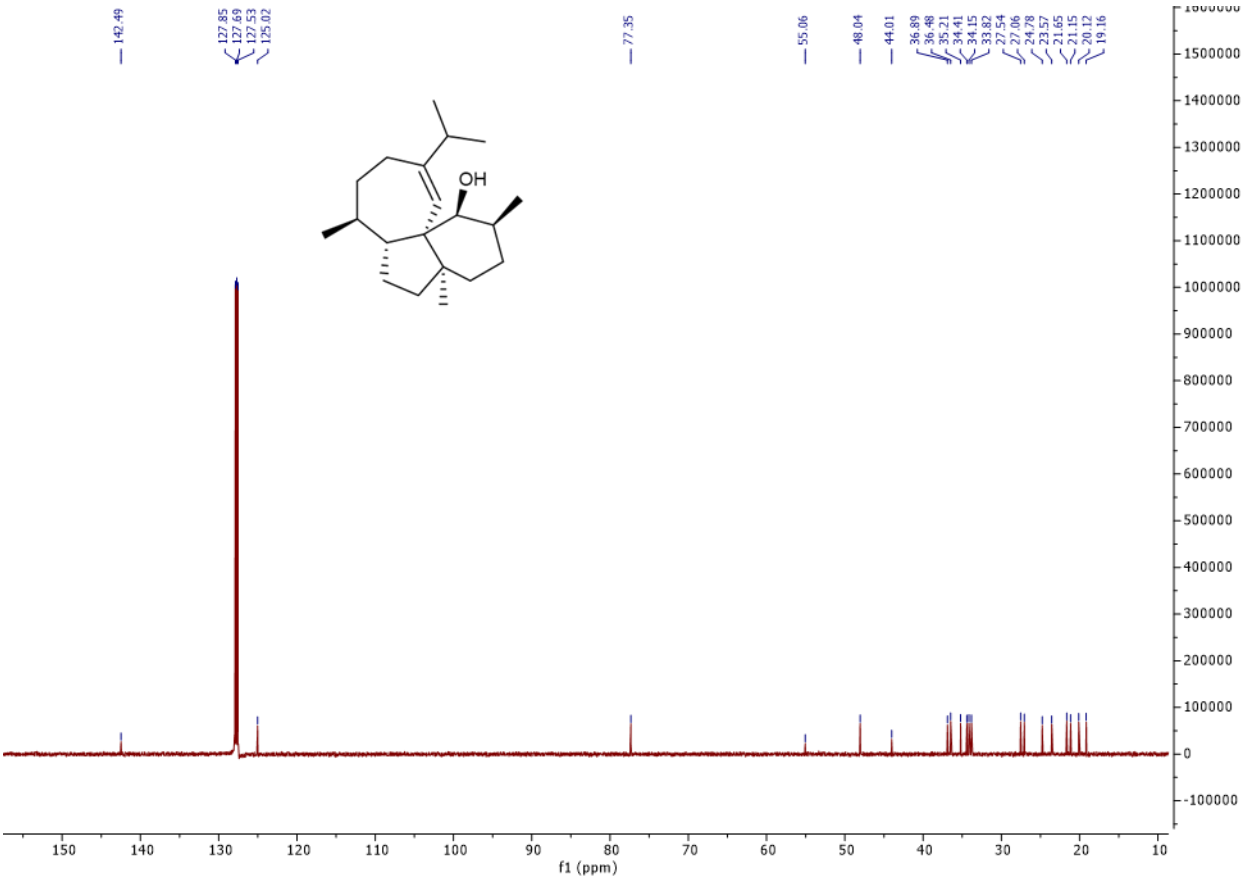

Supplementary Fig. 15. ^{13}C NMR spectrum of salbirenol (**2**) in C_6D_6 (151 MHz).

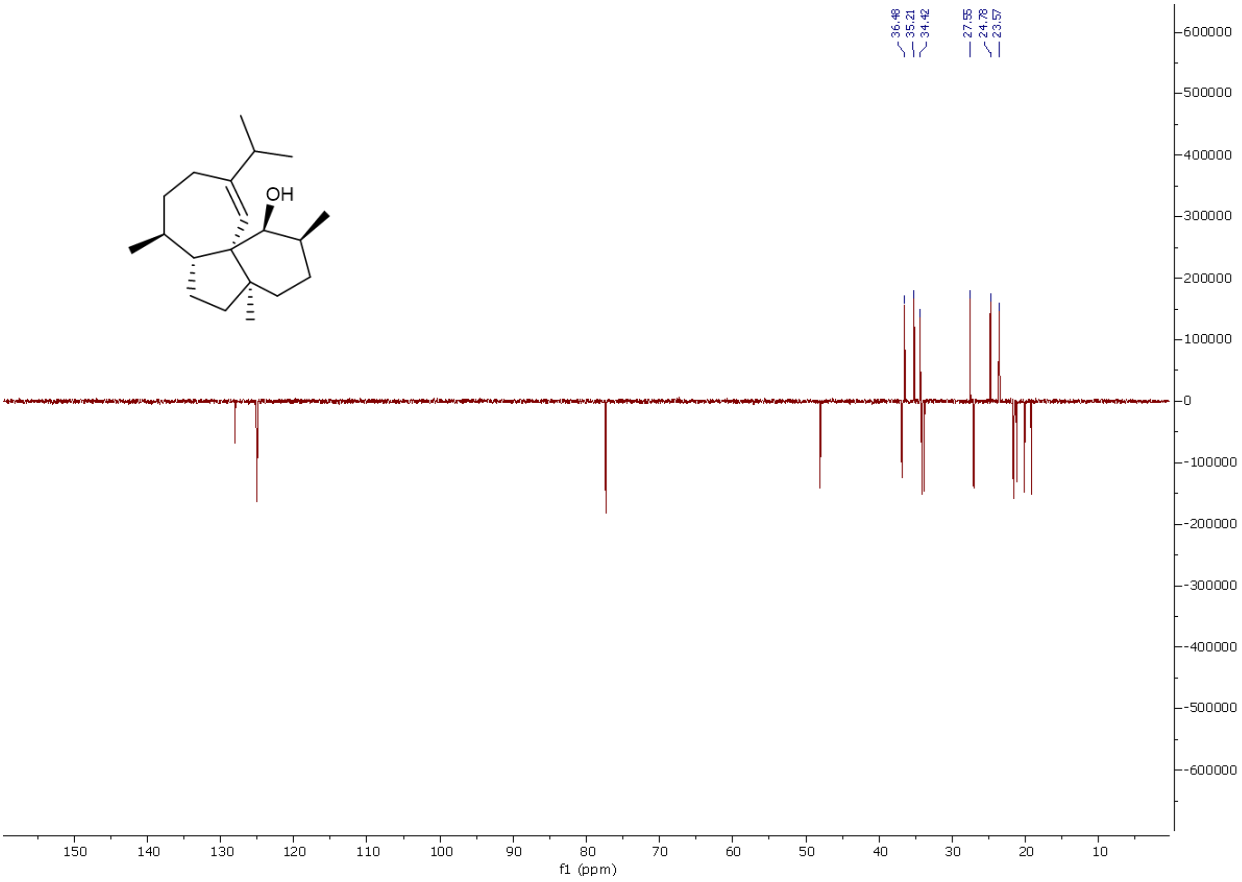

Supplementary Fig. 16. DEPT 135 spectrum of salbirenol (**2**) in C_6D_6 (151 MHz).

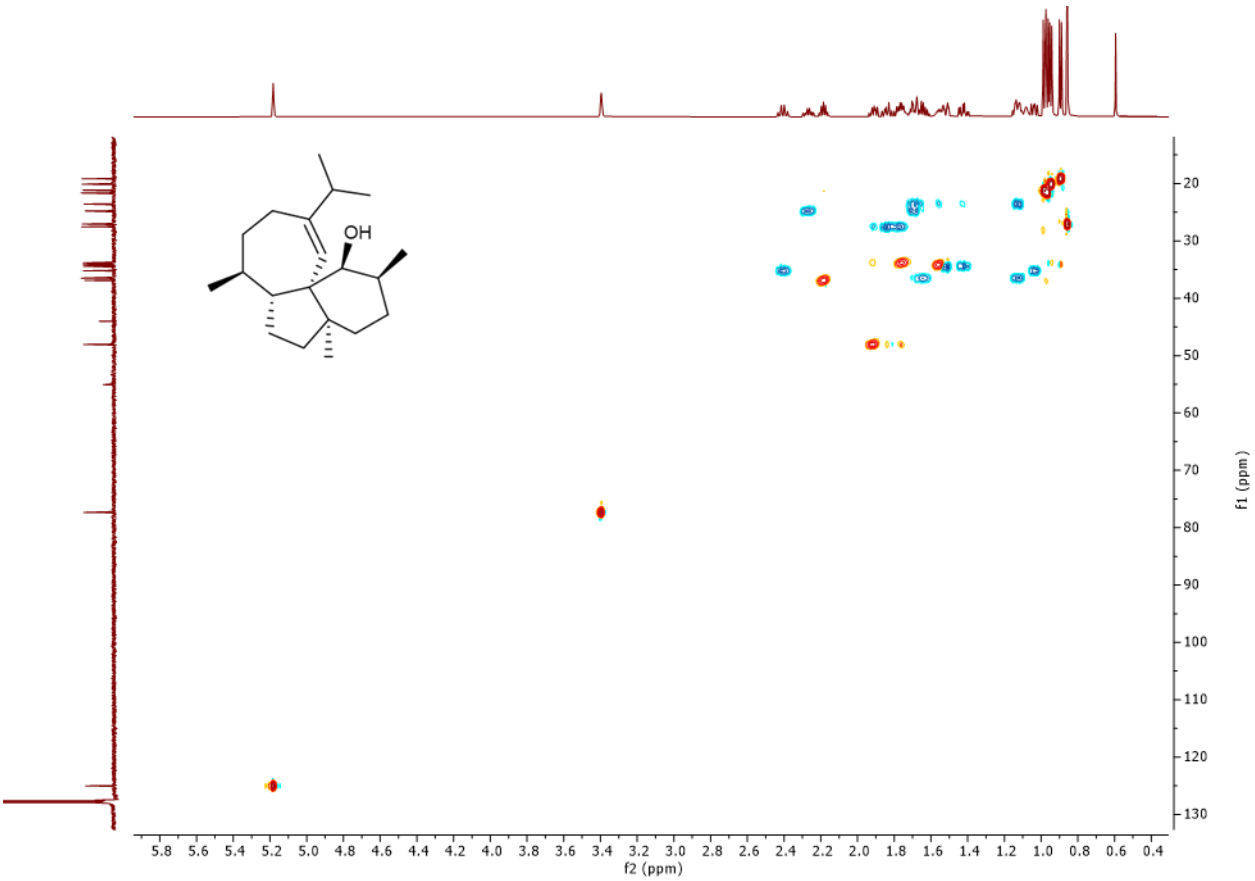

Supplementary Fig. 17. HSQC spectrum of salbirenol (**2**) in C_6D_6.

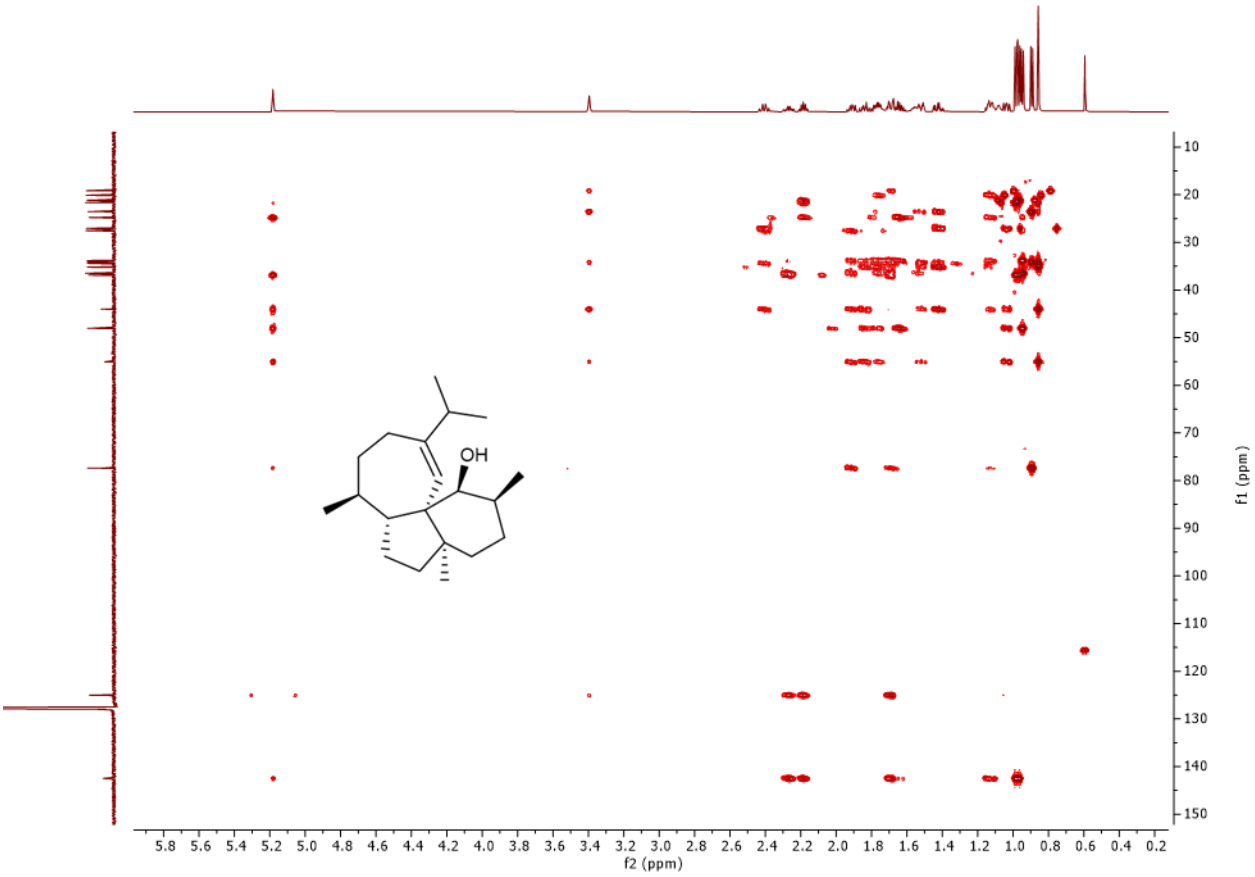

Supplementary Fig. 18. HMBC spectrum of salbirenol (**2**) in C_6D_6.

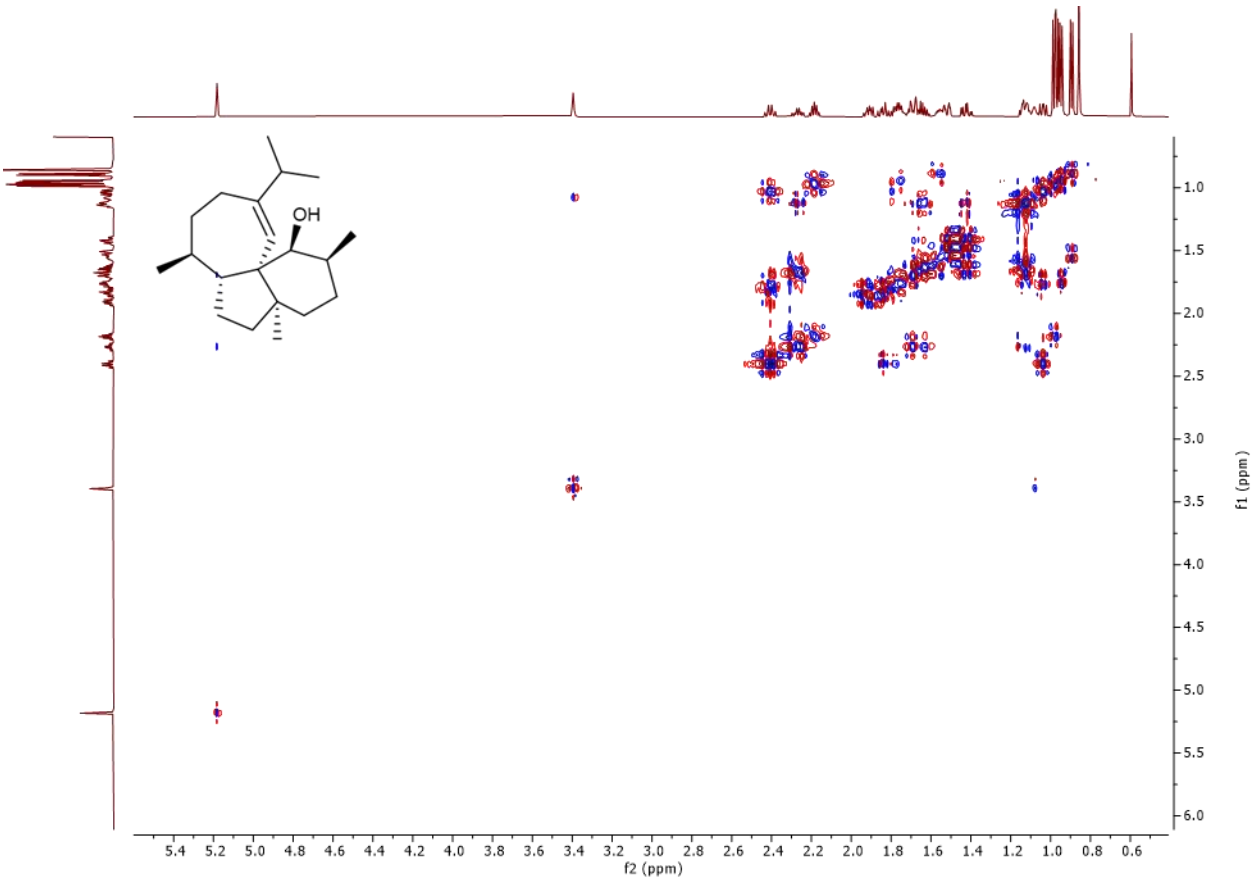

Supplementary Fig. 19. COSY spectrum of salbirenol (**2**) in C_6D_6.

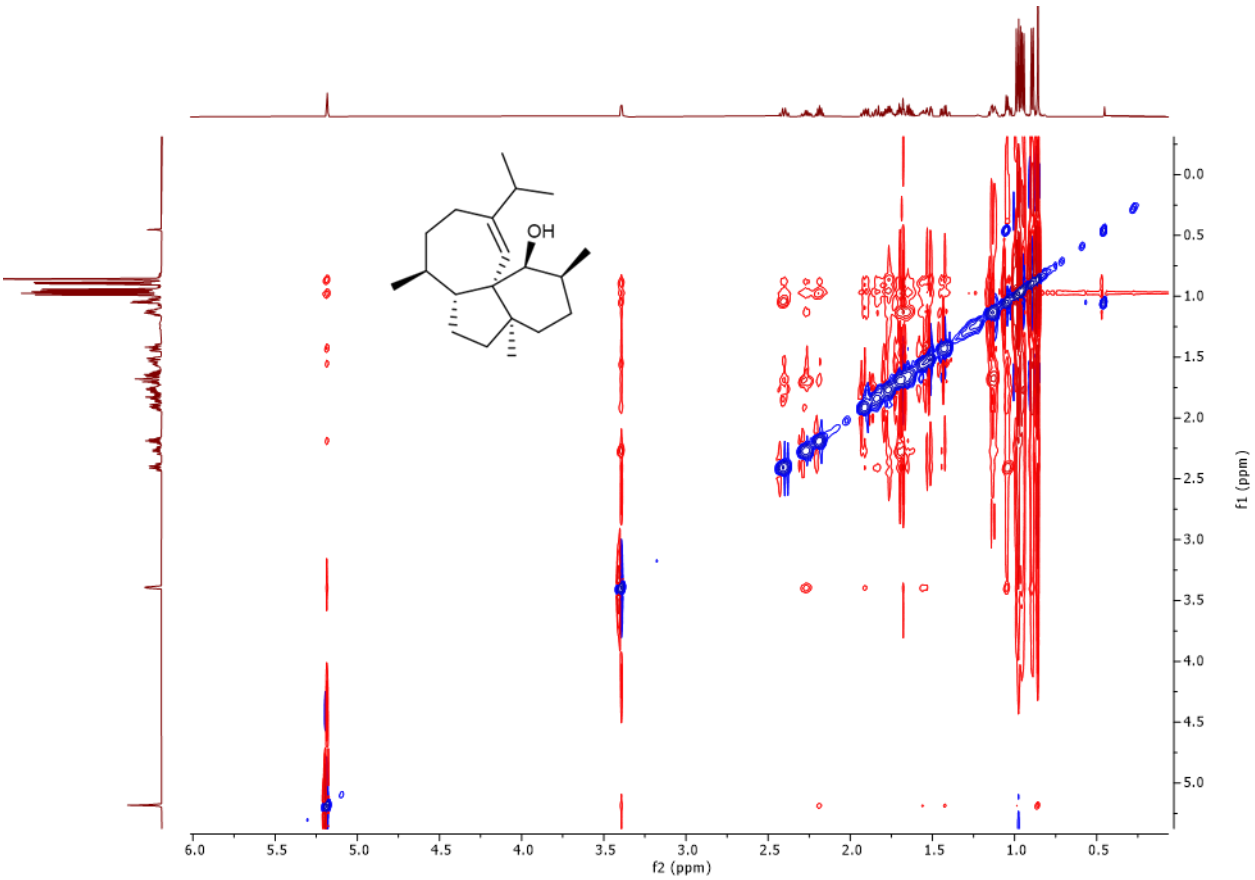

Supplementary Fig. 20. NOESY spectrum of salbirenol (**2**) in C_6D_6.

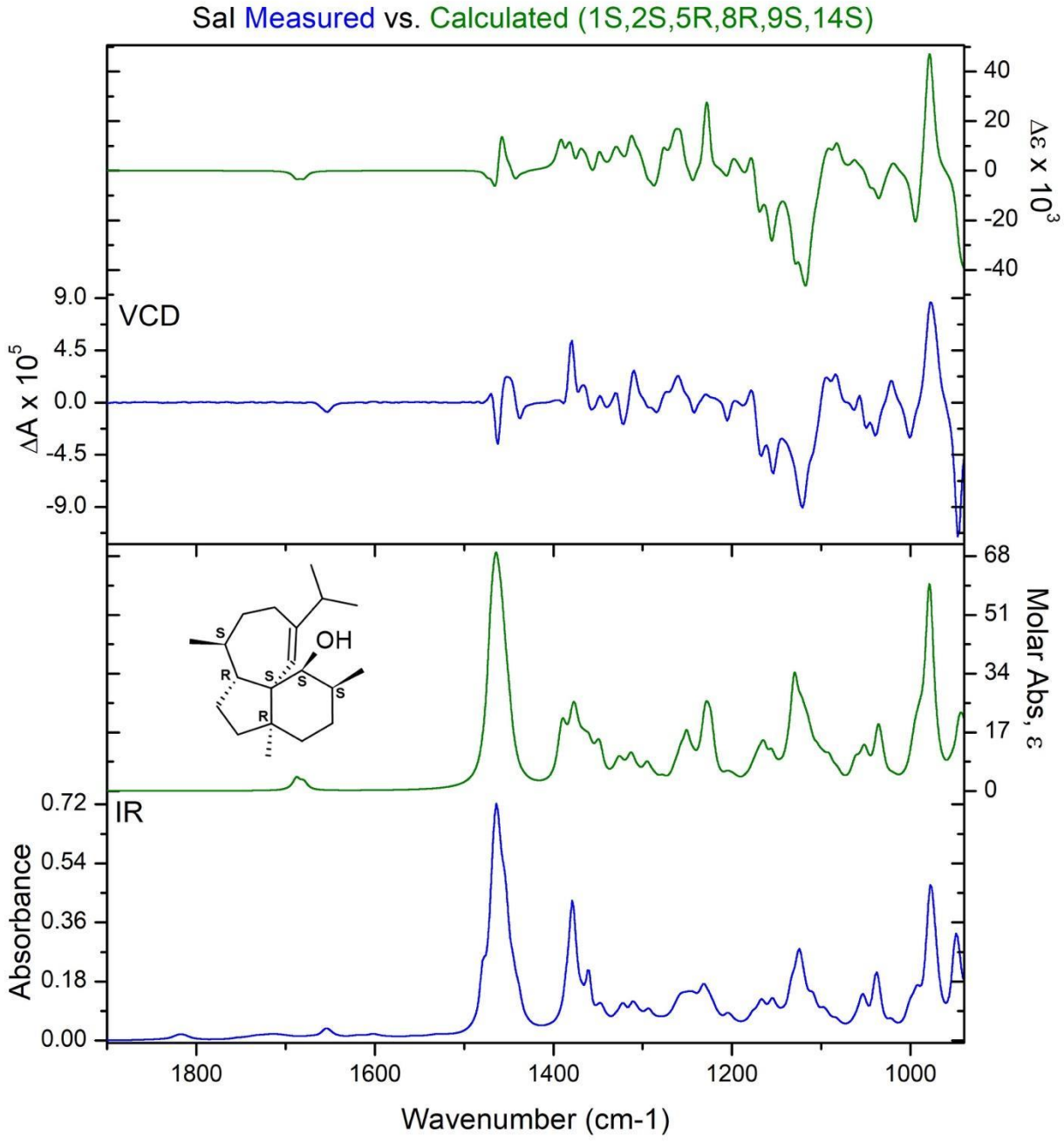

Supplementary Fig. 21. DFT calculated (green) and experimental (blue) VCD and IR spectra of salbirenol **(2)**.

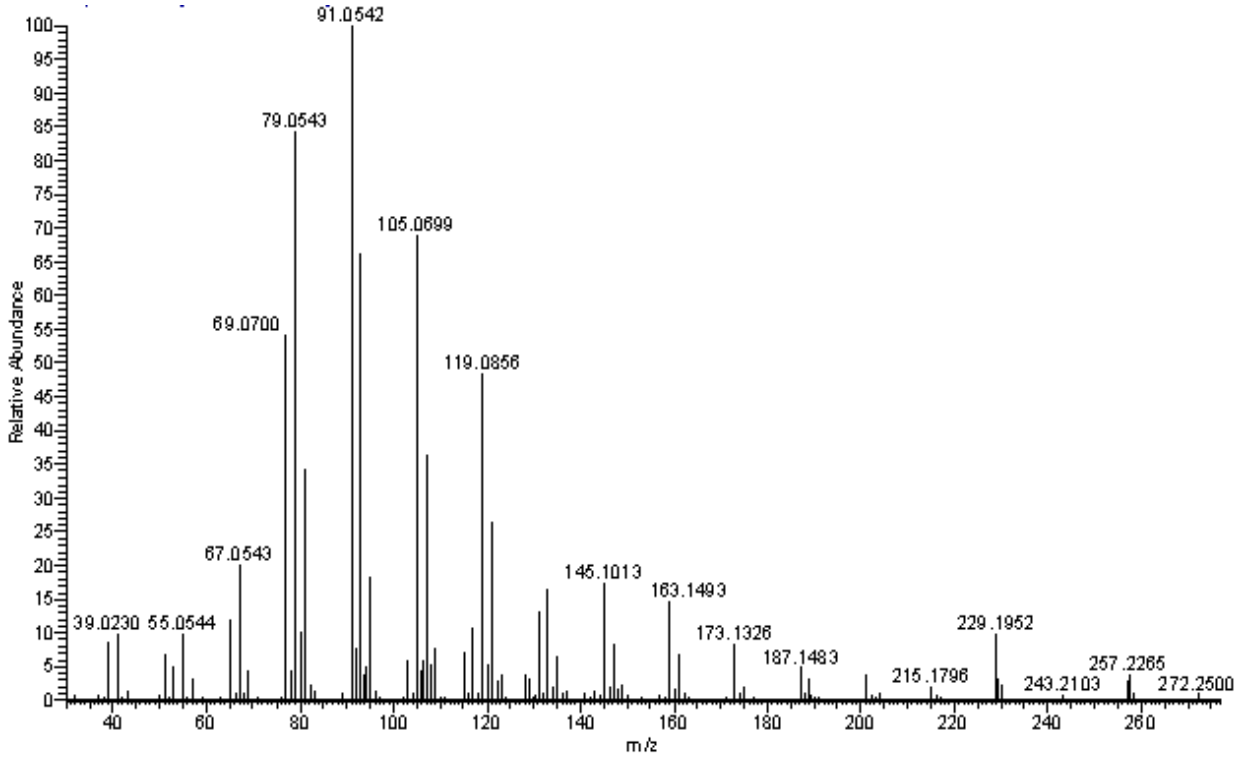

Supplementary Fig. 22. EIMS of chitino-2,5(6),9(10)-triene (**3**).

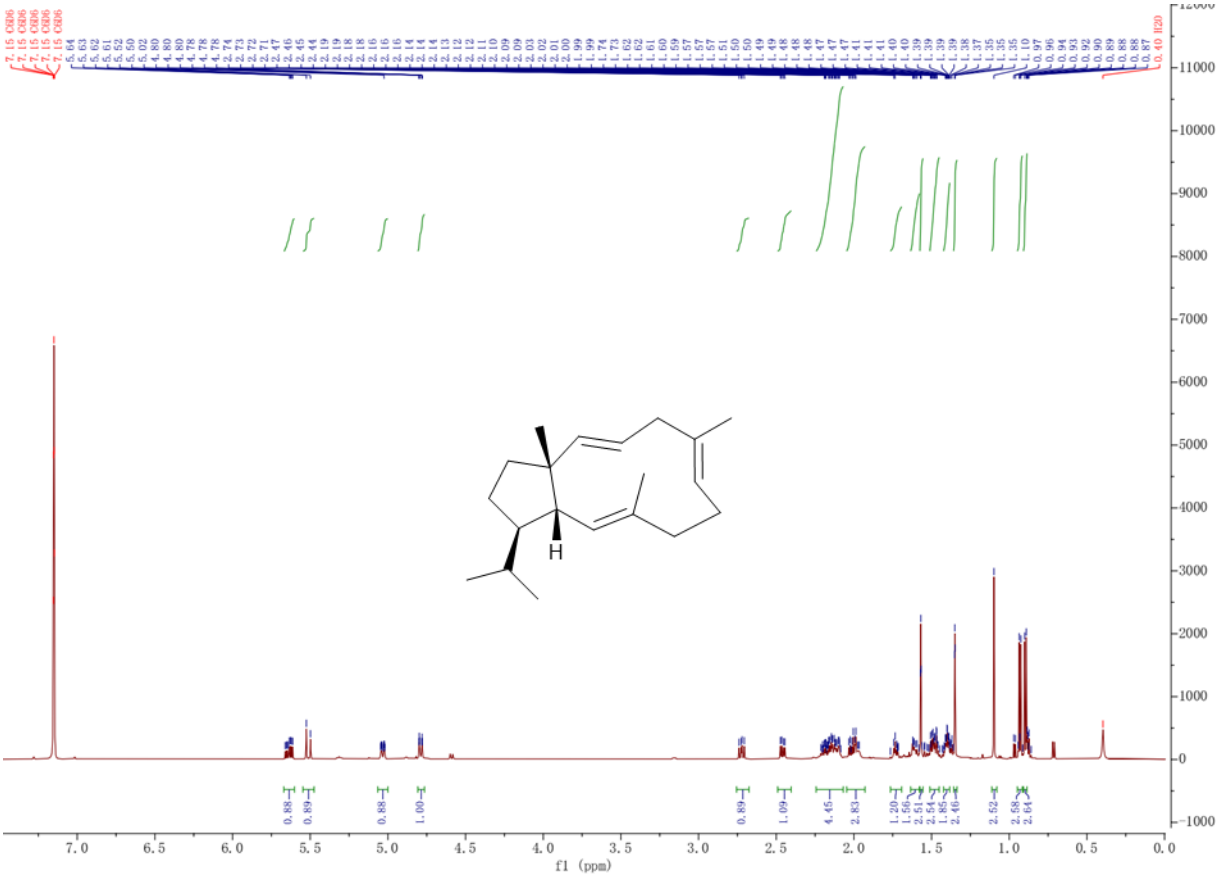

Supplementary Fig. 23. ^{1}H NMR spectrum of chitino-2,5(6),9(10)-triene (**3**) in C_6D_6 (600 MHz).

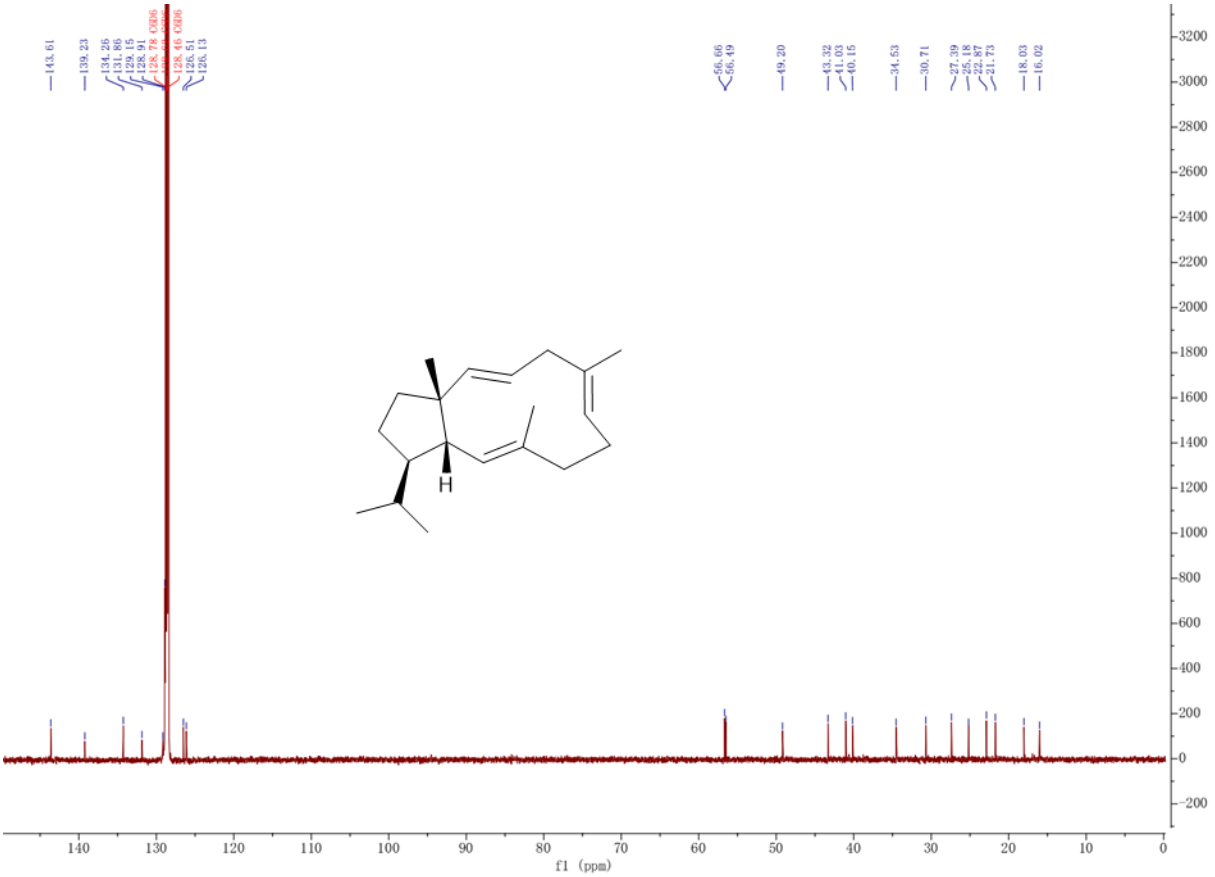

Supplementary Fig. 24. ^{13}C NMR spectrum of chitino-2,5(6),9(10)-triene (**3**) in C_6D_6 (151 MHz).

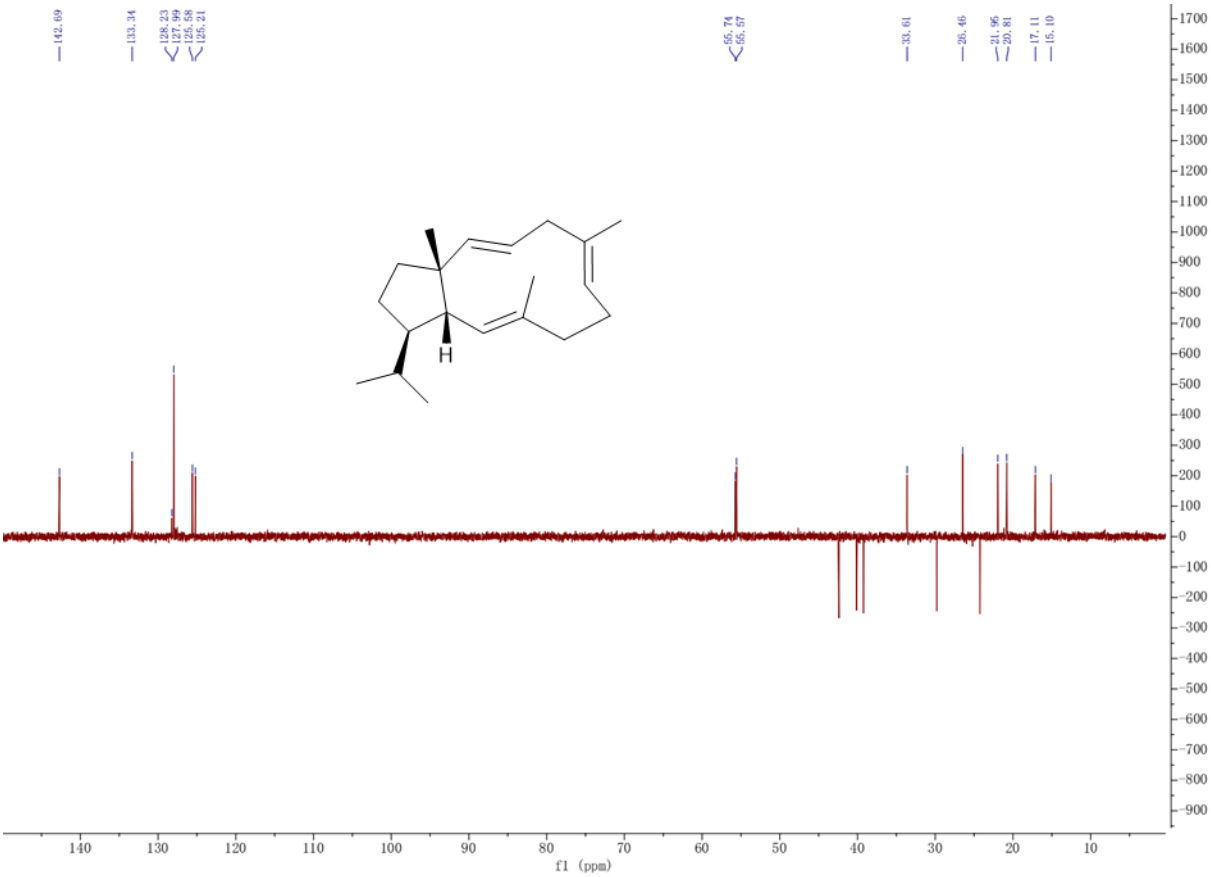

Supplementary Fig. 25. DEPT 135 spectrum of chitino-2,5(6),9(10)-triene (**3**) in C_6D_6 (151 MHz).

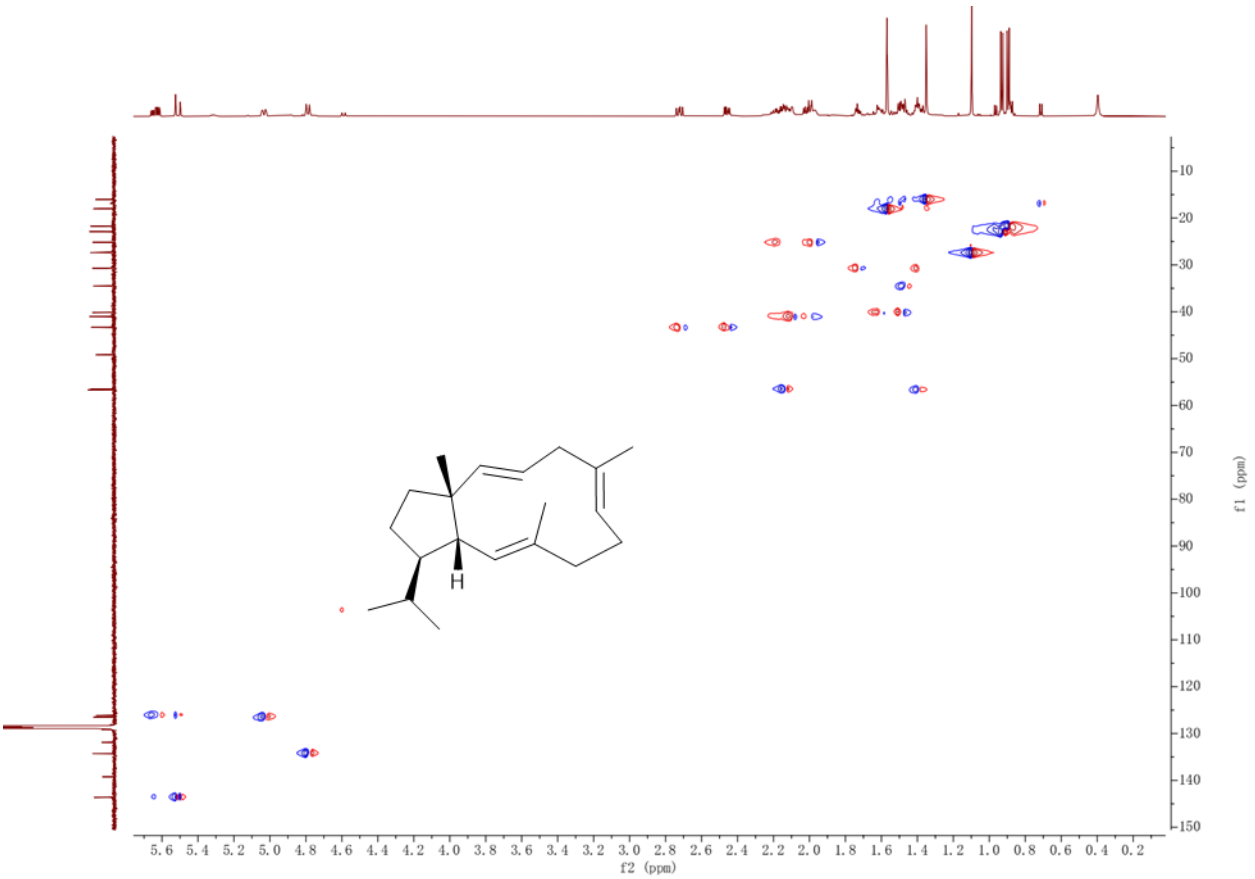

Supplementary Fig. 26. HSQC spectrum of chitino-2,5(6),9(10)-triene (**3**) in C_6D_6.

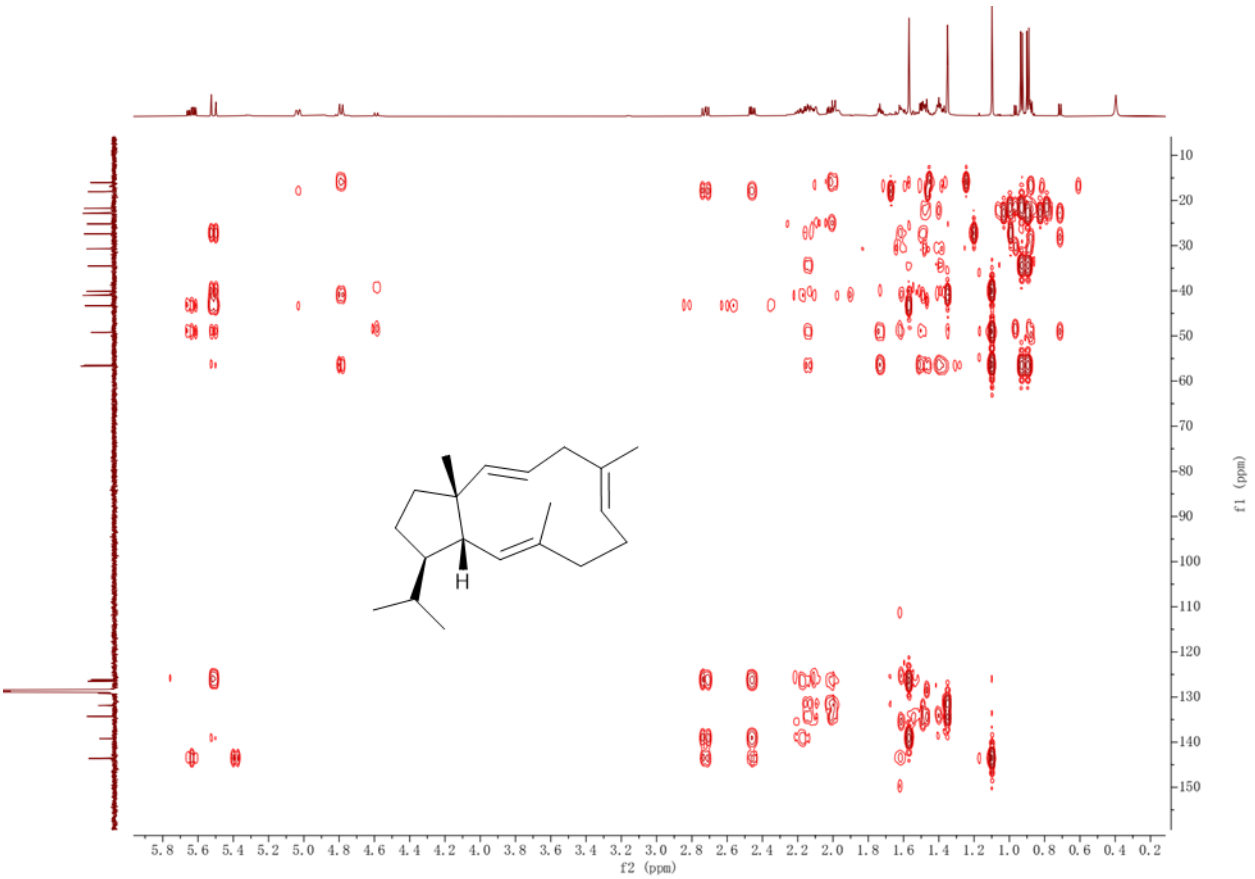

Supplementary Fig. 27. HMBC spectrum of chitino-2,5(6),9(10)-triene (**3**) in C_6D_6.

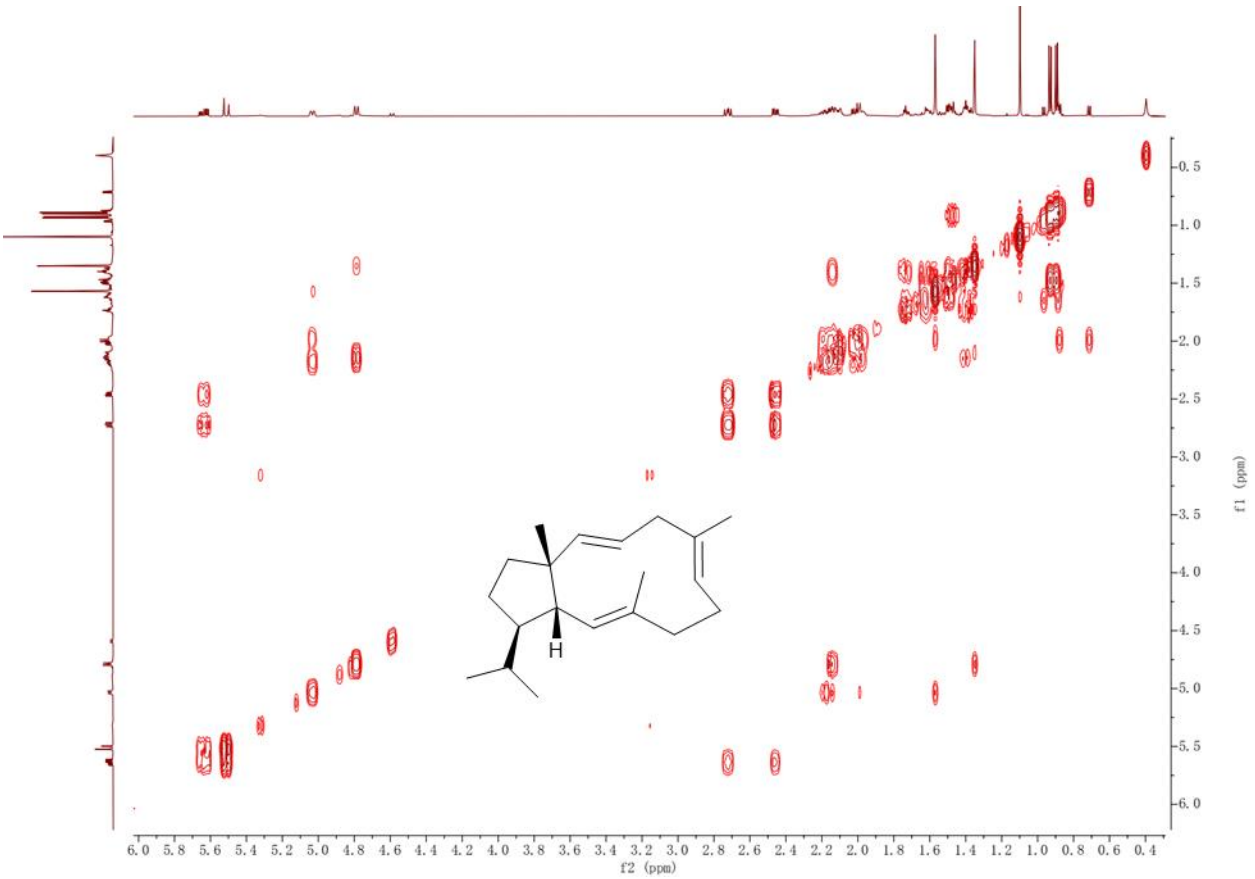

Supplementary Fig. 28. COSY spectrum of chitino-2,5(6),9(10)-triene (**3**) in C_6D_6.

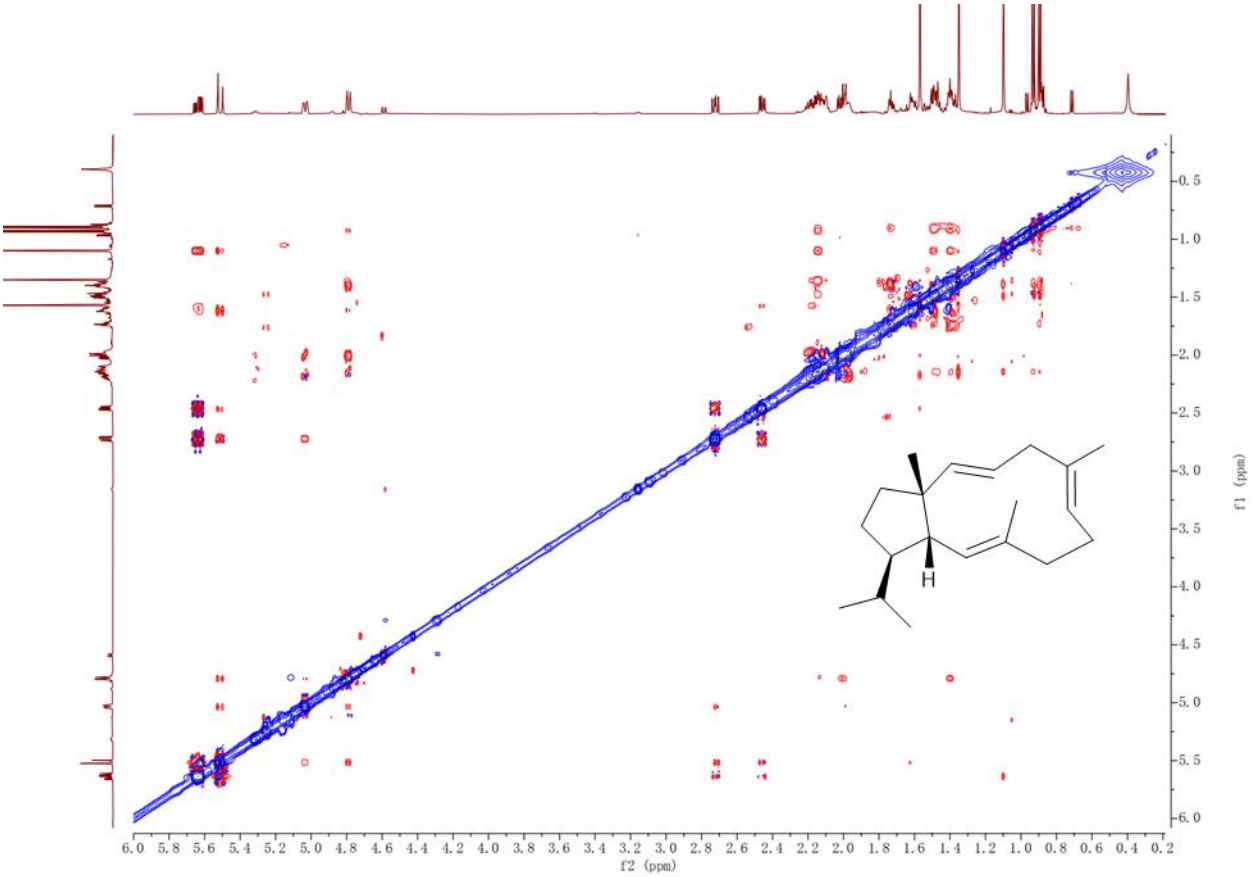

Supplementary Fig. 29. NOESY spectrum of chitino-2,5(6),9(10)-triene (**3**) in C_6D_6.

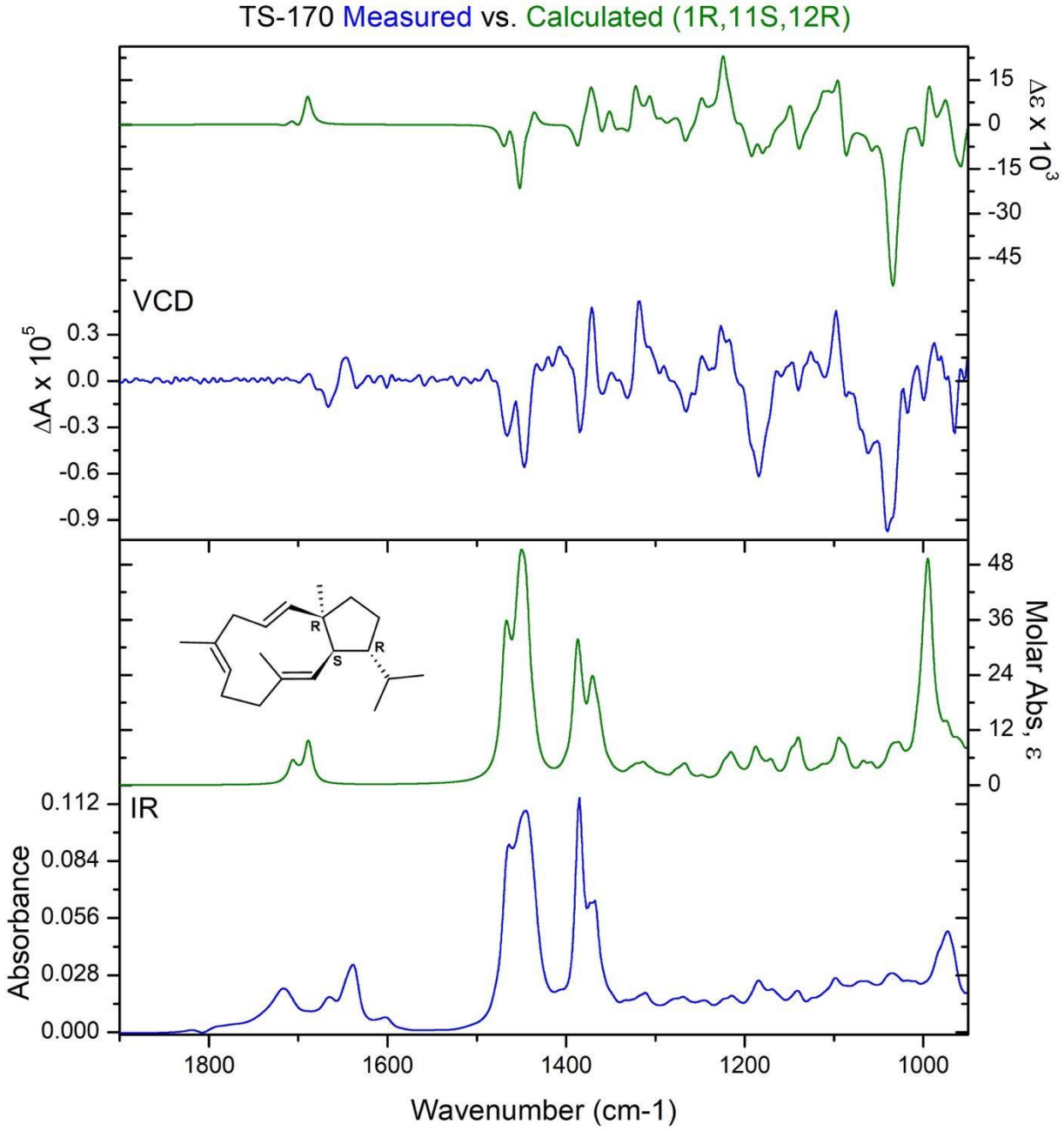

Supplementary Fig. 30. DFT calculated (green) and experimental (blue) VCD and IR spectra of chitino-2,5(6),9(10)-triene (**3**) supporting the absolute configuration as 1*R*,11*S*,12*R*.

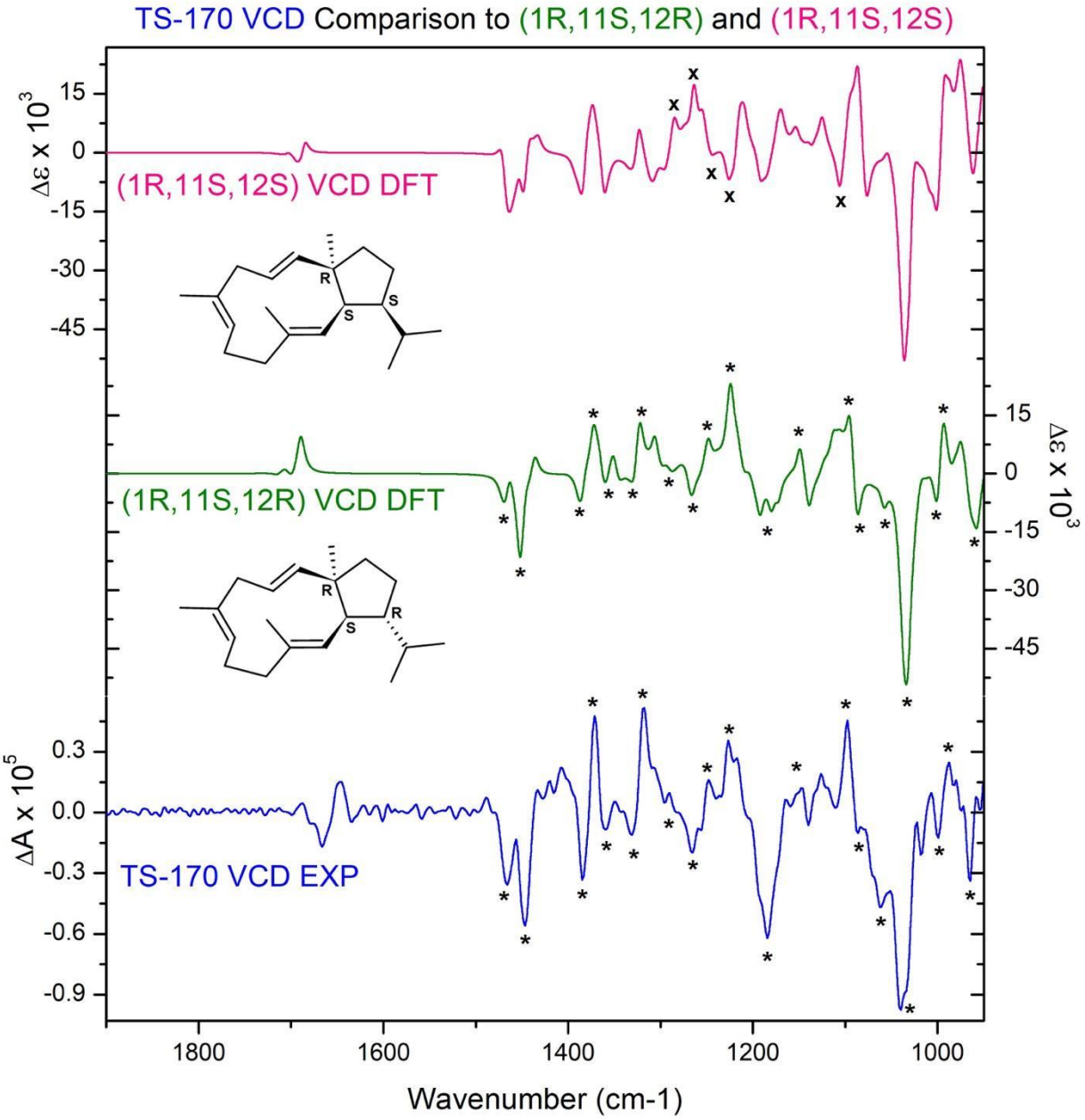

Supplementary Fig. 31. DFT calculated (pink and green) and experimental (blue) VCD and IR spectra of chitino-2,5(6),9(10)-triene (**3**) supporting the absolute configuration as 1*R*,11*S*,12*R*.

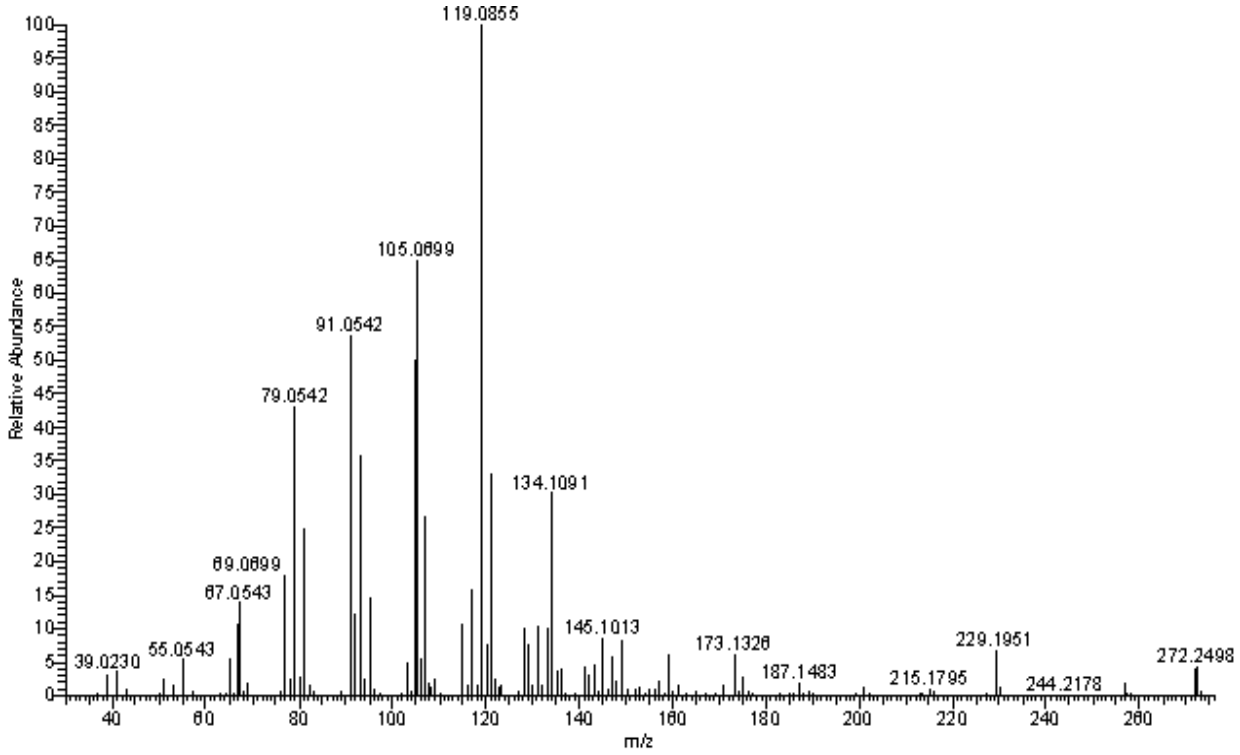

Supplementary Fig. 32. EIMS of peysonnosene (**4**).

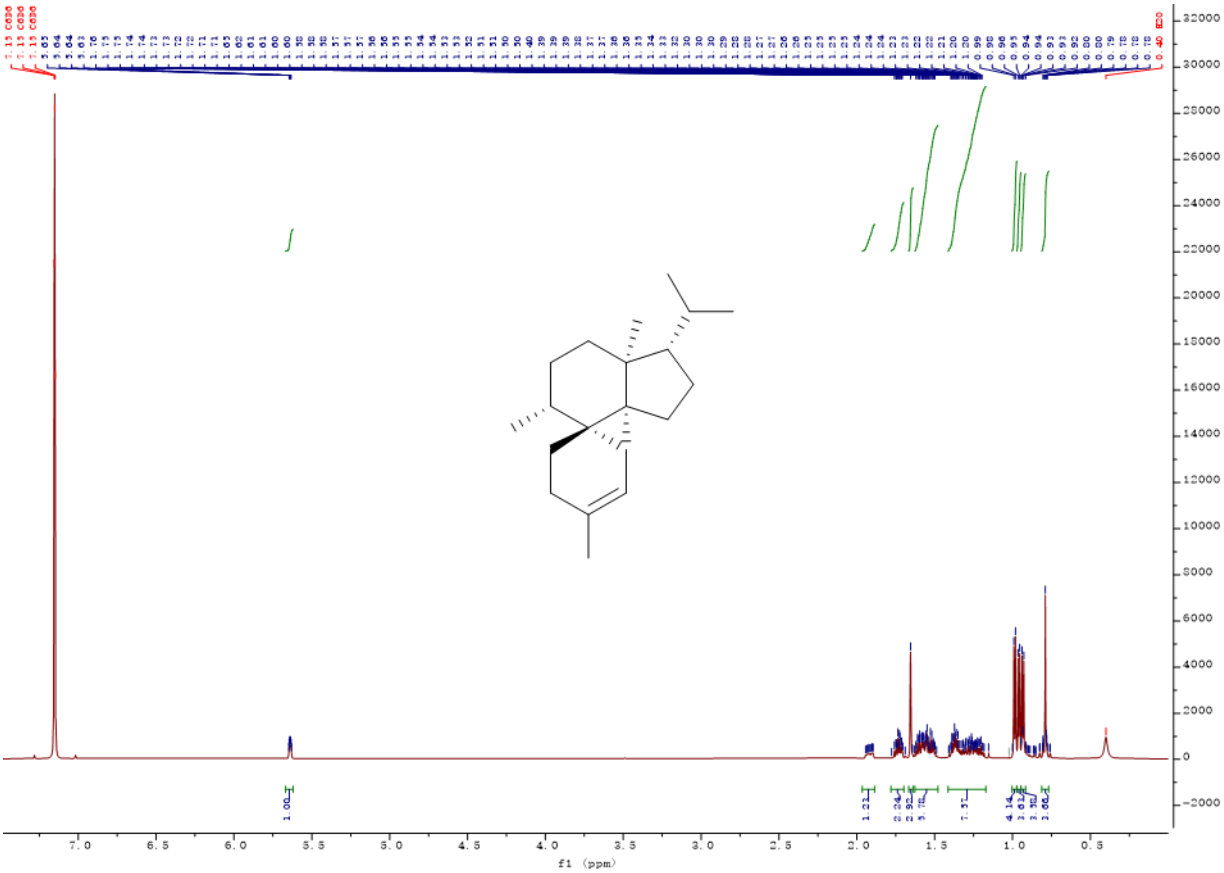

Supplementary Fig. 33. ^{1}H NMR spectrum of peysonnosene (**4**) in C_6D_6 (600 MHz).

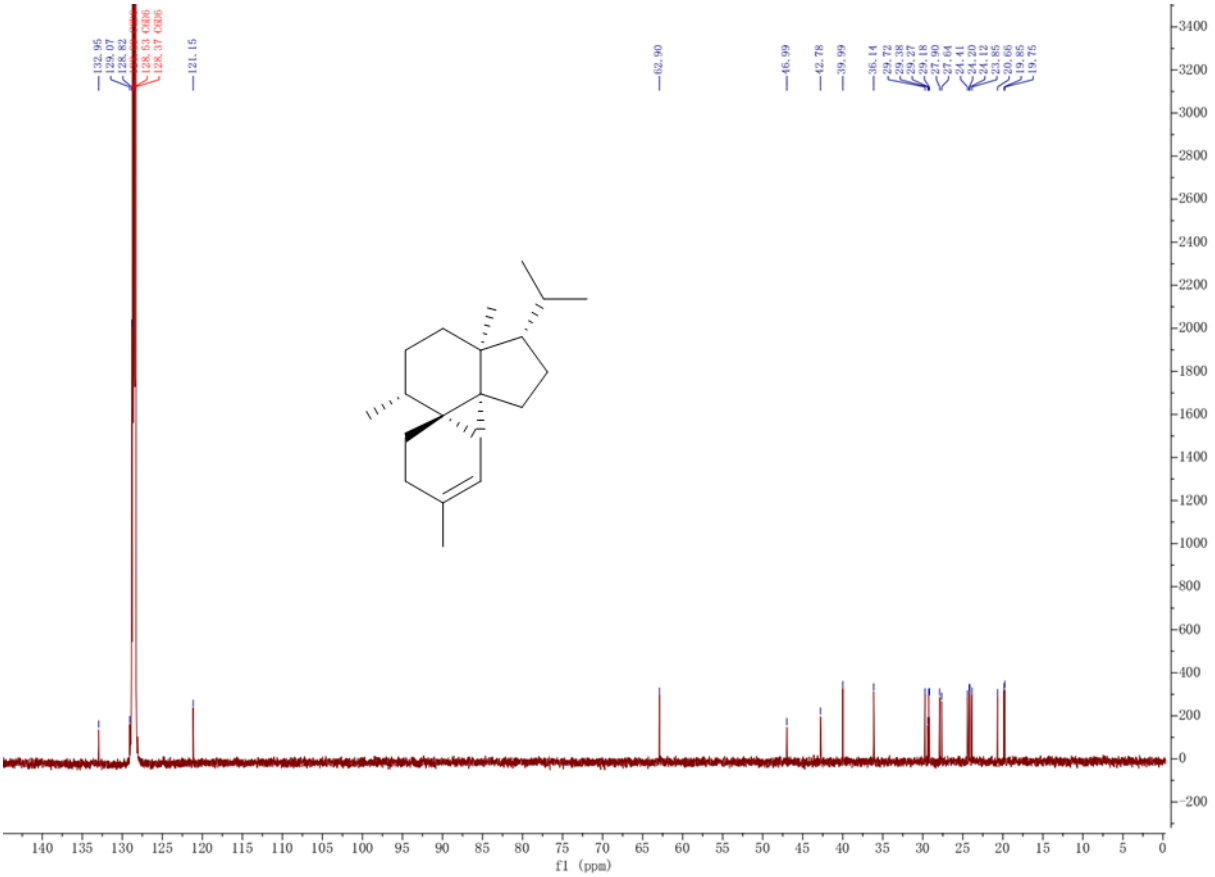

Supplementary Fig. 34. ^{13}C NMR spectrum of peysonnosene (**4**) in C_6D_6 (151 MHz).

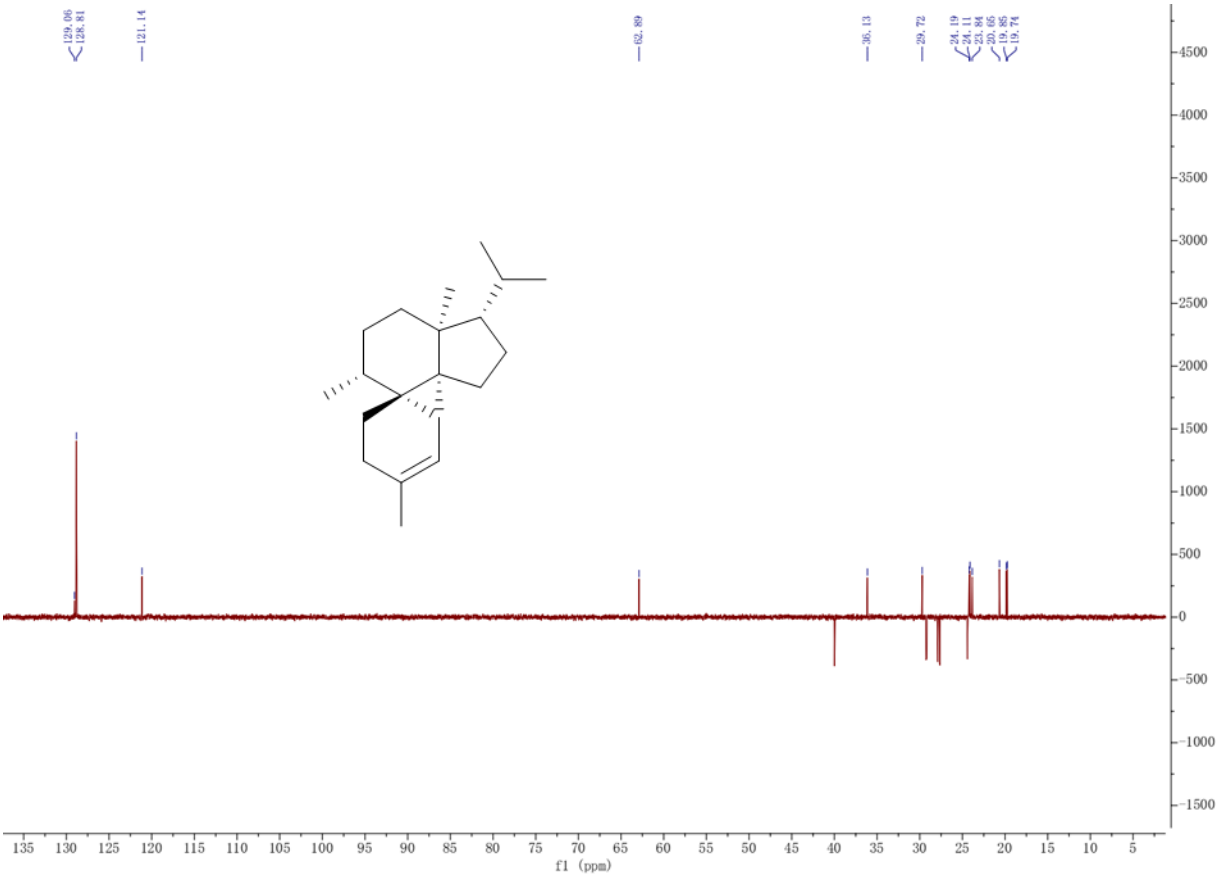

Supplementary Fig. 35. DEPT 135 spectrum peysonnosene (**4**) in C_6D_6.

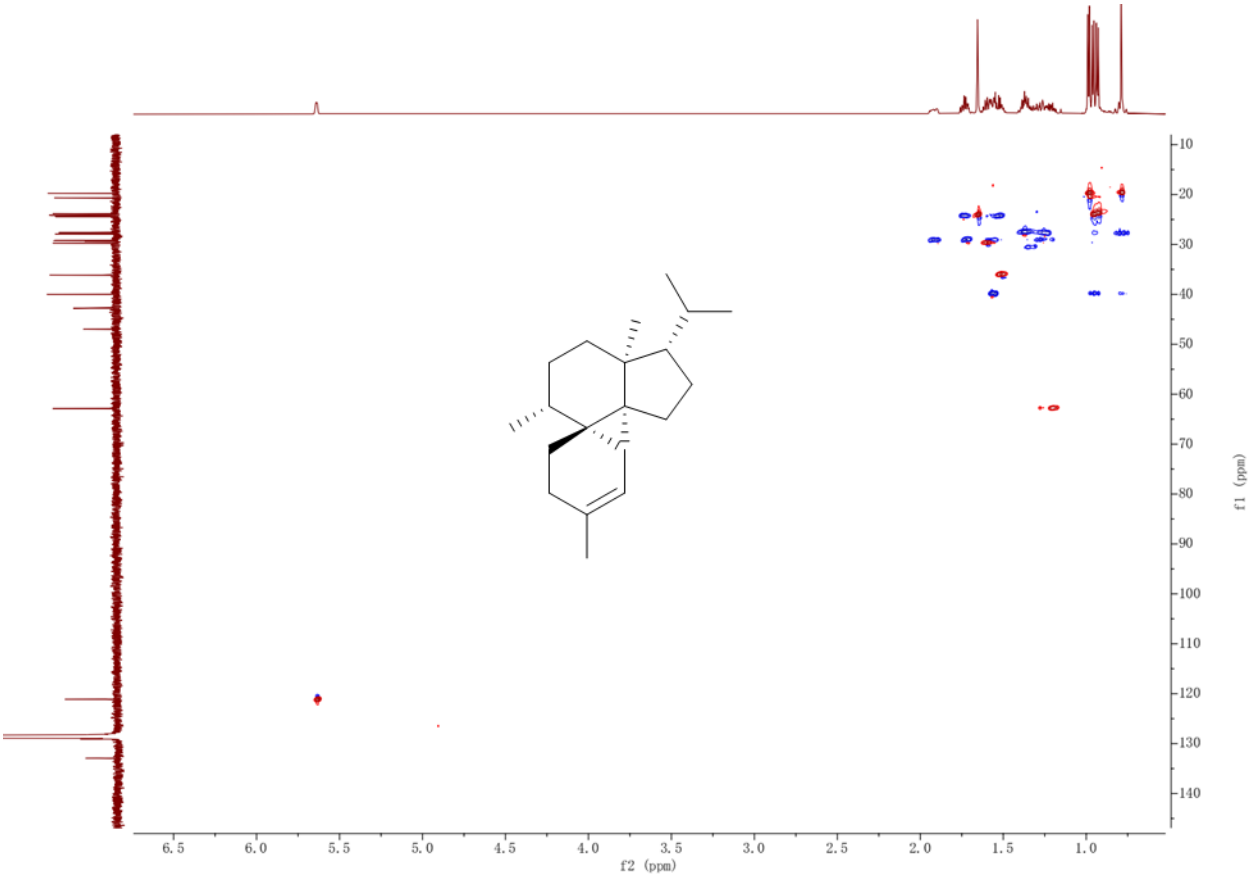

Supplementary Fig. 36. HSQC spectrum of peysonnosene (**4**) in C_6D_6.

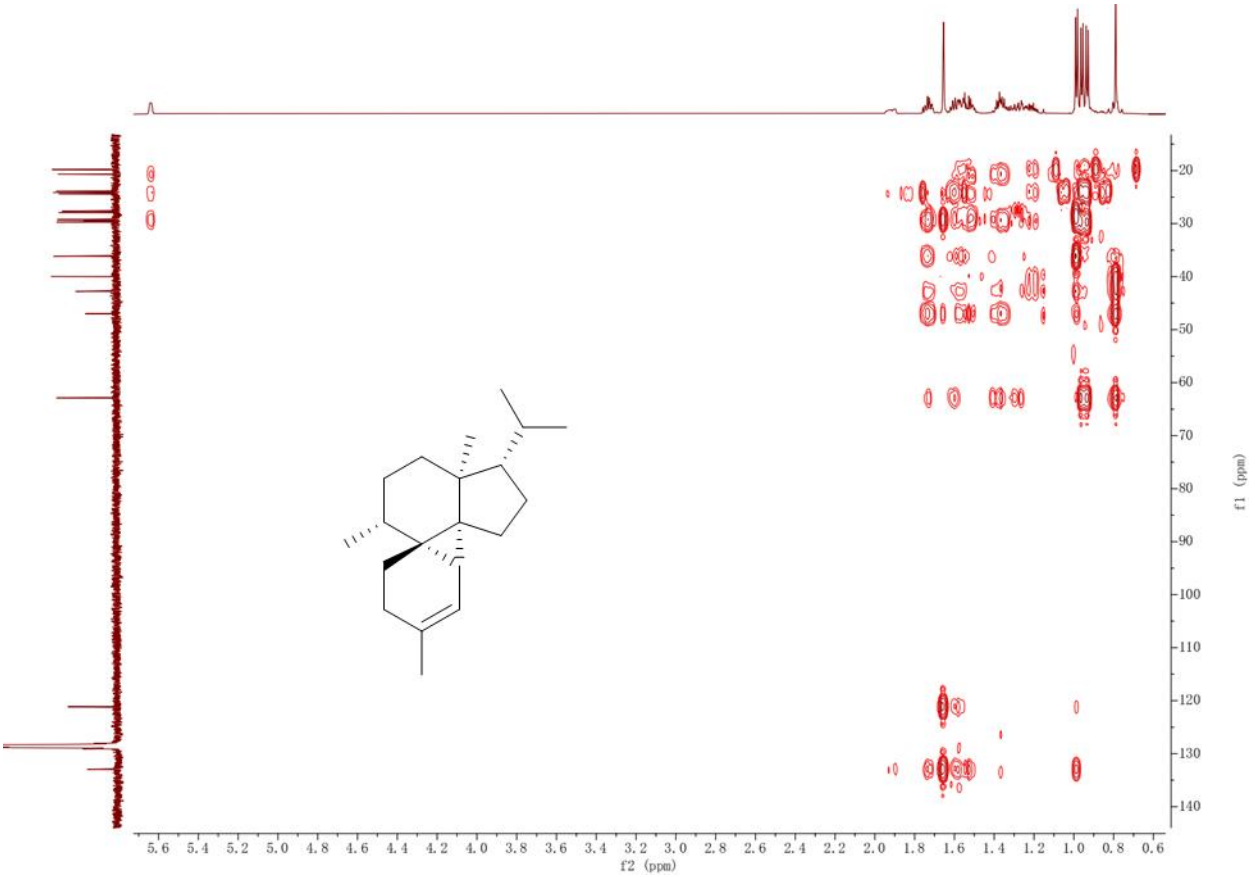

Supplementary Fig. 37. HMBC spectrum of peysonnosene (**4**) in C_6D_6.

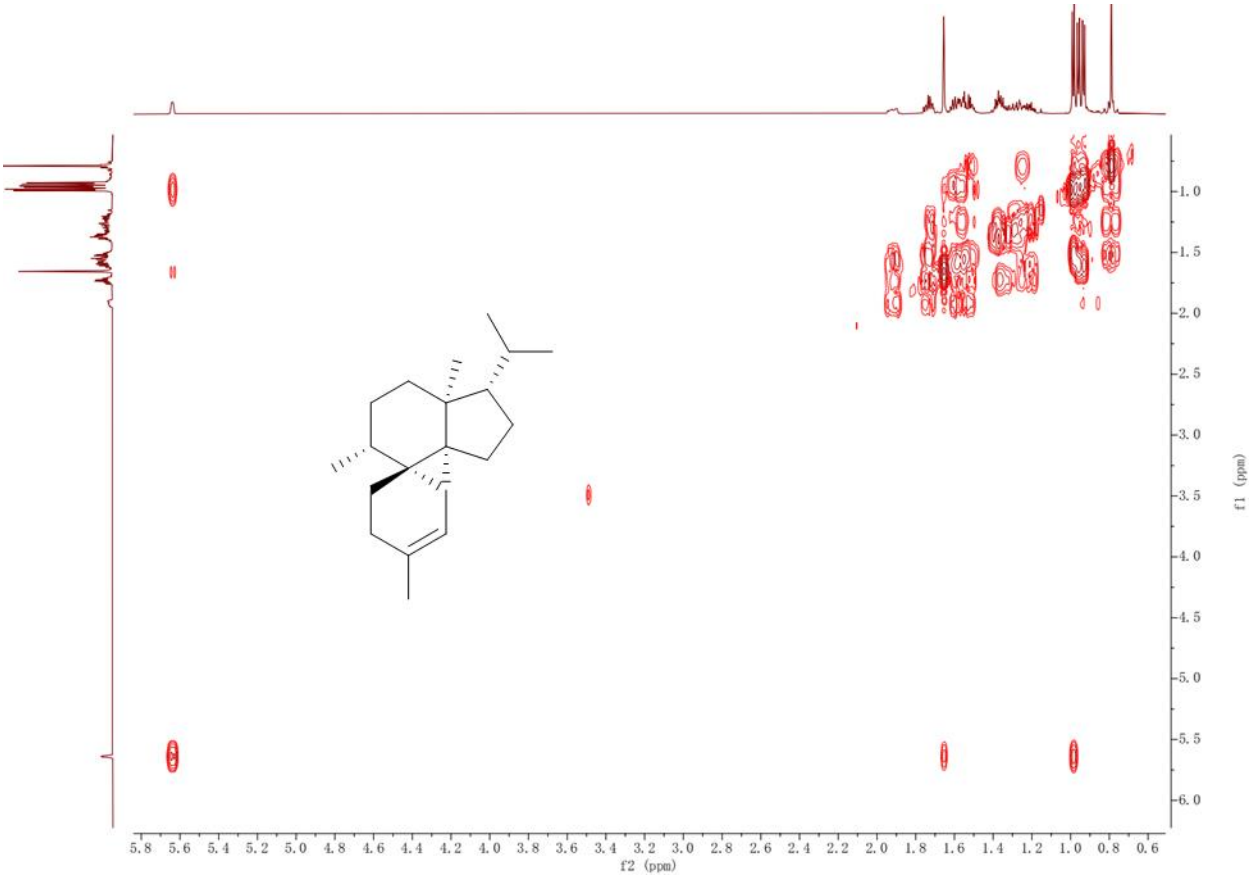

Supplementary Fig. 38. COSY spectrum of peysonnosene (**4**) in C_6D_6.

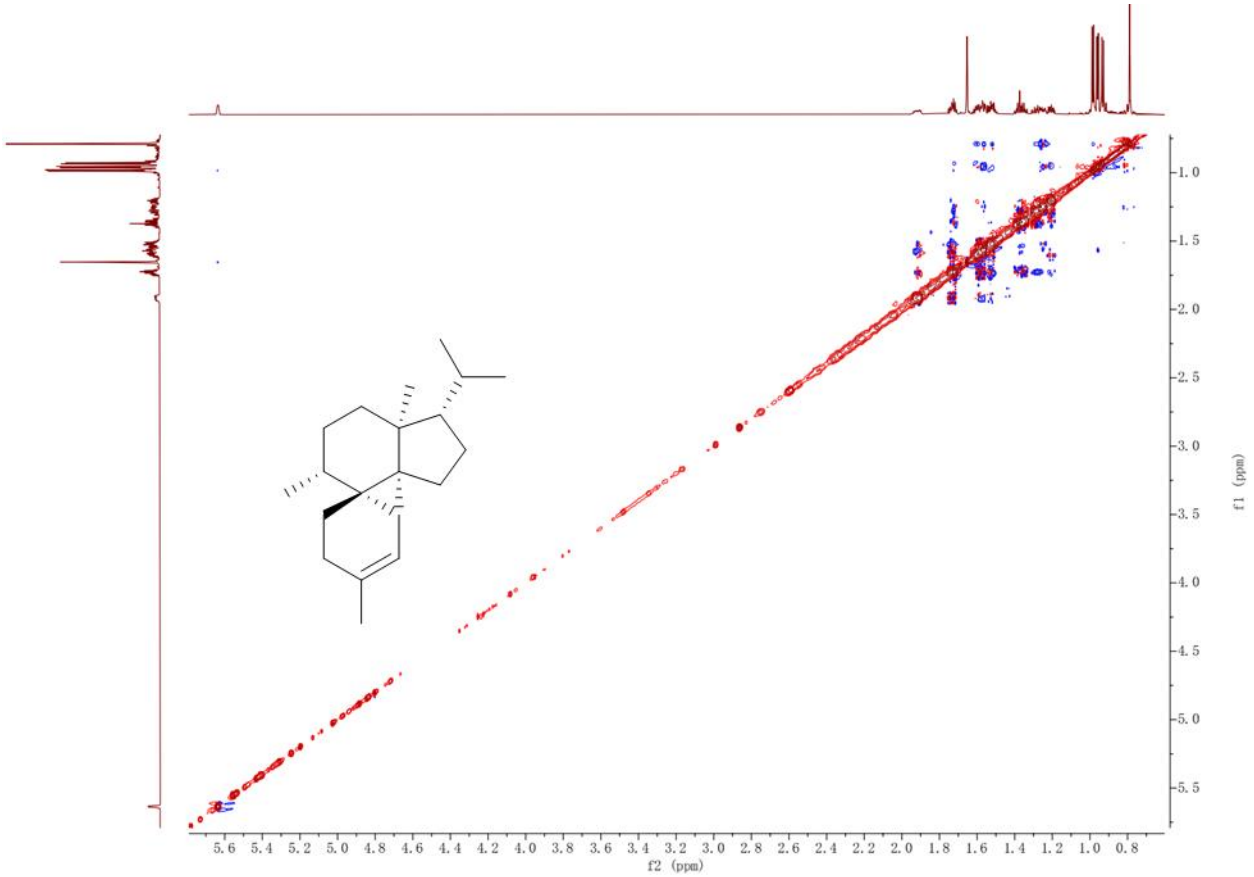

Supplementary Fig. 39. NOESY spectrum of peysonnosene (**4**) in C_6D_6 (800 MHz).

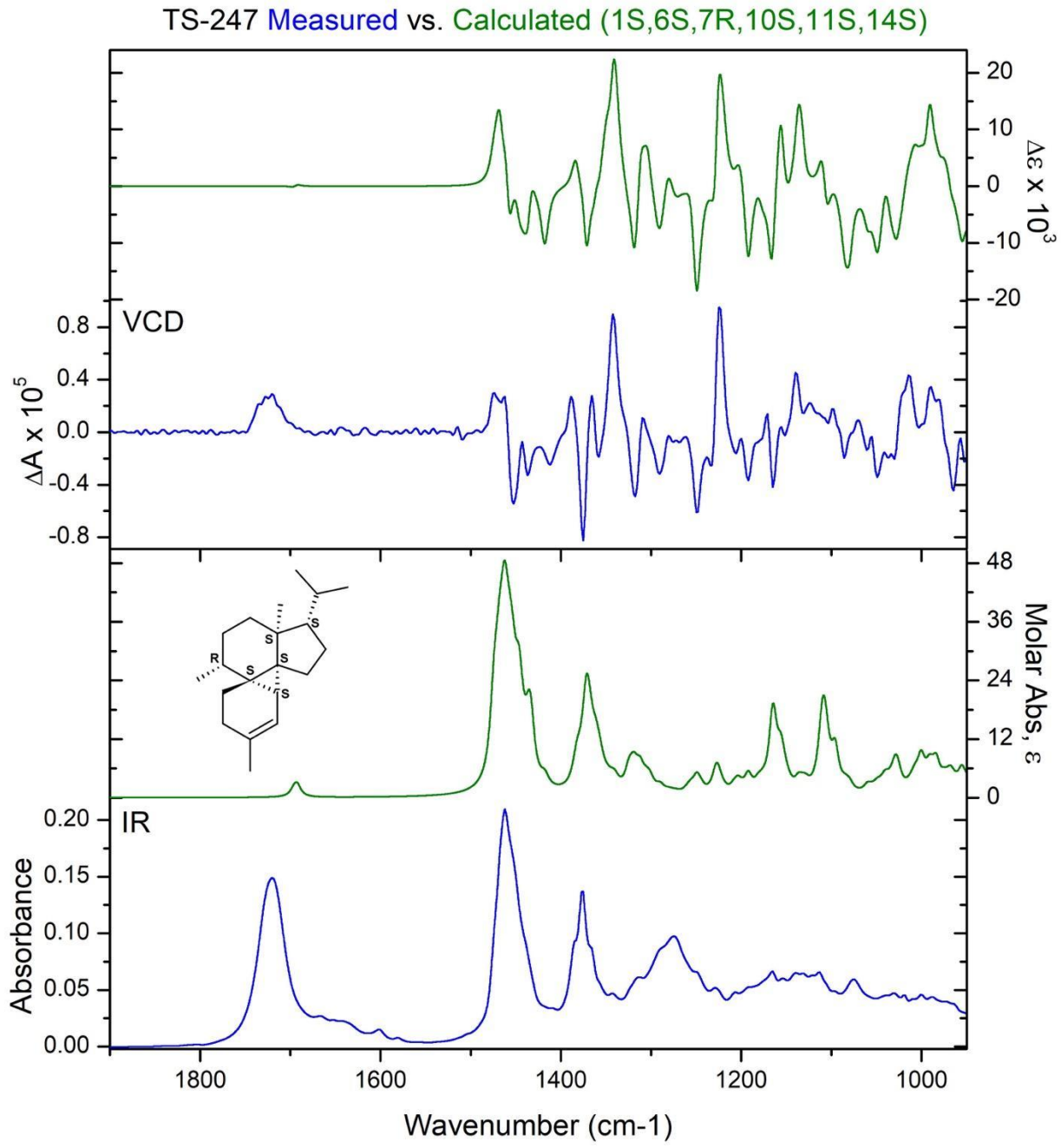

Supplementary Fig. 40. DFT calculated (green) and experimental (blue) VCD and IR spectra of peysonnosene (**4**).

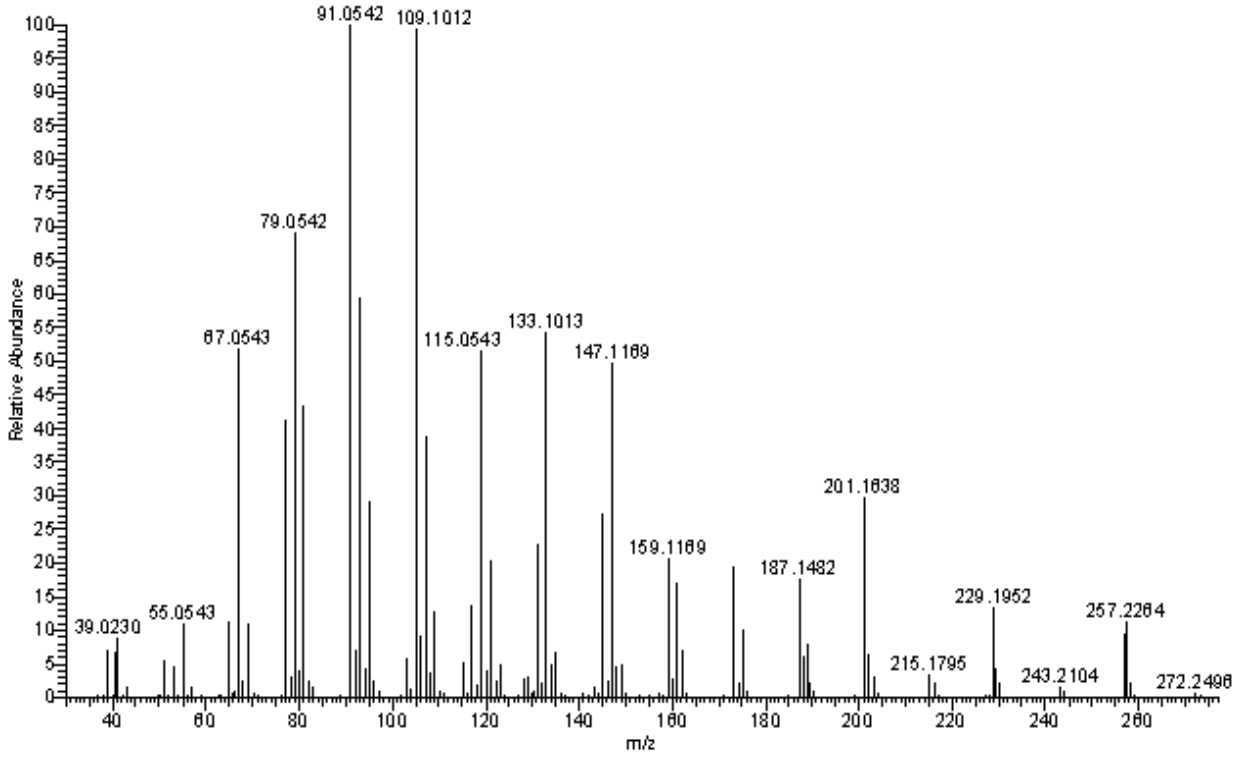

Supplementary Fig. 41. EIMS of clavulara-1(15),17-diene (**5**).

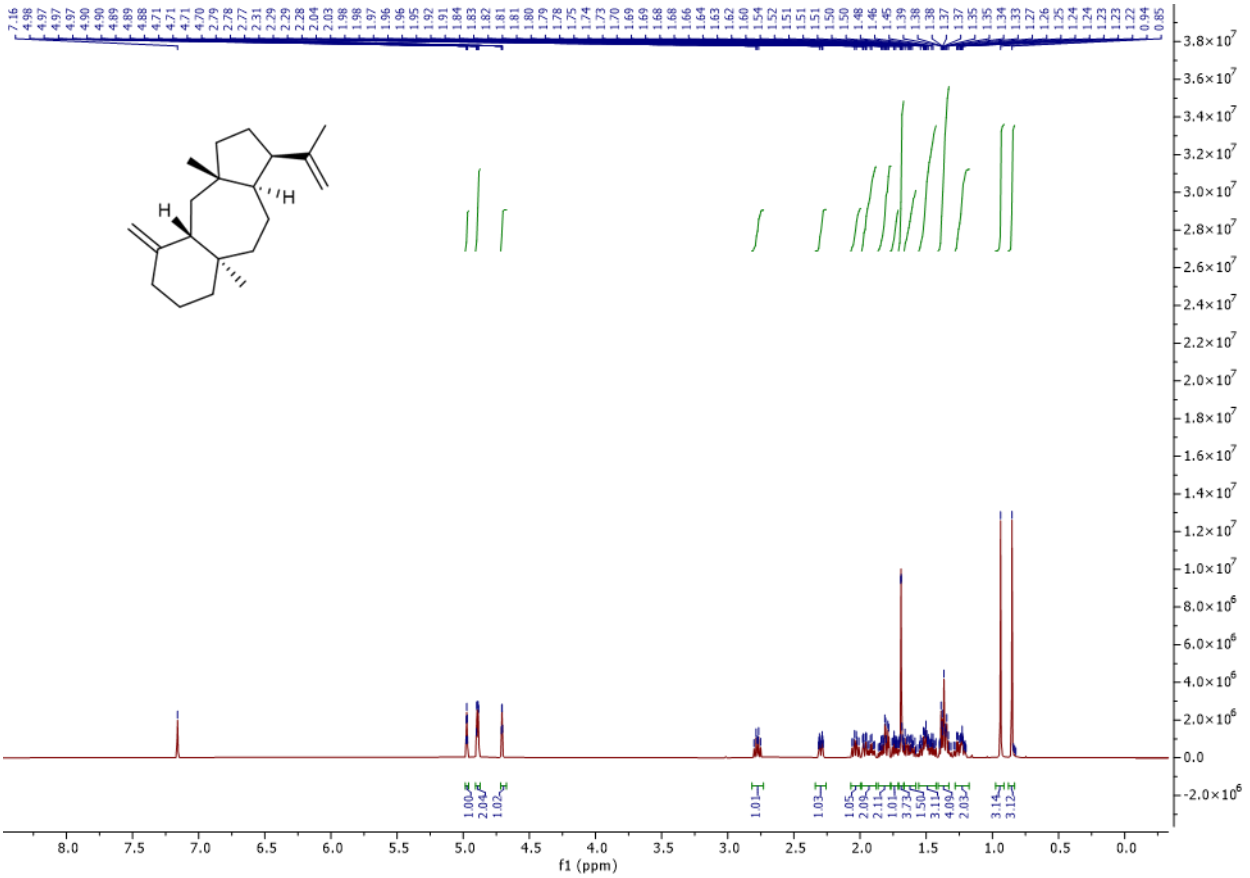

Supplementary Fig. 42. ^{1}H NMR spectrum of clavulara-1(15),17-diene (**5**) in C_6D_6 (600 MHz).

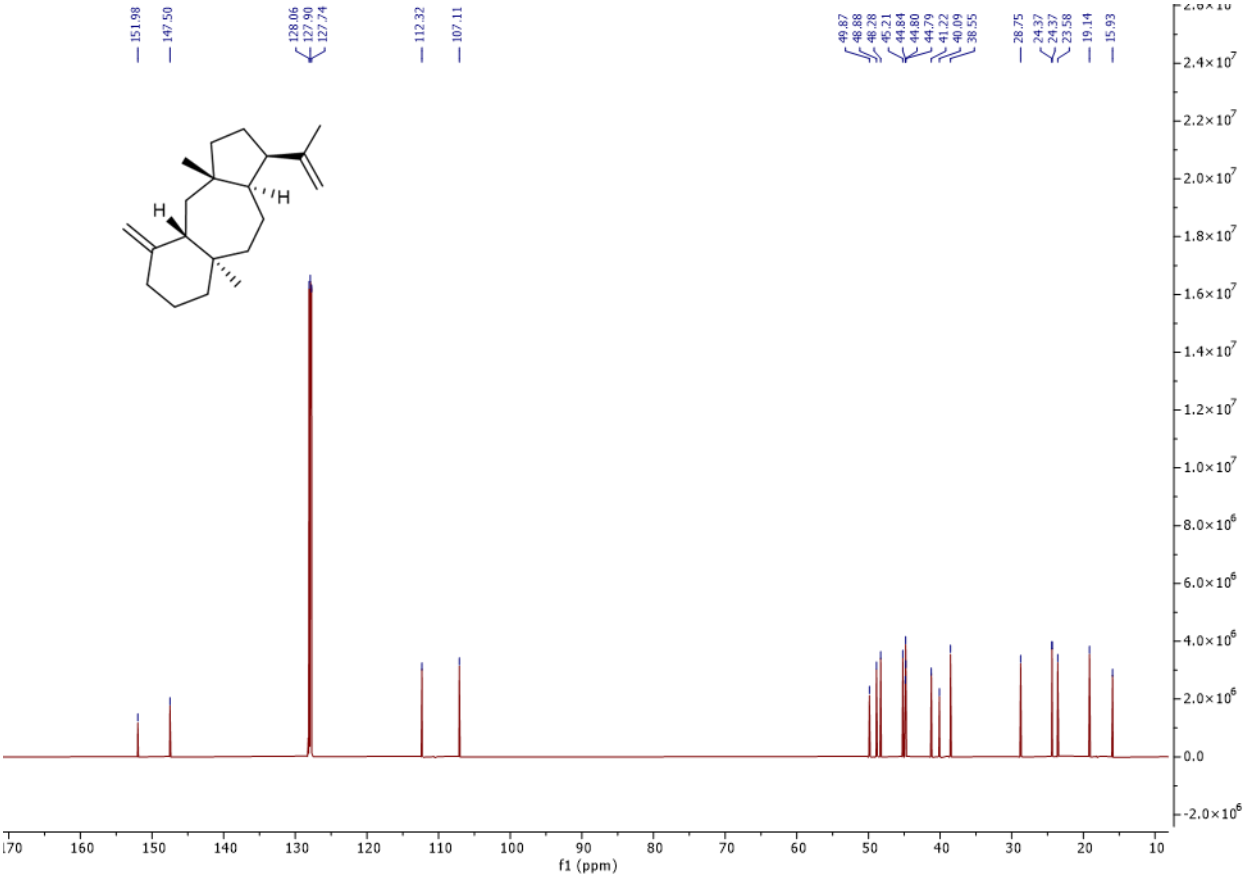

Supplementary Fig. 43. ^{13}C NMR spectrum of clavulara-1(15),17-diene (**5**) in C_6D_6 (151 MHz).

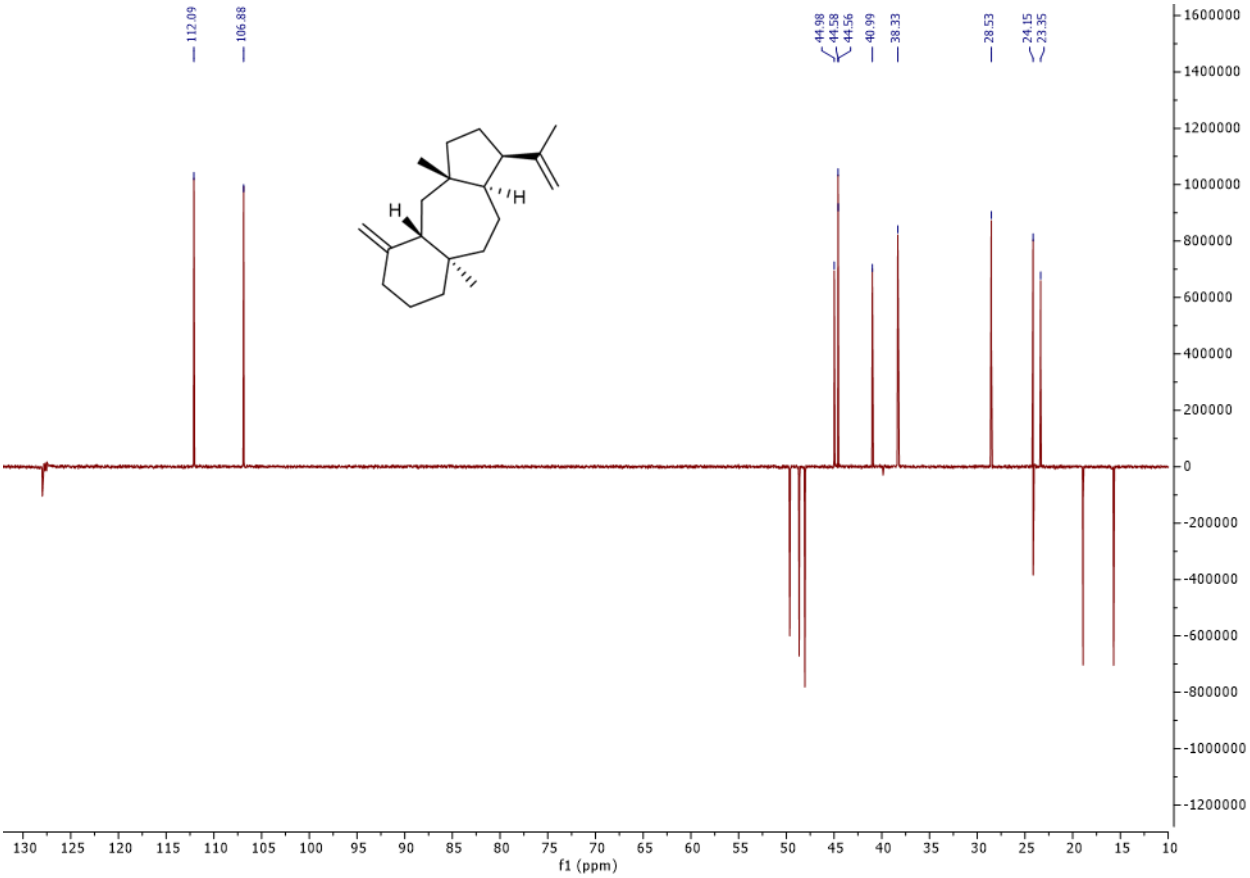

Supplementary Fig. 44. DEPT 135 spectrum of clavulara-1(15),17-diene (**5**) in C_6D_6 (151 MHz).

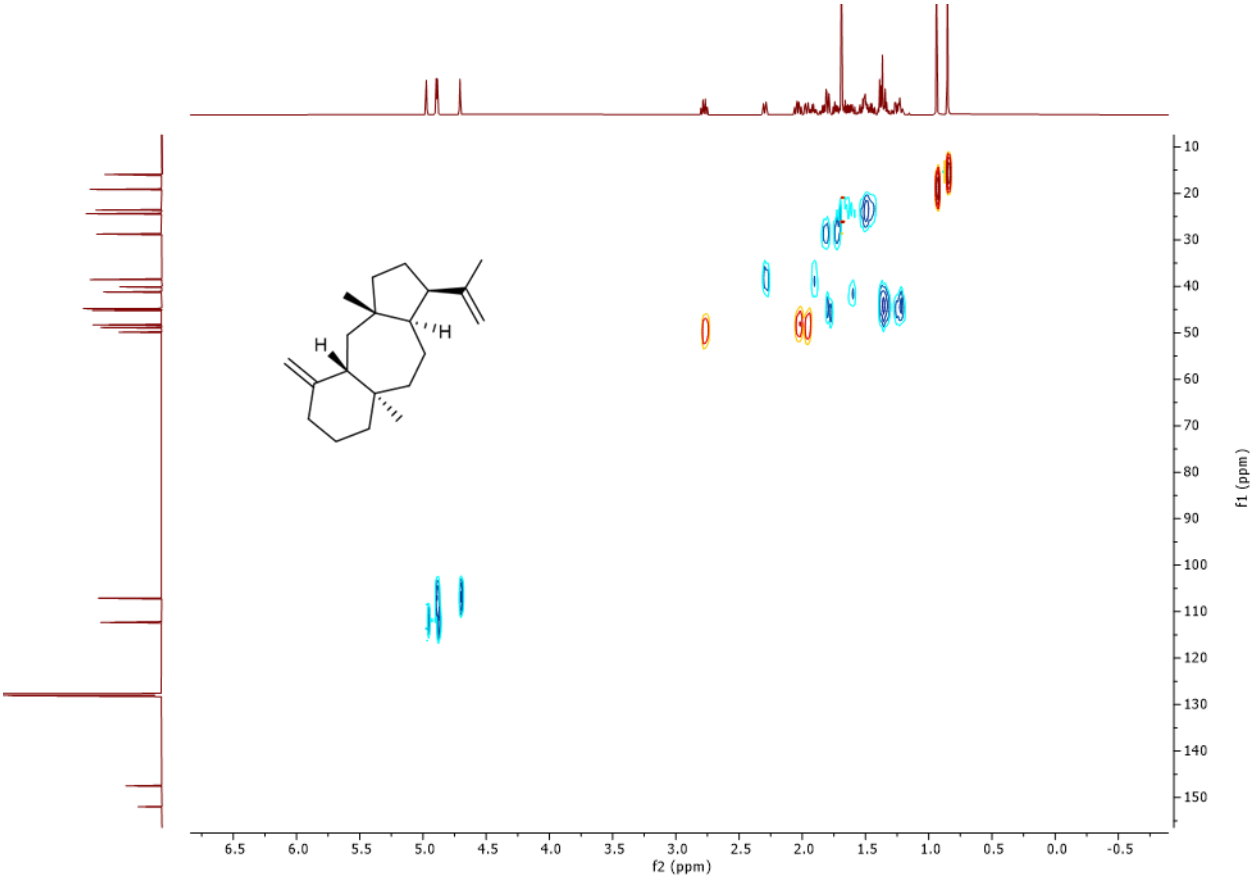

Supplementary Fig. 45. HSQC spectrum of clavulara-1(15),17-diene (**5**) in C_6D_6.

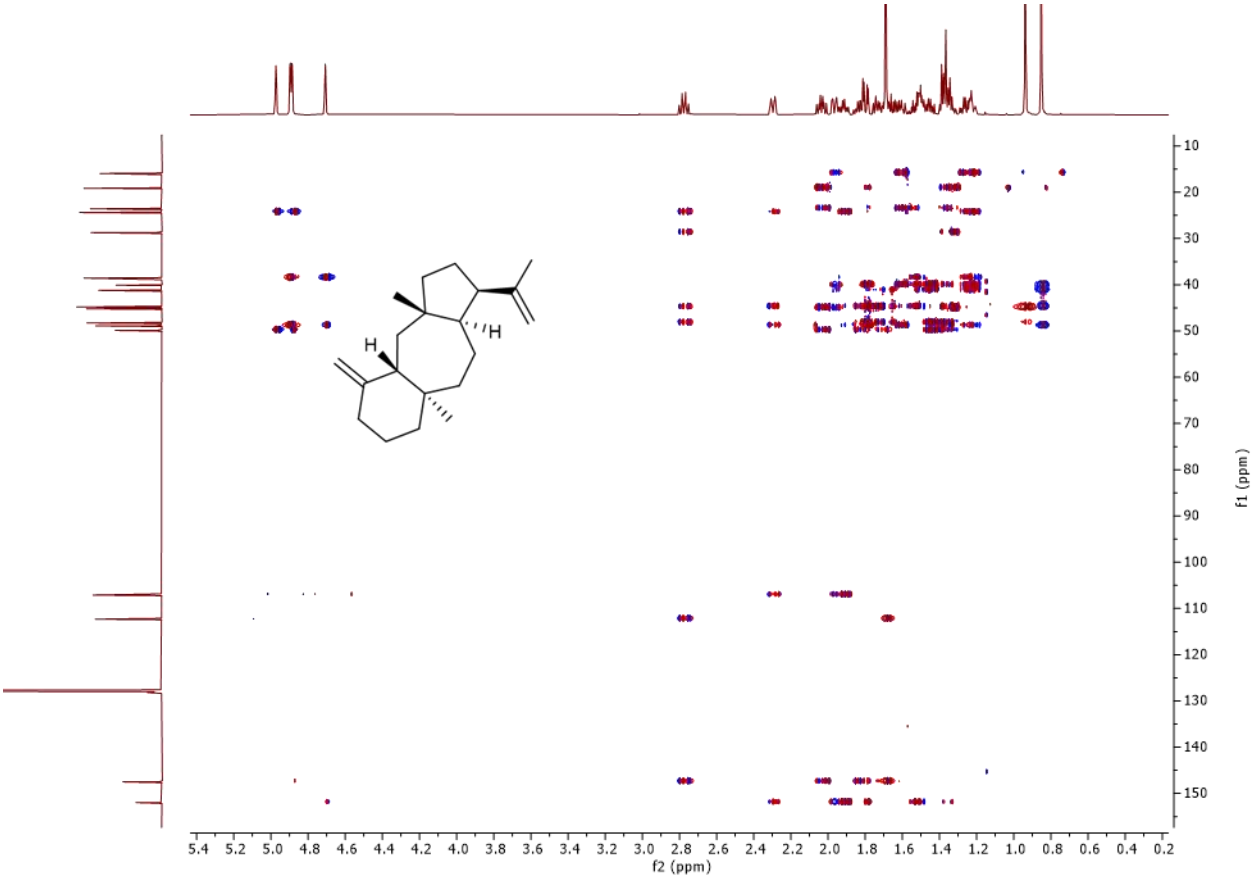

Supplementary Fig. 46. HMBC spectrum of clavulara-1(15),17-diene (**5**) in C_6D_6.

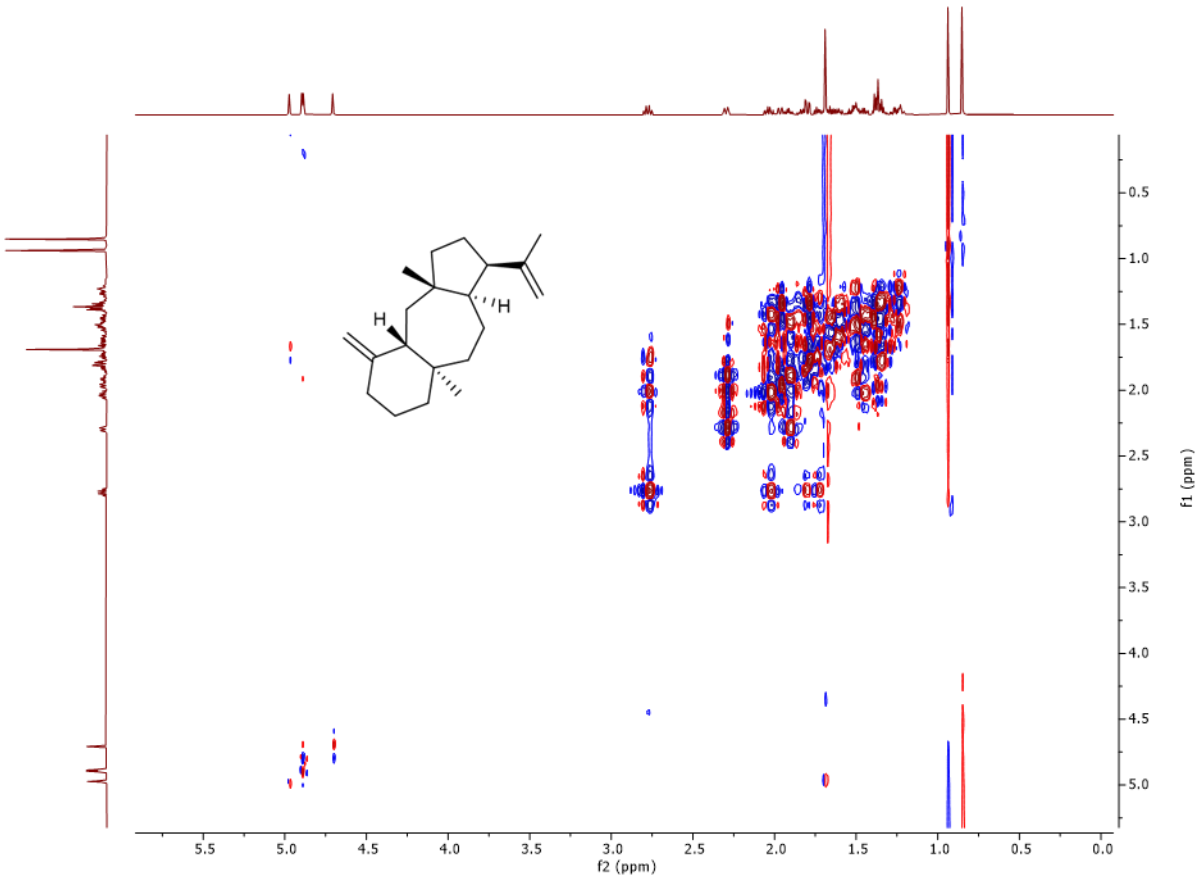

Supplementary Fig. 47. COSY spectrum of clavulara-1(15),17-diene (**5**) in C_6D_6.

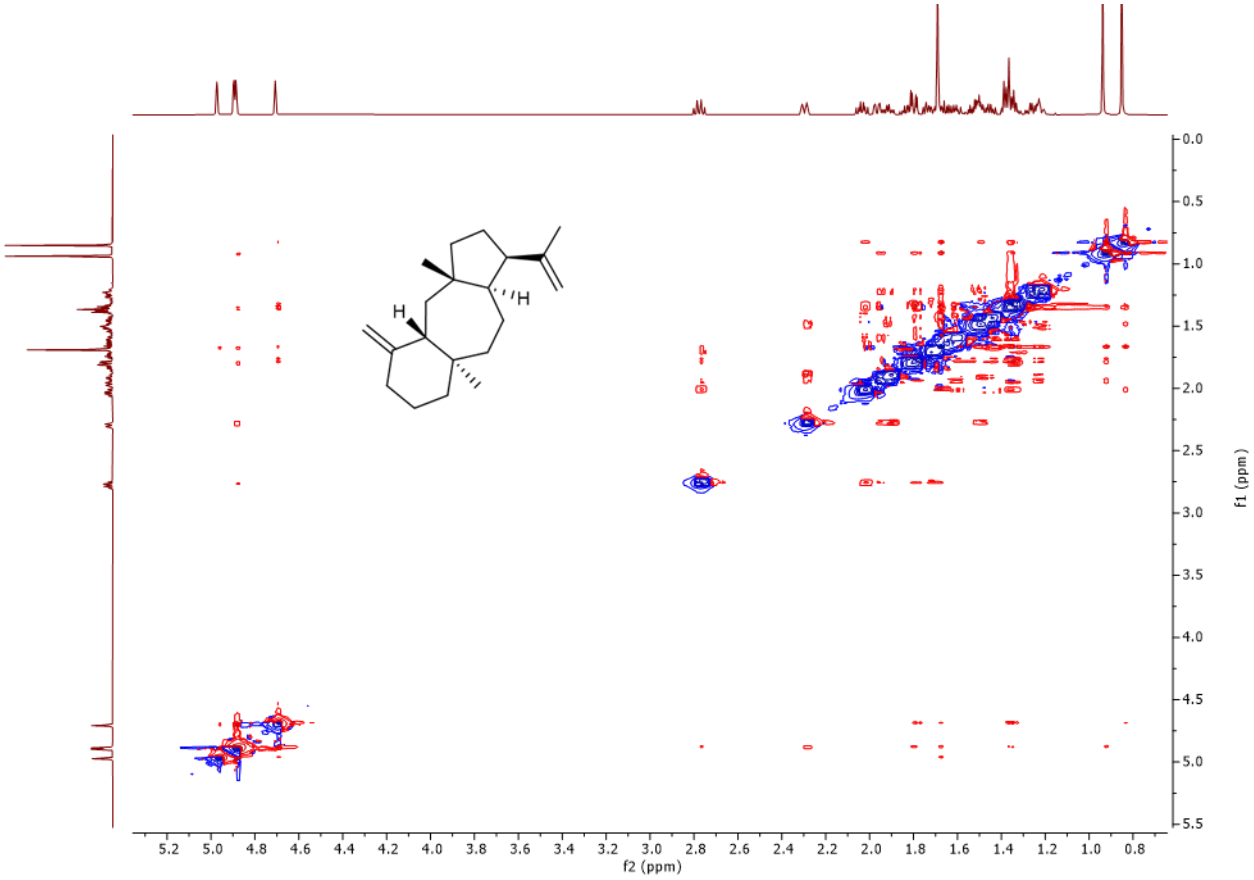

Supplementary Fig. 48. NOESY spectrum of clavulara-1(15),17-diene (**5**) in C_6D_6 (800 MHz).

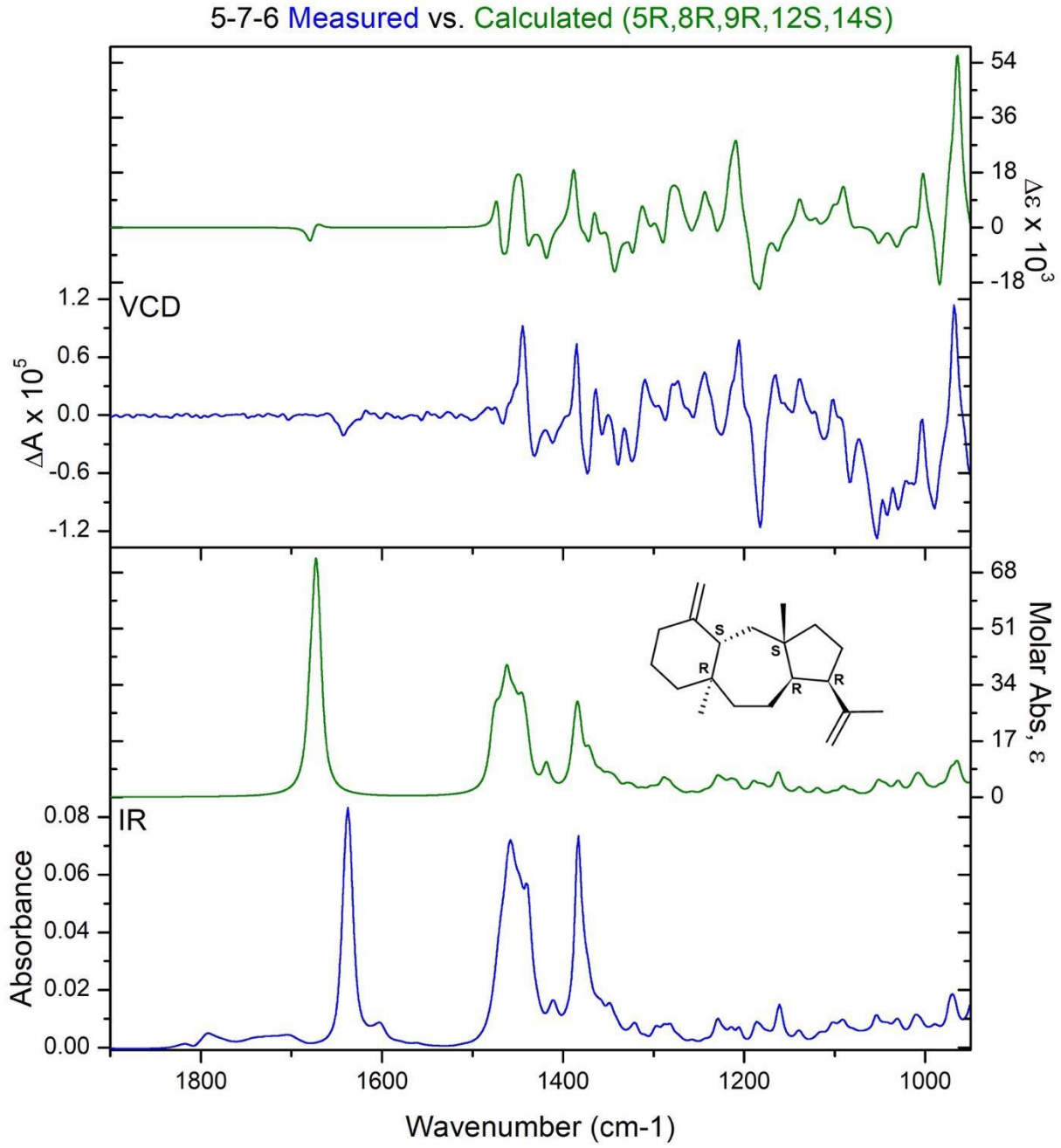

Supplementary Fig. 49. DFT calculated (green) and experimental (blue) VCD and IR spectra of clavulara-1(15),17-diene (**5**) supporting the absolute configuration as 5*R*,8*R*,9*R*,*12*S,14*S*.

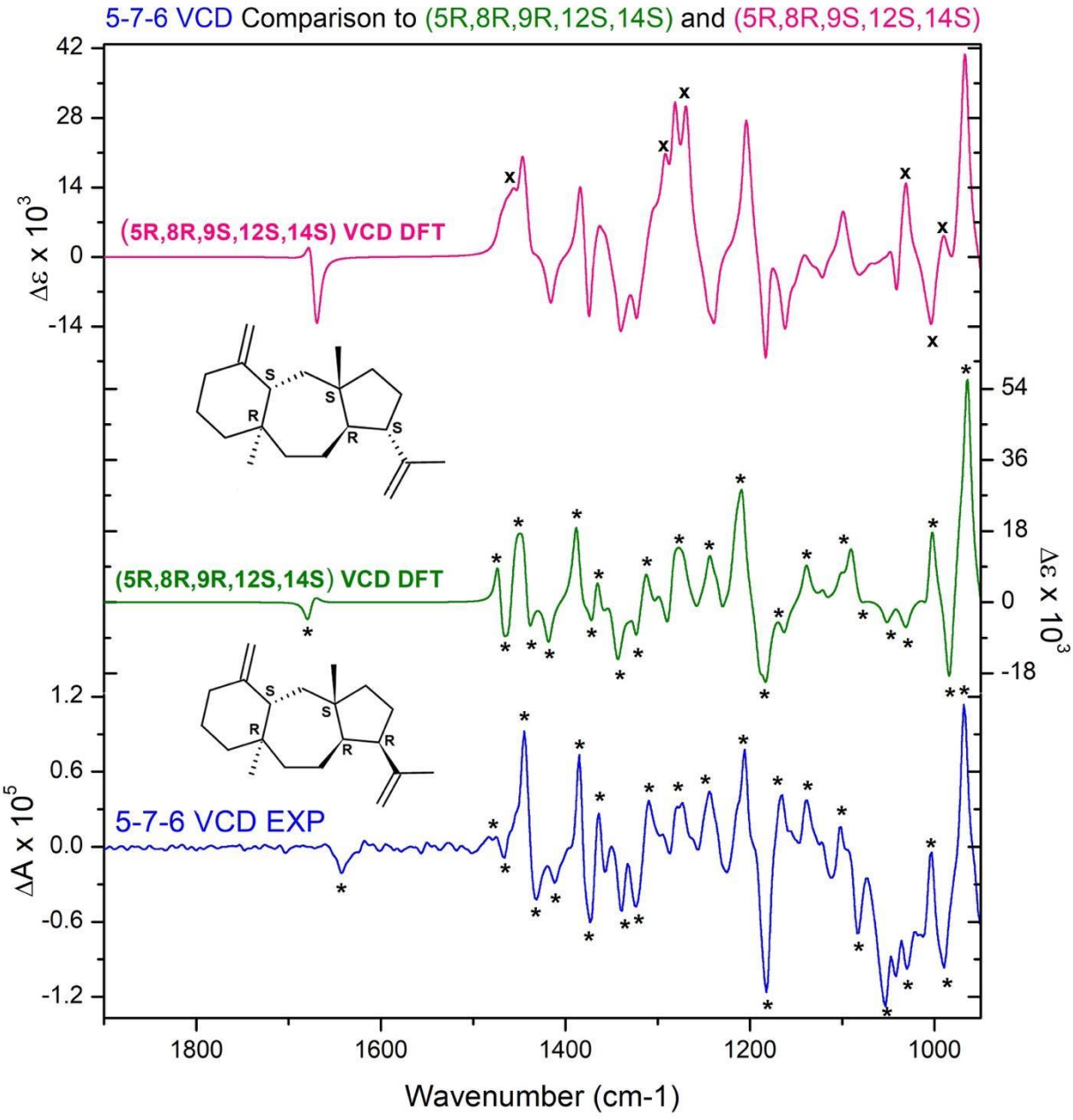

Supplementary Fig. 50. DFT calculated (pink and green) and experimental (blue) VCD and IR spectra of clavulara-1(15),17-diene (**5**) supporting the absolute configuration as 5*R*,8*R*,9*R*,*12*S,14*S*.

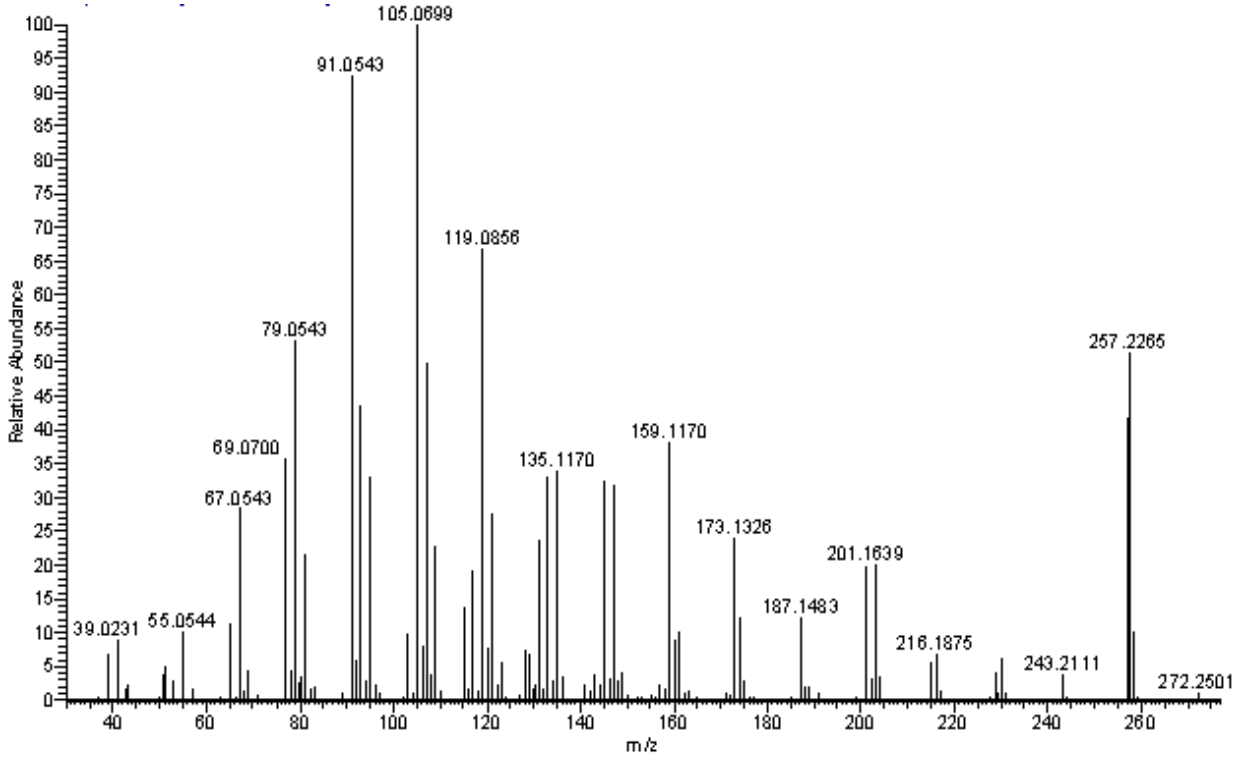

Supplementary Fig. 51. EIMS of variediene (**6**). The fragmentation matched the literature[25].

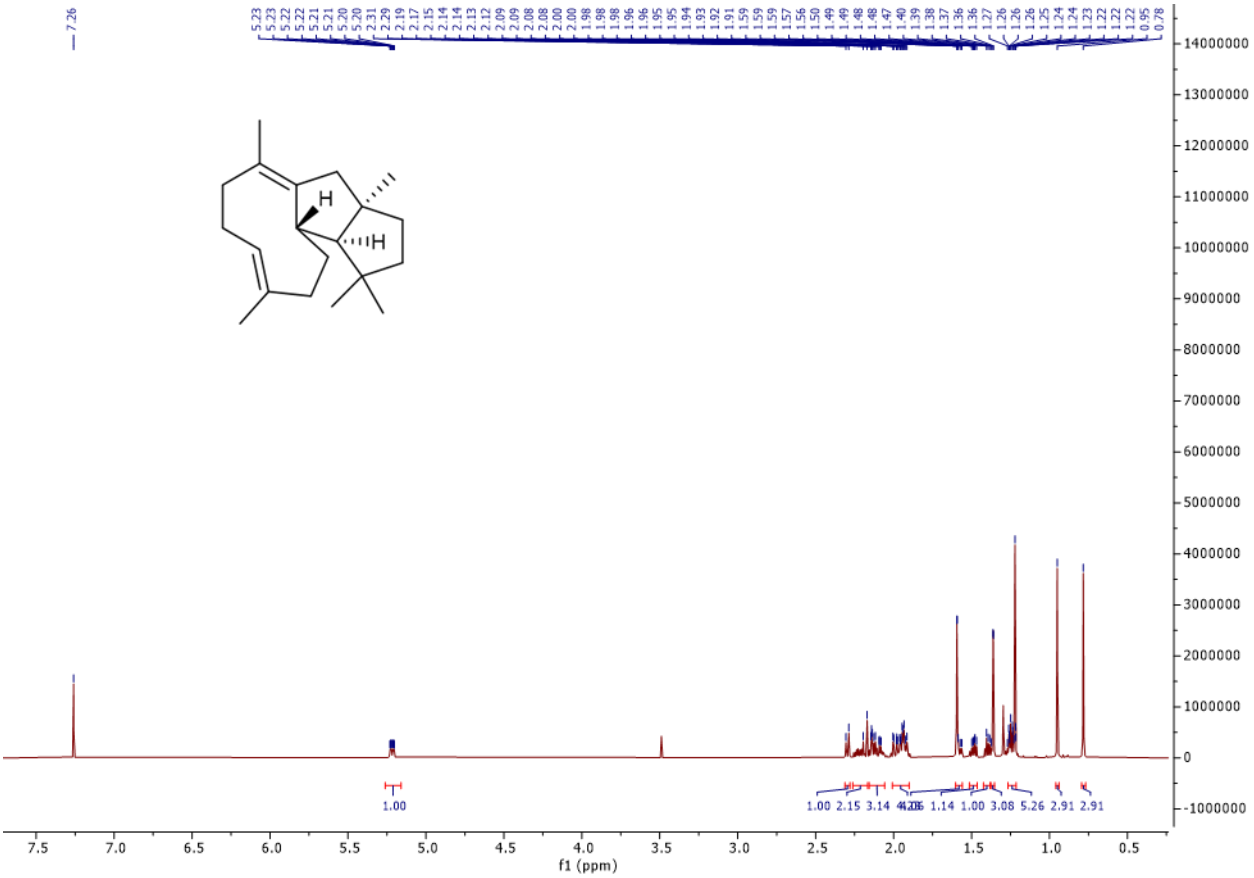

Supplementary Fig. 52. ^{1}H NMR spectrum of variediene (**6**) in $CDCl_3$ (600 MHz).

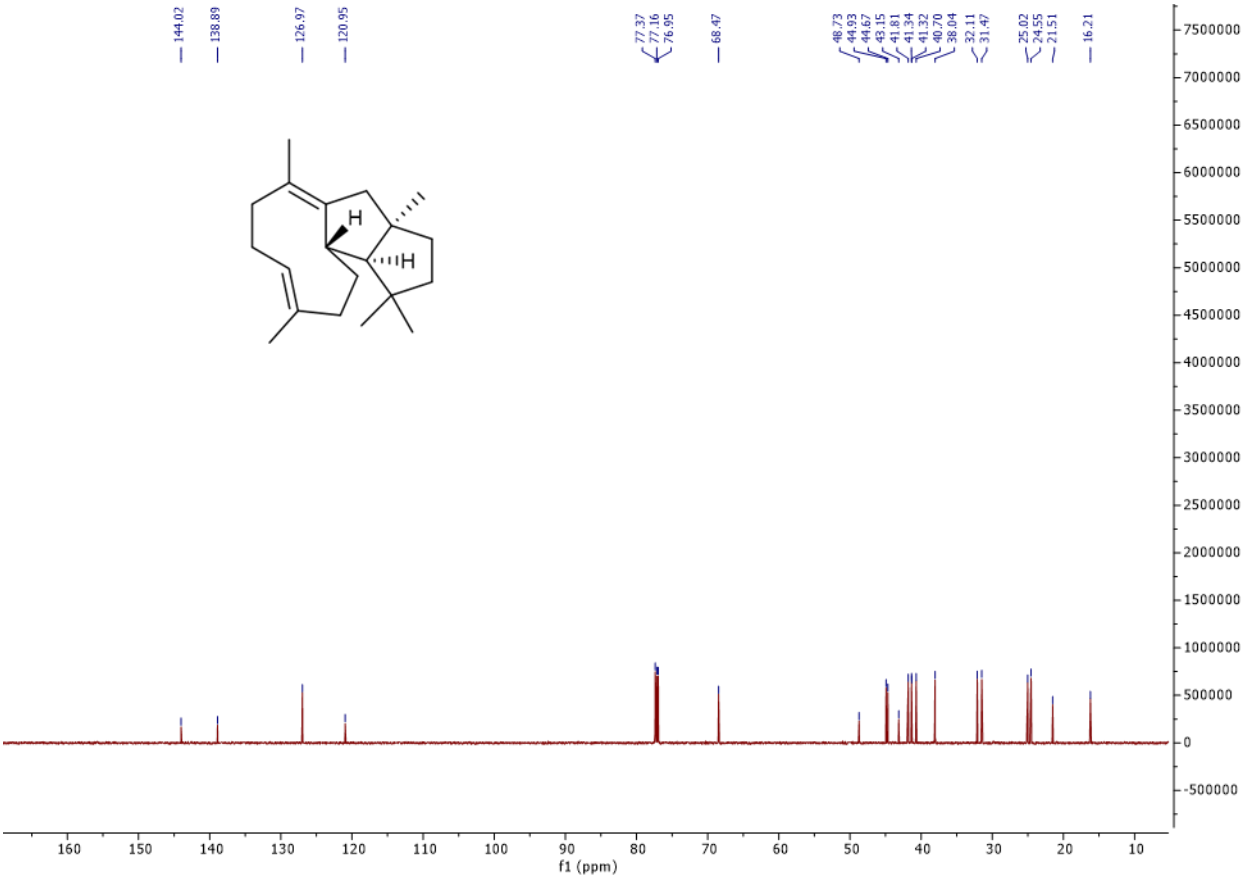

Supplementary Fig. 53. ^{13}C NMR spectrum of variediene (**6**) in $CDCl_3$ (151 MHz).

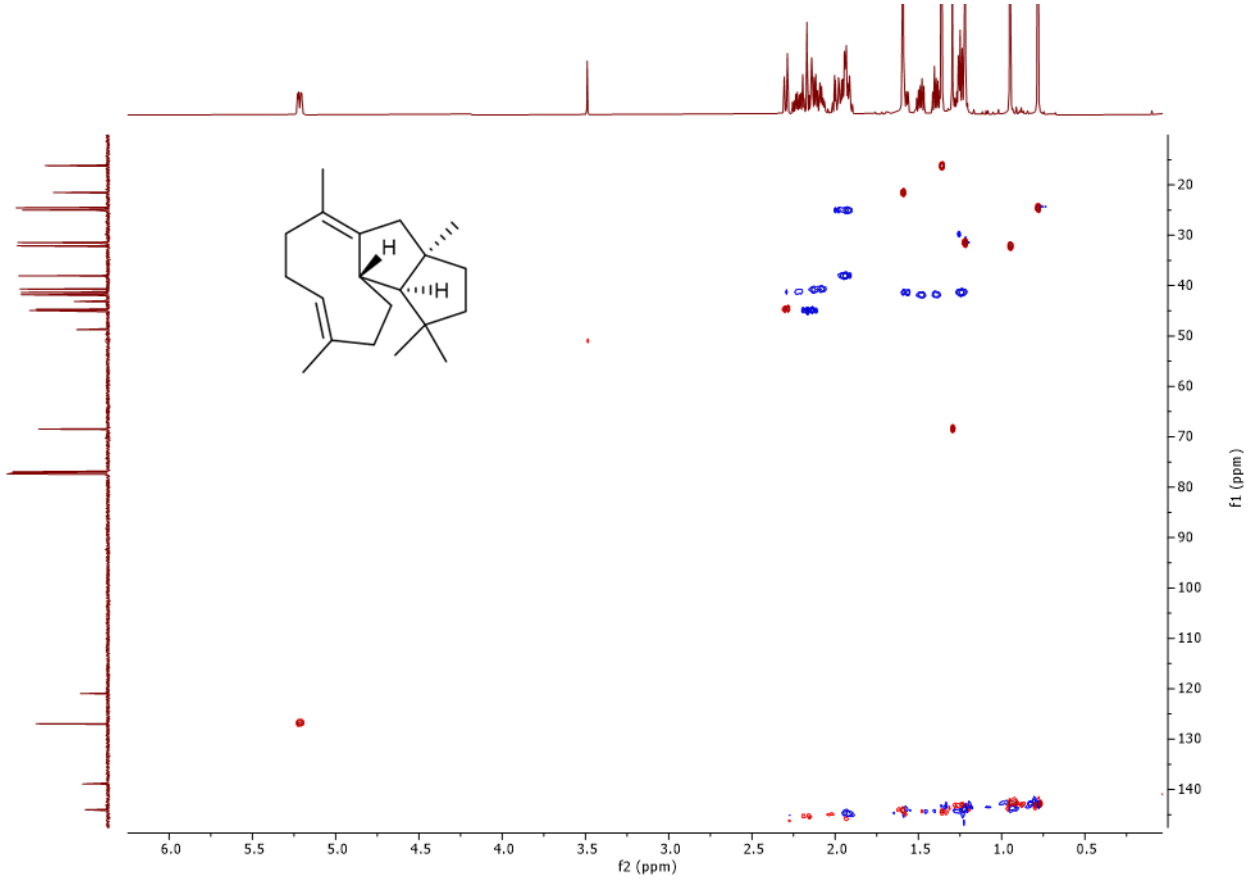

Supplementary Fig. 54. HSQC spectrum of variediene (**6**) in $CDCl_3$.

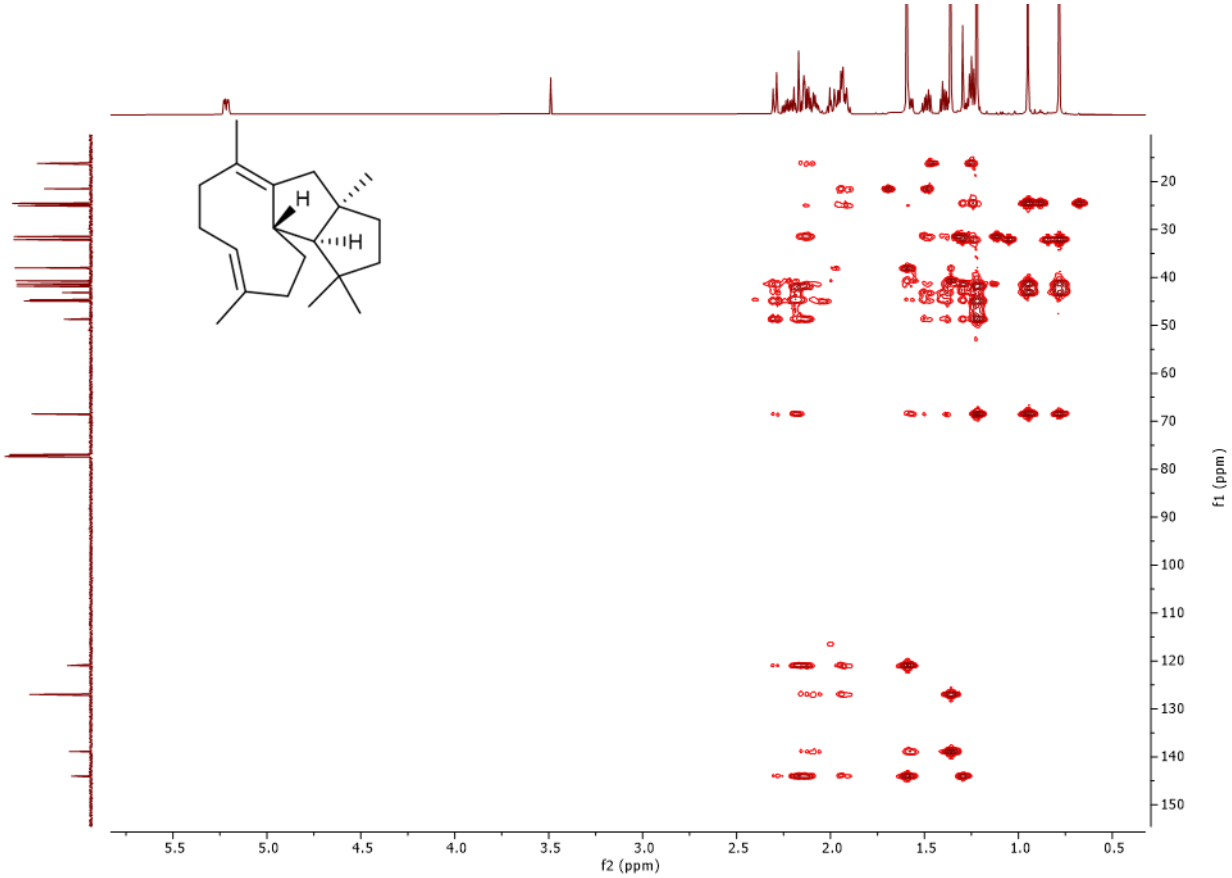

Supplementary Fig. 55. HMBC spectrum of variediene (**6**) in $CDCl_3$.

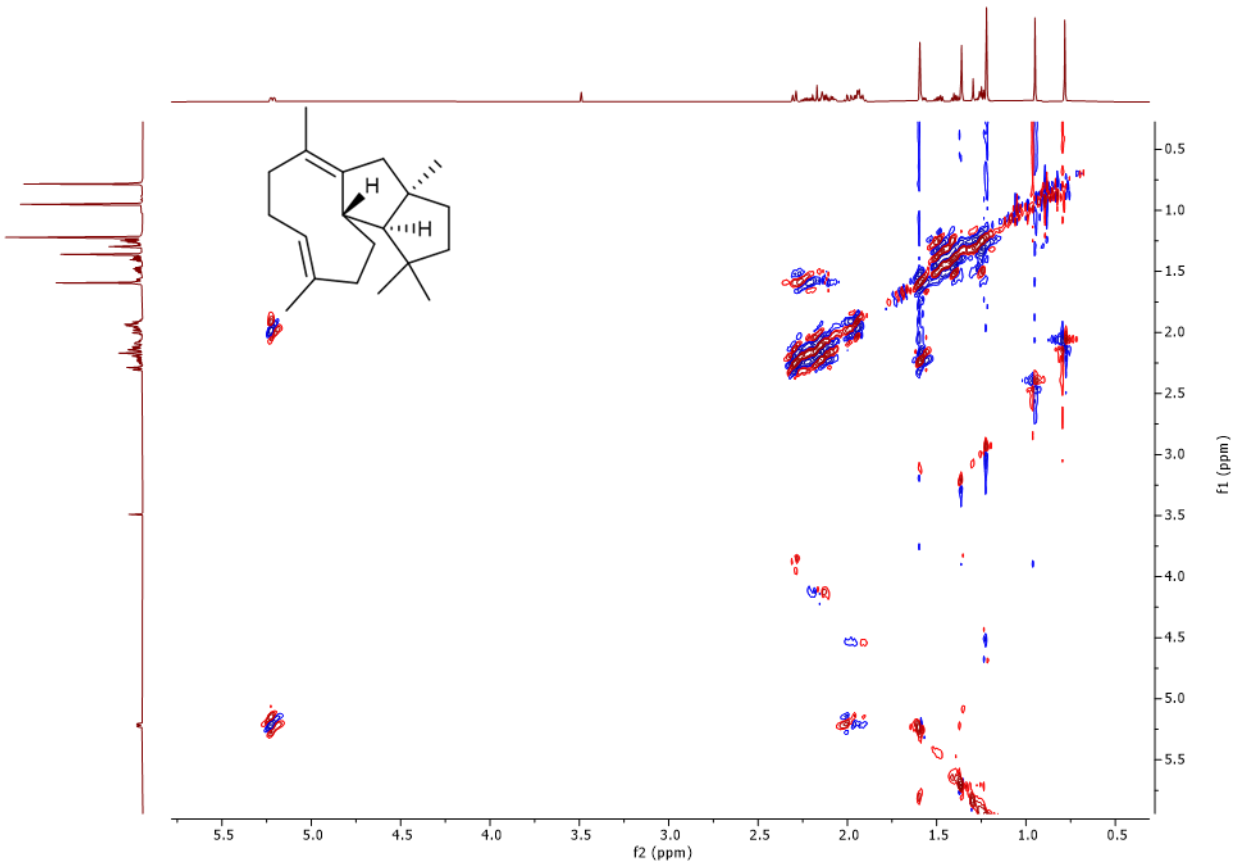

Supplementary Fig. 56. COSY spectrum of variediene (**6**) in $CDCl_3$.

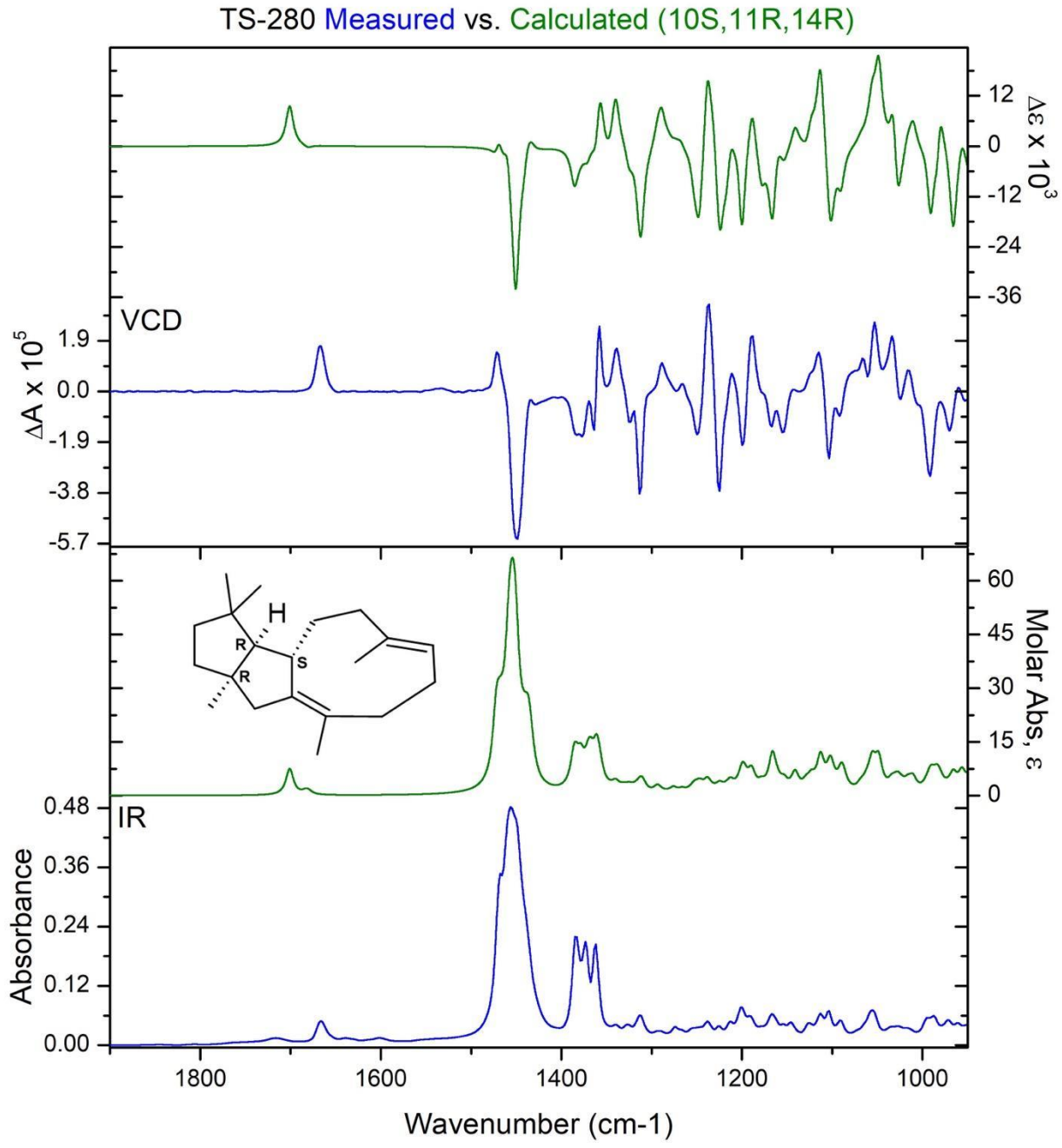

Supplementary Fig. 57. DFT calculated (green) and experimental (blue) VCD and IR spectra of variediene (**6**).

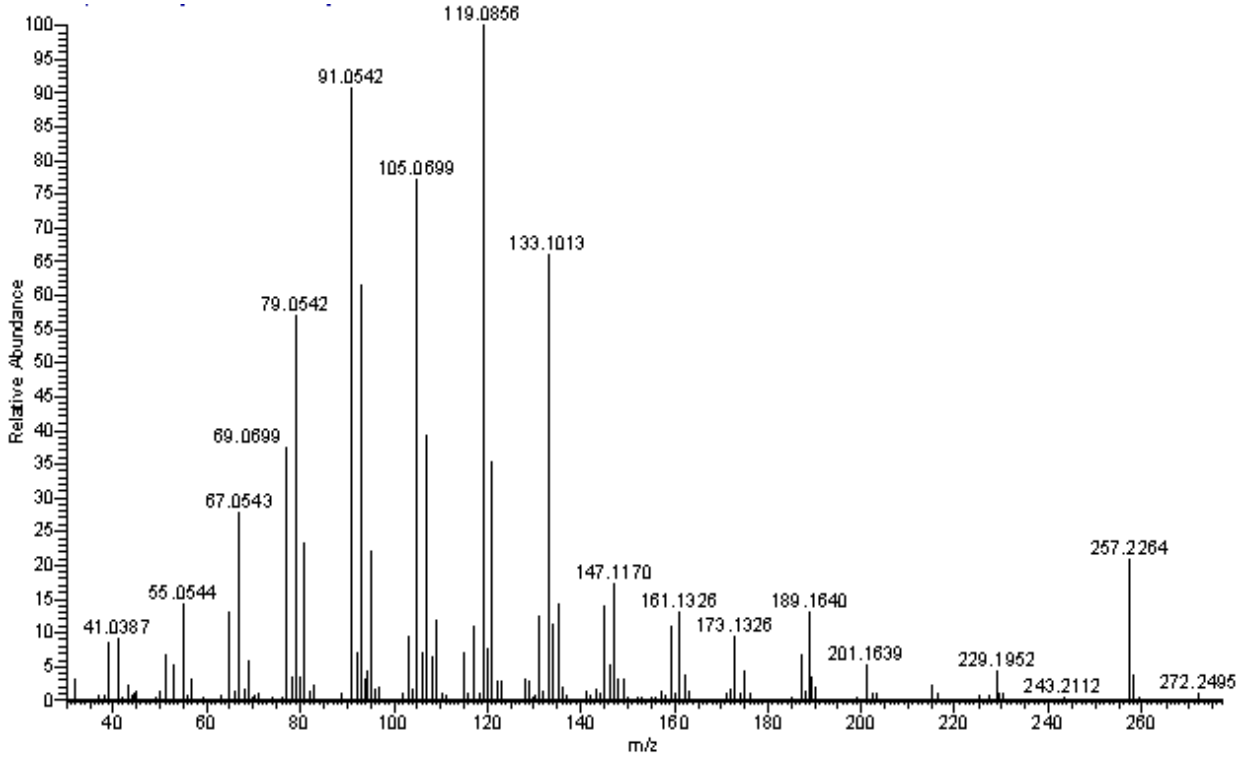

Supplementary Fig. 58. EIMS of 1*S*-verticilla-3,7,11(12)-triene (**7**).

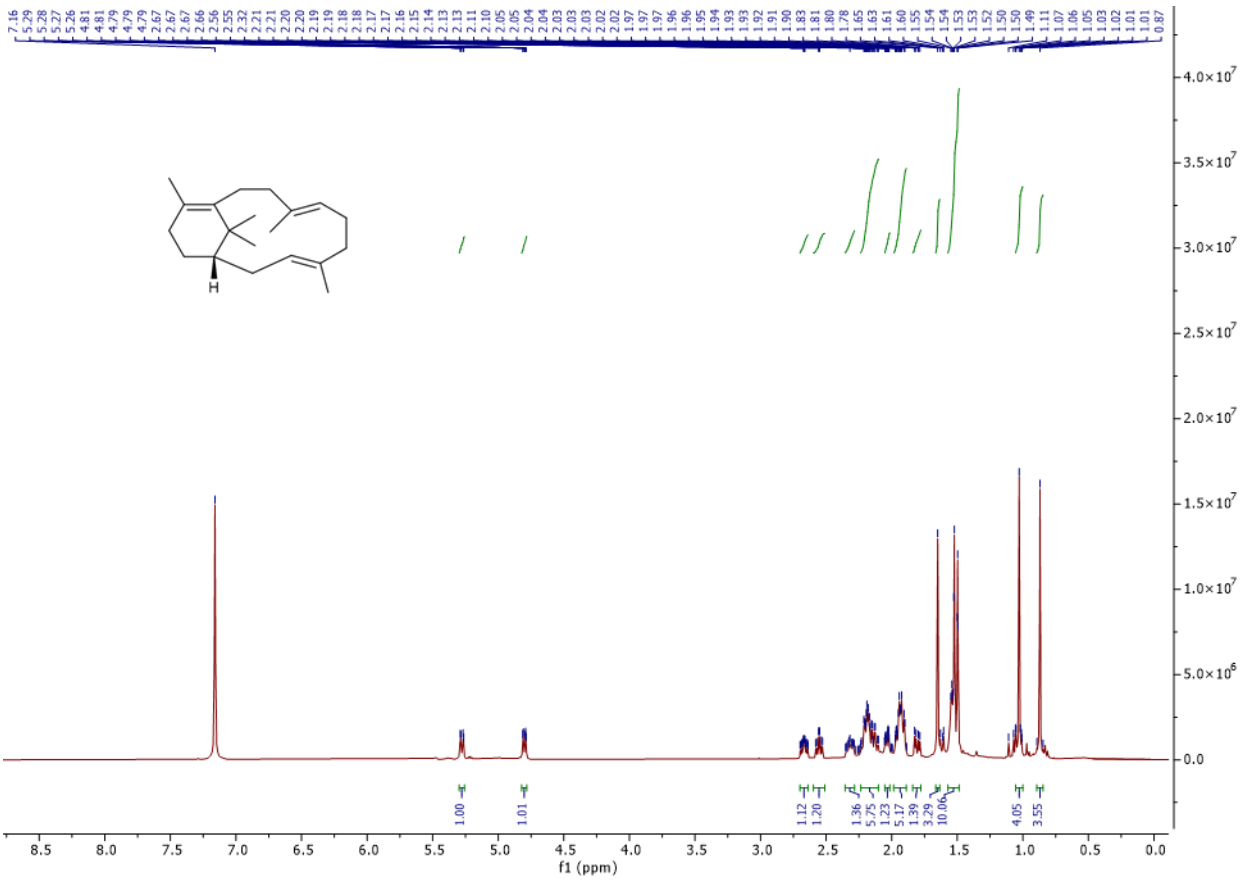

Supplementary Fig. 59. ^{1}H NMR spectrum of 1*S*-verticilla-3,7,11(12)-triene (**7**) in C_6D_6 (600 MHz).

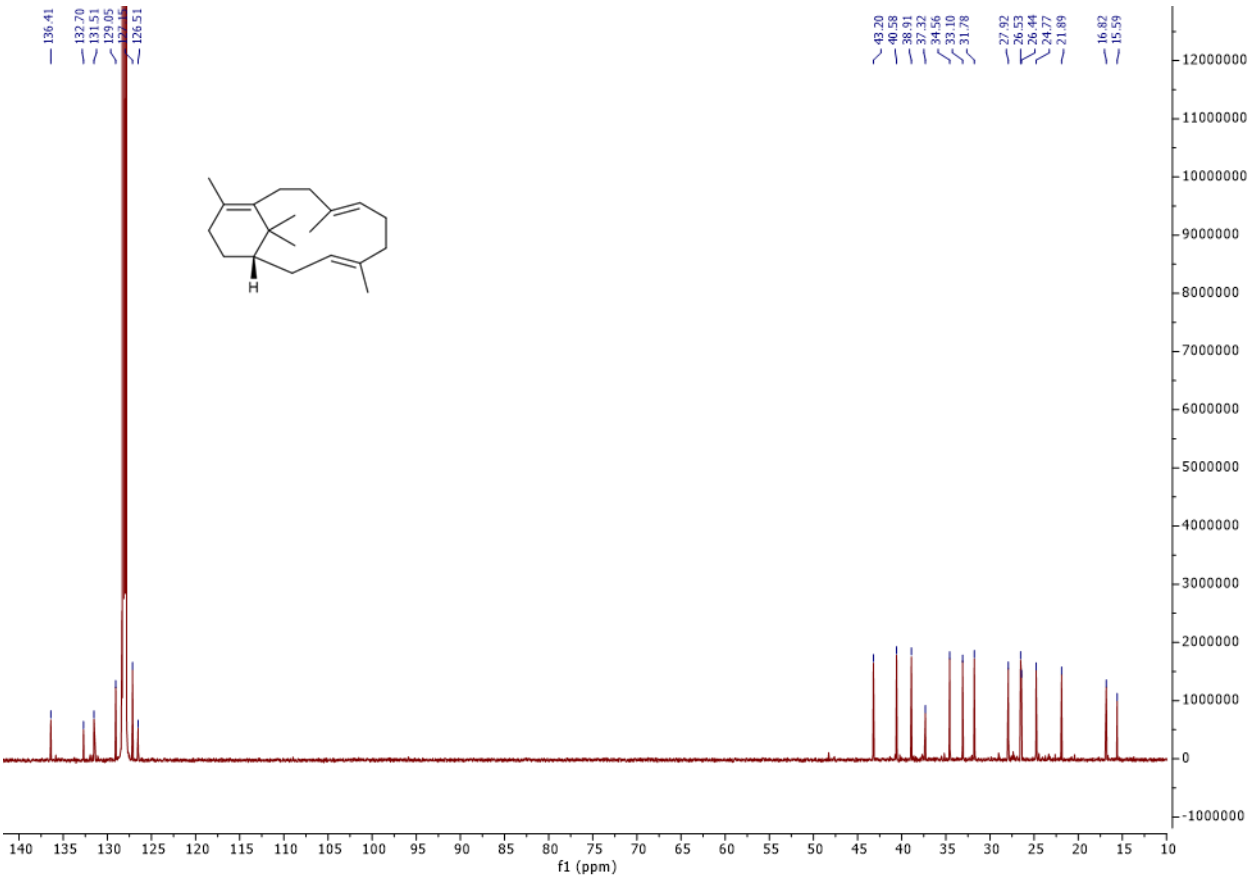

Supplementary Fig. 60. ^{13}C NMR spectrum of 1*S*-verticilla-3,7,11(12)-triene (**7**) in C_6D_6 (151 MHz).

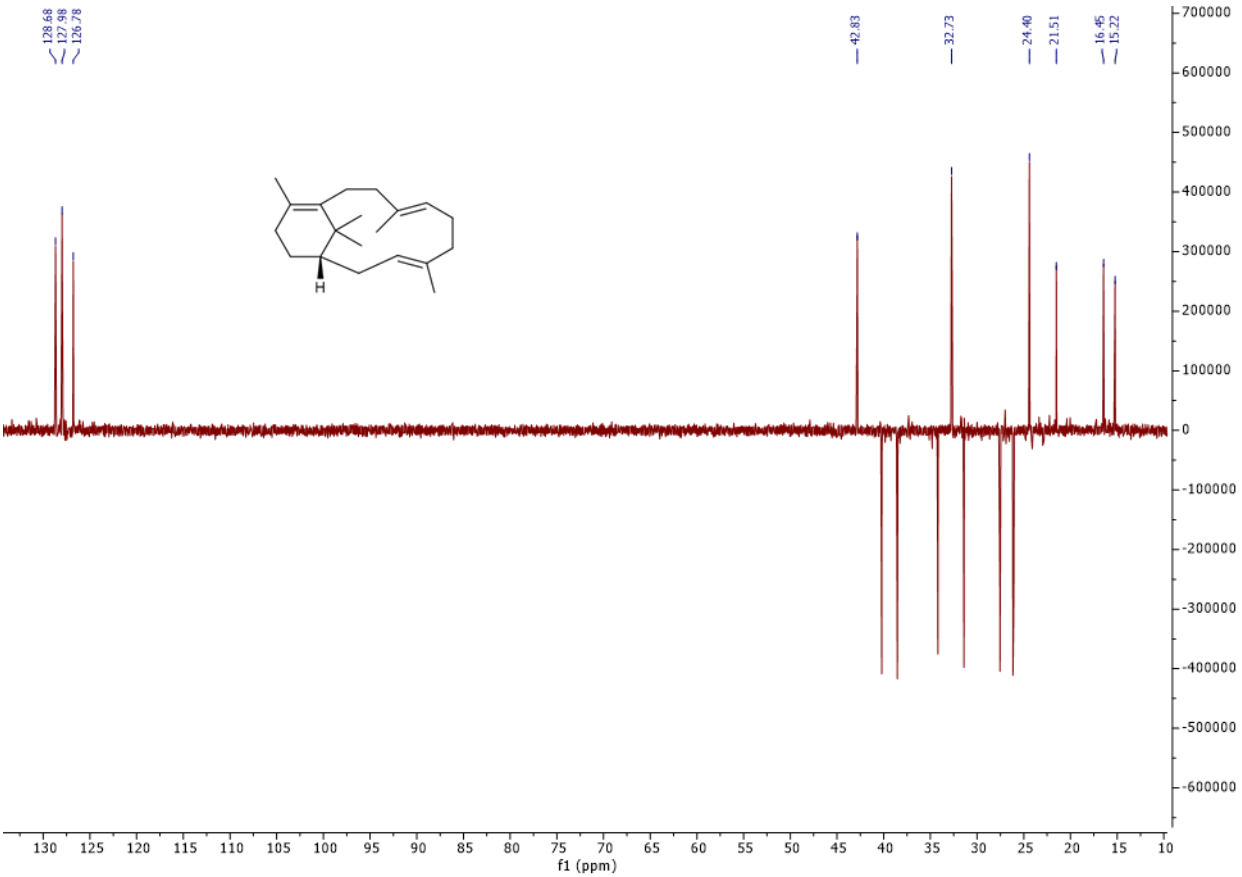

Supplementary Fig. 61. DEPT 135 spectrum of 1*S*-verticilla-3,7,11(12)-triene (**7**) in C_6D_6 (151 MHz).

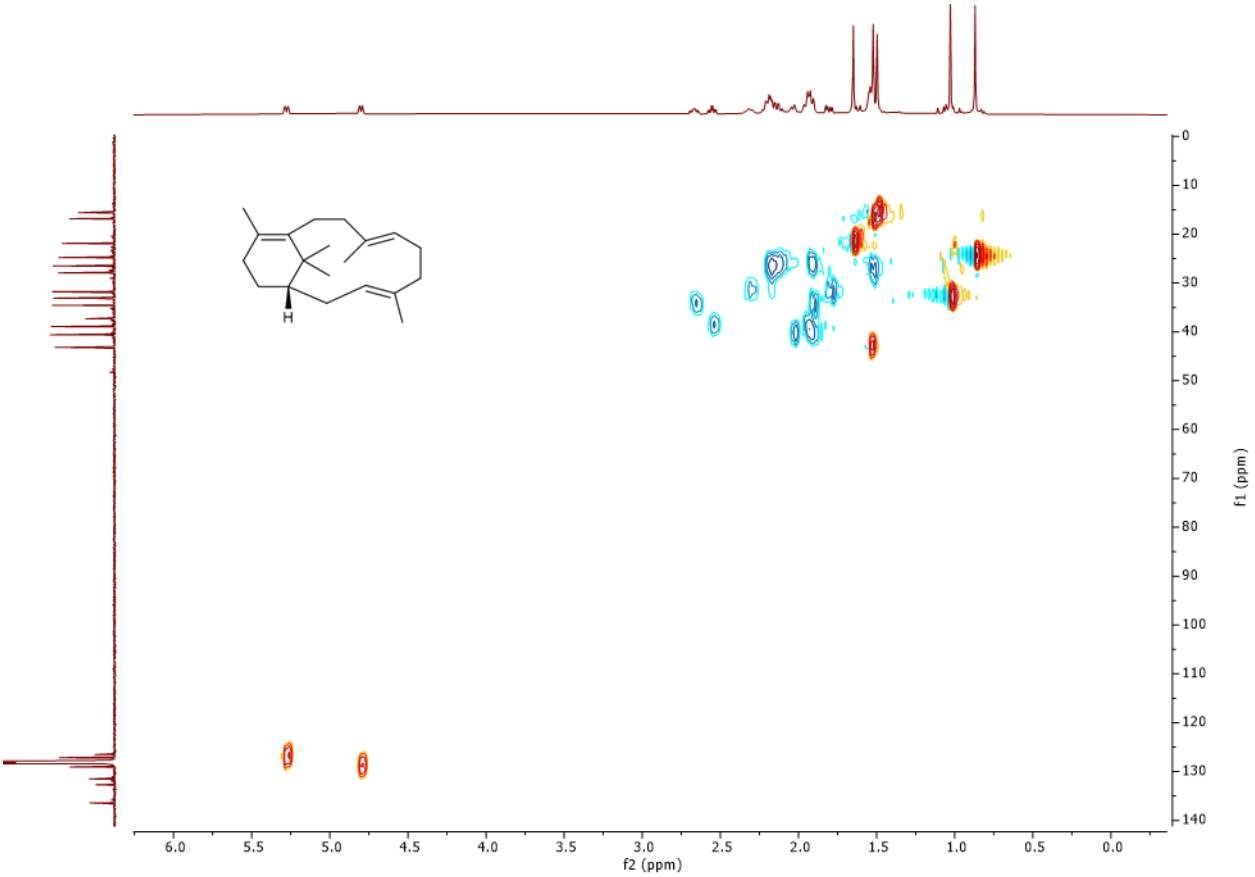

Supplementary Fig. 62. HSQC spectrum of 1*S*-verticilla-3,7,11(12)-triene (**7**) in C_6D_6.

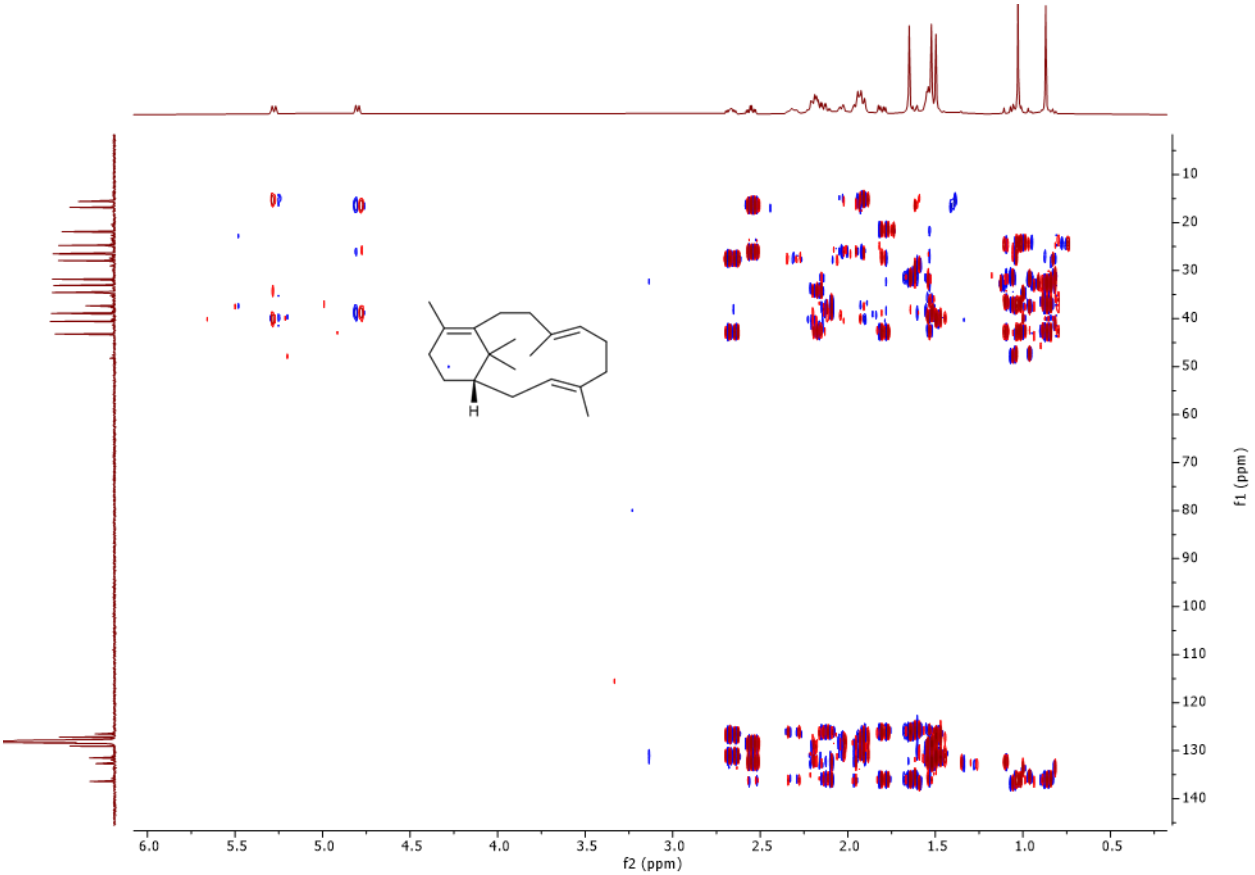

Supplementary Fig. 63. HMBC spectrum of 1*S*-verticilla-3,7,11(12)-triene (**7**) in C_6D_6.

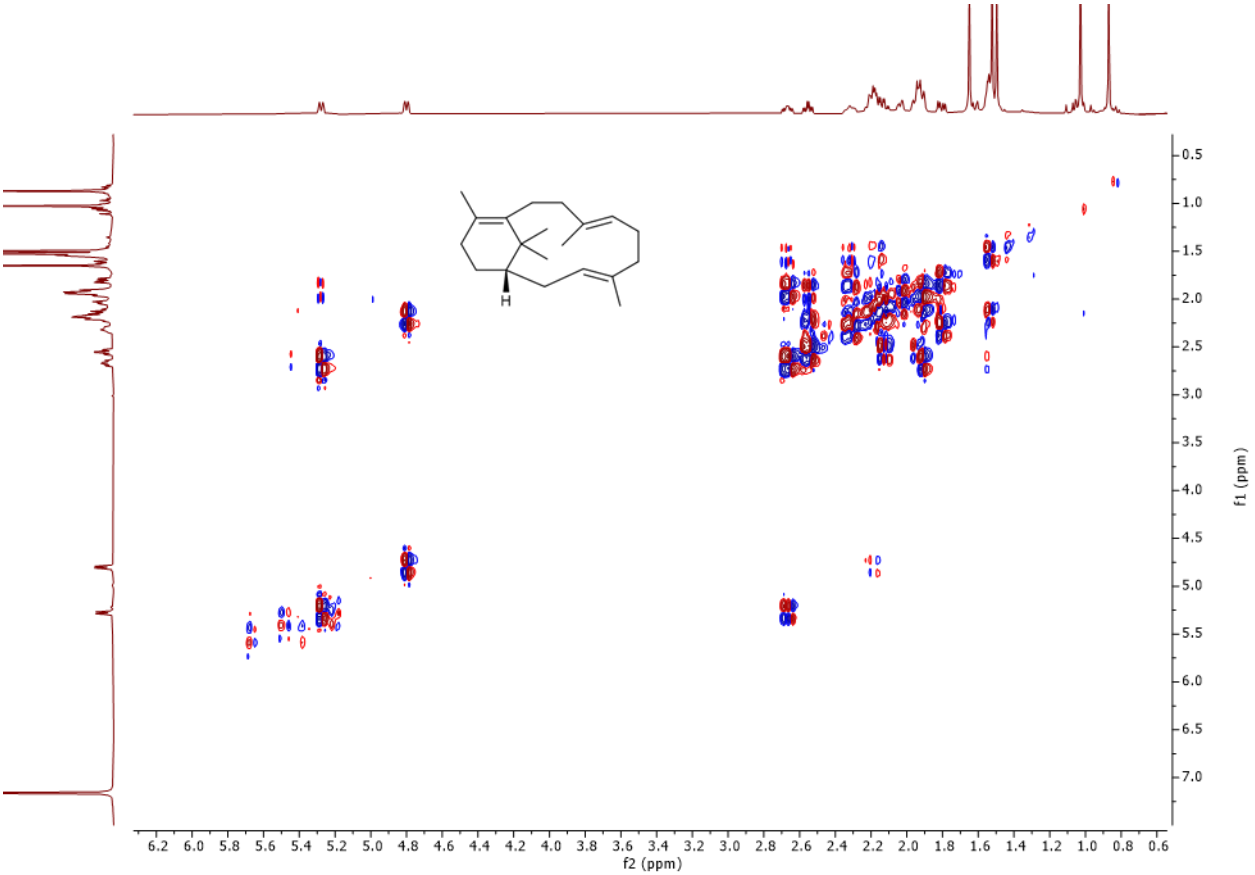

Supplementary Fig. 64. COSY spectrum of 1*S*-verticilla-3,7,11(12)-triene (**7**) in C_6D_6.

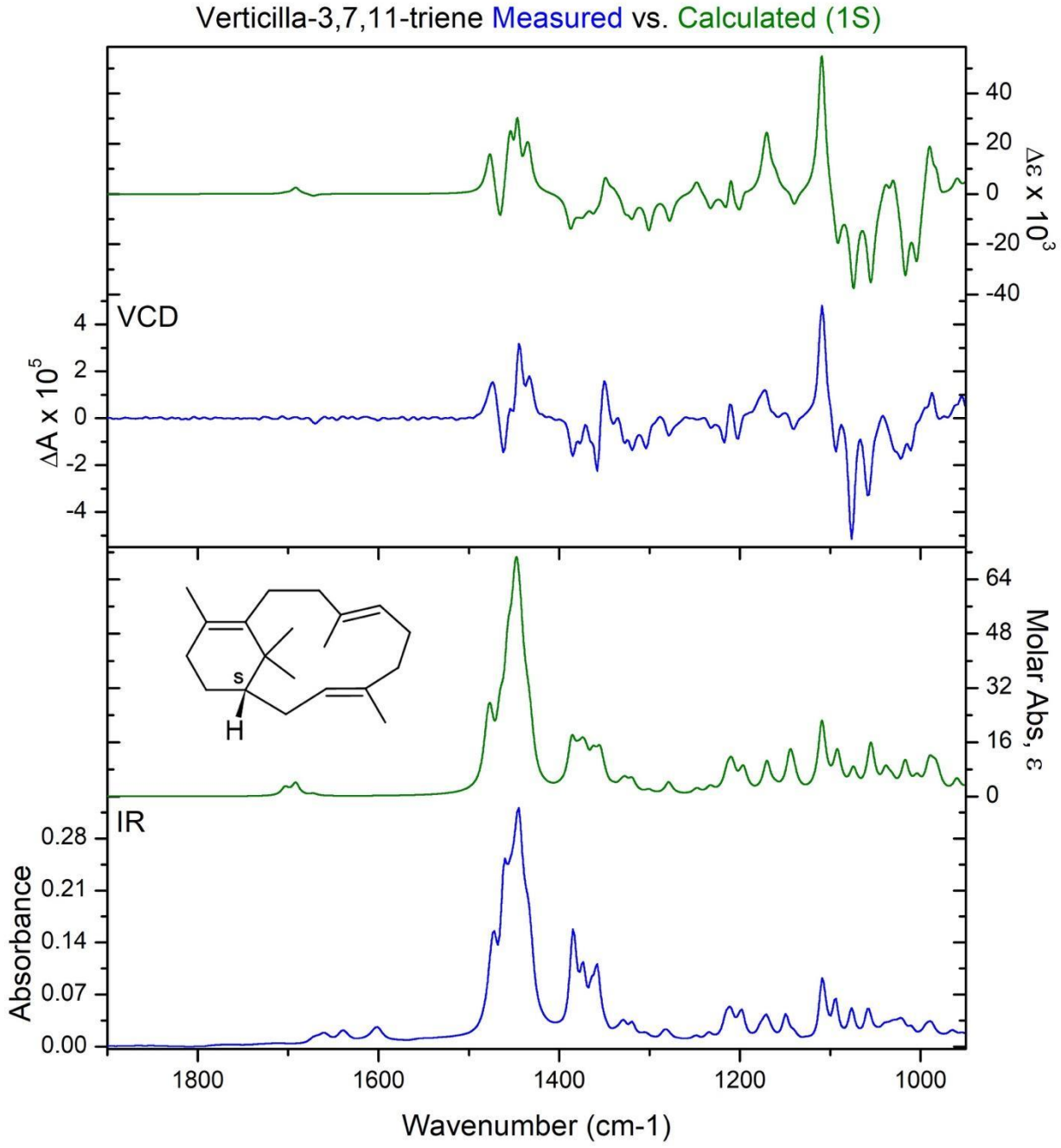

Supplementary Fig. 65. DFT calculated (green) and experimental (blue) VCD and IR spectra of 1*S*-verticilla-3,7,11(12)-triene (**7**).

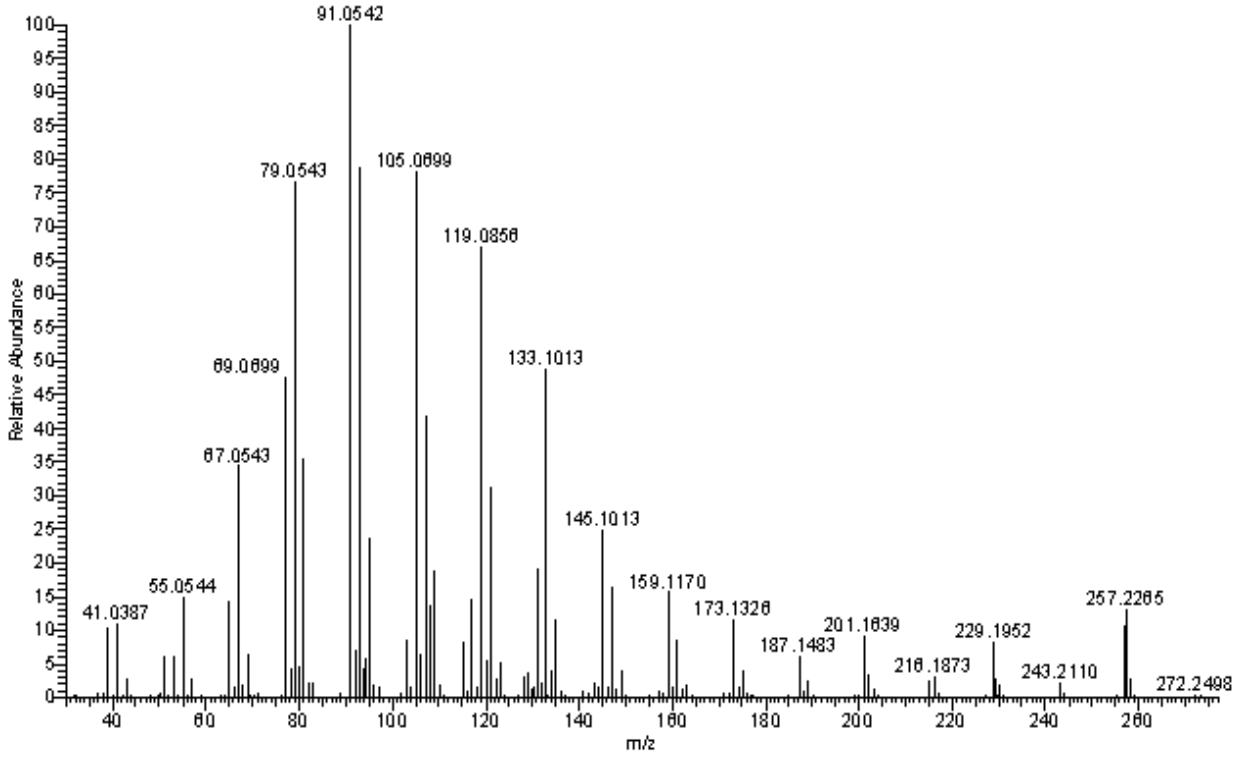

Supplementary Fig. 66. EIMS of 1*S*-verticilla-3,8(19),11(12)-triene (**8**).

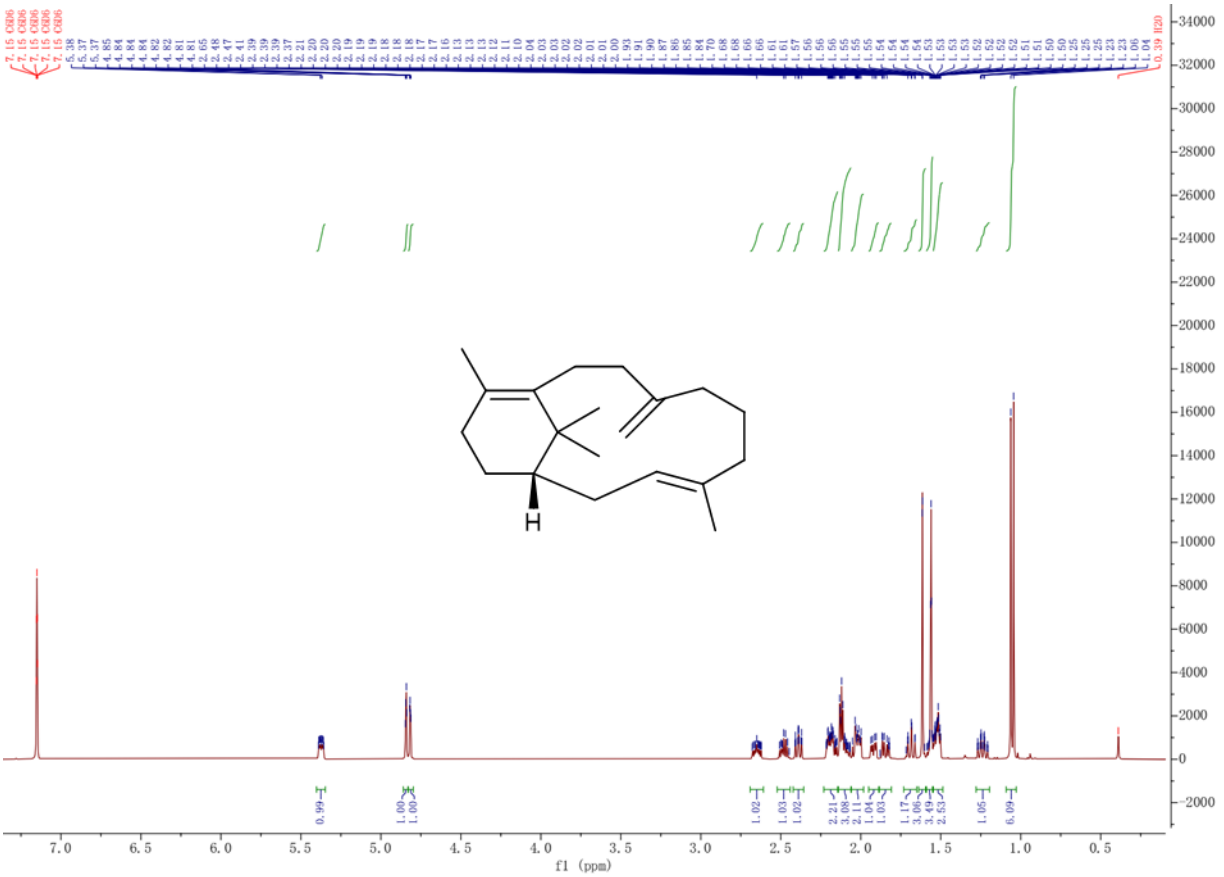

Supplementary Fig. 67. ^{1}H NMR spectrum of 1*S*-verticilla-3,8(19),11(12)-triene (**8**) in C_6D_6 (600 MHz).

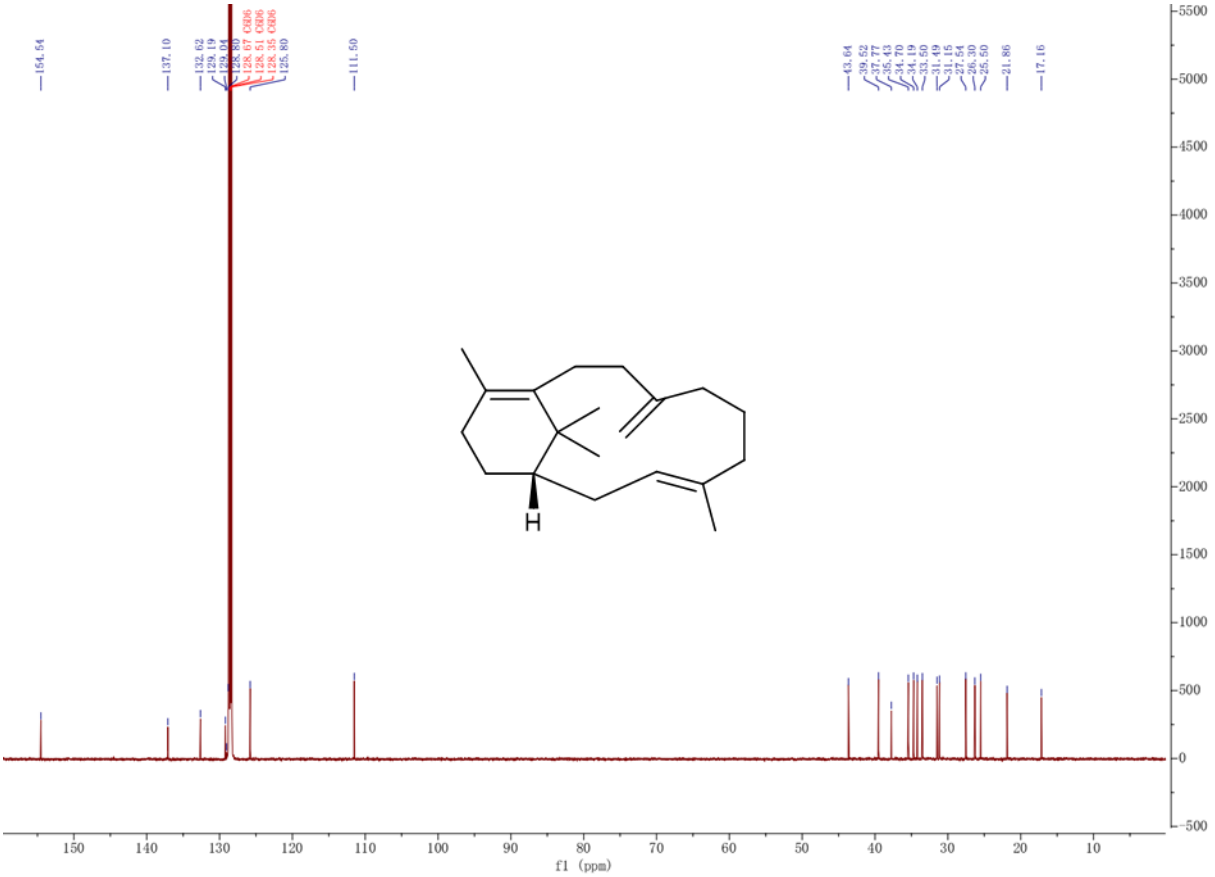

Supplementary Fig. 68. ^{13}C NMR spectrum of 1*S*-verticilla-3,8(19),11(12)-triene (**8**) in C_6D_6 (151 MHz).

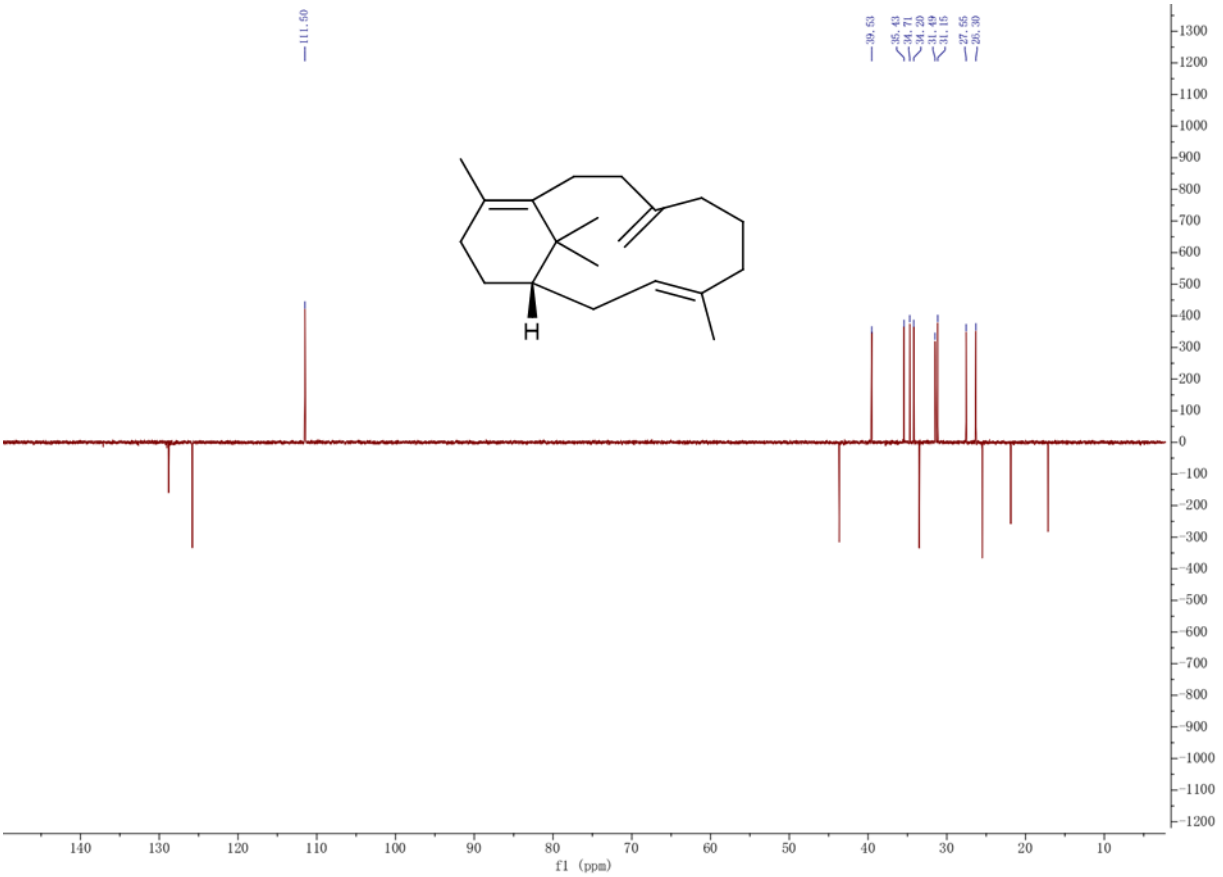

Supplementary Fig. 69. DEPT 135 spectrum of 1*S*-verticilla-3,8(19),11(12)-triene (**8**) in C_6D_6 (151 MHz).

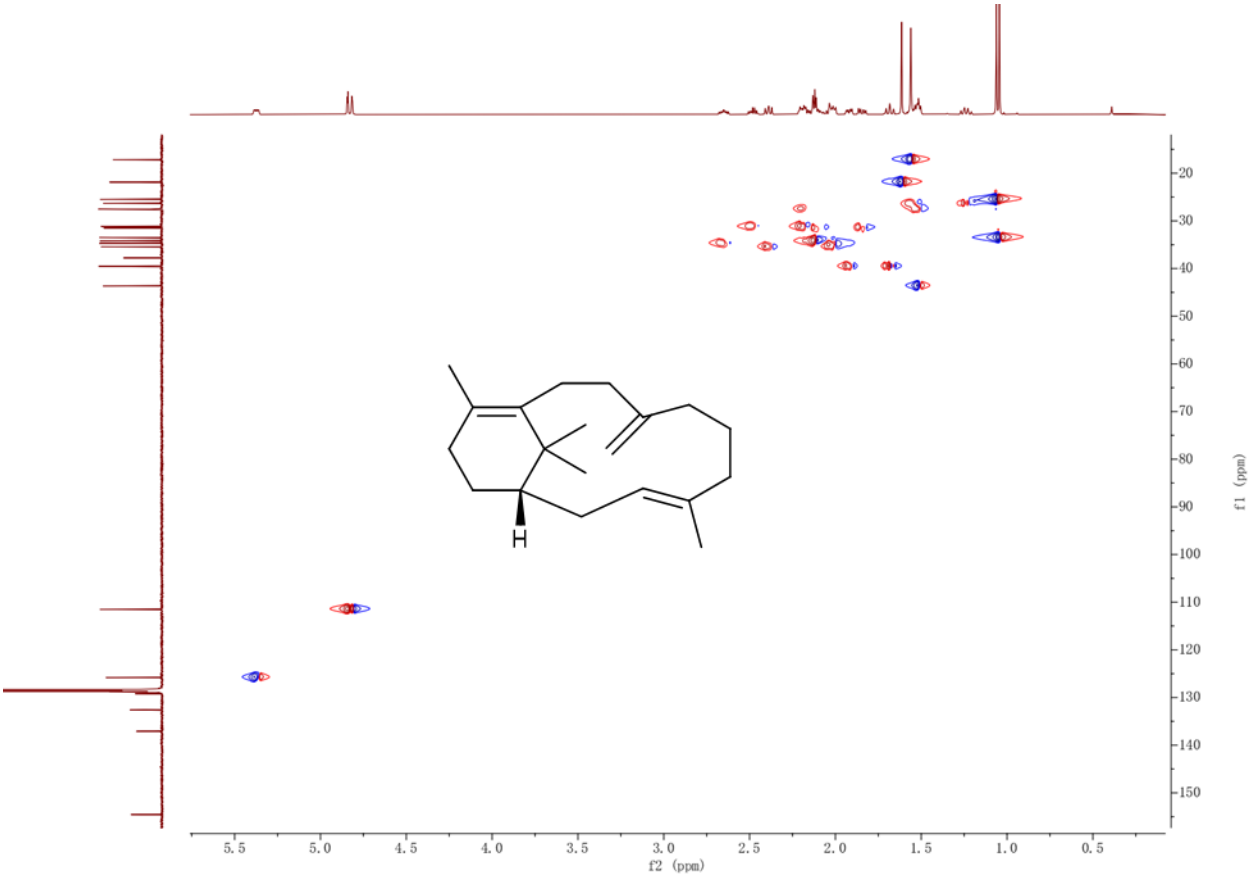

Supplementary Fig. 70. HSQC spectrum of 1*S*-verticilla-3,8(19),11(12)-triene (**8**) in C_6D_6.

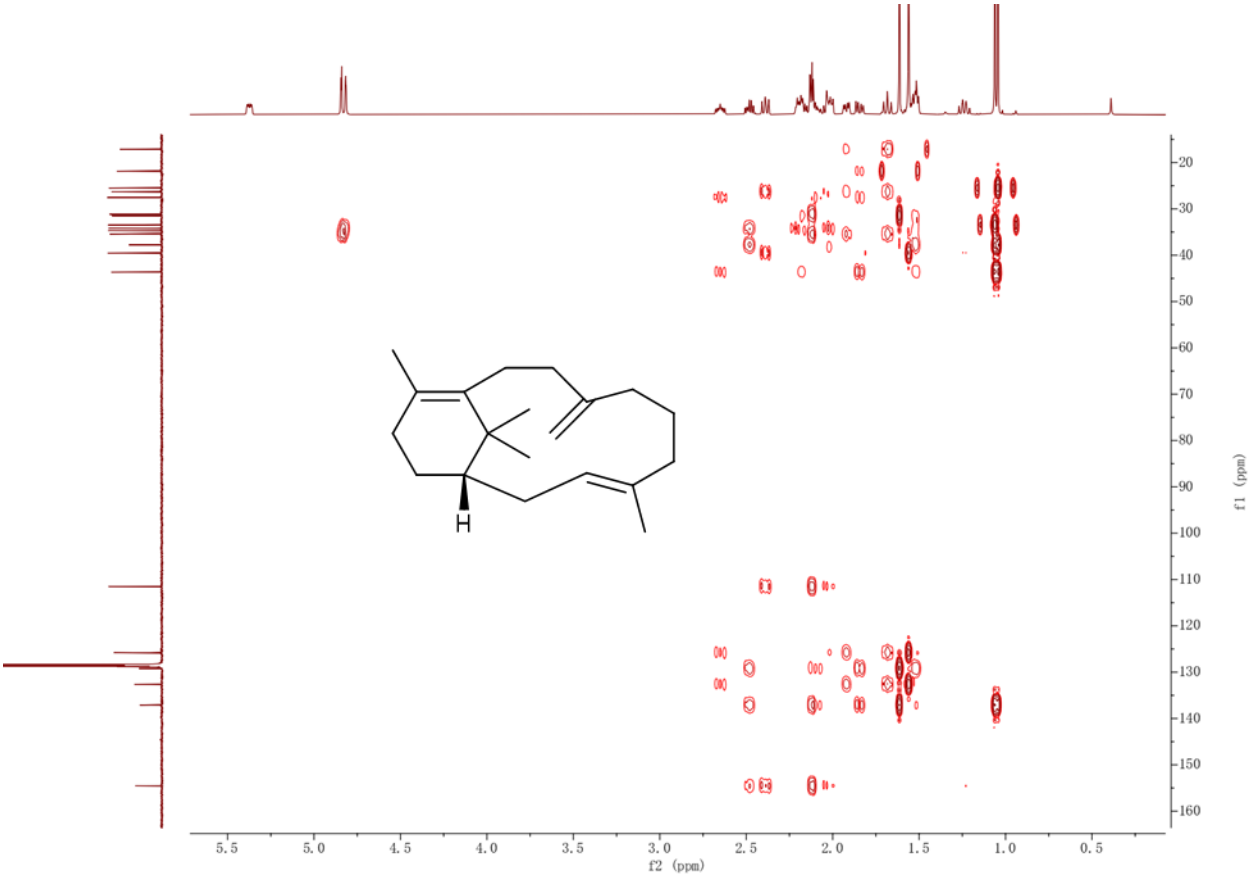

Supplementary Fig. 71. HMBC spectrum of 1*S*-Verticilla-3,8(19),11(12)-triene (**8**) in C_6D_6.

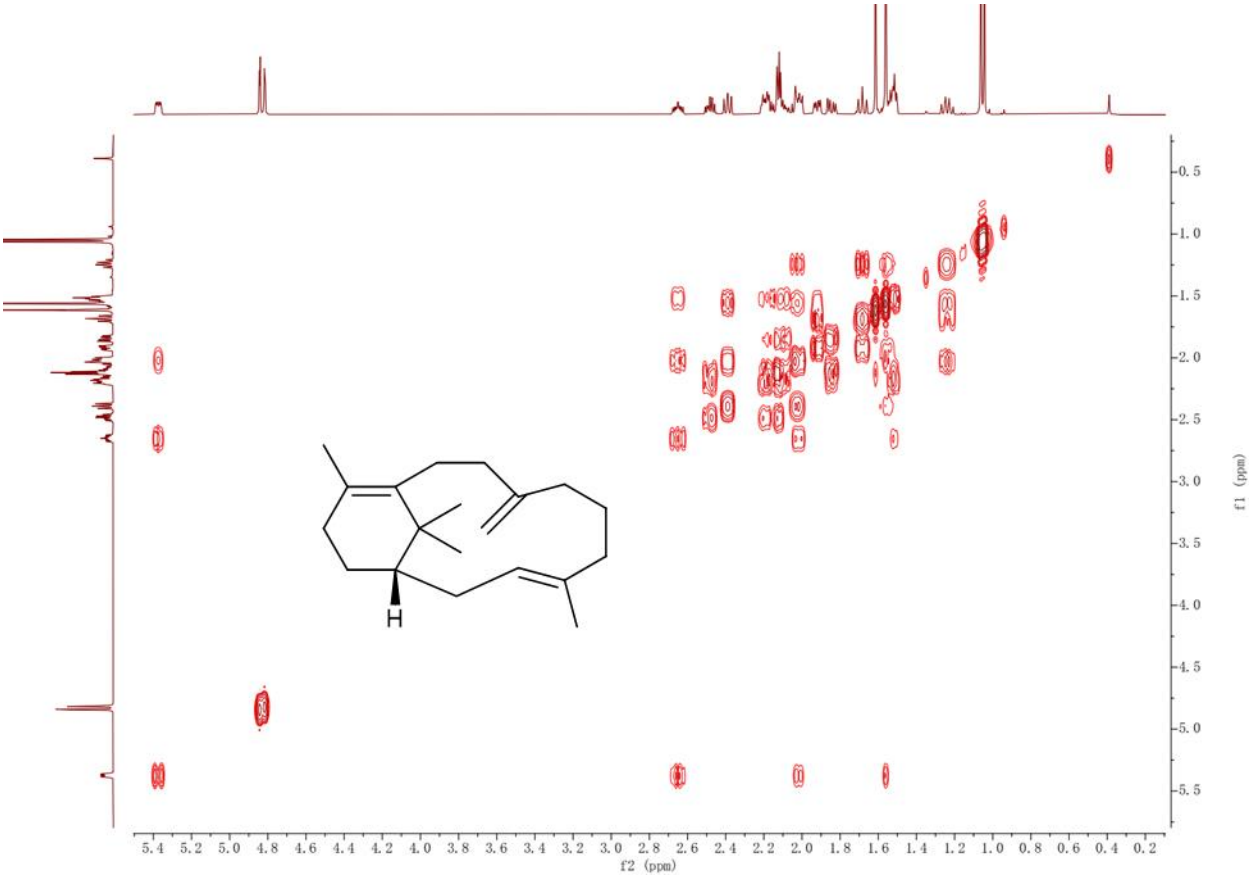

Supplementary Fig. 72. COSY spectrum of 1*S*-Verticilla-3,8(19),11(12)-triene (**8**) in C_6D_6.

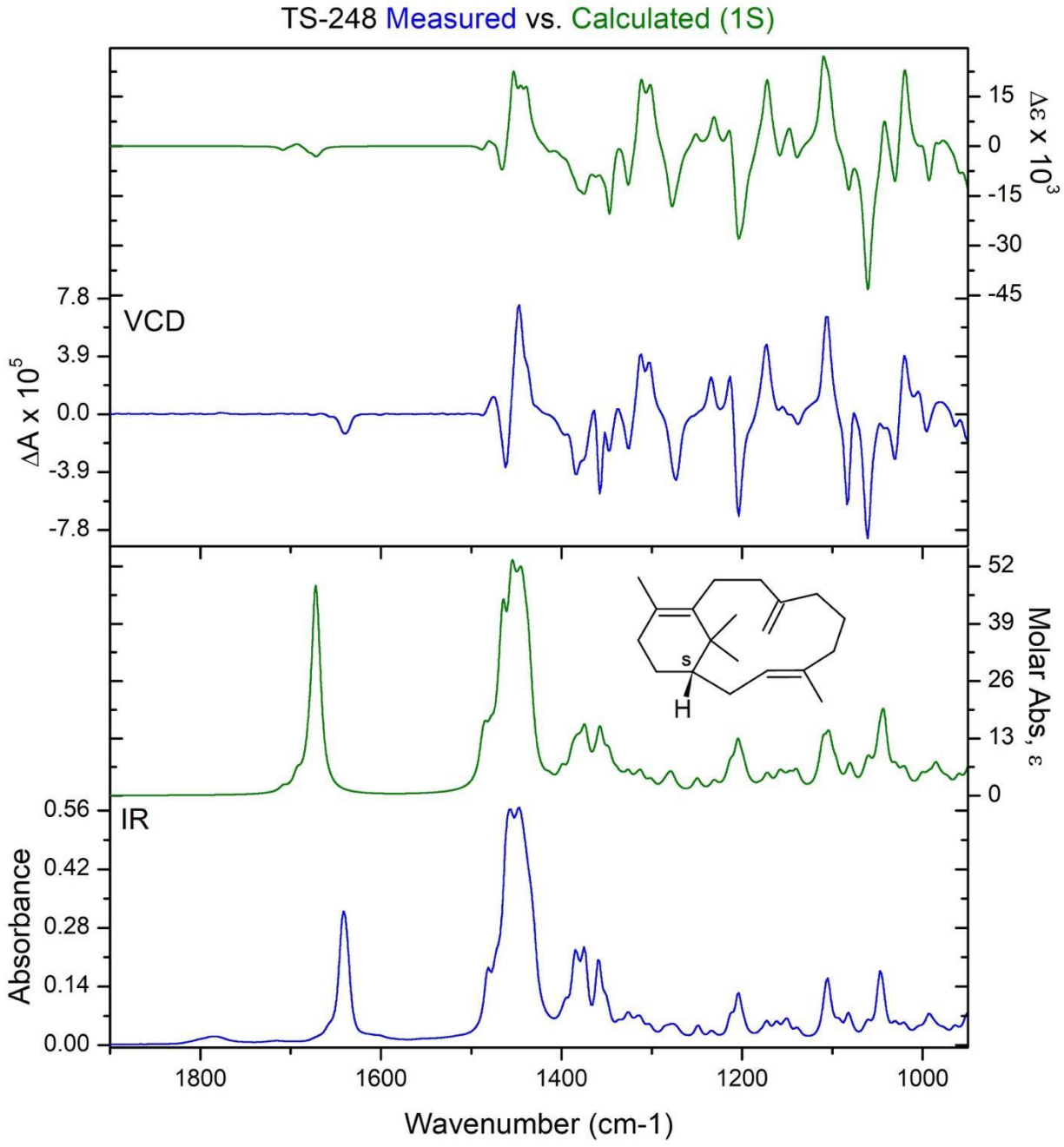

Supplementary Fig. 73. DFT calculated (green) and experimental (blue) VCD and IR spectra of 1*S*-Verticilla-3,8(19),11(12)-triene (**8**).

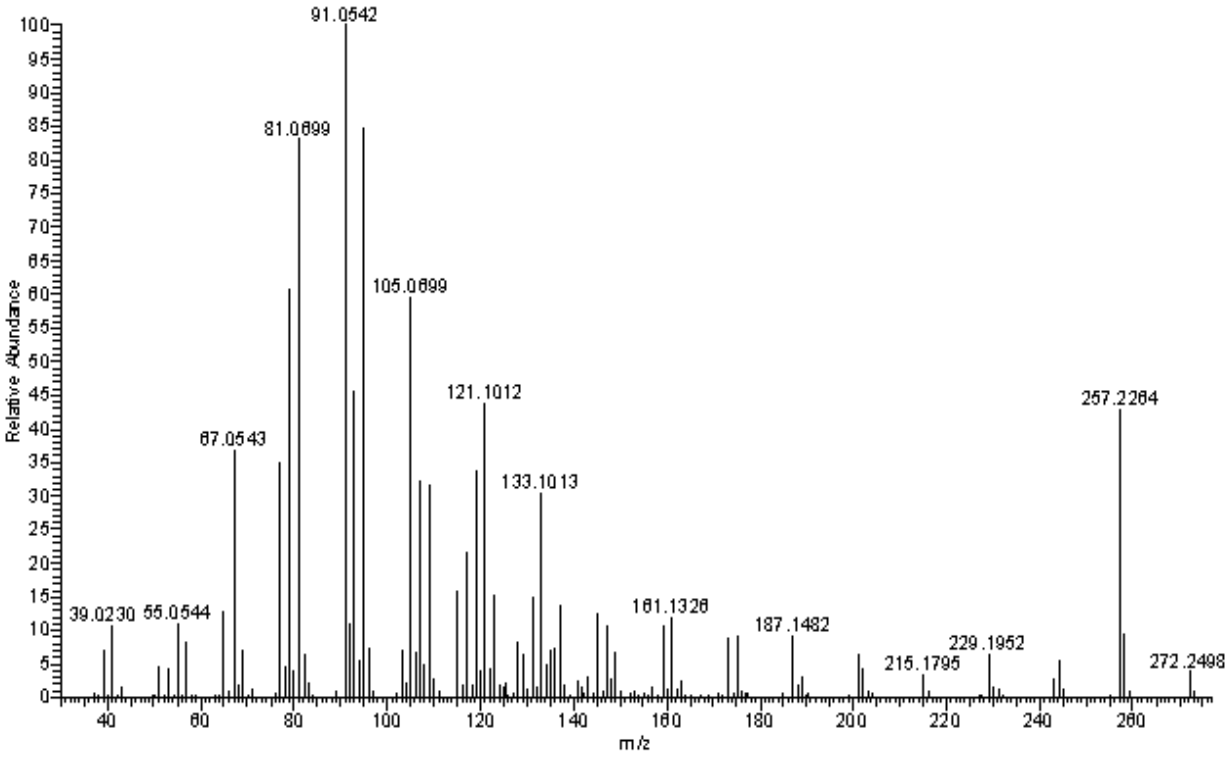

Supplementary Fig. 74. EIMS of (-)-sandaracopimaradiene (**9**). The fragmentation and retention index (RI = 1996) matched the literature (RI = 1999)[26].

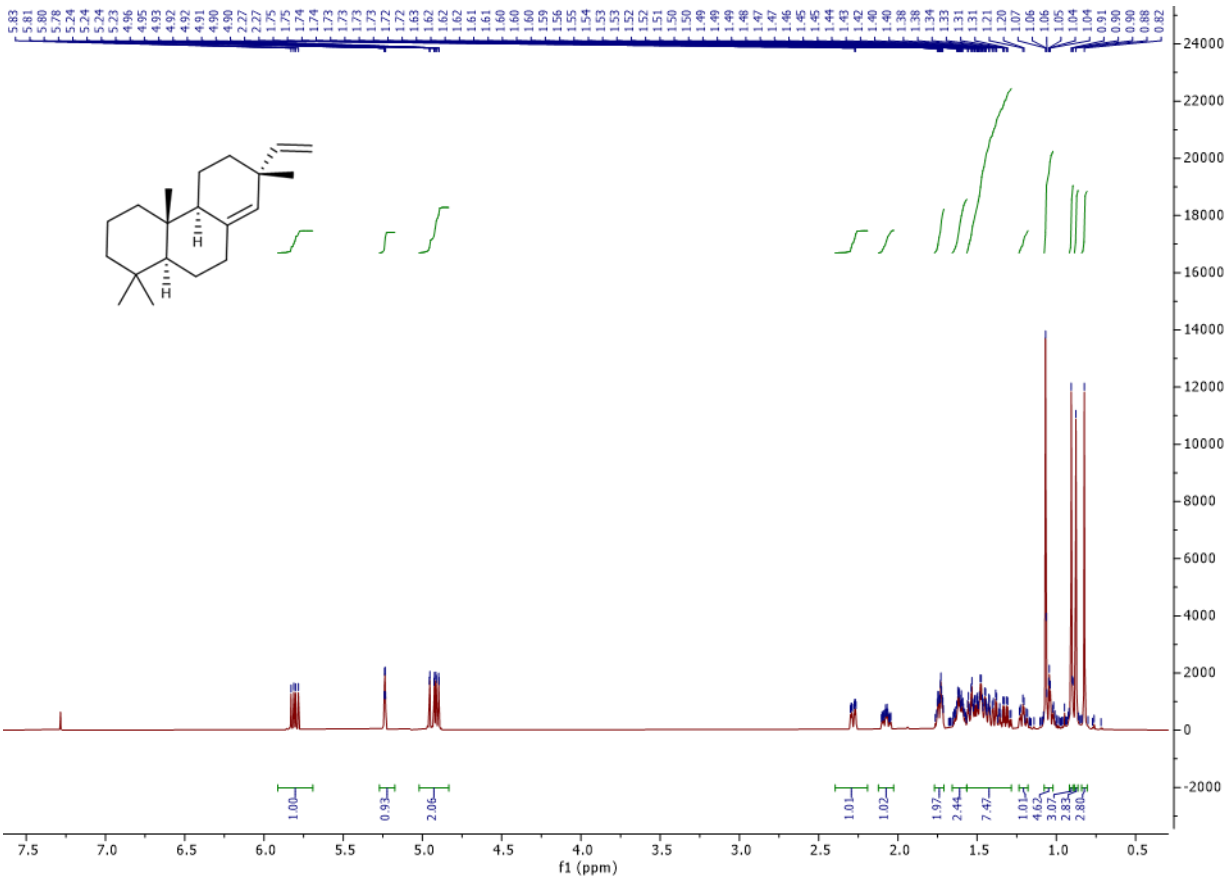

Supplementary Fig. 75. ^{1}H NMR spectrum of (-)-sandaracopimaradiene (**9**) in $CDCl_3$ (600 MHz).

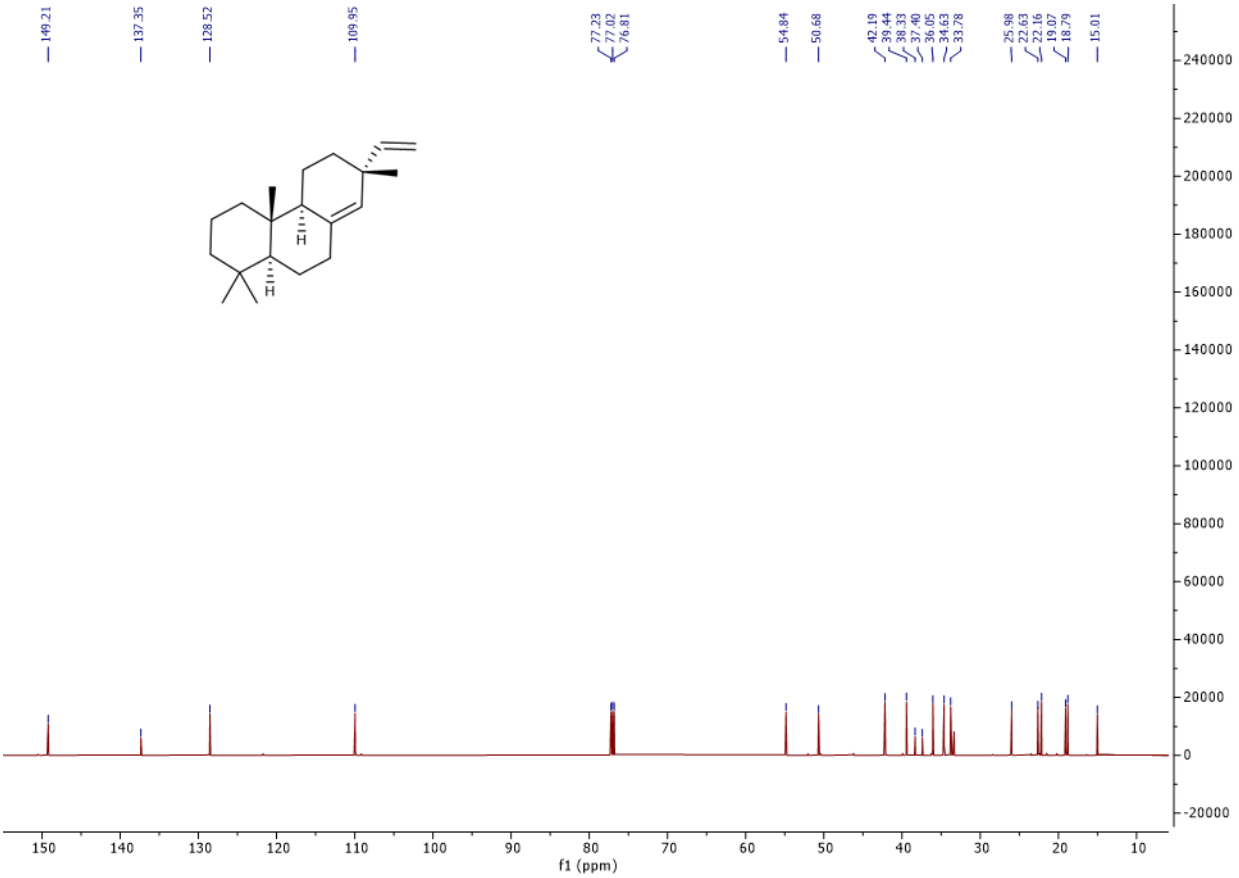

Supplementary Fig. 76. ^{13}C NMR spectrum of (-)-sandaracopimaradiene (**9**) in $CDCl_3$ (151 MHz).

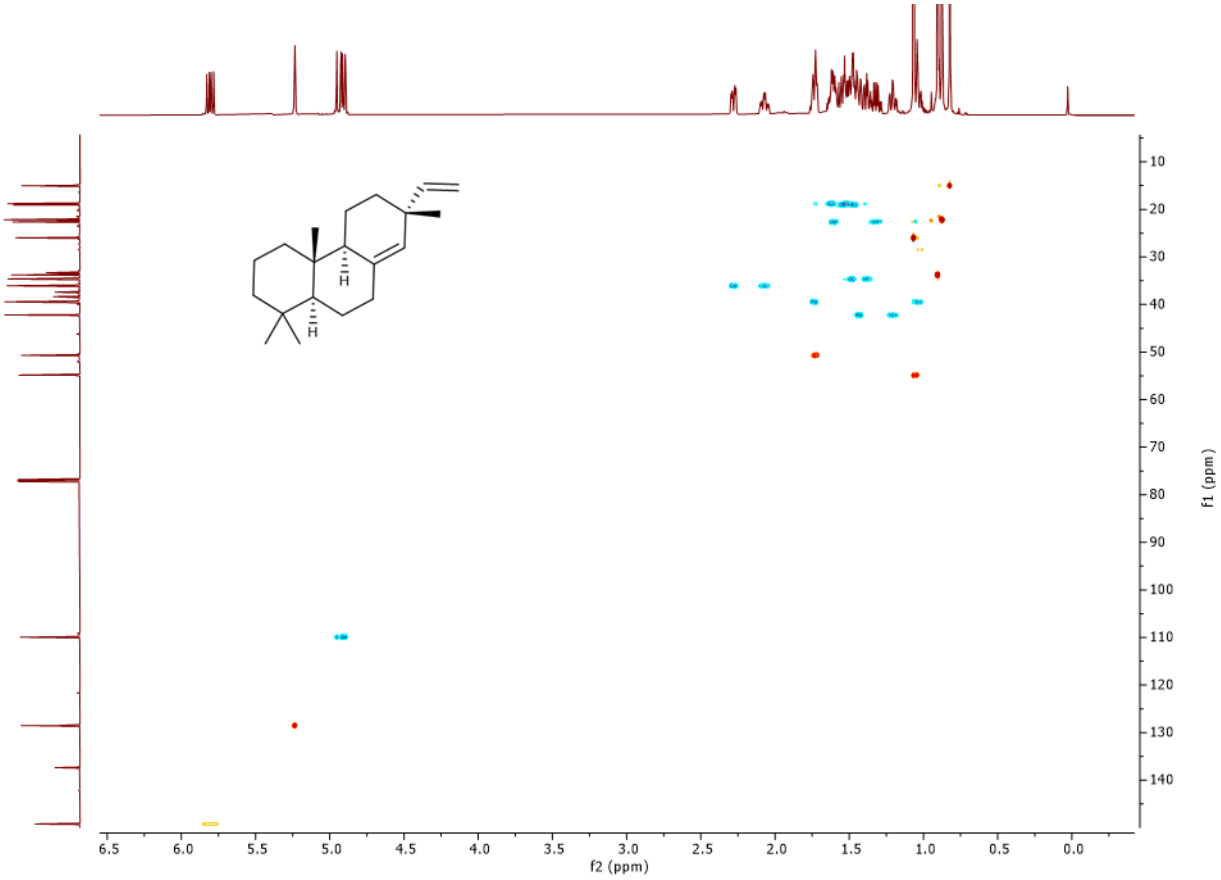

Supplementary Fig. 77. HSQC spectrum of (-)-sandaracopimaradiene (**9**) in $CDCl_3$.

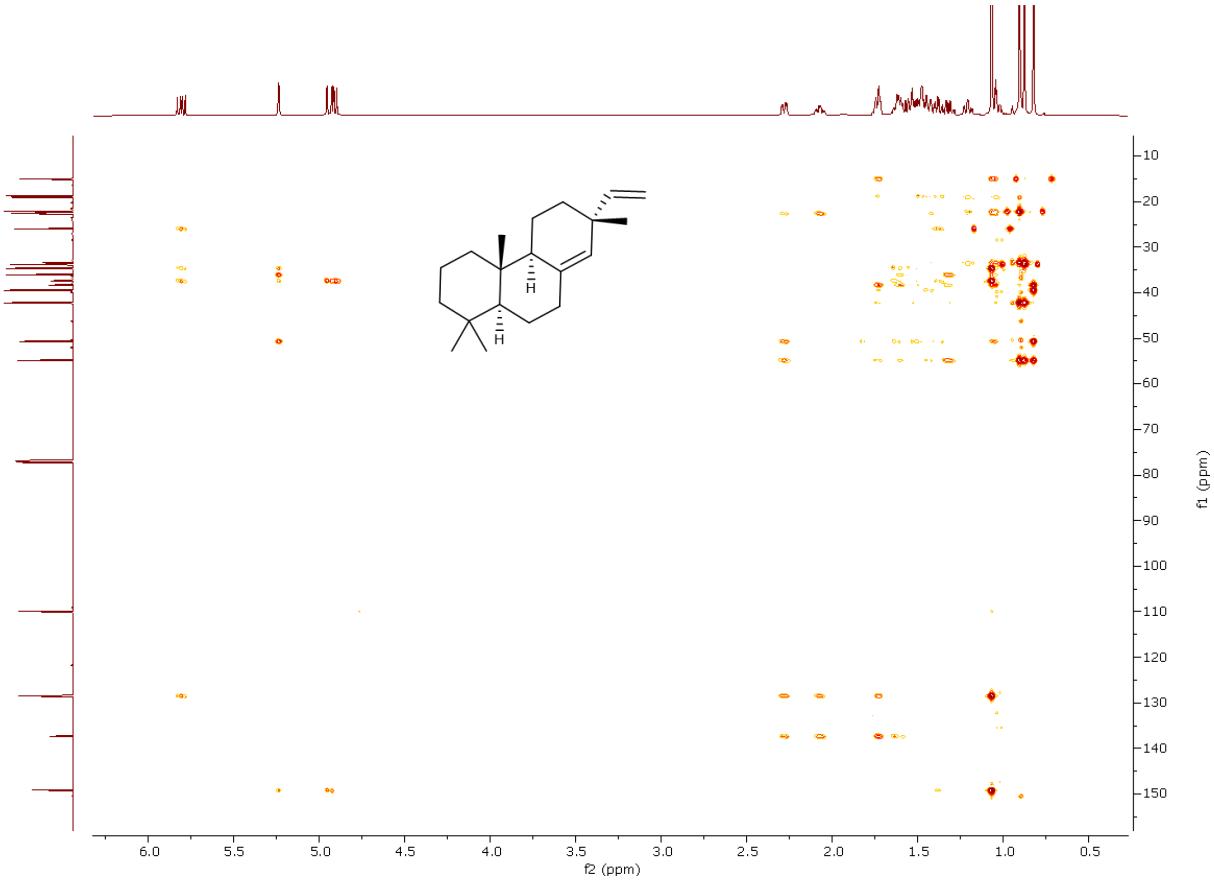

Supplementary Fig. 78. HMBC spectrum of (-)-sandaracopimaradiene (**9**) in $CDCl_3$.

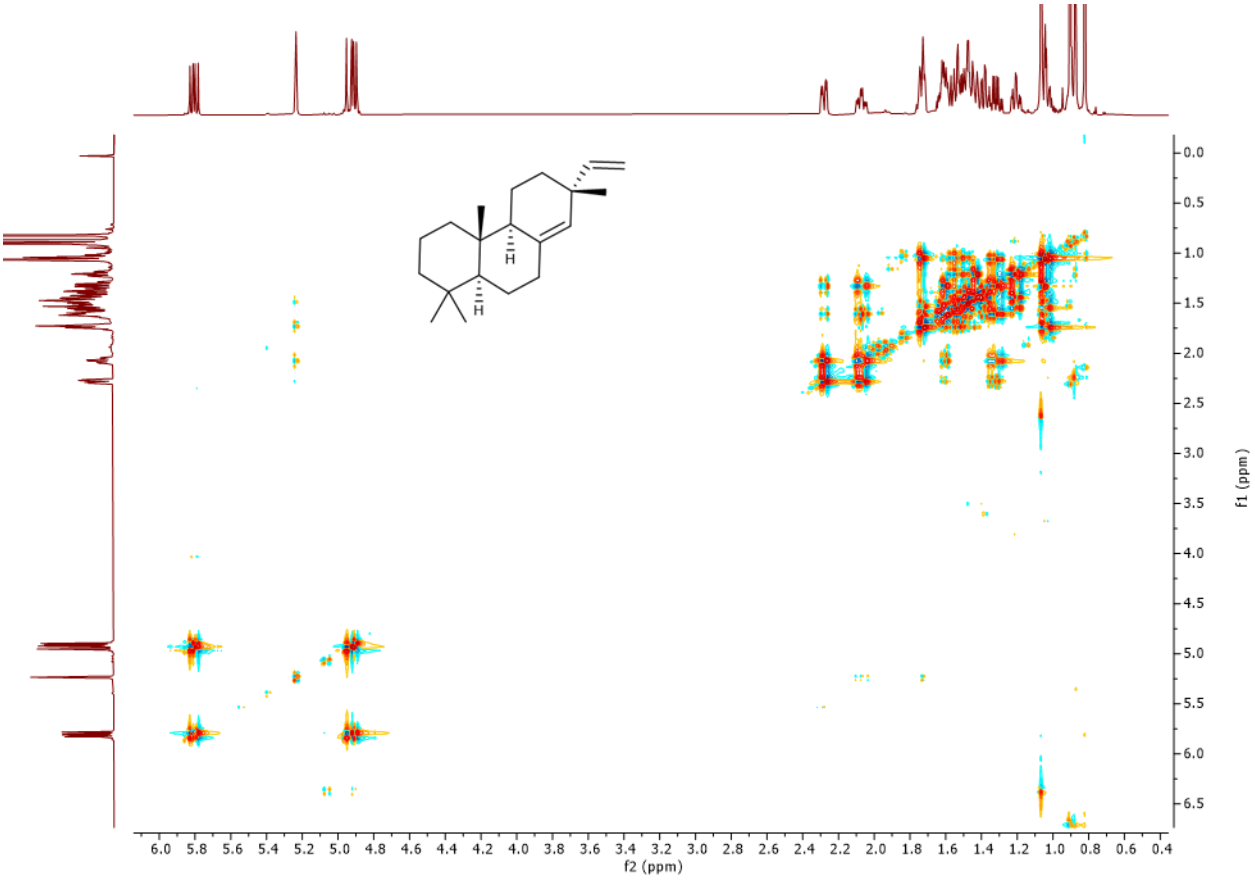

Supplementary Fig. 79. COSY spectrum of (-)-sandaracopimaradiene (**9**) in $CDCl_3$.

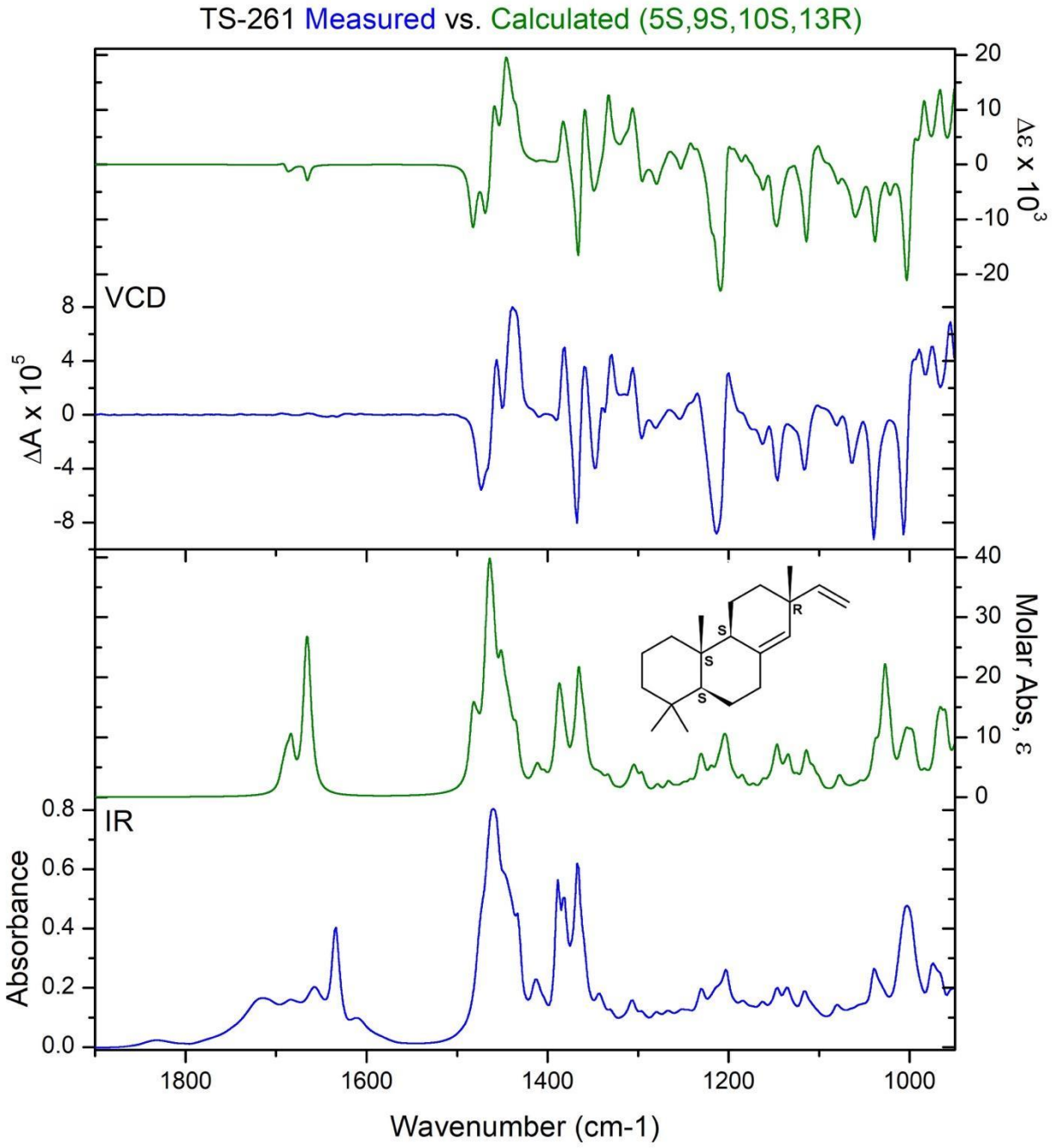

Supplementary Fig. 80. DFT calculated (green) and experimental (blue) VCD and IR spectra of (-)-sandaracopimaradiene (**9**).

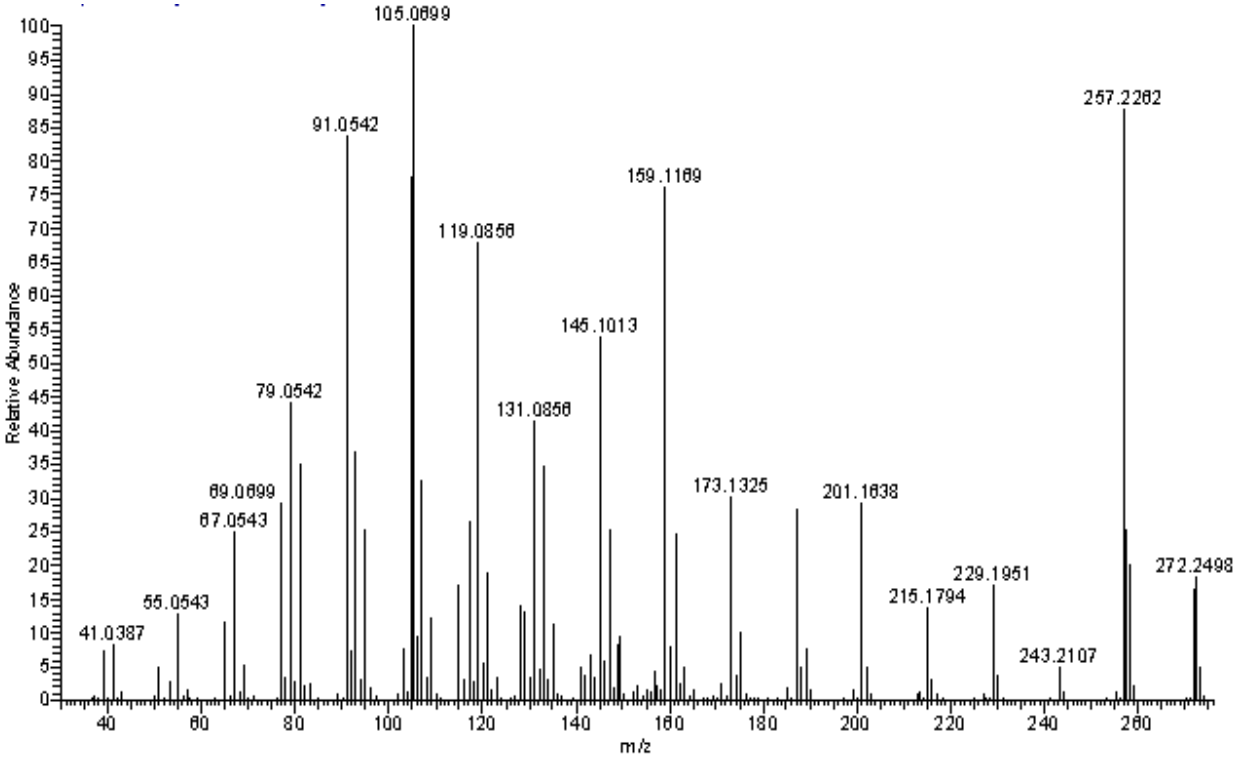

Supplementary Fig. 81. EIMS of venezuelaene A (**10**). The fragmentation matched the literature[11].

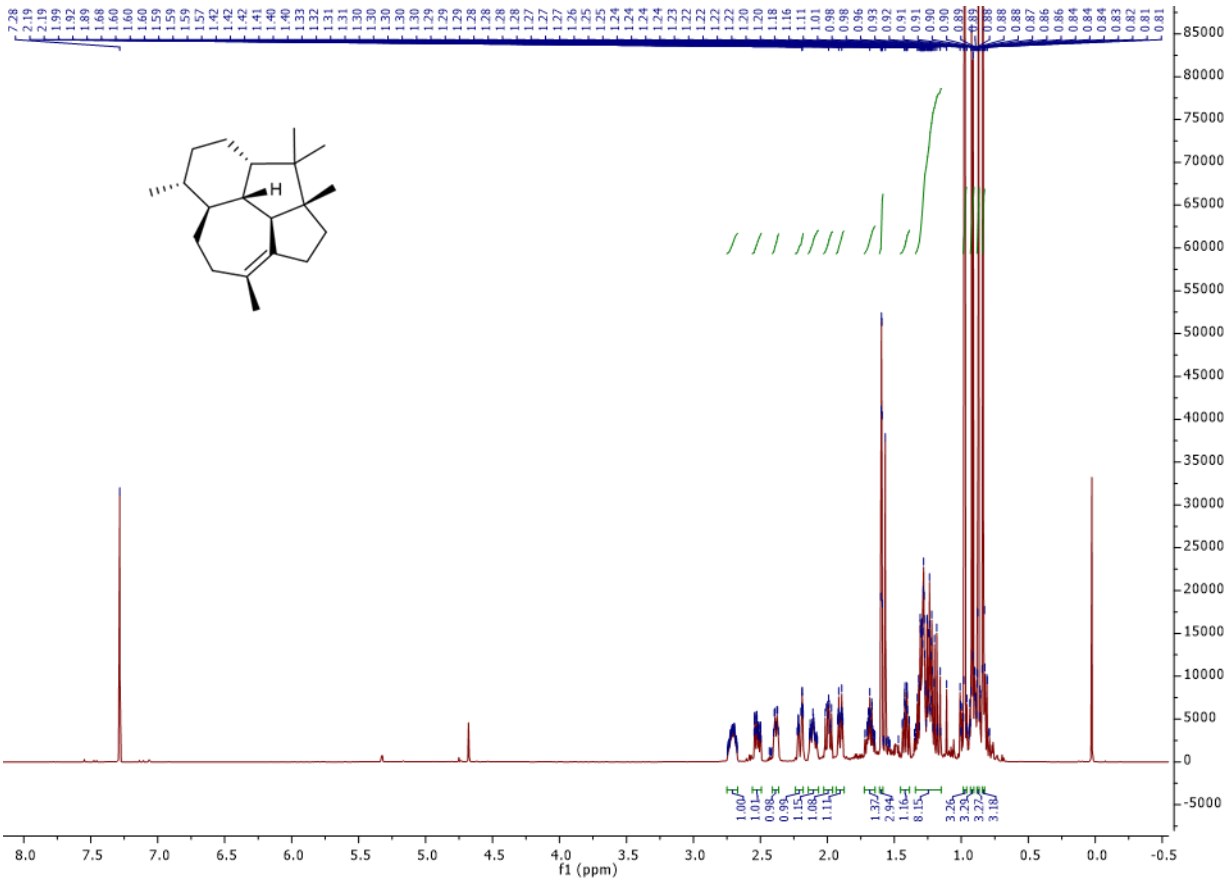

Supplementary Fig. 82. ^{1}H NMR spectrum of venezuelaene A (**10**) in $CDCl_3$ (600 MHz).

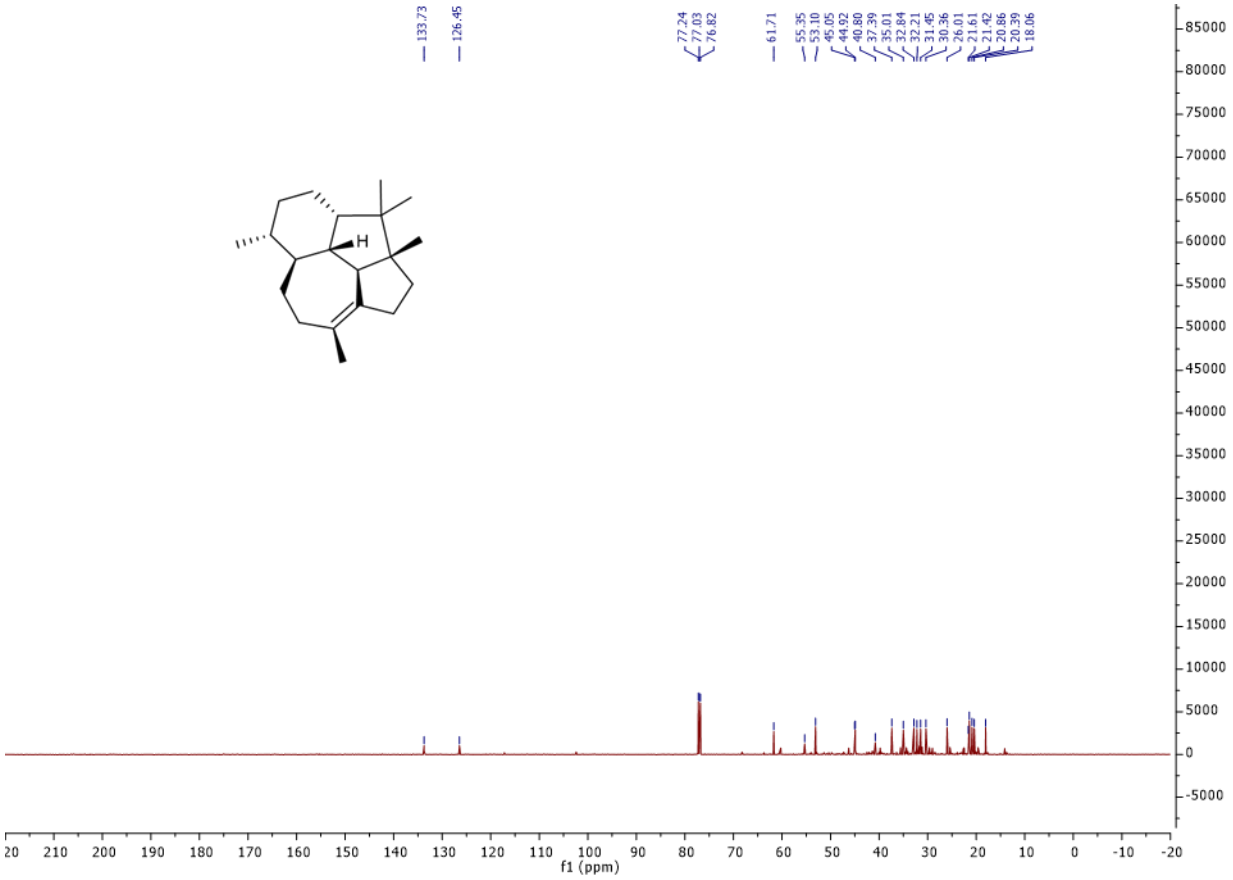

Supplementary Fig. 83. ^{13}C NMR spectrum of venezuelaene A (**10**) in $CDCl_3$ (151 MHz).

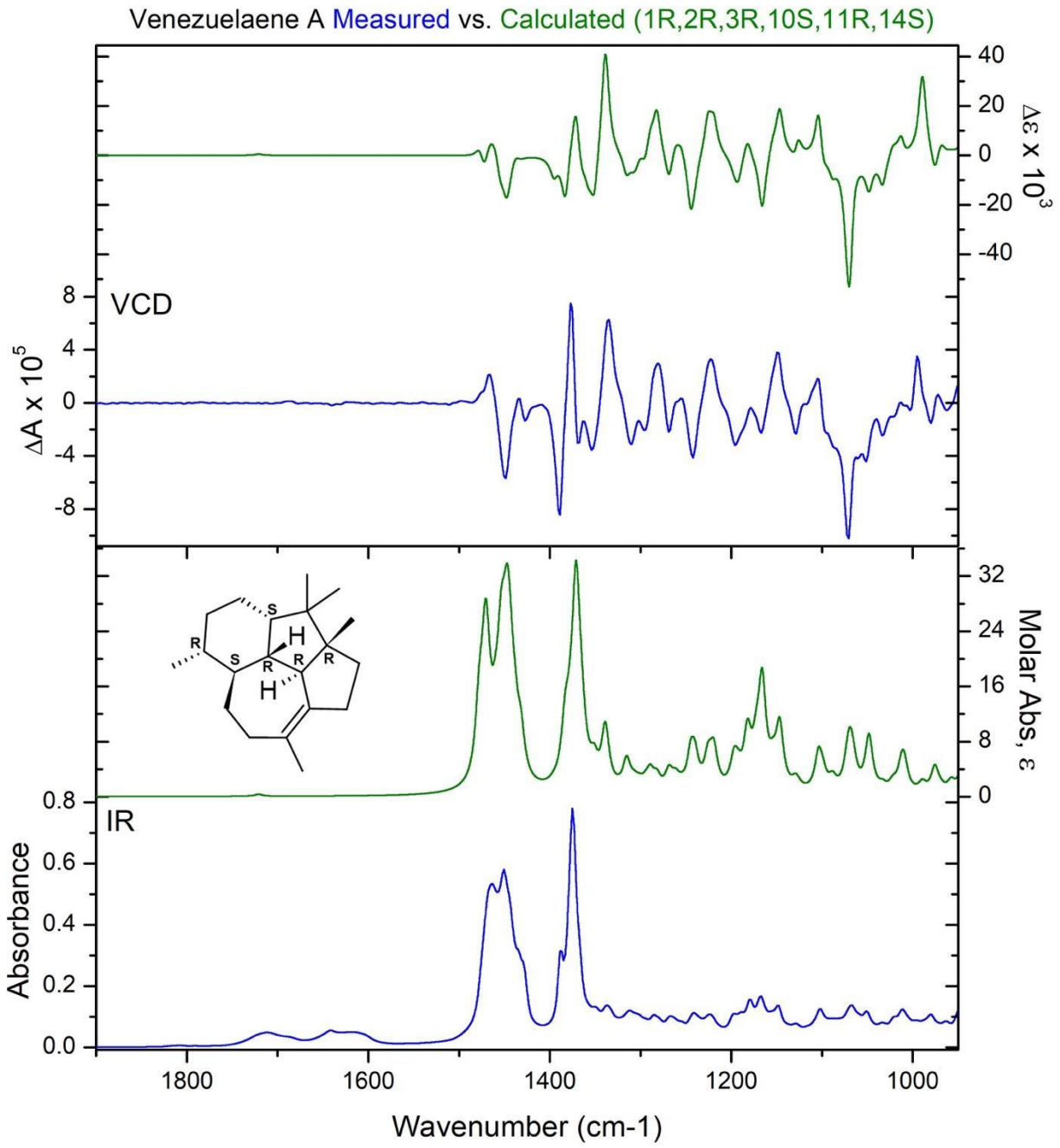

Supplementary Fig. 84. DFT calculated (green) and experimental (blue) VCD and IR spectra of venezuelaene A (**10**).

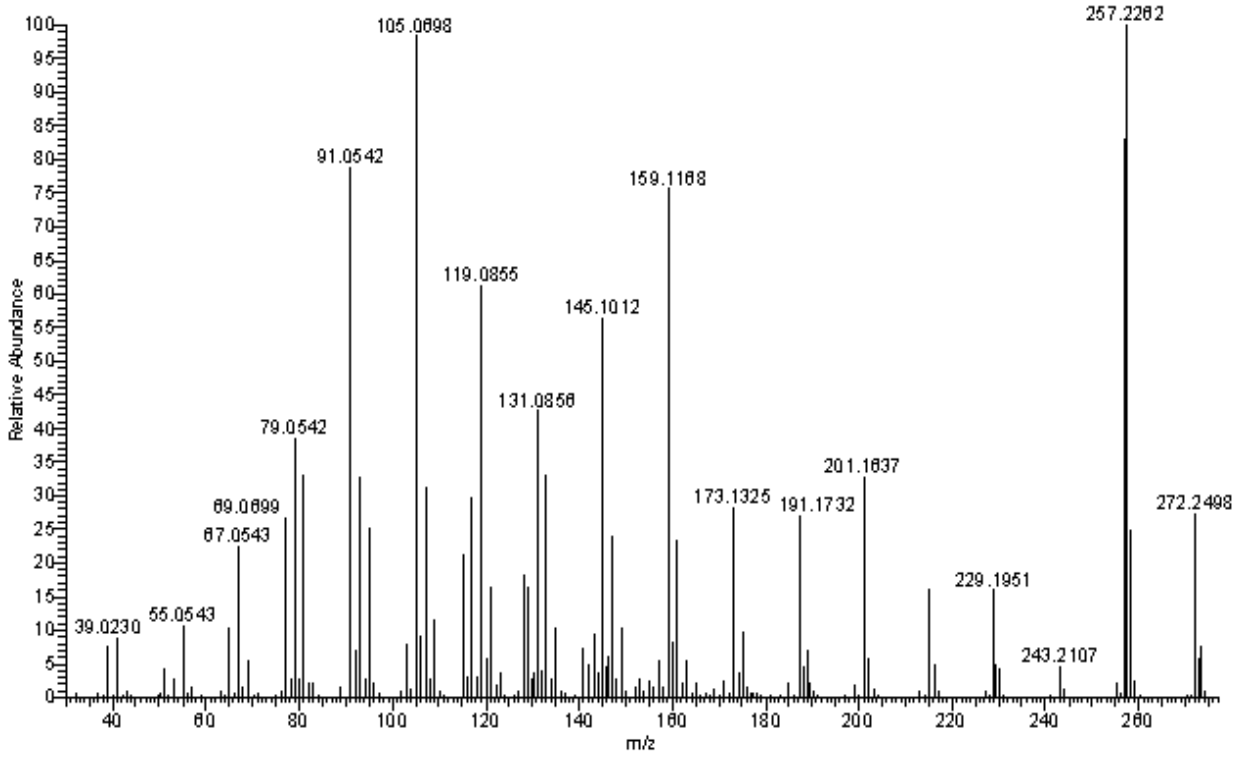

Supplementary Fig. 85. EIMS of venezuelaene A2 (**11**).

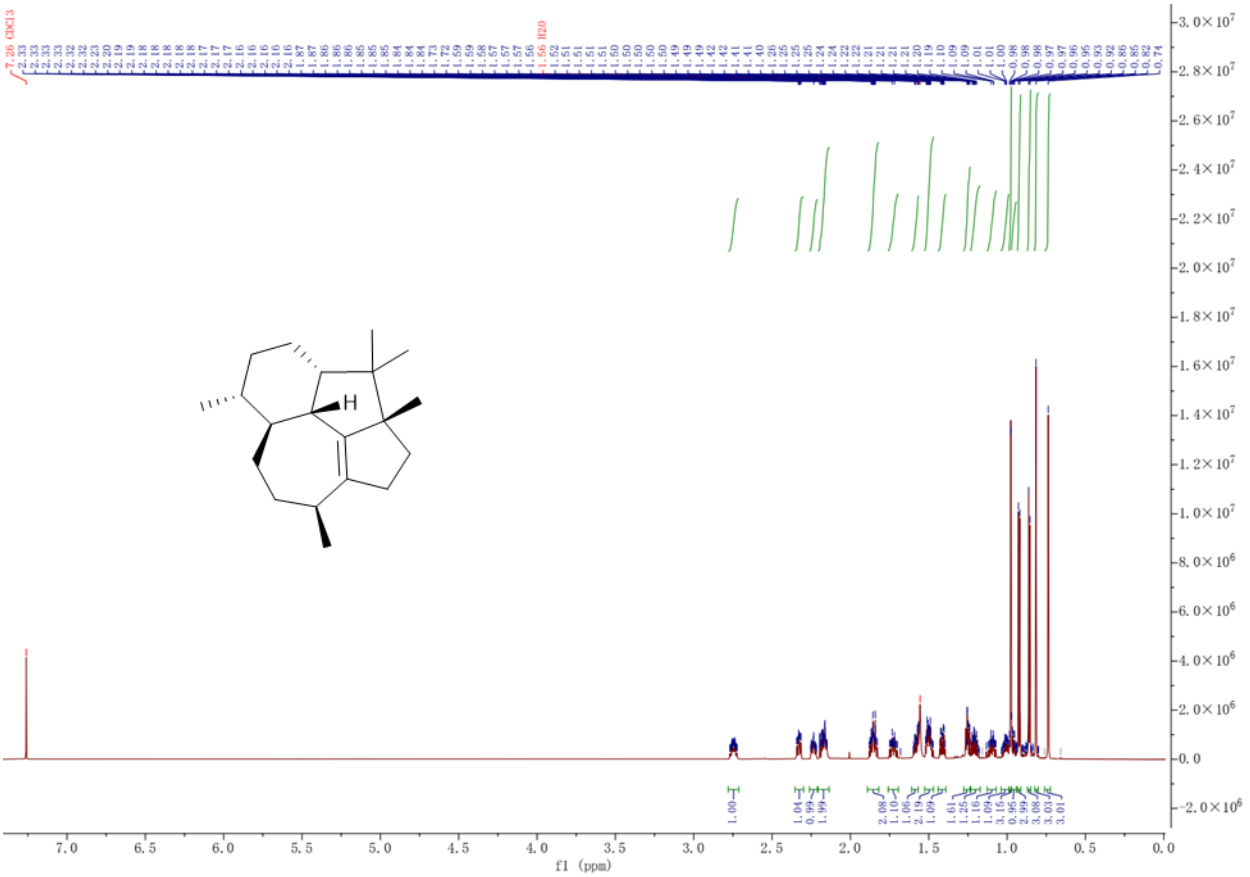

Supplementary Fig. 86. ^{1}H NMR spectrum of venezuelaene A2 (**11**) in $CDCl_3$ (800 MHz).

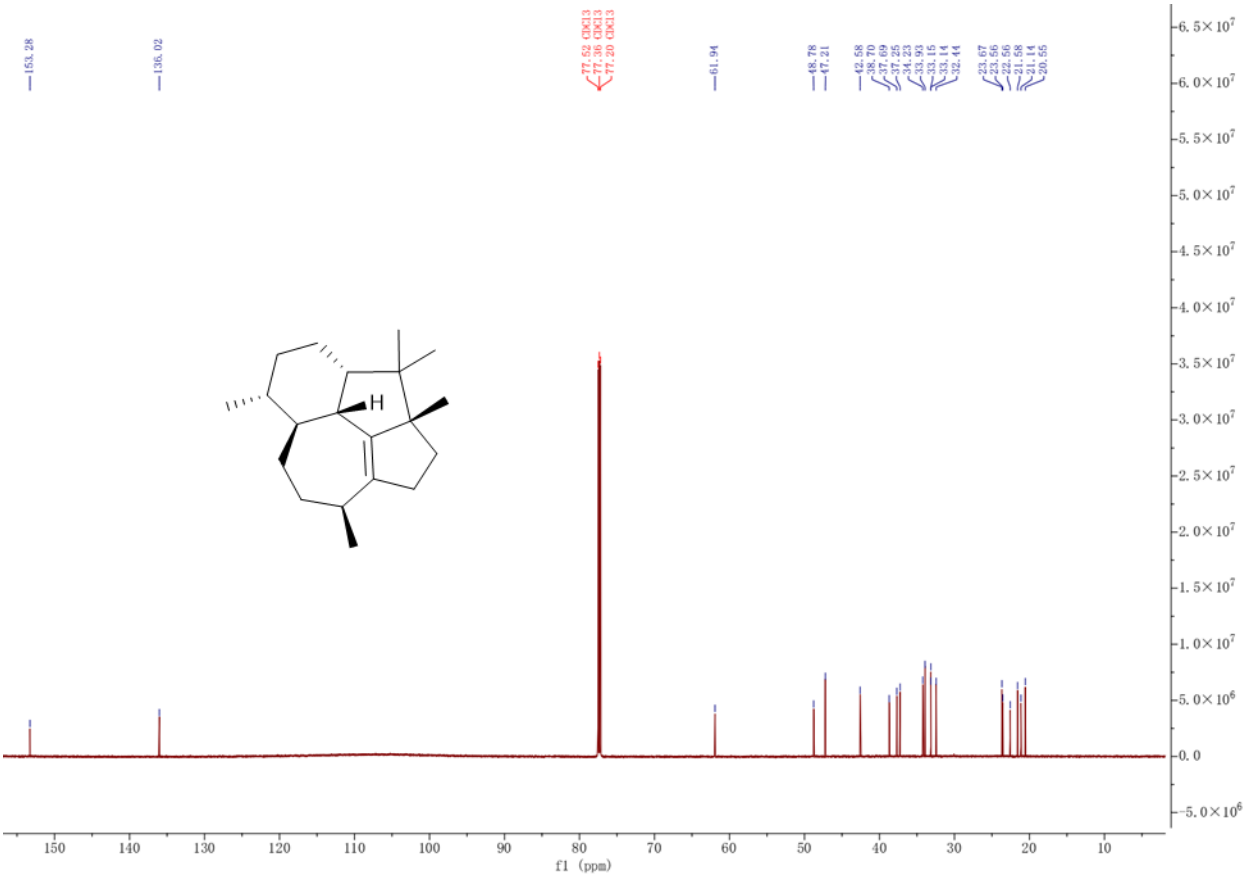

Supplementary Fig. 87. ^{13}C NMR spectrum of venezuelaene A2 (**11**) in $CDCl_3$ (200 MHz).

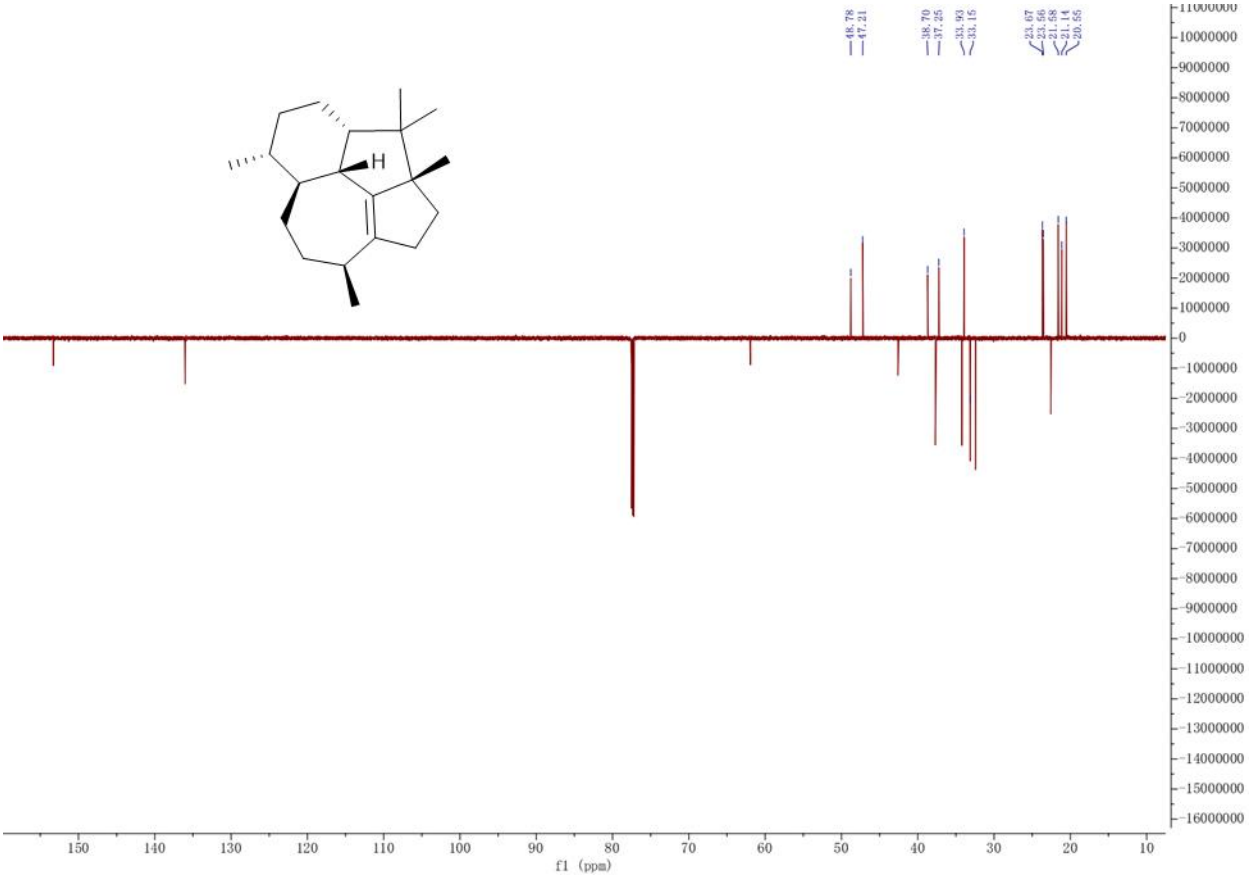

Supplementary Fig. 88. DEPTQ 135 spectrum of venezuelaene A2 (**11**) in $CDCl_3$ (151 MHz).

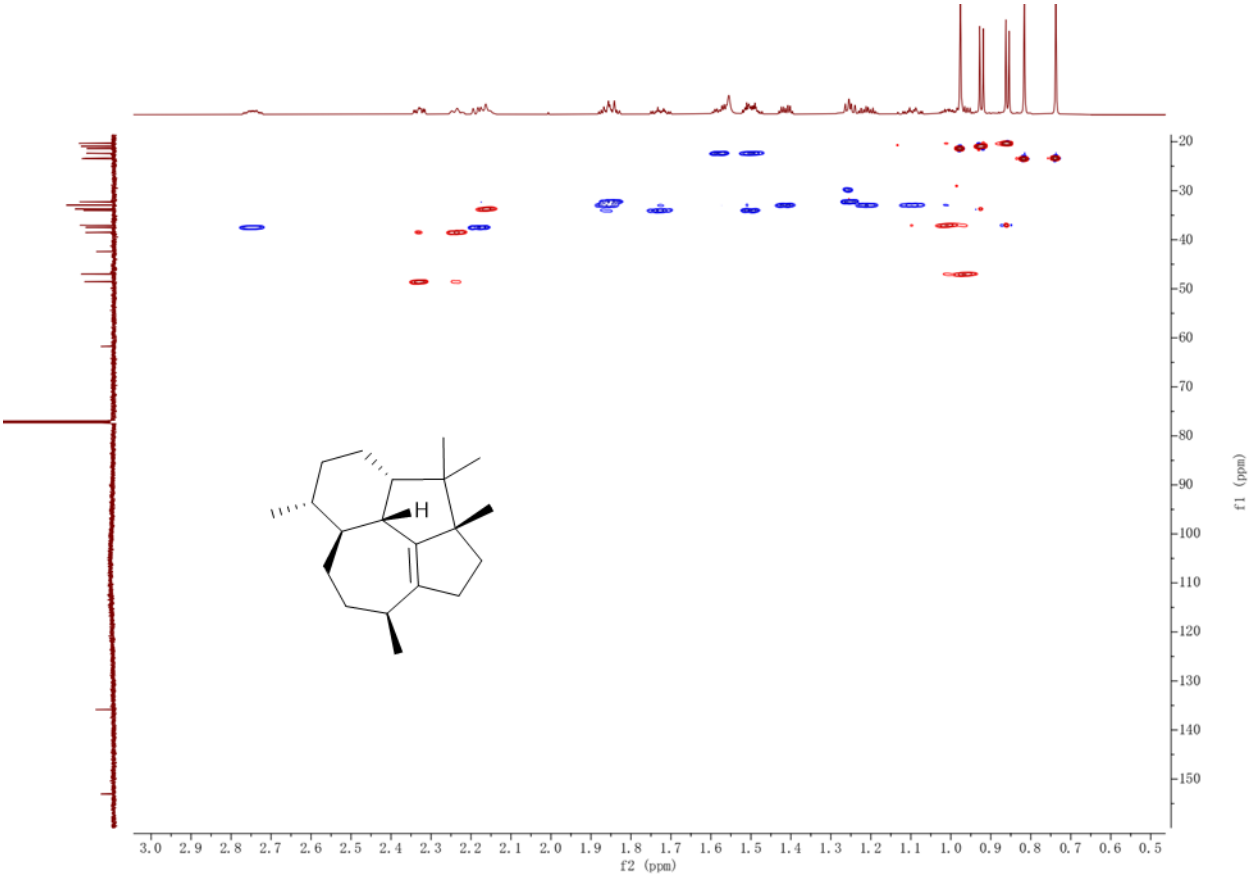

Supplementary Fig. 89. HSQC spectrum of venezuelaene A2 (**11**) in $CDCl_3$.

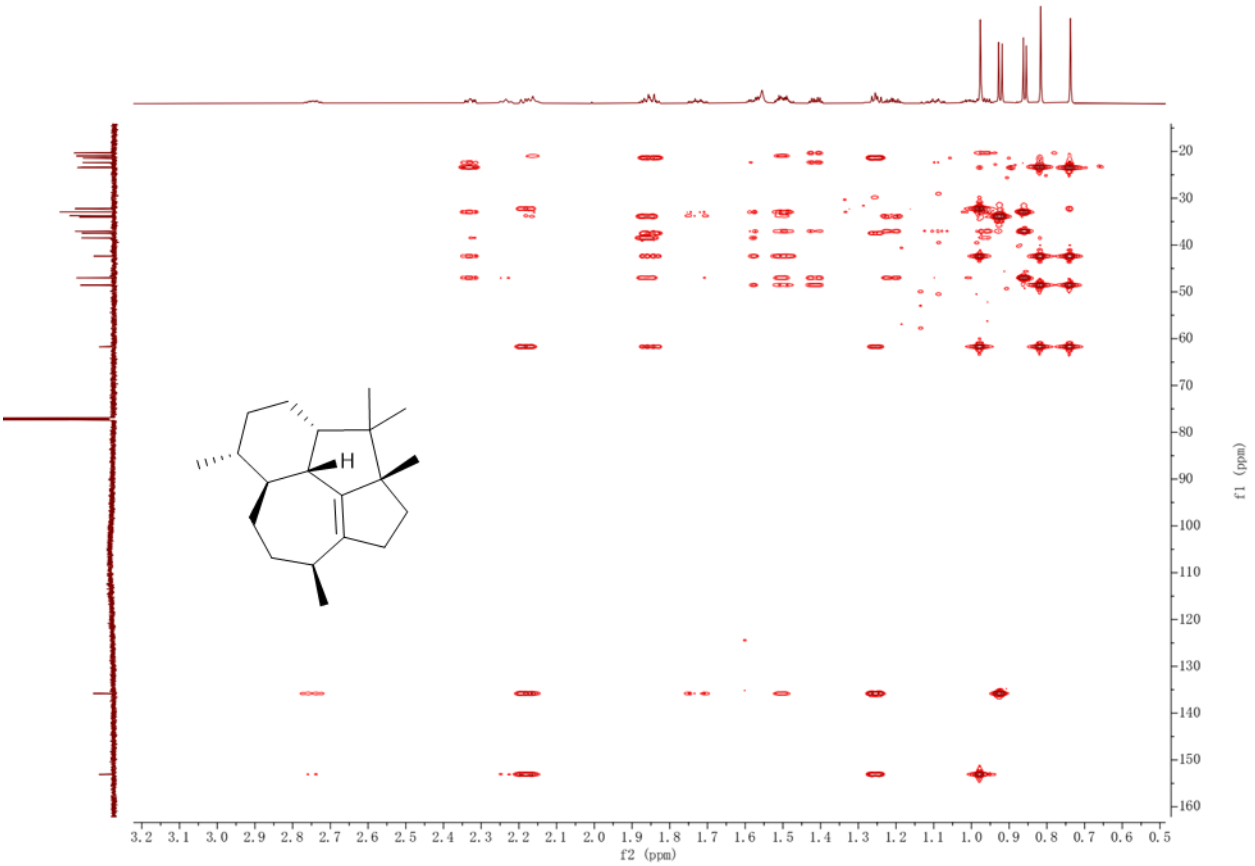

Supplementary Fig. 90. HMBC spectrum of venezuelaene A2 (**11**) in $CDCl_3$.

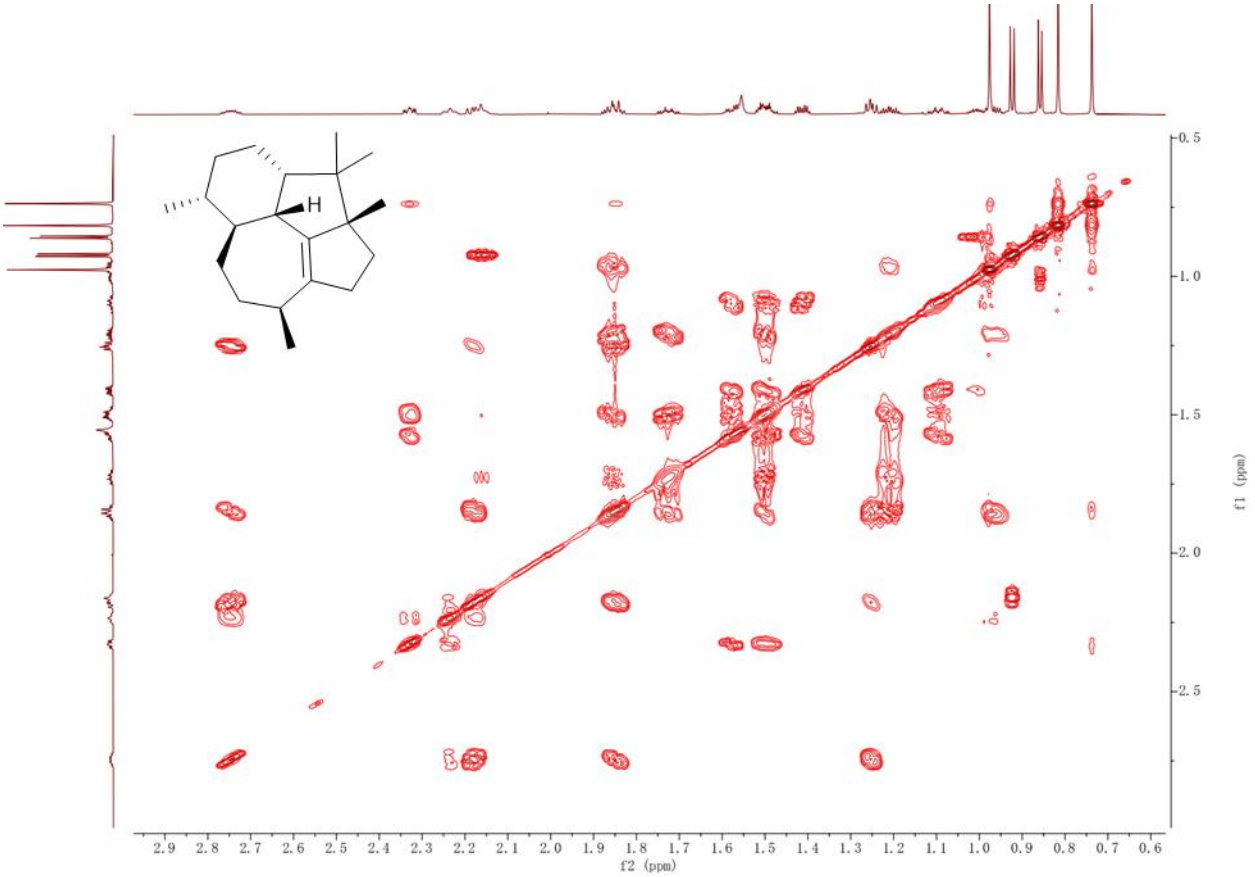

Supplementary Fig. 91. COSY spectrum of venezuelaene A2 (**11**) in $CDCl_3$.

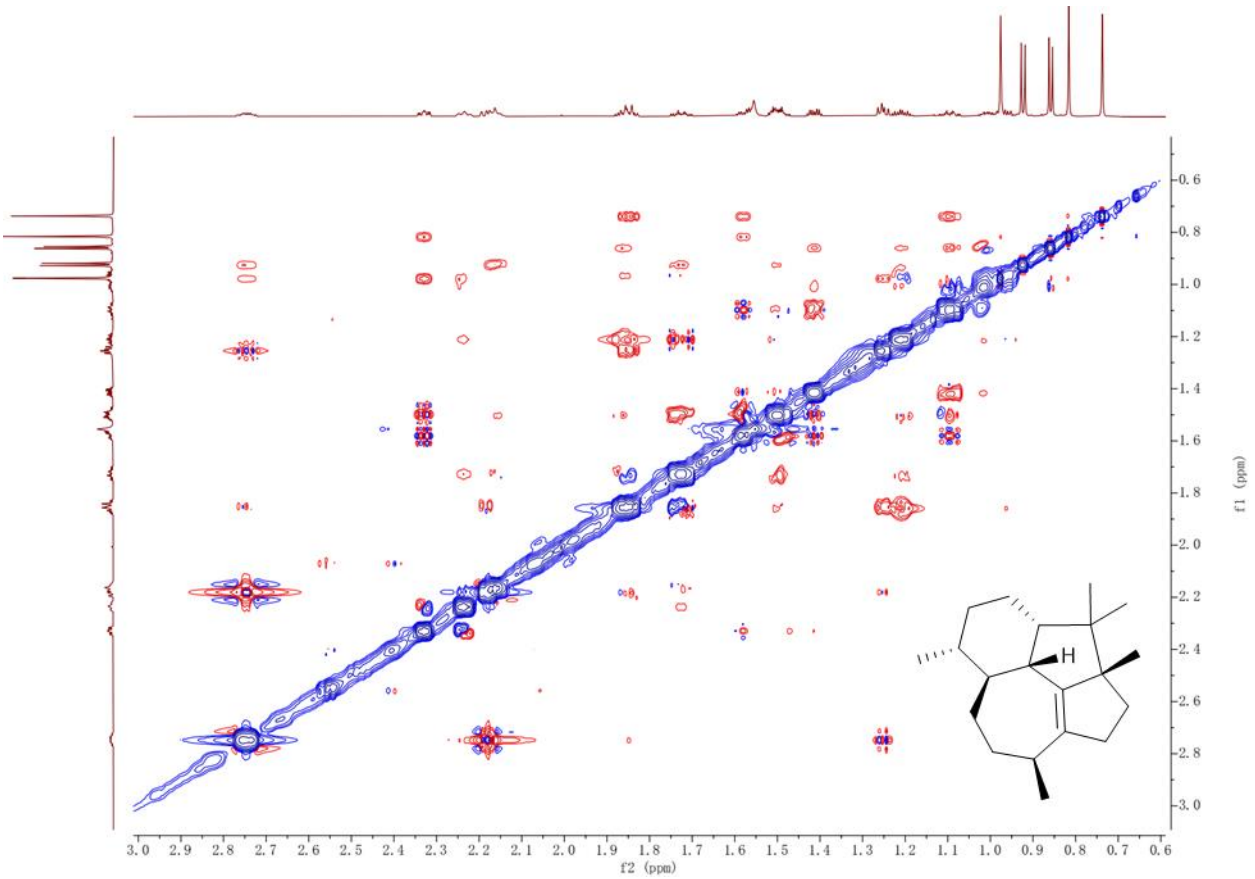

Supplementary Fig. 92. NOESY spectrum of venezuelaene A2 (**11**) in $CDCl_3$ (800 MHz).

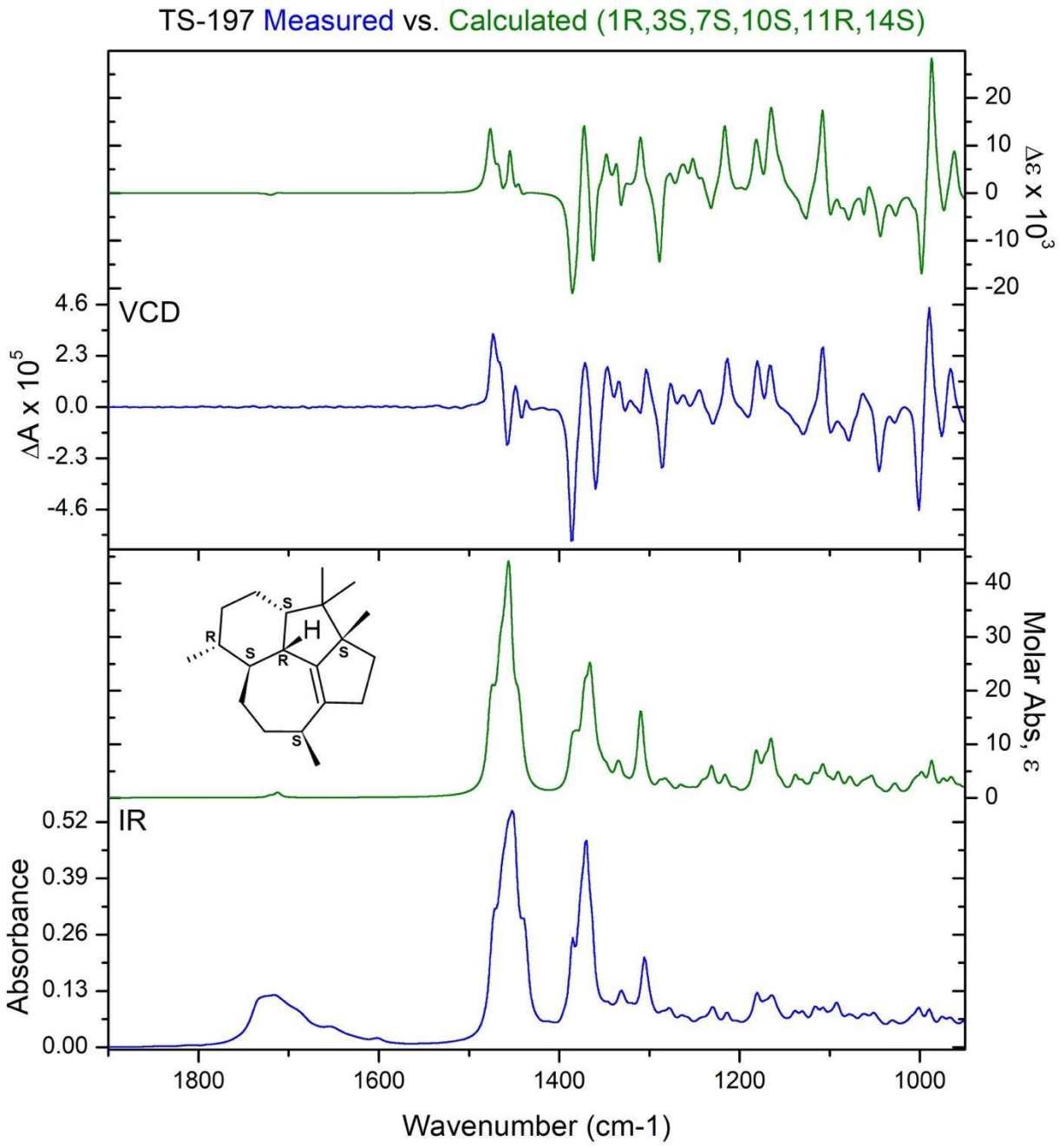

Supplementary Fig. 93. DFT calculated (green) and experimental (blue) VCD and IR spectra of venezuelaene A2 (**11**) supporting the absolute configuration as 1*R*,3*S*,7*S*,10*S*,11*R*,14*S*.

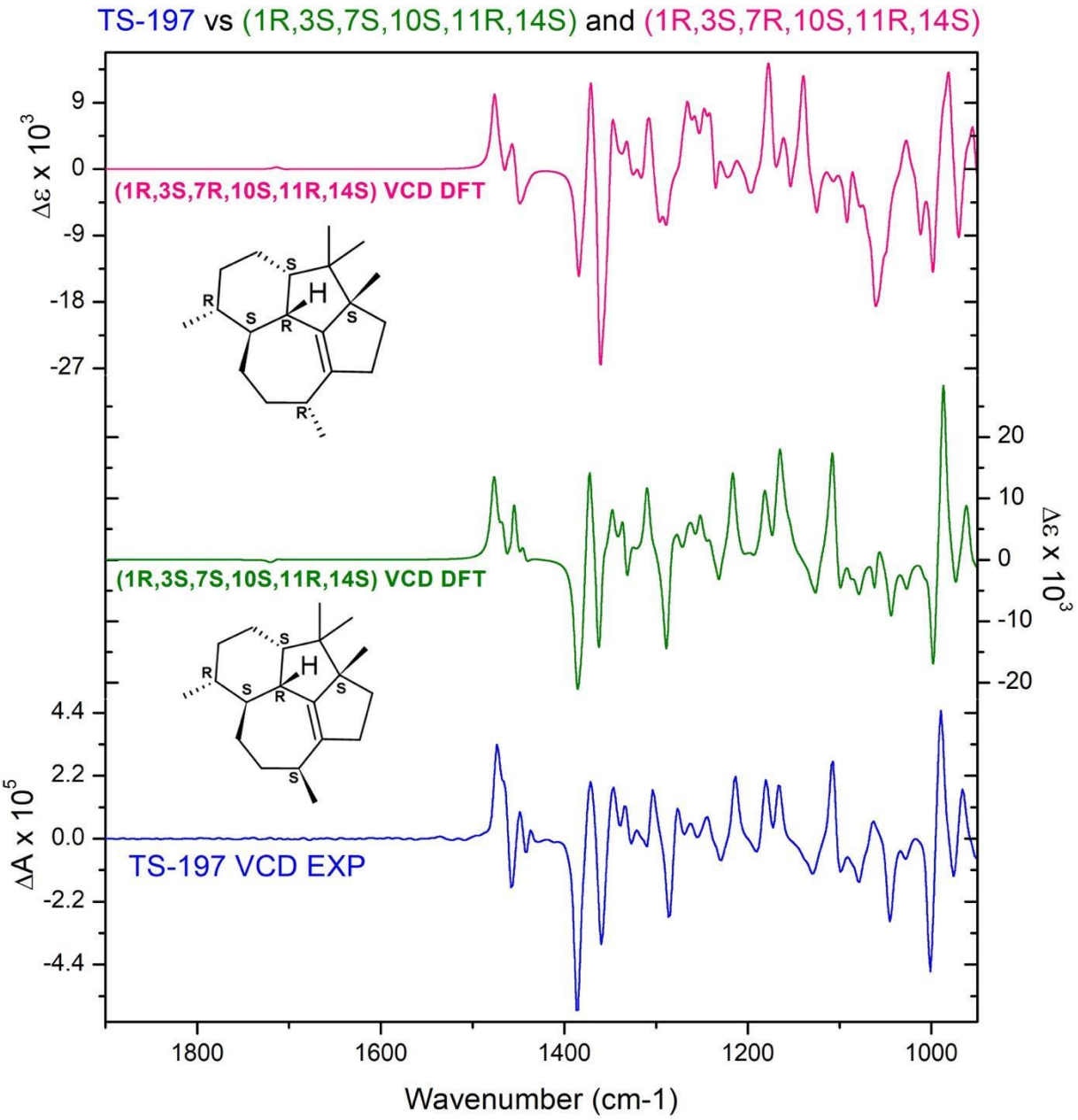

Supplementary Fig. 94. DFT calculated (pink and green) and experimental (blue) VCD and IR spectra of venezuelaene A2 (**11**) supporting the absolute configuration as 1*R*,3*S*,7*S*,10*S*,11*R*,14*S*.

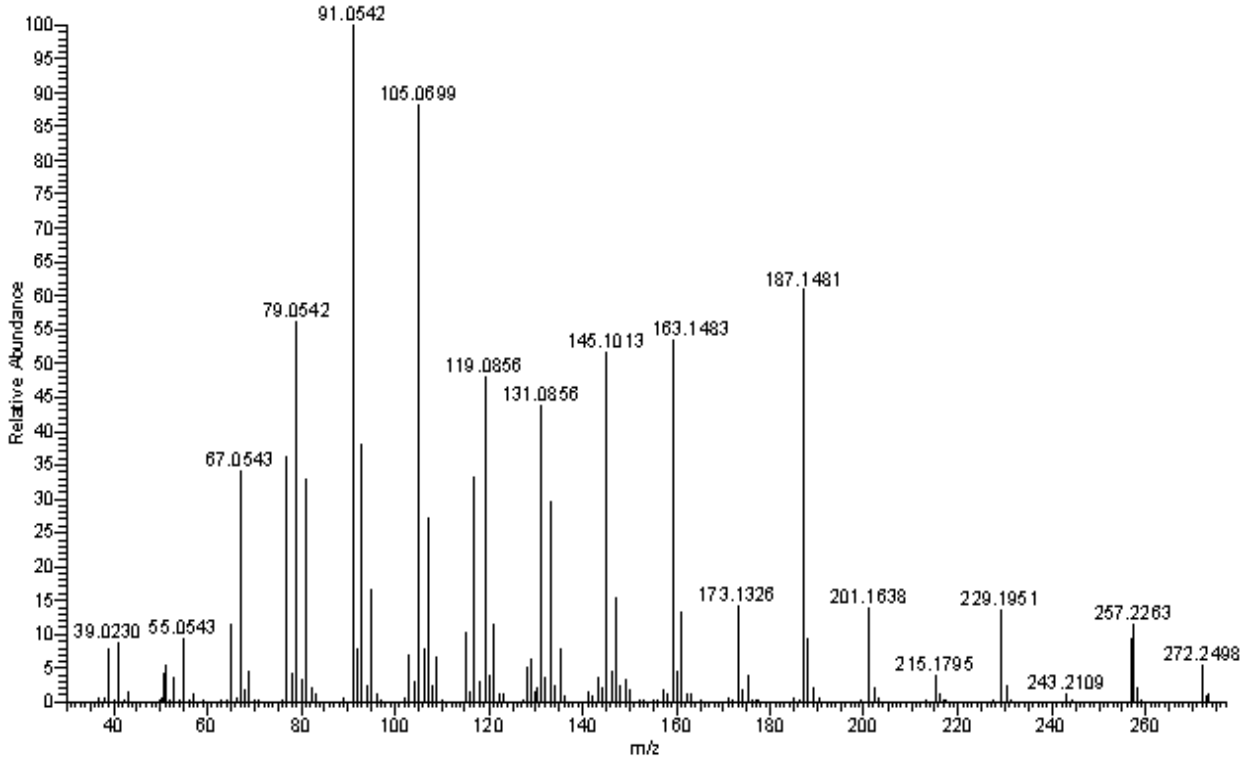

Supplementary Fig. 95. EIMS of odyverdiene B2 (**12**).

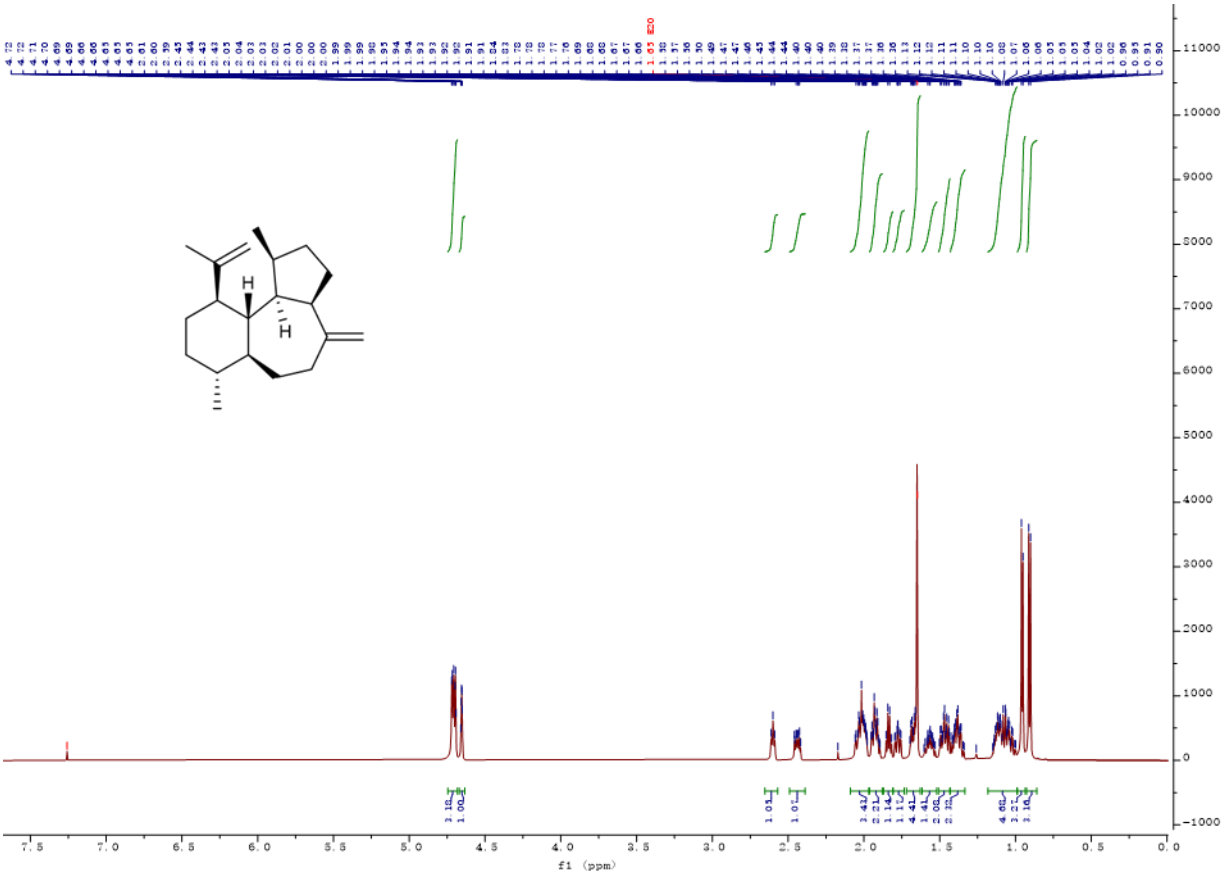

Supplementary Fig. 96. ^{1}H NMR spectrum of odyverdiene B2 (**12**) $CDCl_3$ (600 MHz).

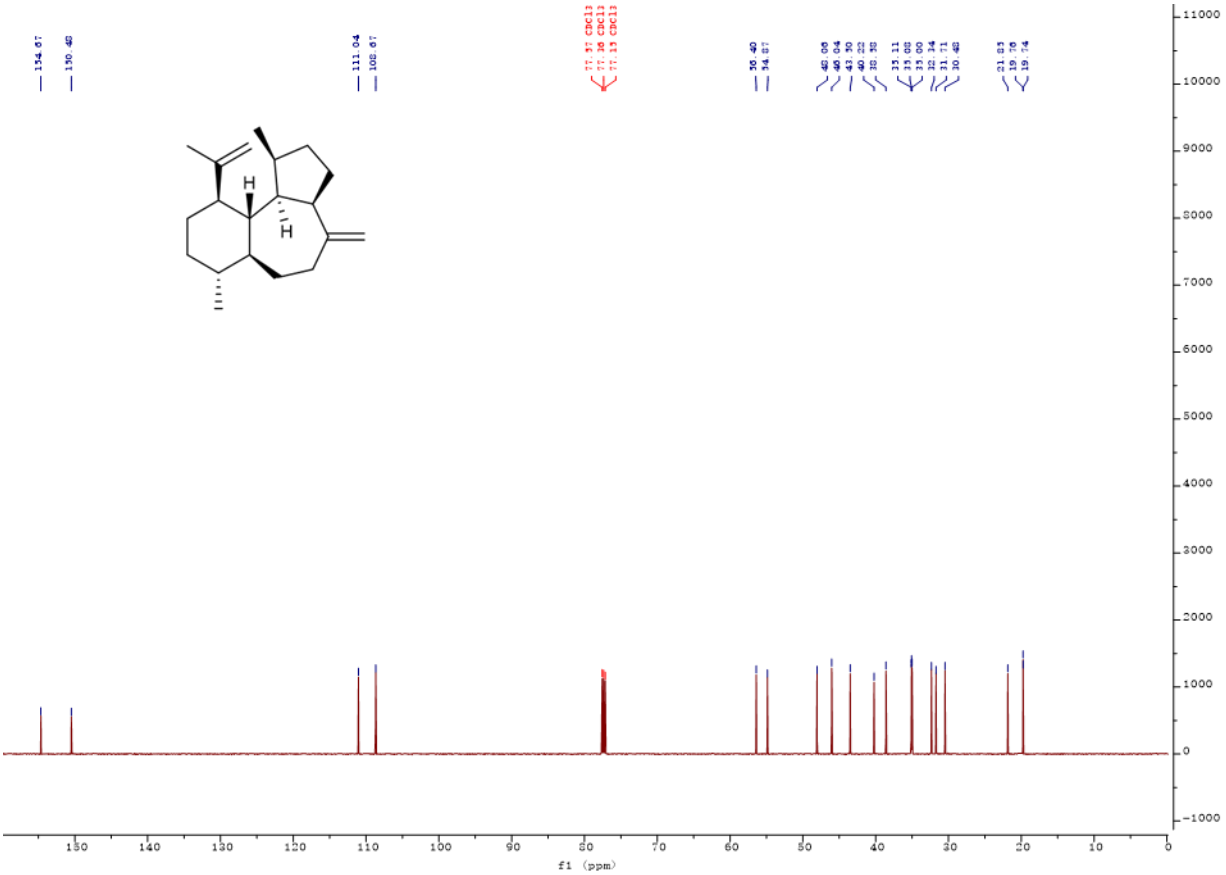

Supplementary Fig. 97. ^{13}C NMR spectrum of odyverdiene B2 (**12**) $CDCl_3$ (151 MHz).

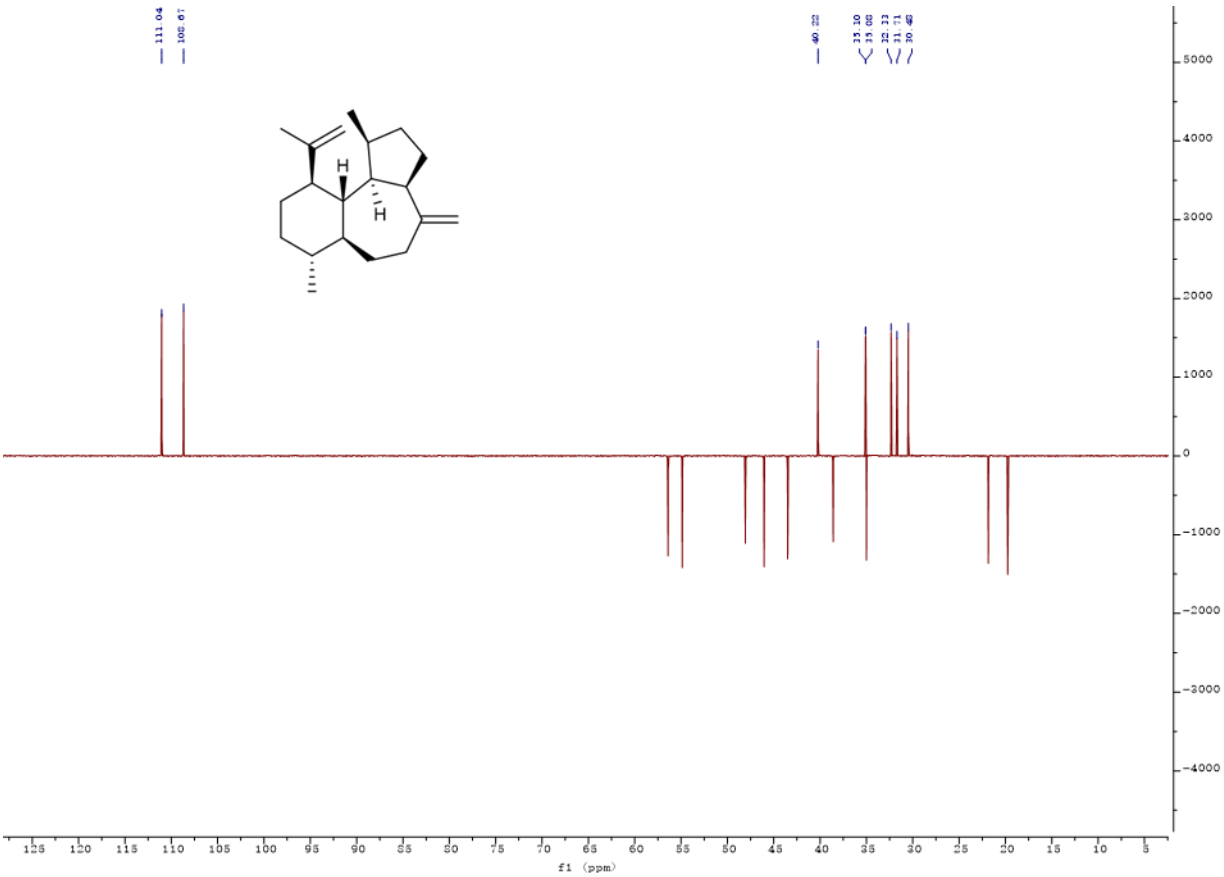

Supplementary Fig. 98. DEPT 135 spectrum of odyverdiene B2 (**12**) $CDCl_3$ (151 MHz).

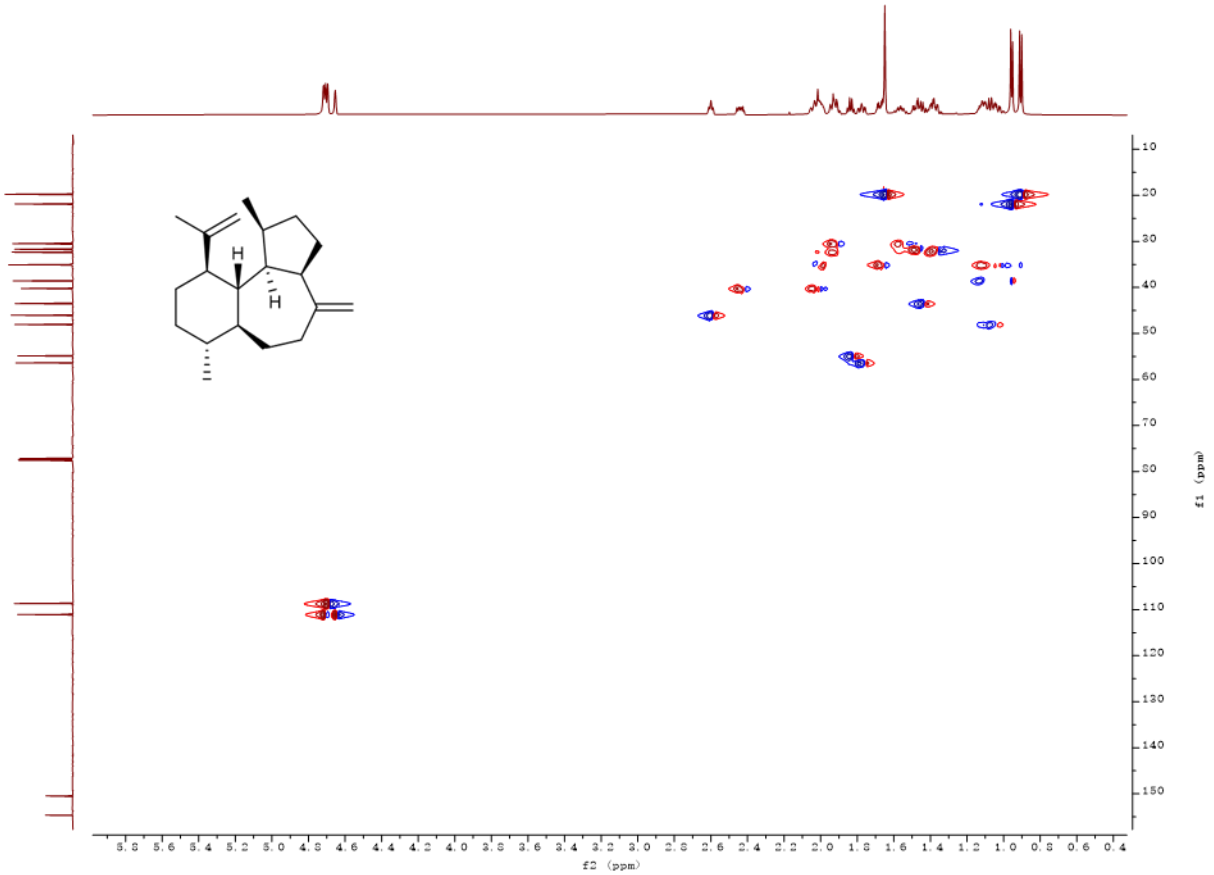

Supplementary Fig. 99. HSQC spectrum of odyverdiene B2 (**12**) $CDCl_3$.

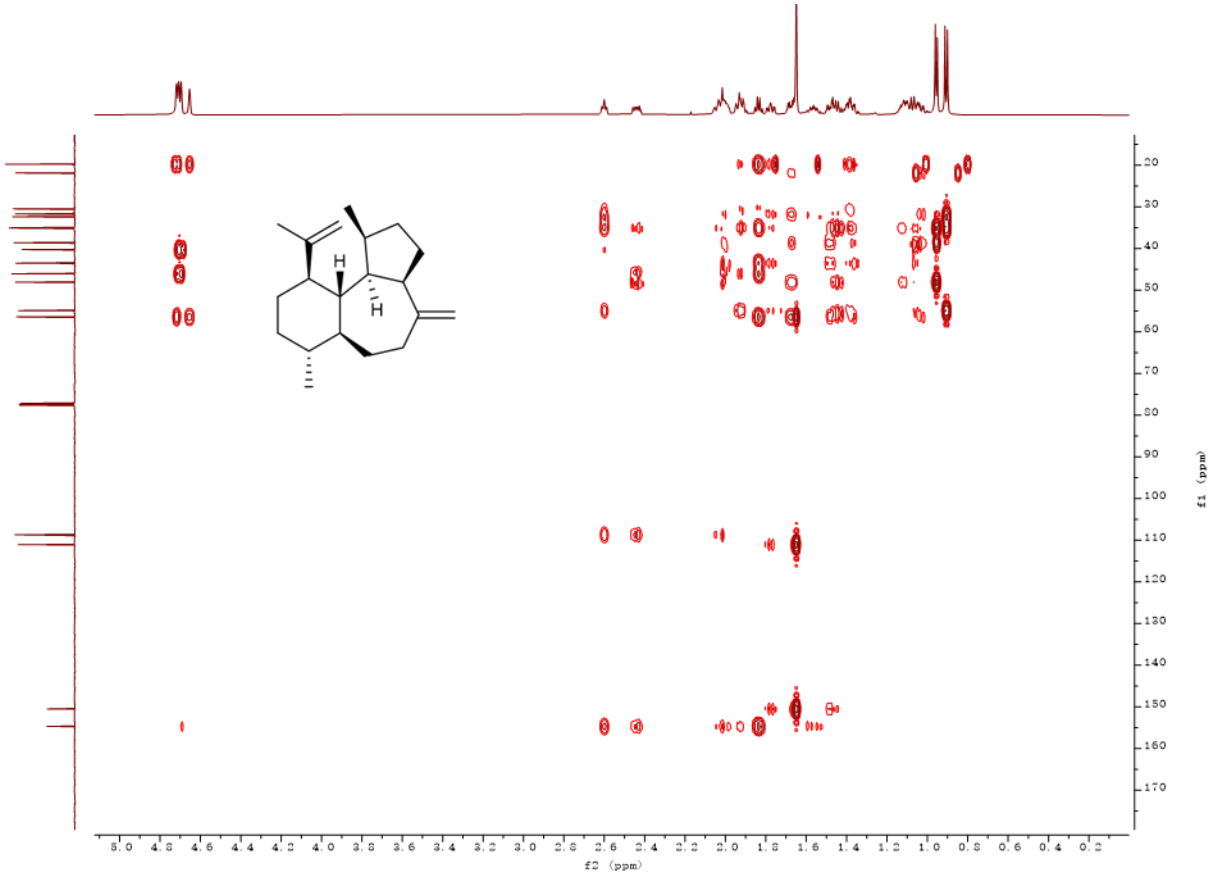

Supplementary Fig. 100. HMBC spectrum of odyverdiene B2 (**12**) $CDCl_3$.

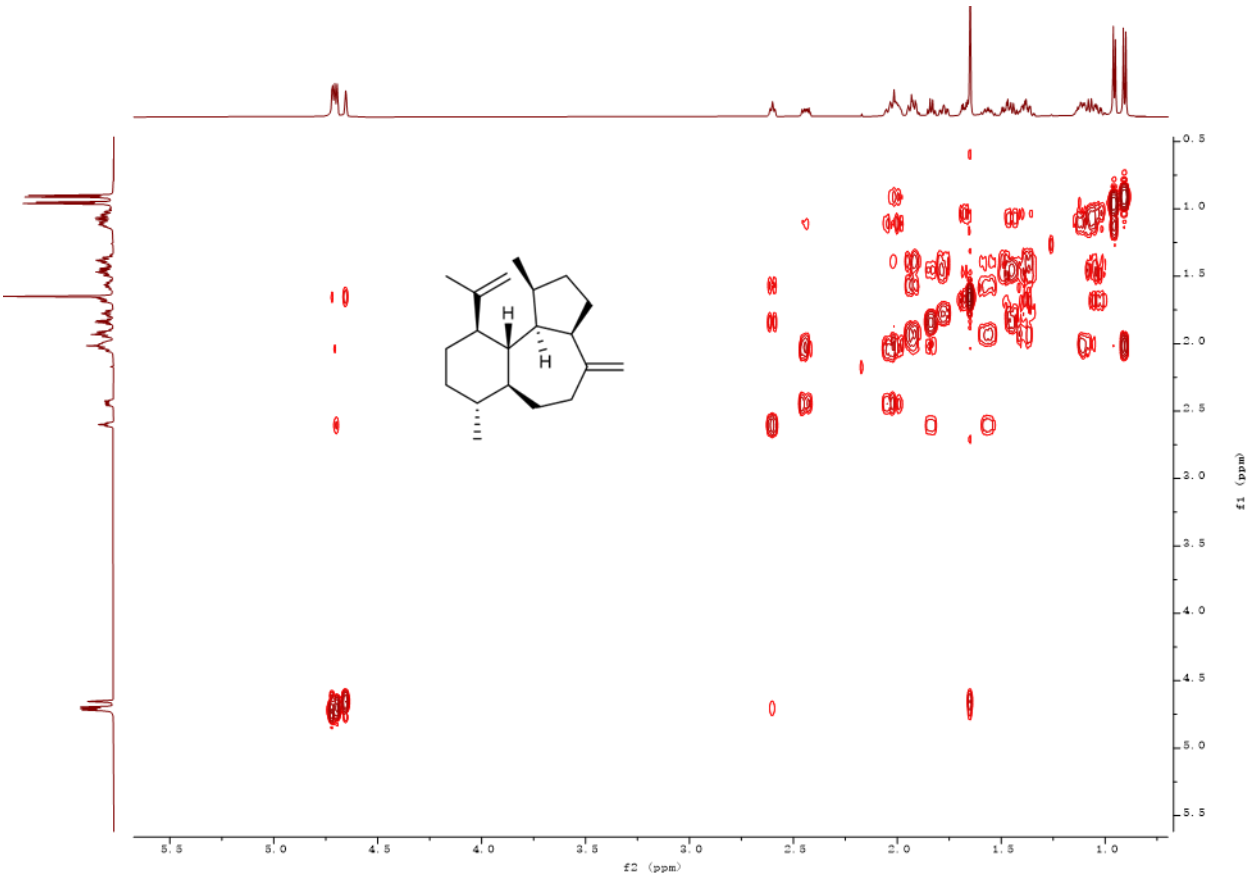

Supplementary Fig. 101. COSY spectrum of odyverdiene B2 (**12**) $CDCl_3$.

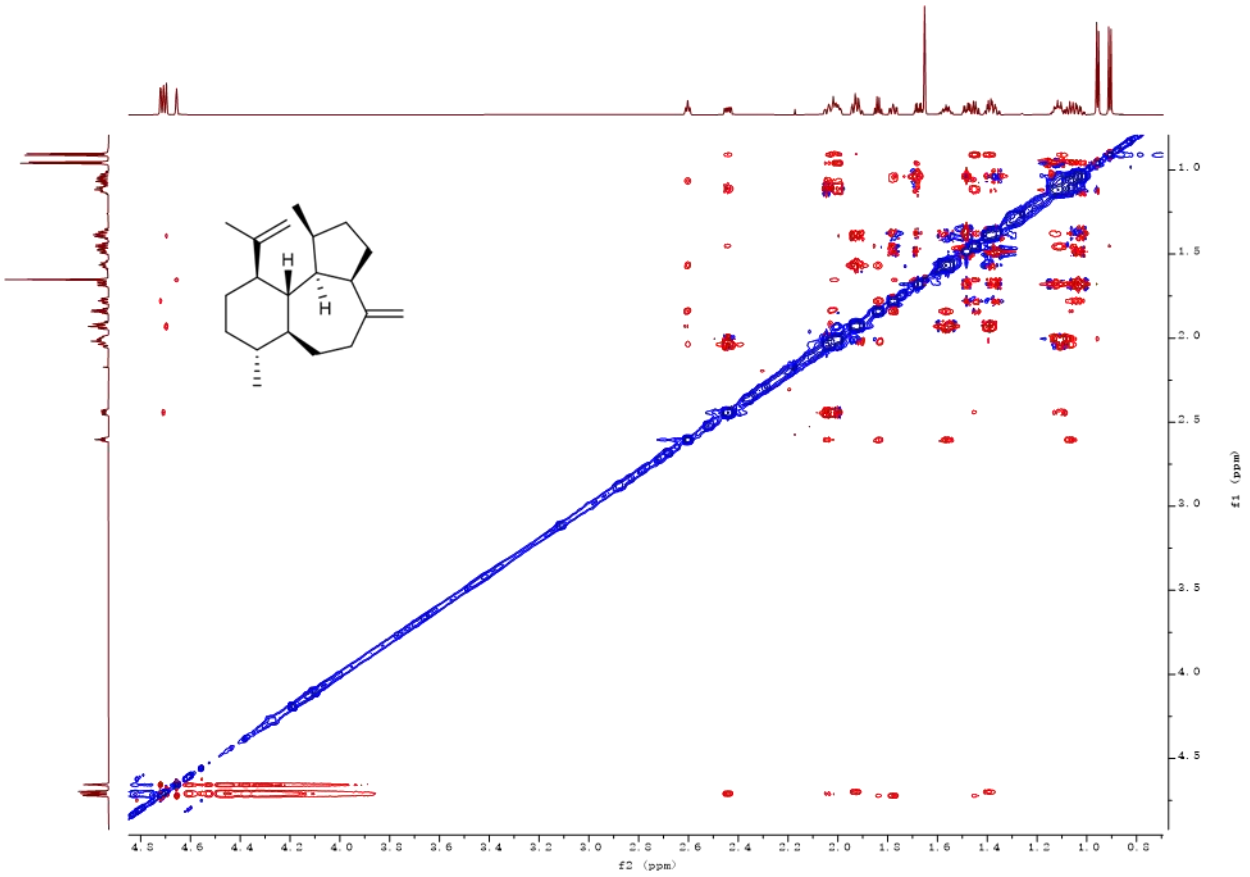

Supplementary Fig. 102. NOESY spectrum of odyverdiene B2 (**12**) $CDCl_3$ (800 MHz).

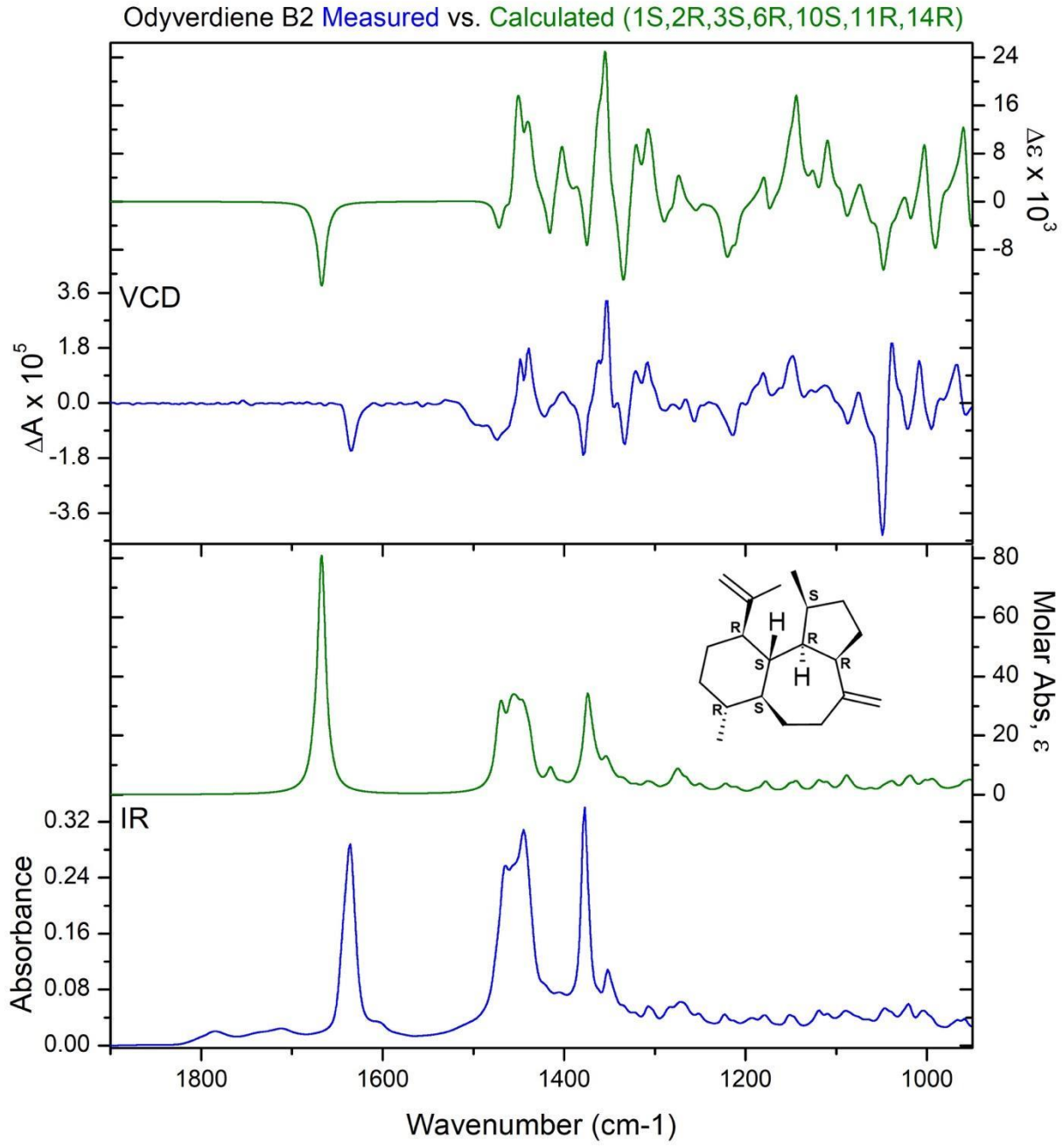

Supplementary Fig. 103. DFT calculated (green) and experimental (blue) VCD and IR spectra of odyverdiene B2 (**12**) supporting the absolute configuration as 1*S*,2*R*,3*S*,6*R*,10*S*,11*R*,14*R*.

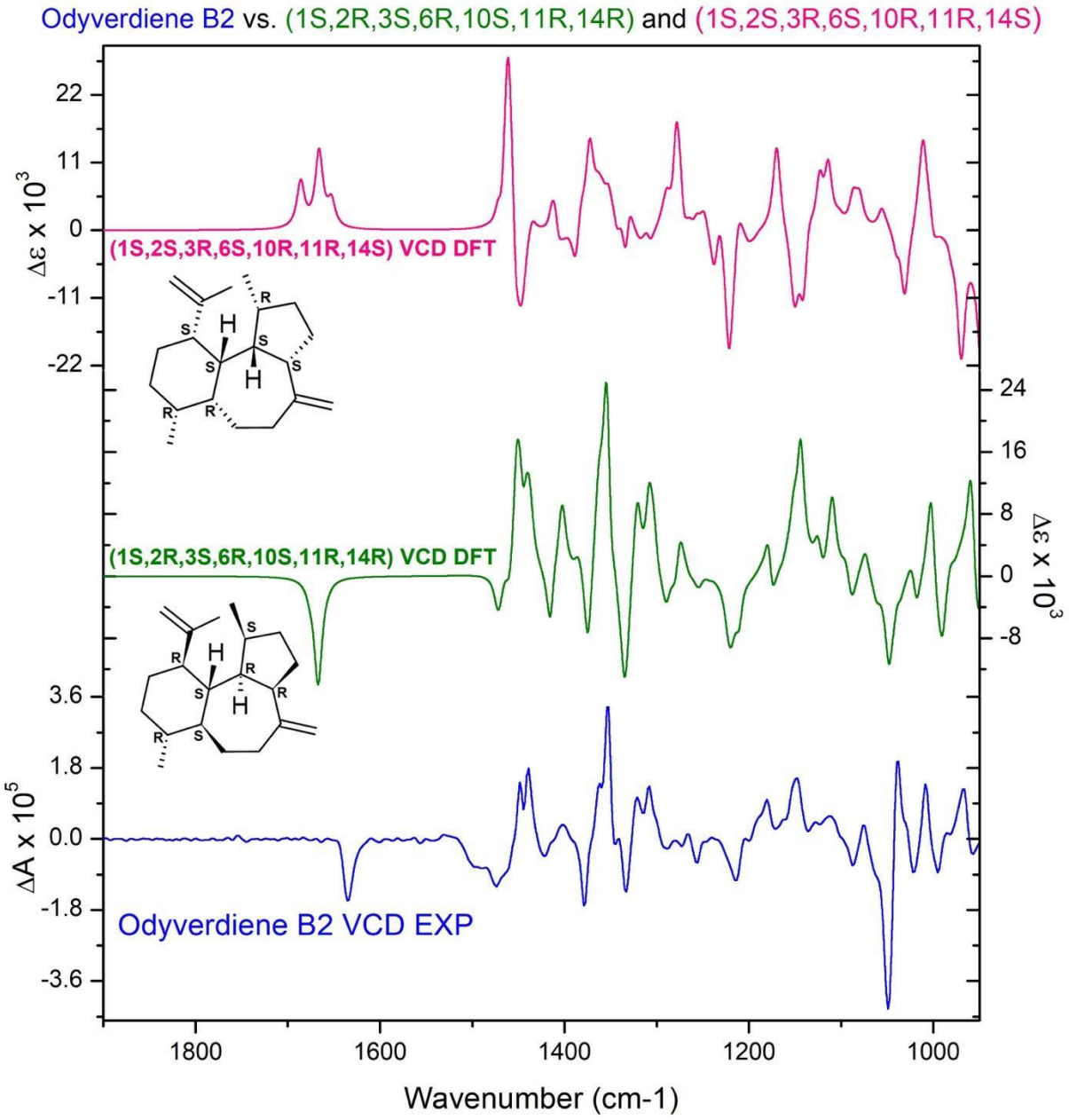

Supplementary Fig. 104. DFT calculated (pink and green) and experimental (blue) VCD and IR spectra of odyverdiene B2 (**12**) supporting the absolute configuration as 1*S*,2*R*,3*S*,6*R*,10*S*,11*R*,14*R*.

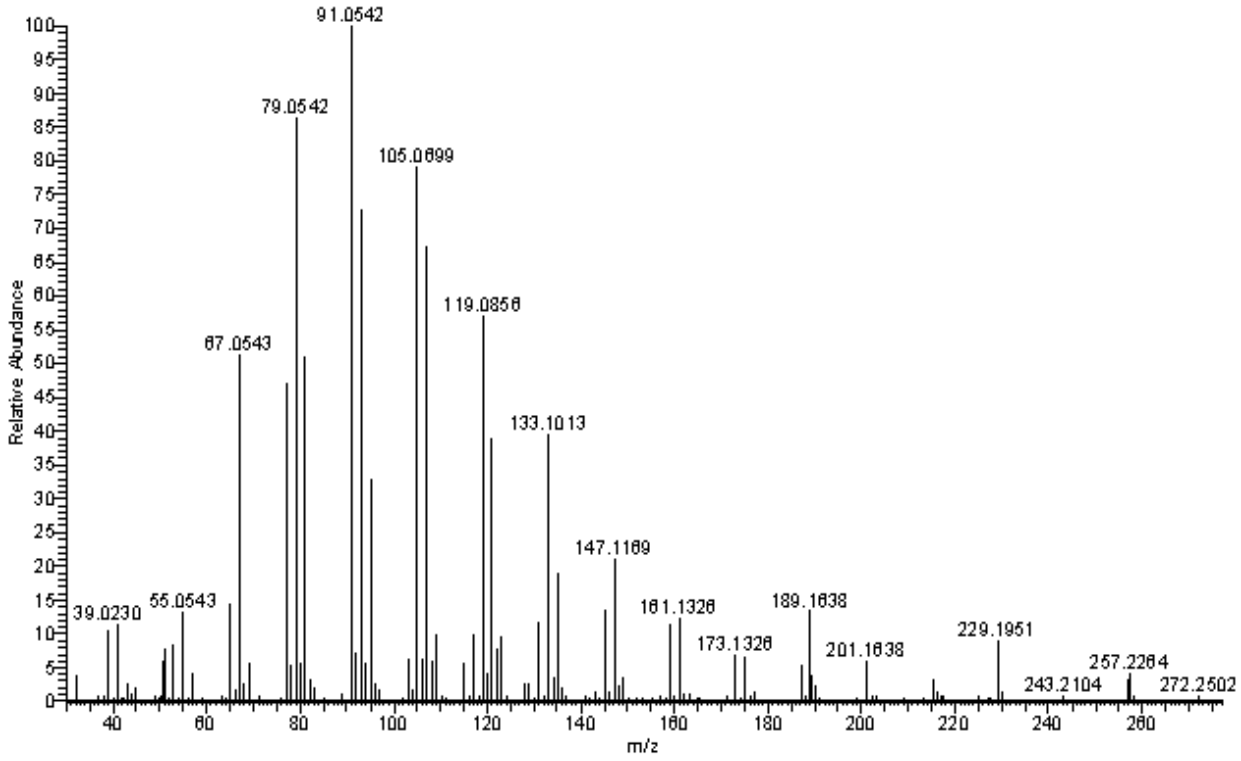

Supplementary Fig. 105. EIMS of 1*S*,3*E*,7*E*,11*R*,12*S*-dolabella-3,7,18-triene (**13**). The fragmentation and retention index (RI = 1961) matched the literature (RI =1956)[12].

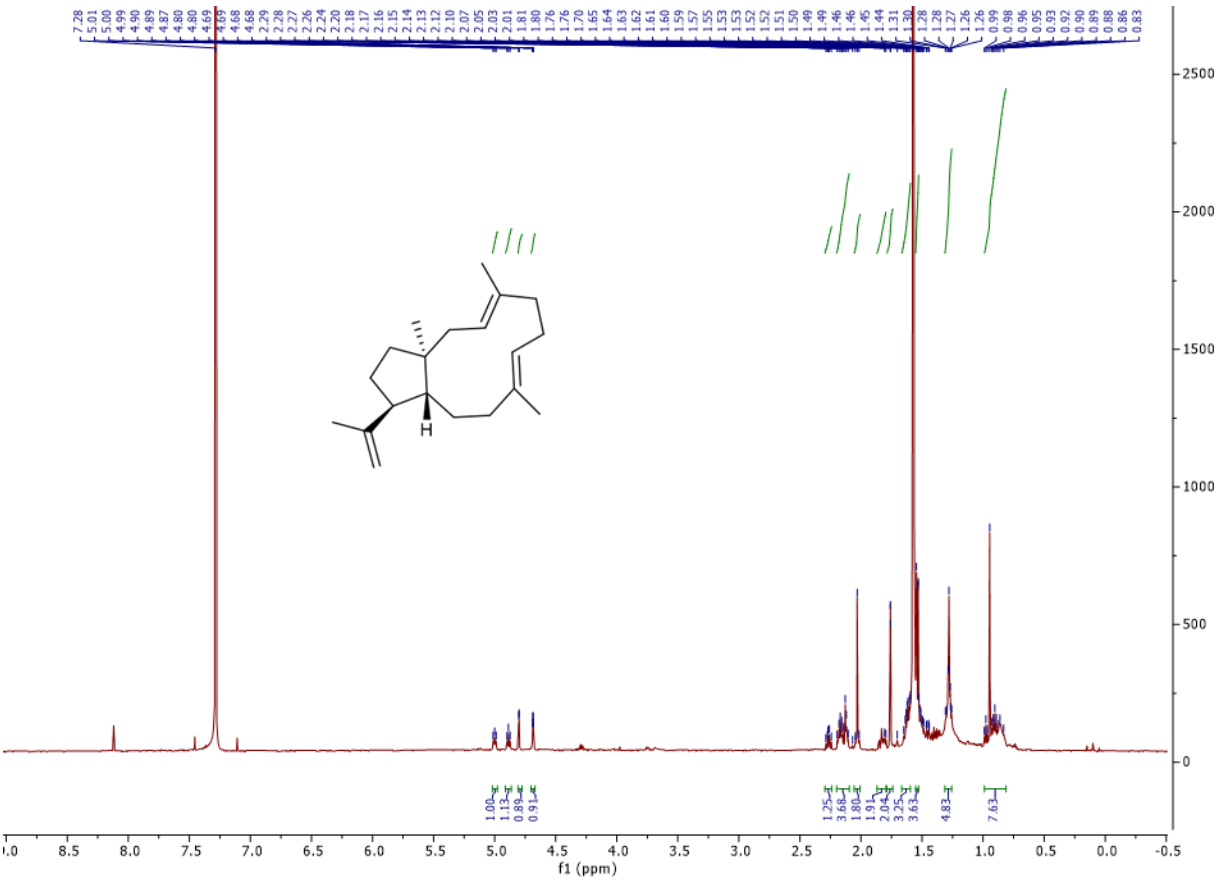

Supplementary Fig. 106. ^{1}H NMR spectrum of 1*S*,3*E*,7*E*,11*R*,12*S*-dolabella-3,7,18-triene (**13**) in $CDCl_3$ (600 MHz).

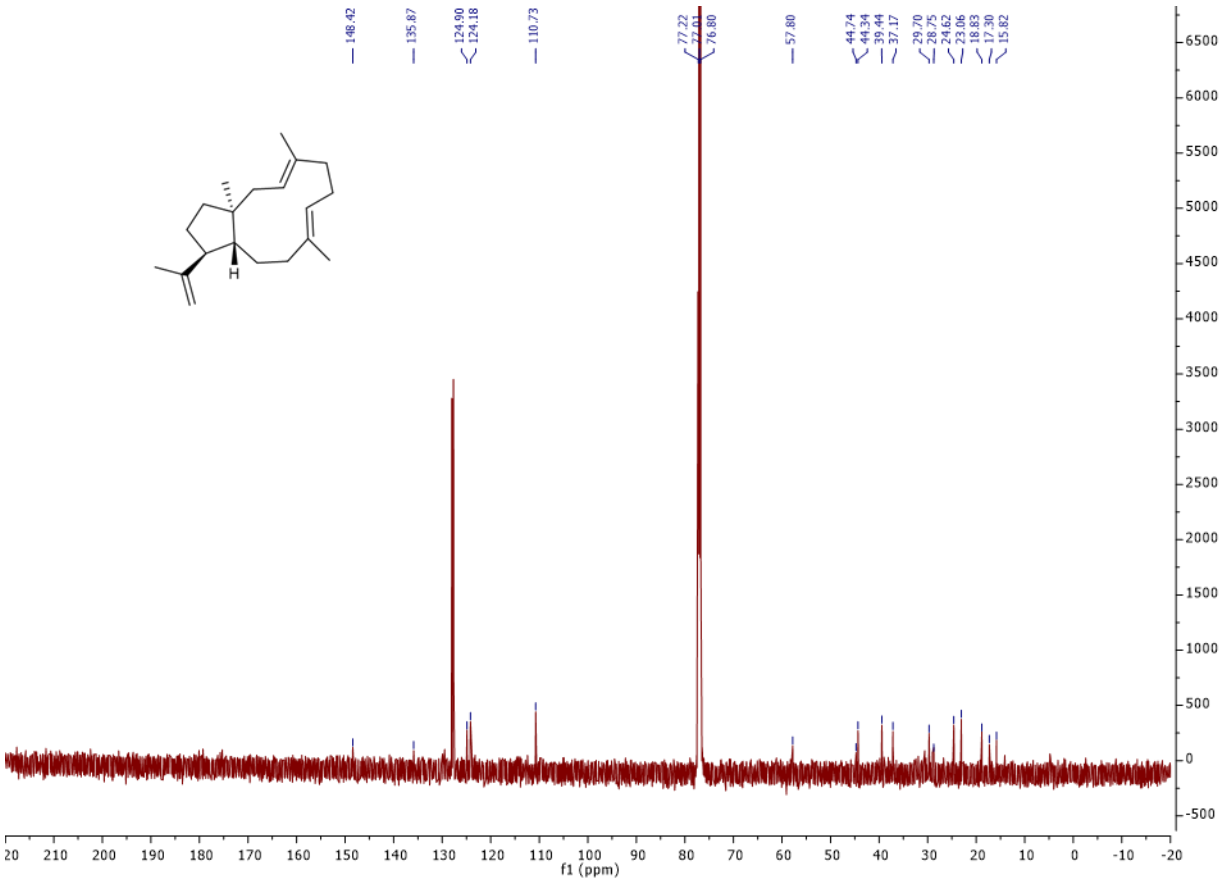

Supplementary Fig. 107. ^{13}C NMR spectrum of 1*S*,3*E*,7*E*,11*R*,12*S*-dolabella-3,7,18-triene (**13**) in $CDCl_3$ (151 MHz).

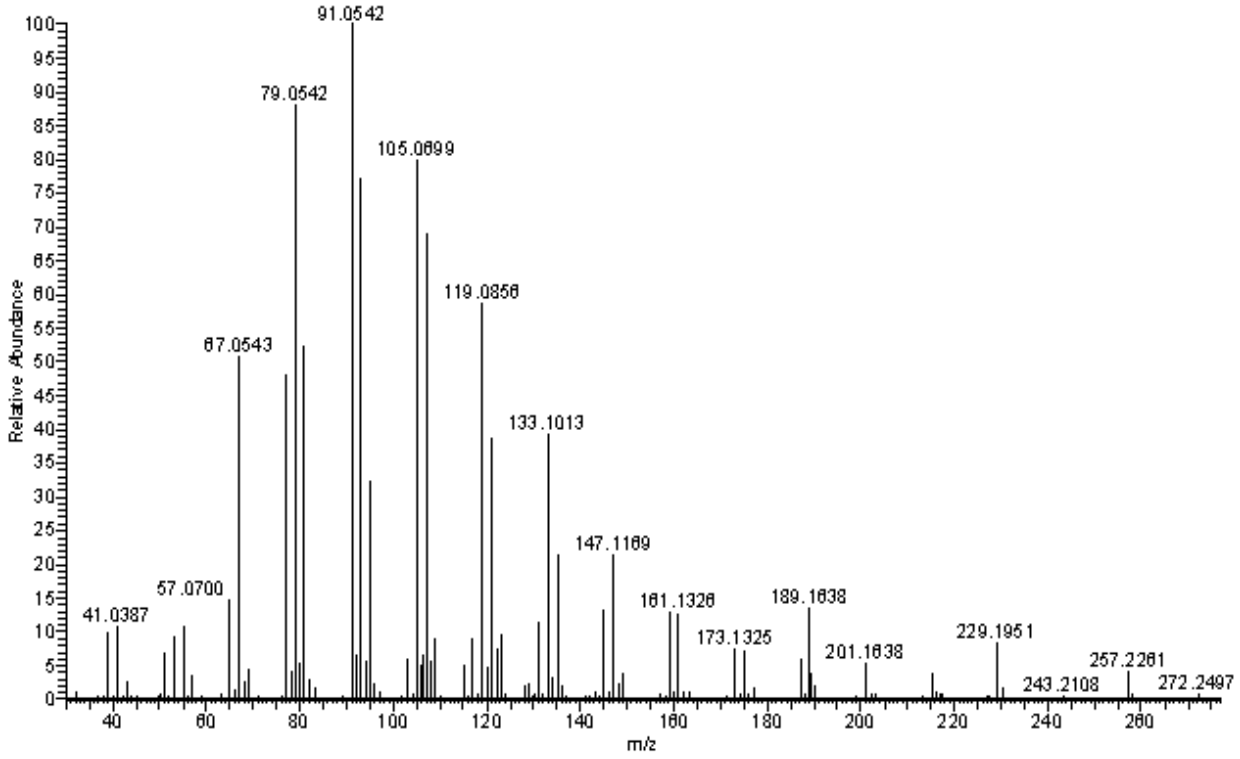

Supplementary Fig. 108. EIMS of 1*R**,3*E*,7*E*,11*S**,12*S**-dolabella-3,7,18-triene (**14**).

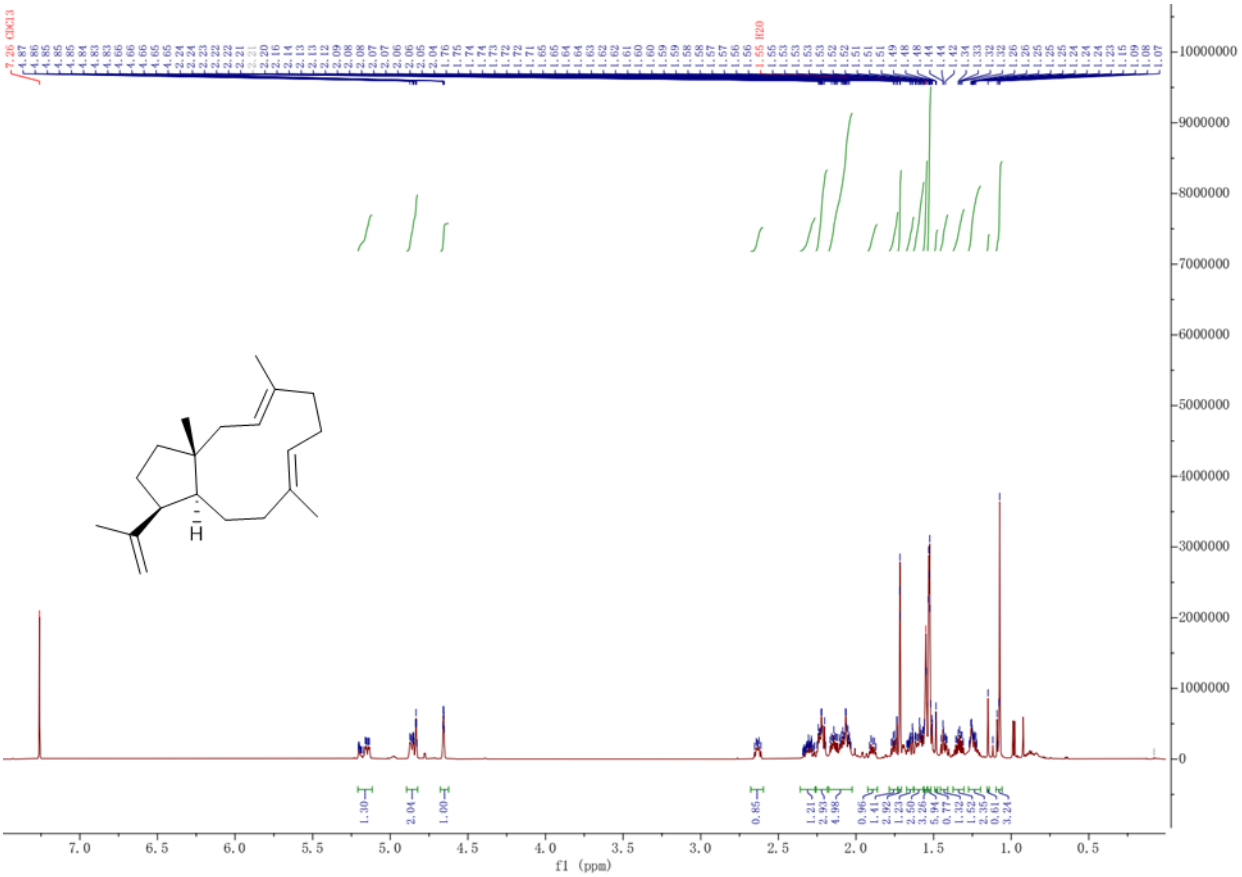

Supplementary Fig. 109. ^{1}H NMR spectrum of 1*R**,3*E*,7*E*,11*S**,12*S**-dolabella-3,7,18-triene (**14**) in $CDCl_3$ (600 MHz).

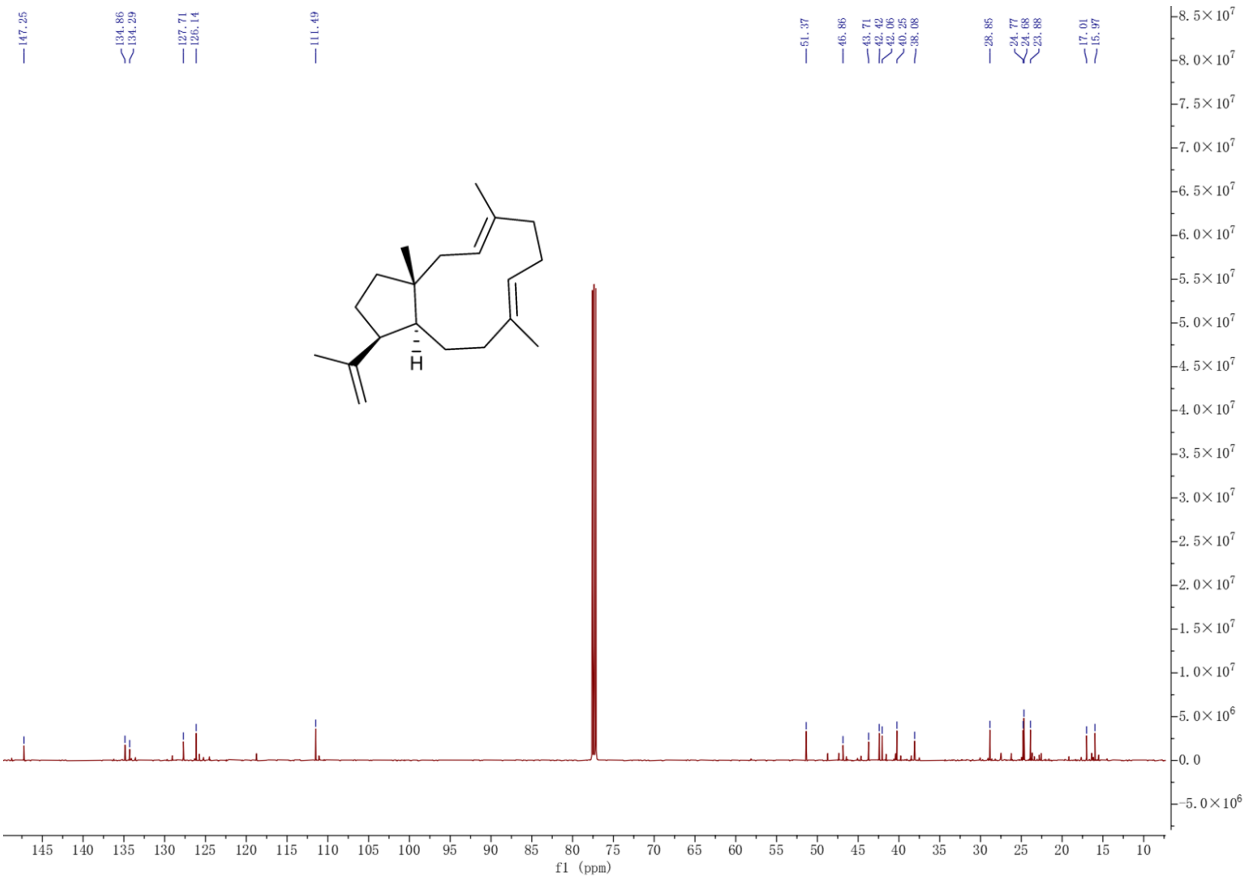

Supplementary Fig. 110. ^{13}C NMR spectrum of 1*R**,3*E*,7*E*,11*S**,12*S**-dolabella-3,7,18-triene (**14**) in $CDCl_3$ (151 MHz).

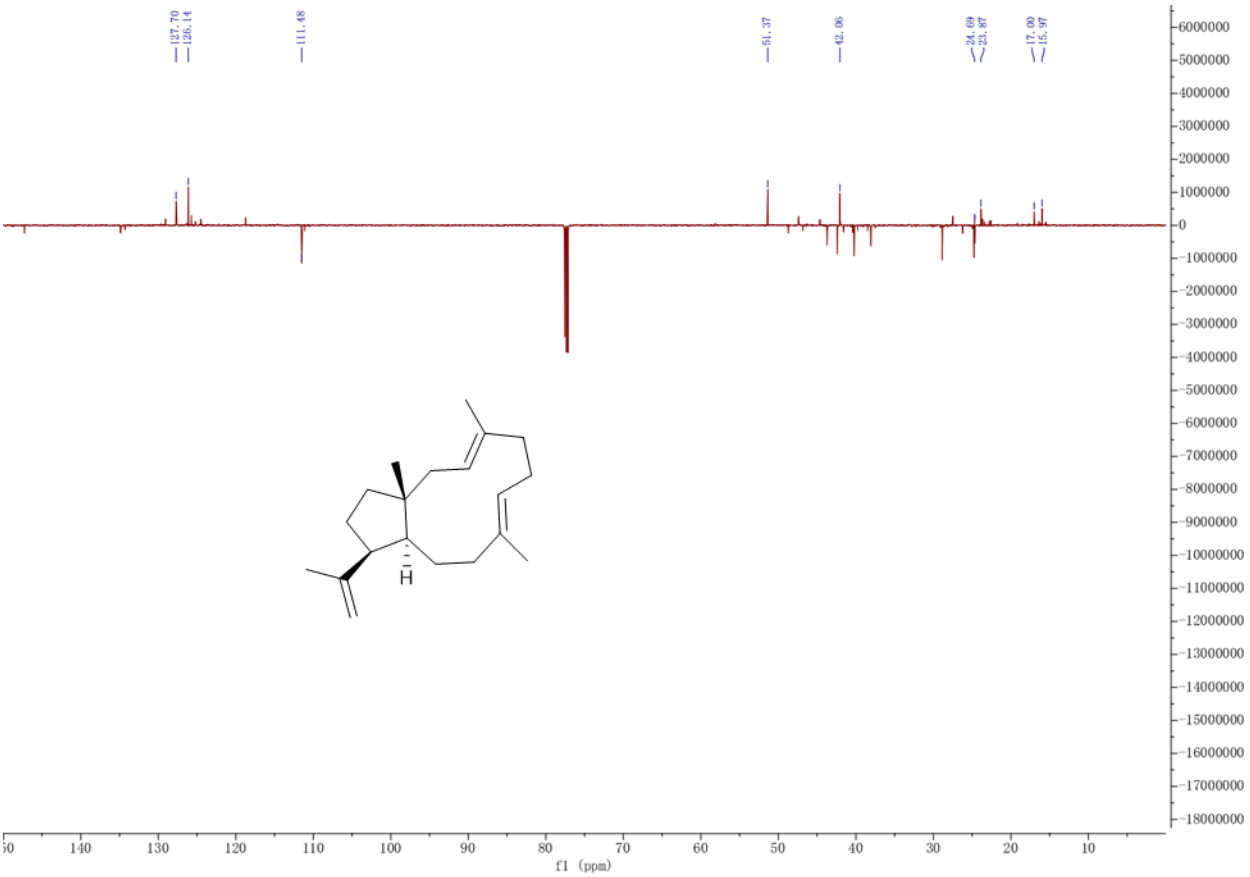

Supplementary Fig. 111. DEPT 135 spectrum of 1*R**,3*E*,7*E*,11*S**,12*S**-dolabella-3,7,18-triene (**14**) in $CDCl_3$ (151 MHz).

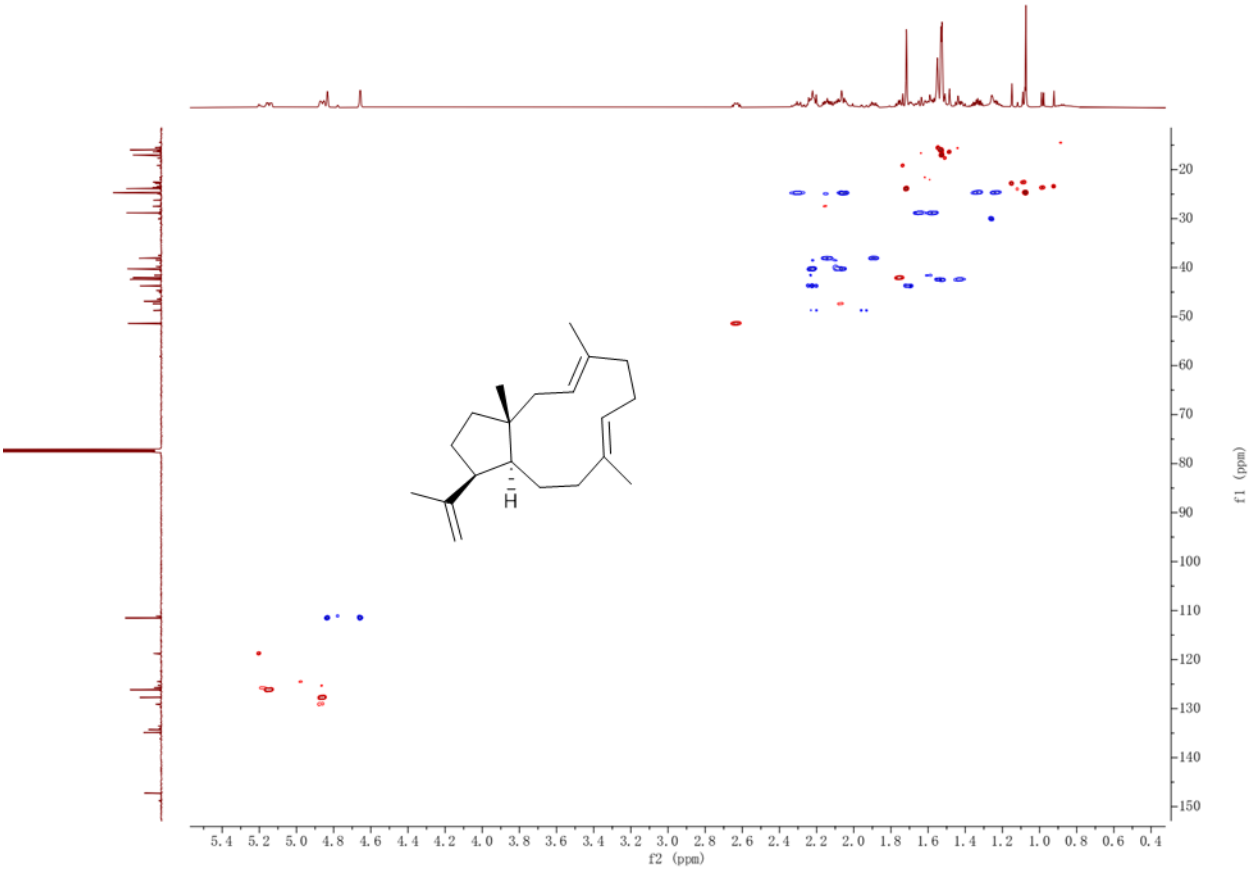

Supplementary Fig. 112. HSQC spectrum of 1*R**,3*E*,7*E*,11*S**,12*S**-dolabella-3,7,18-triene (**14**) in $CDCl_3$.

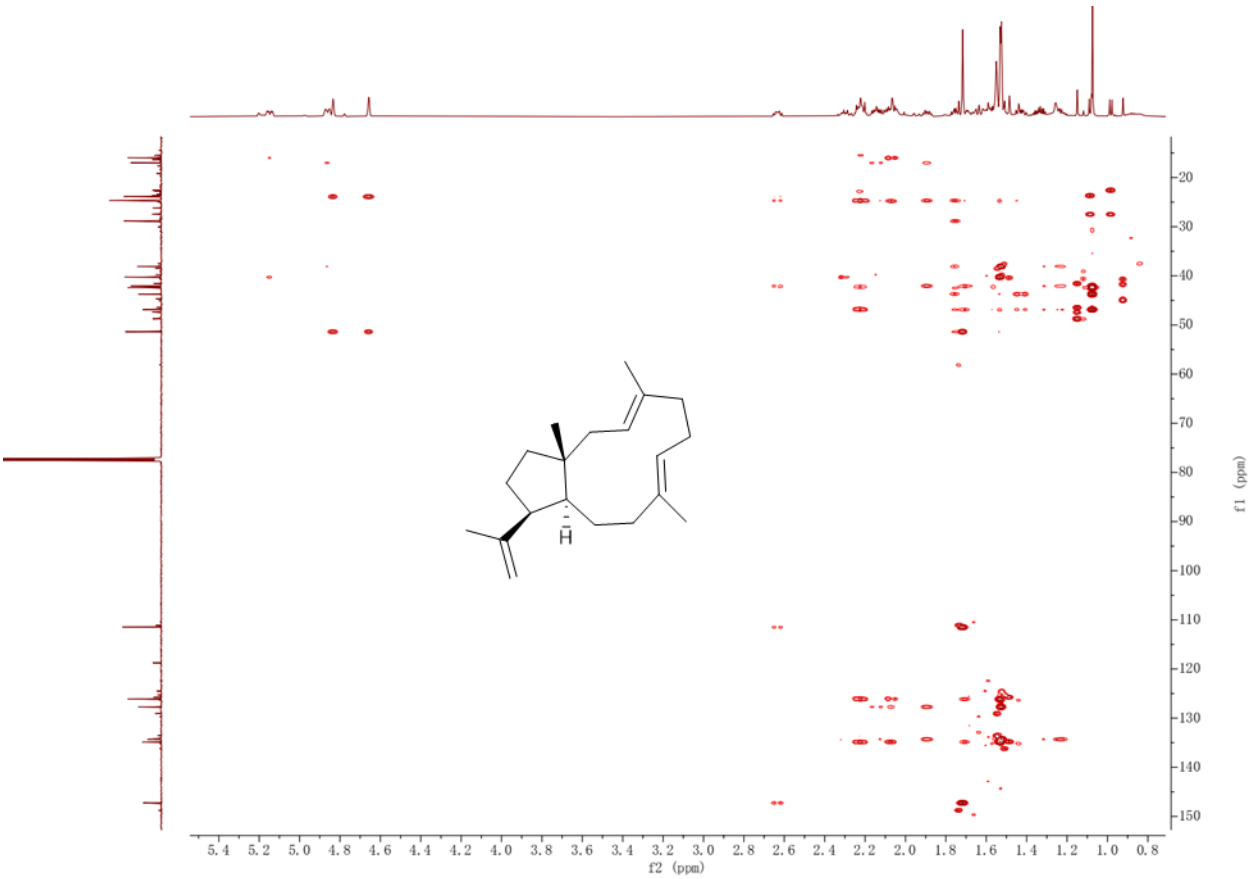

Supplementary Fig. 113. HMBC spectrum of 1*R**,3*E*,7*E*,11*S**,12*S**-dolabella-3,7,18-triene (**14**) in $CDCl_3$.

.

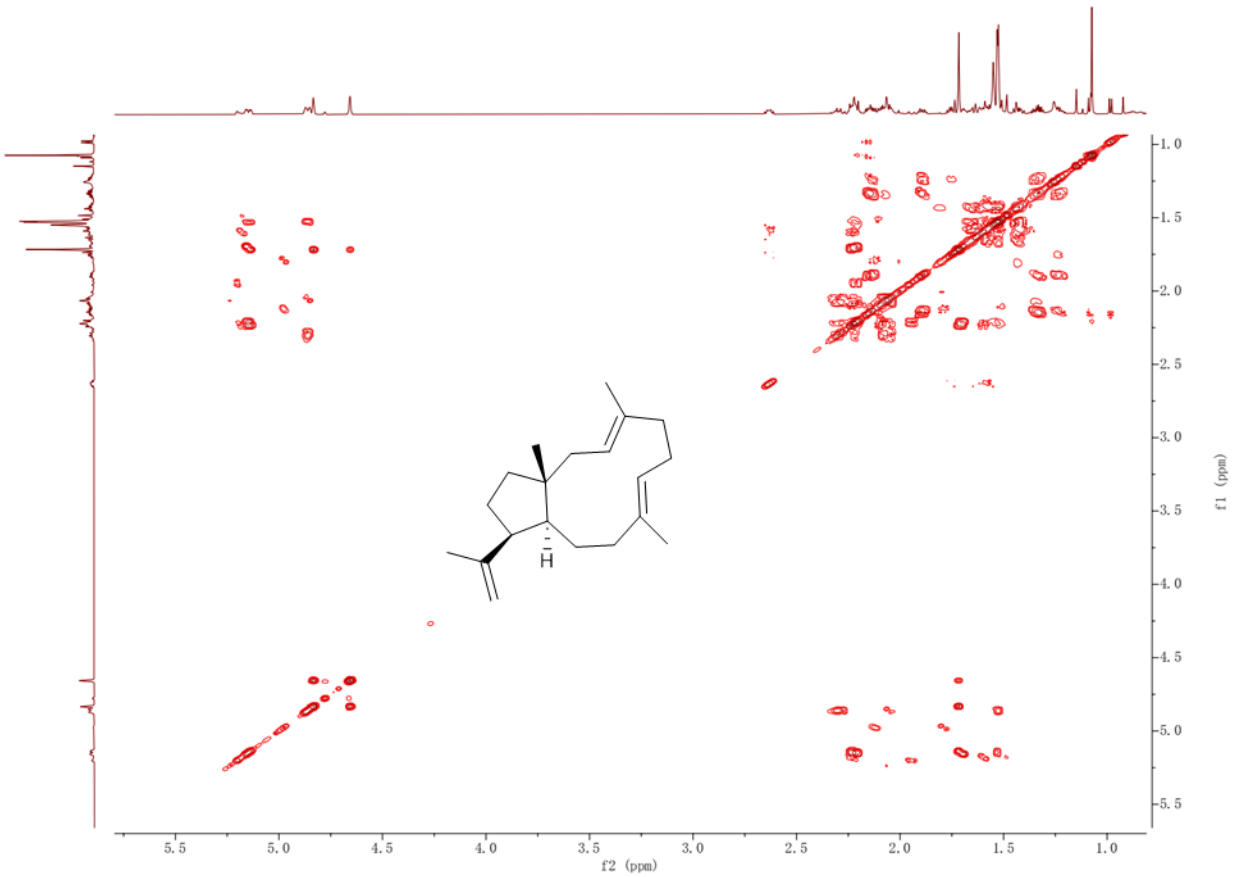

Supplementary Fig. 114. COSY spectrum of 1*R**,3*E*,7*E*,11*S**,12*S**-dolabella-3,7,18-triene (**14**) in $CDCl_3$

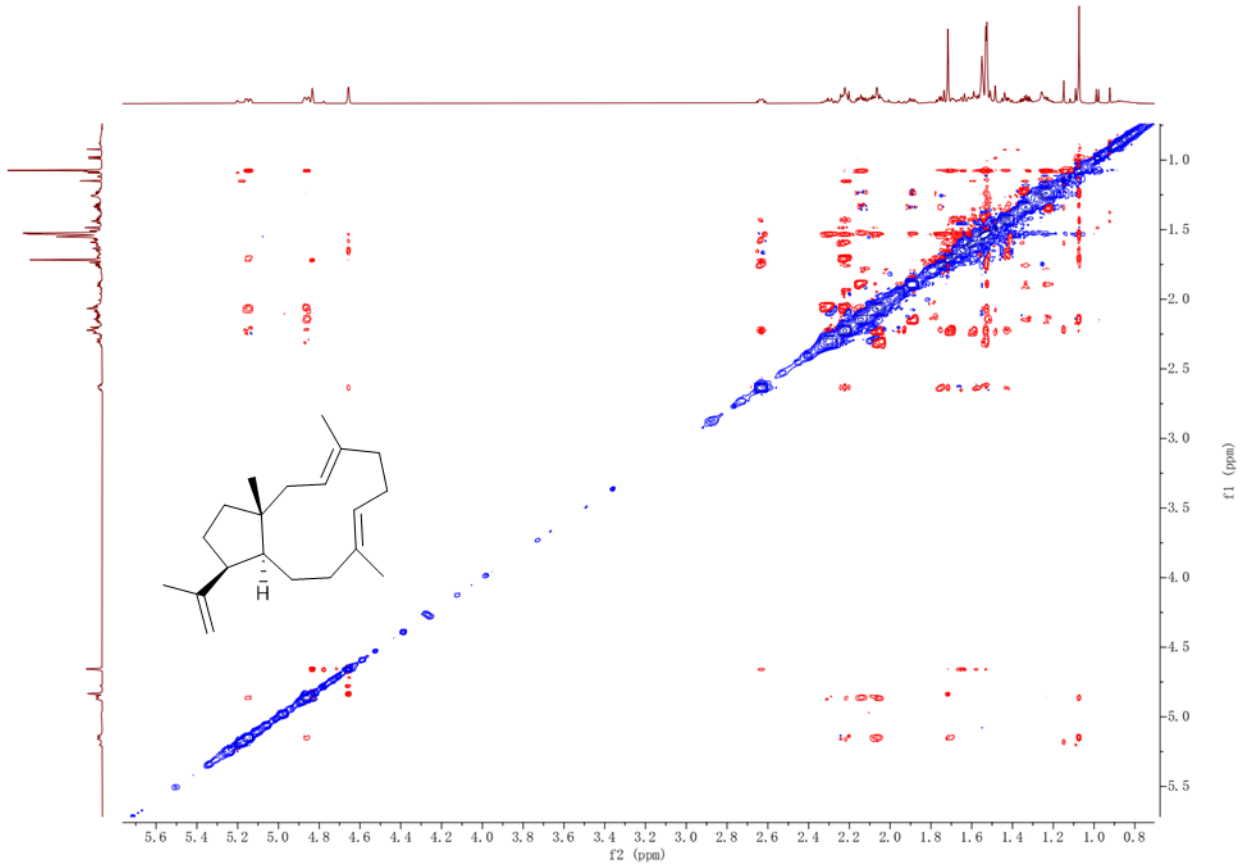

Supplementary Fig. 115. NOESY spectrum of 1*R**,3*E*,7*E*,11*S**,12*S**-dolabella-3,7,18-triene (**14**) in $CDCl_3$.

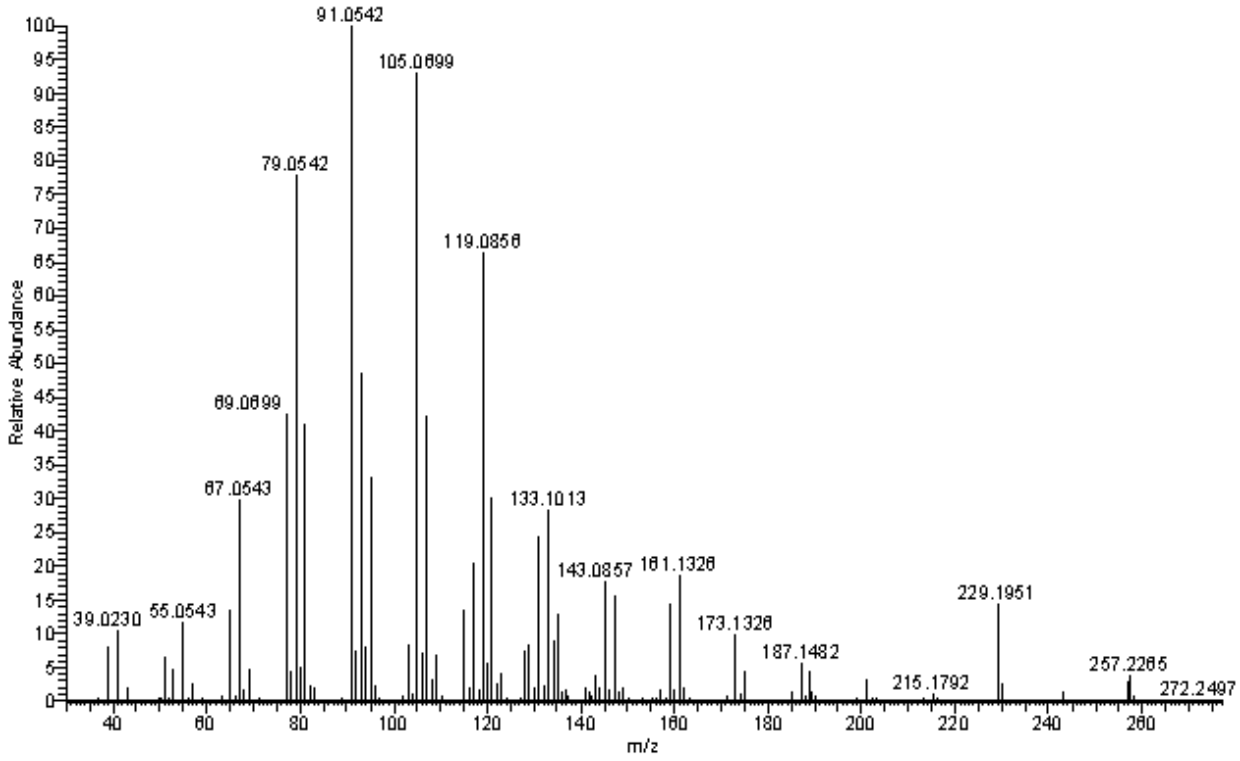

Supplementary Fig. 116. EIMS of 1*R*,7*E*,10*E*,12*R*-dolabella-4(16),7,10-triene (**15**).

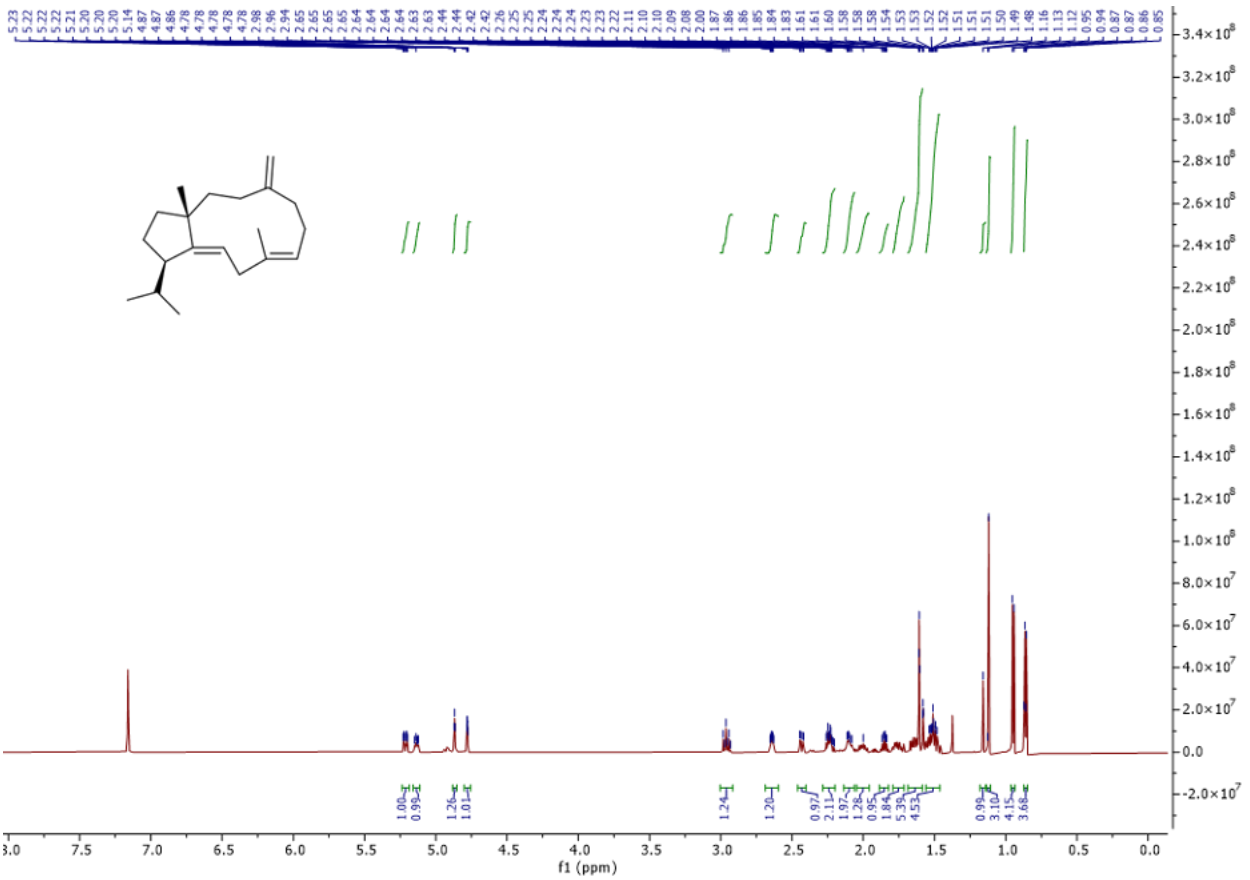

Supplementary Fig. 117. ^{1}H NMR spectrum of 1*R*,7*E*,10*E*,12*R*-dolabella-4(16),7,10-triene (**15**) in C_6D_6 (600 MHz).

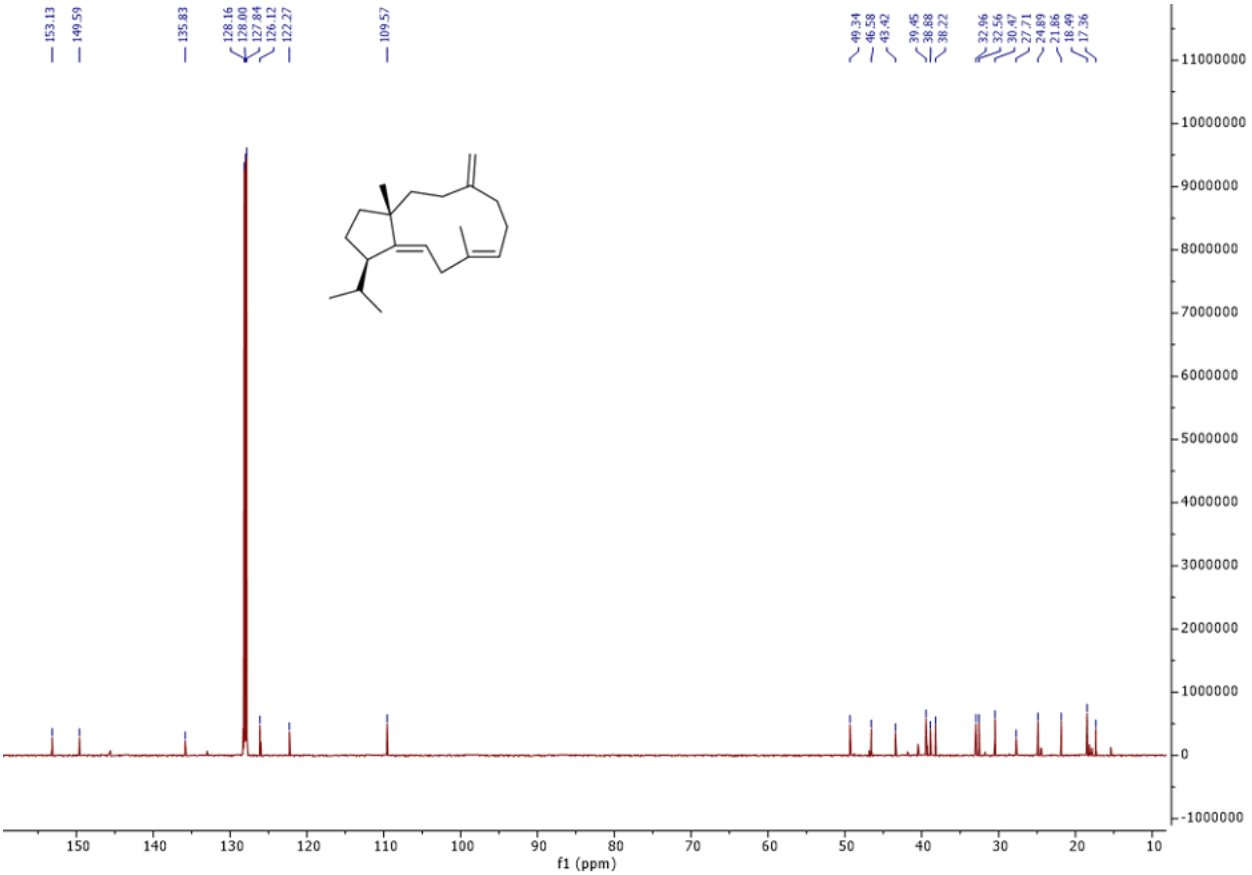

Supplementary Fig. 118. ^{13}C NMR spectrum of 1*R*,7*E*,10*E*,12*R*-dolabella-4(16),7,10-triene (**15**) in C_6D_6 (151 MHz).

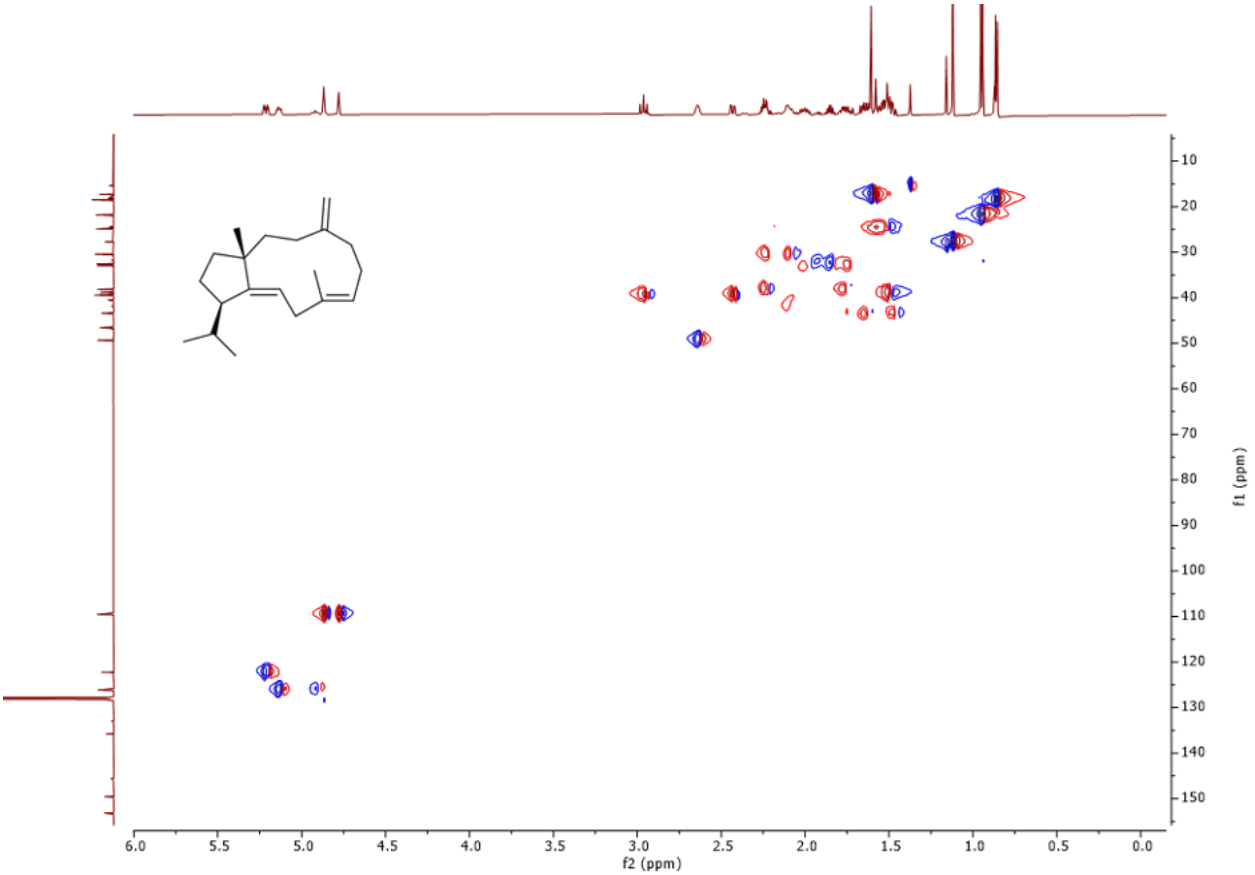

Supplementary Fig. 119. HSQC spectrum of 1*R*,7*E*,10*E*,12*R*-dolabella-4(16),7,10-triene (**15**) in C_6D_6.

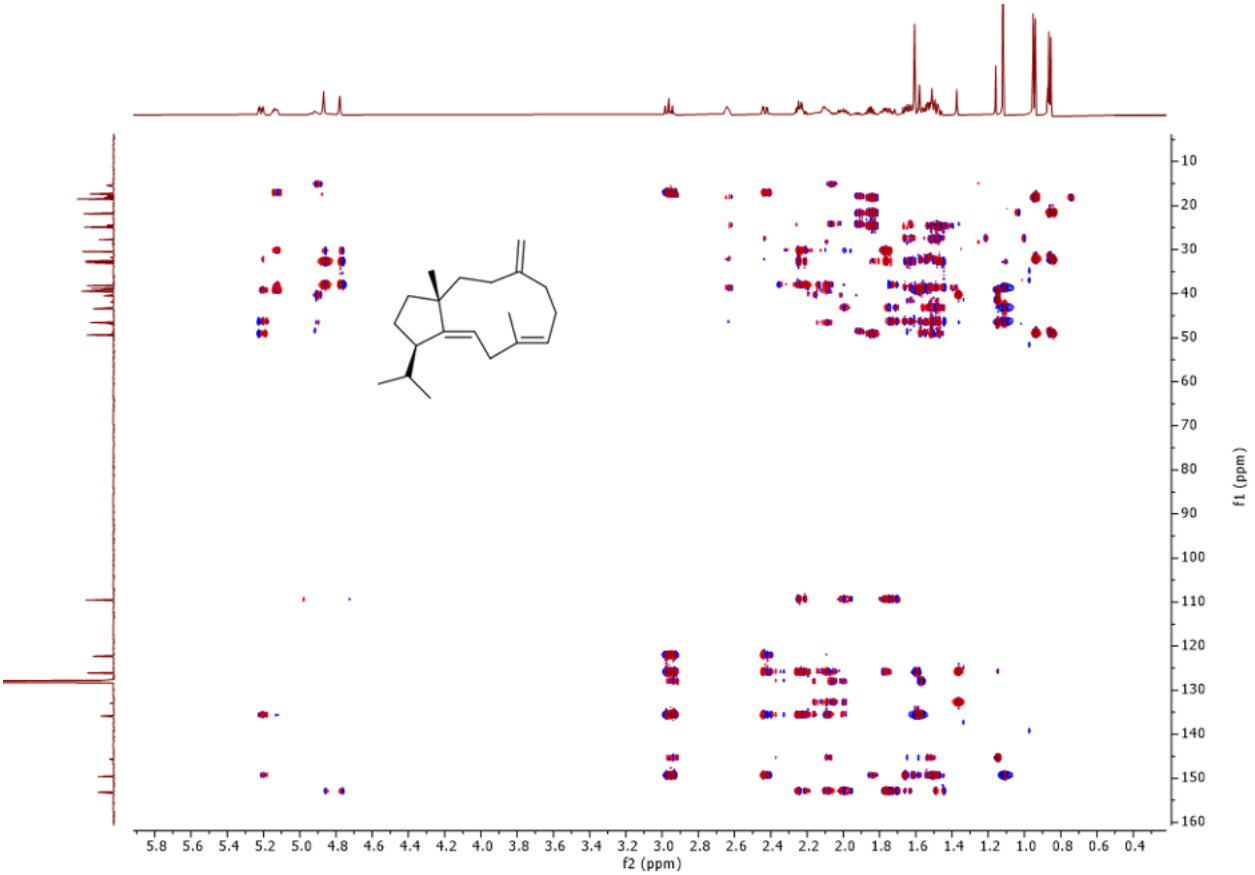

Supplementary Fig. 120. HMBC spectrum of 1*R*,7*E*,10*E*,12*R*-dolabella-4(16),7,10-triene (**15**) in C_6D_6 (151 MHz).

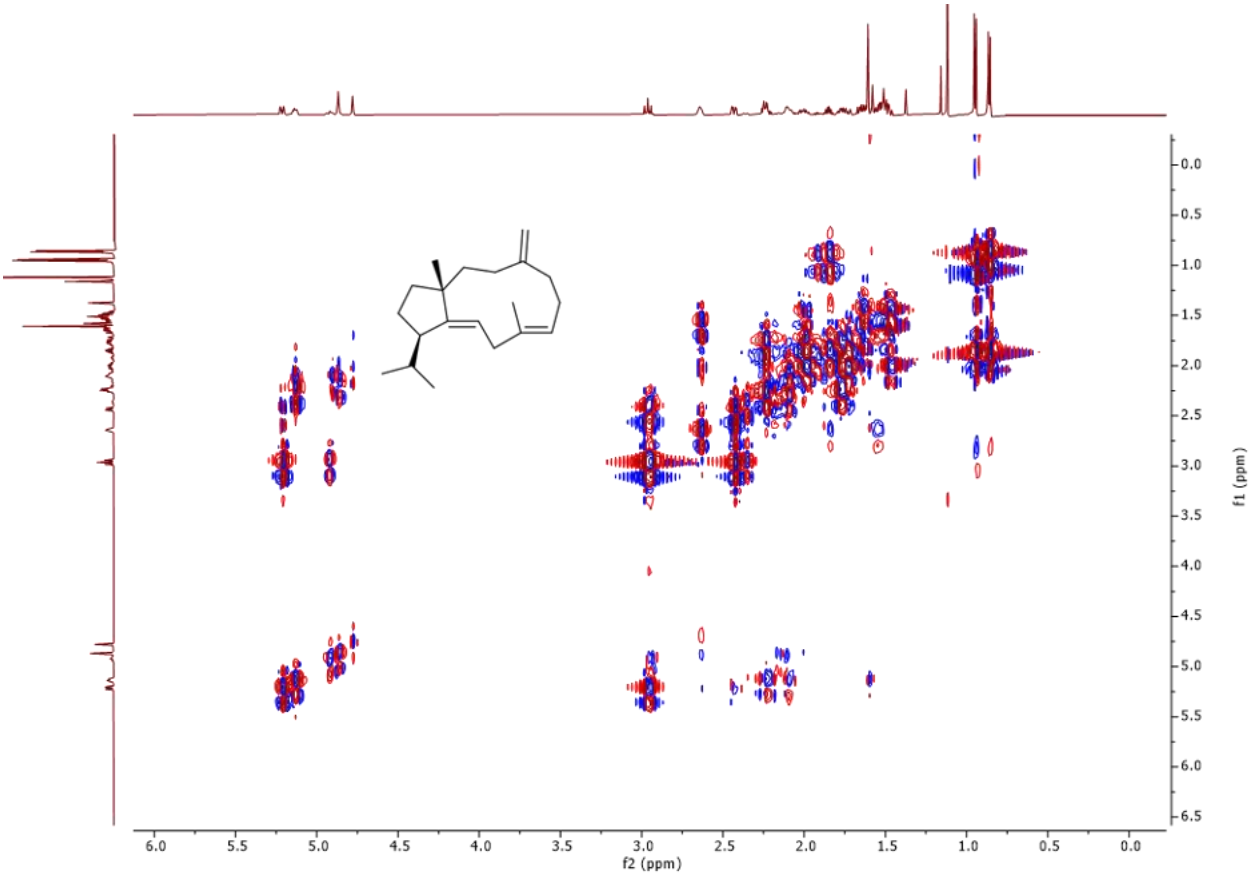

Supplementary Fig. 121. COSY spectrum of 1*R*,7*E*,10*E*,12*R*-dolabella-4(16),7,10-triene (**15**) in C_6D_6.

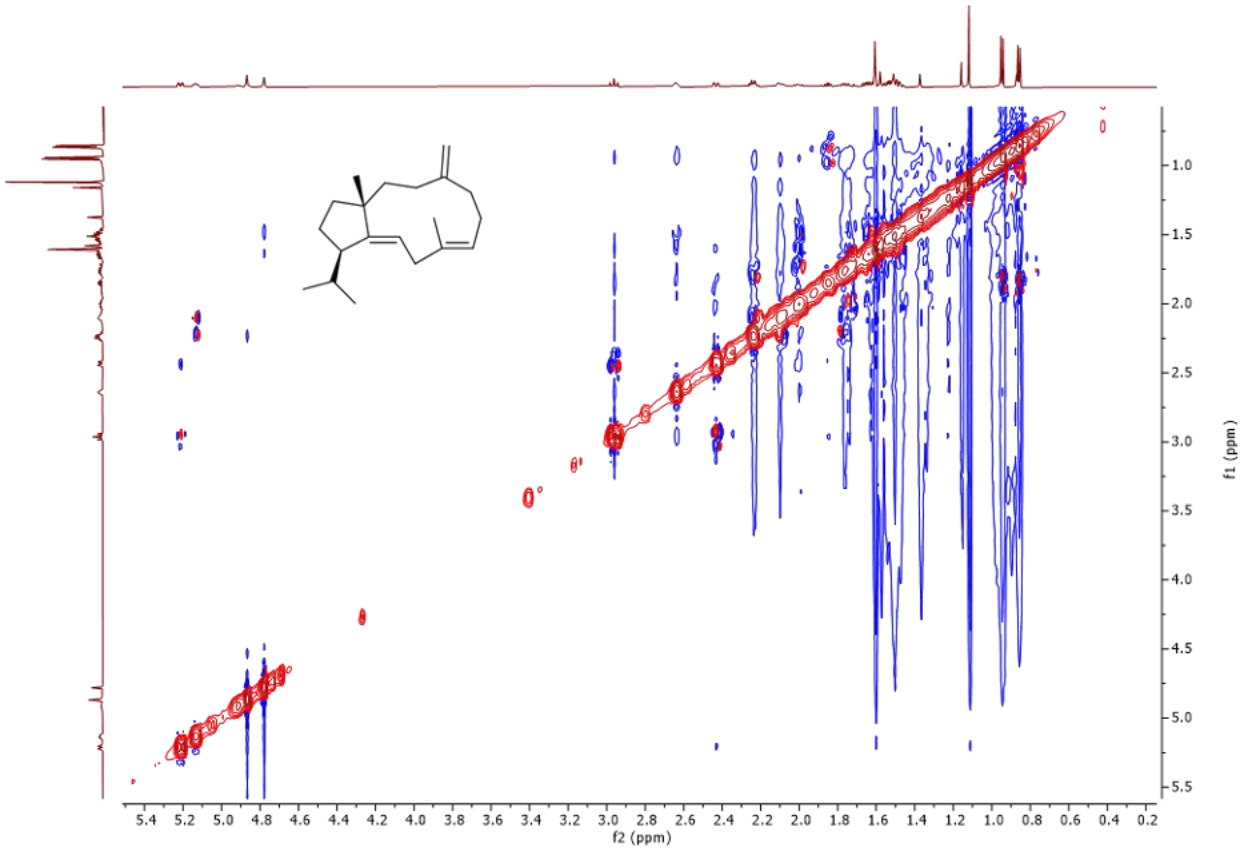

Supplementary Fig. 122. NOESY spectrum of 1*R*,7*E*,10*E*,12*R*-dolabella-4(16),7,10-triene (**15**) in C_6D_6.

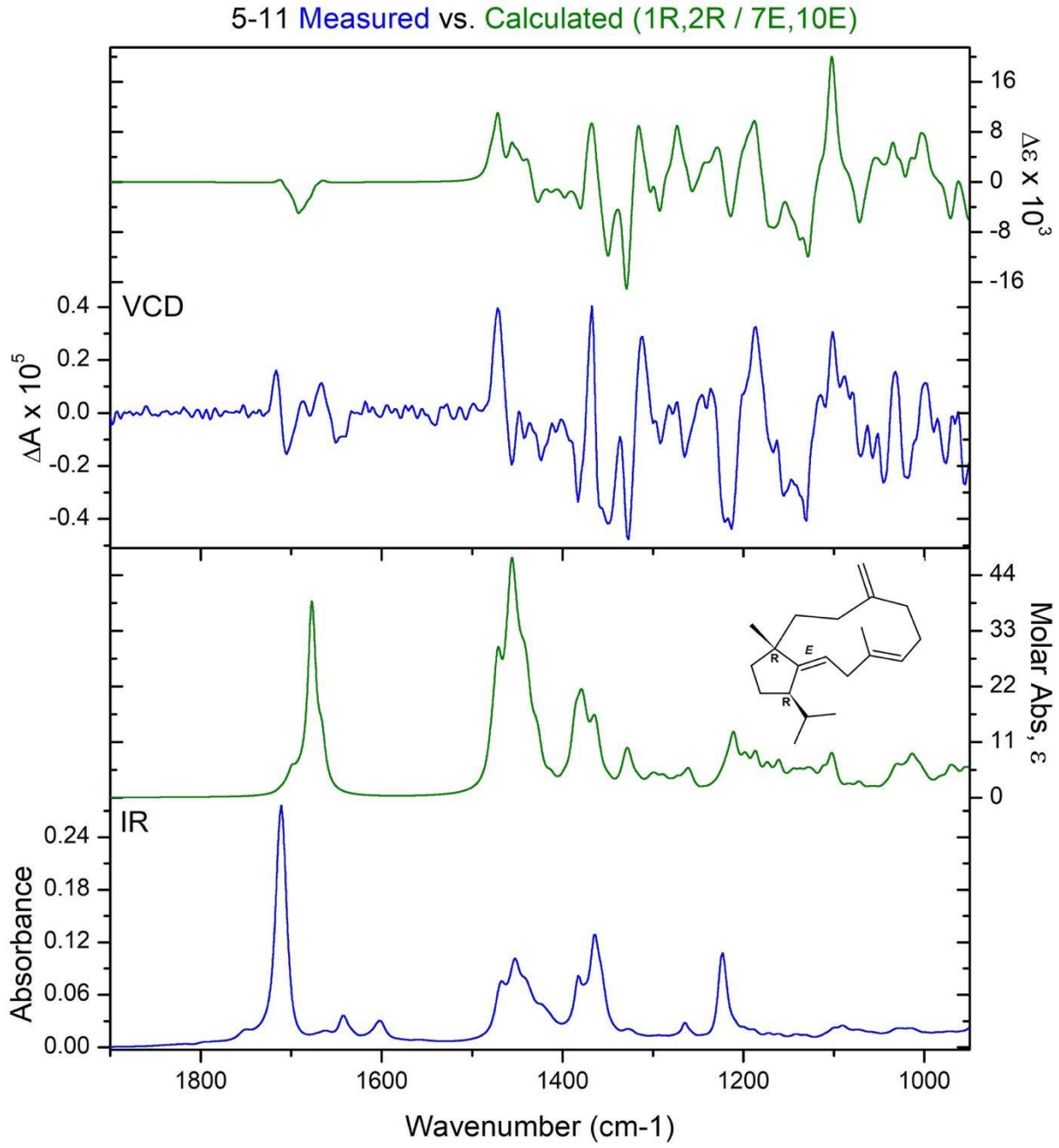

Supplementary Fig. 123. DFT calculated (green) and experimental (blue) VCD and IR spectra of 1*R*,7*E*,10*E*,12*R*-dolabella-4(16),7,10-triene (**15**) supporting the absolute configuration as 1*R*,7*E*,10*E*,12*R*.

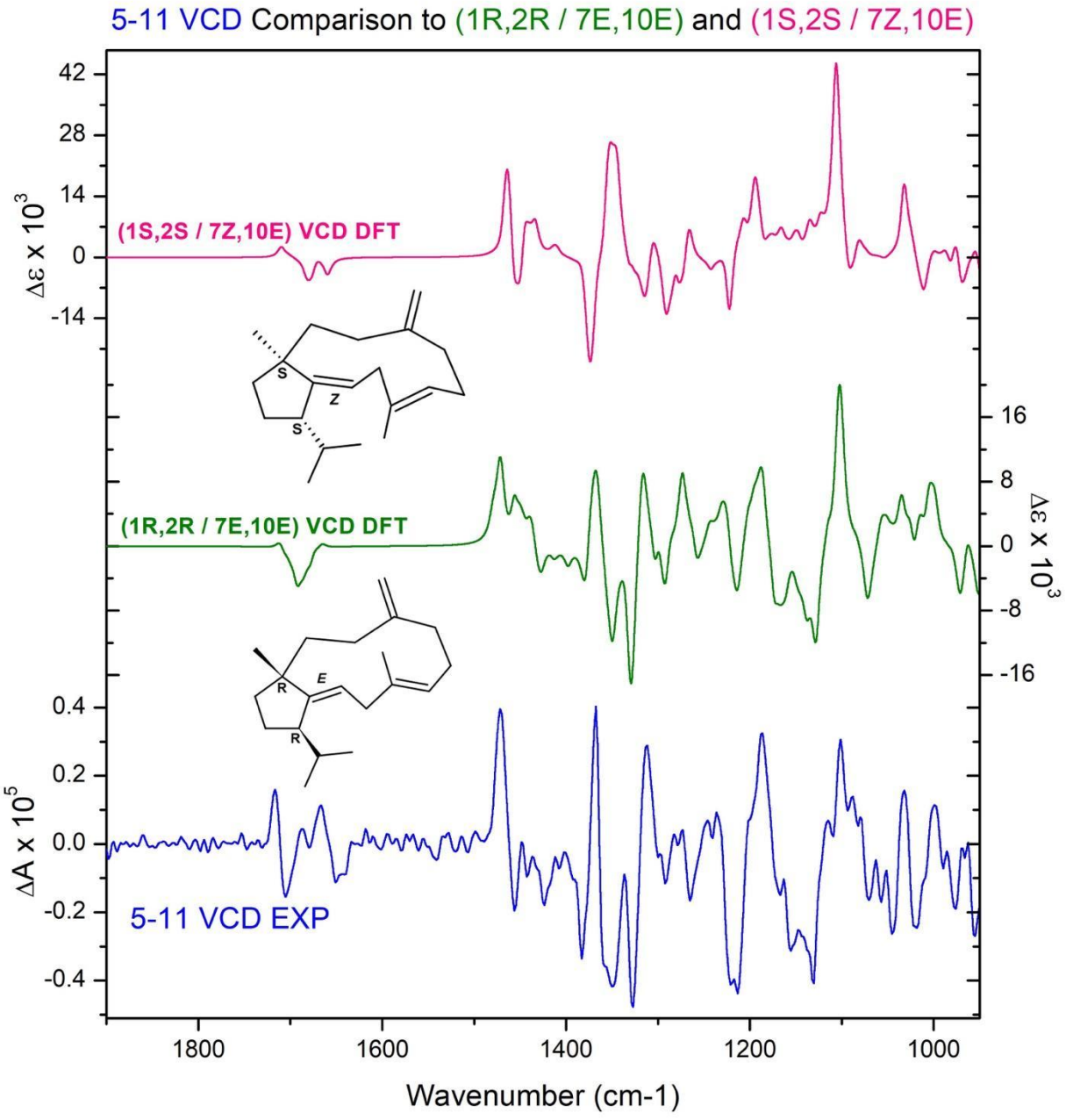

Supplementary Fig. 124. DFT calculated (pink and green) and experimental (blue) VCD and IR spectra of 1*R*,7*E*,10*E*,12*R*-dolabella-4(16),7,10-triene (**15**) supporting the absolute configuration as 1*R*,7*E*,10*E*,12*R*.

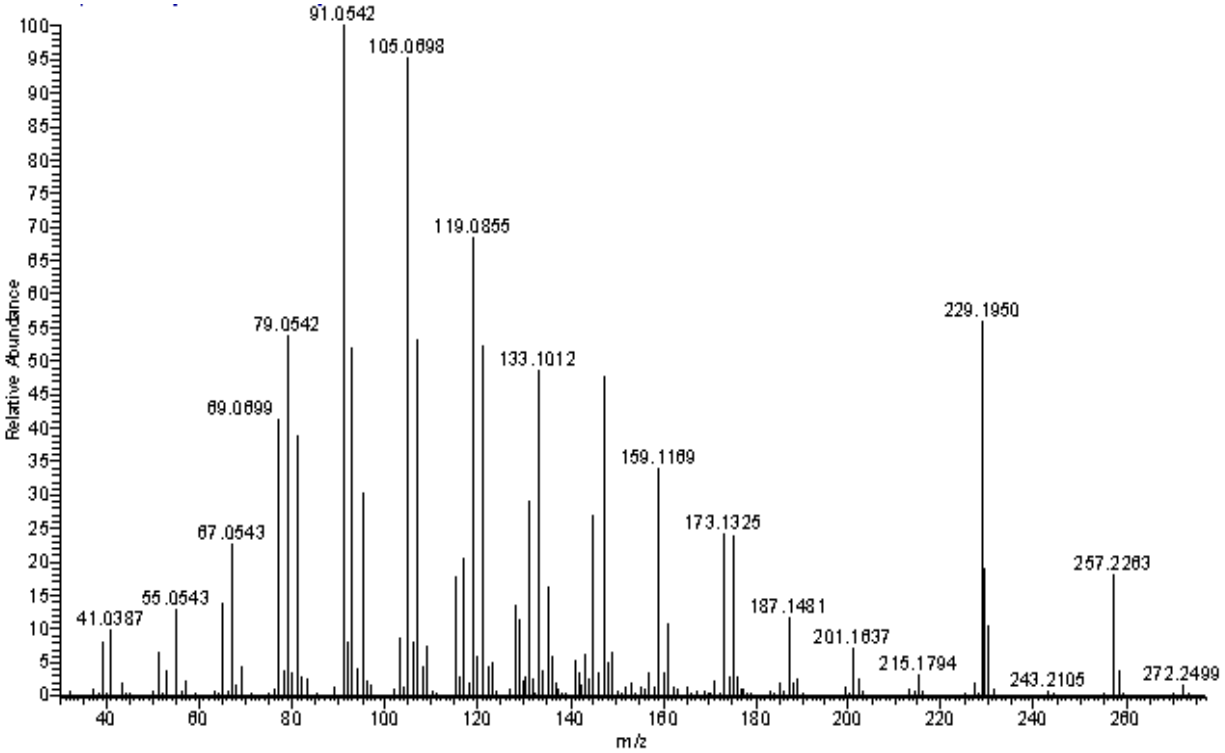

Supplementary Fig. 125. EIMS of (+)-2*S*,3*S*,6*R*,7*Z*,10*Z*,11*R*-cyclooctat-7(8),10(14)-diene (**16**).

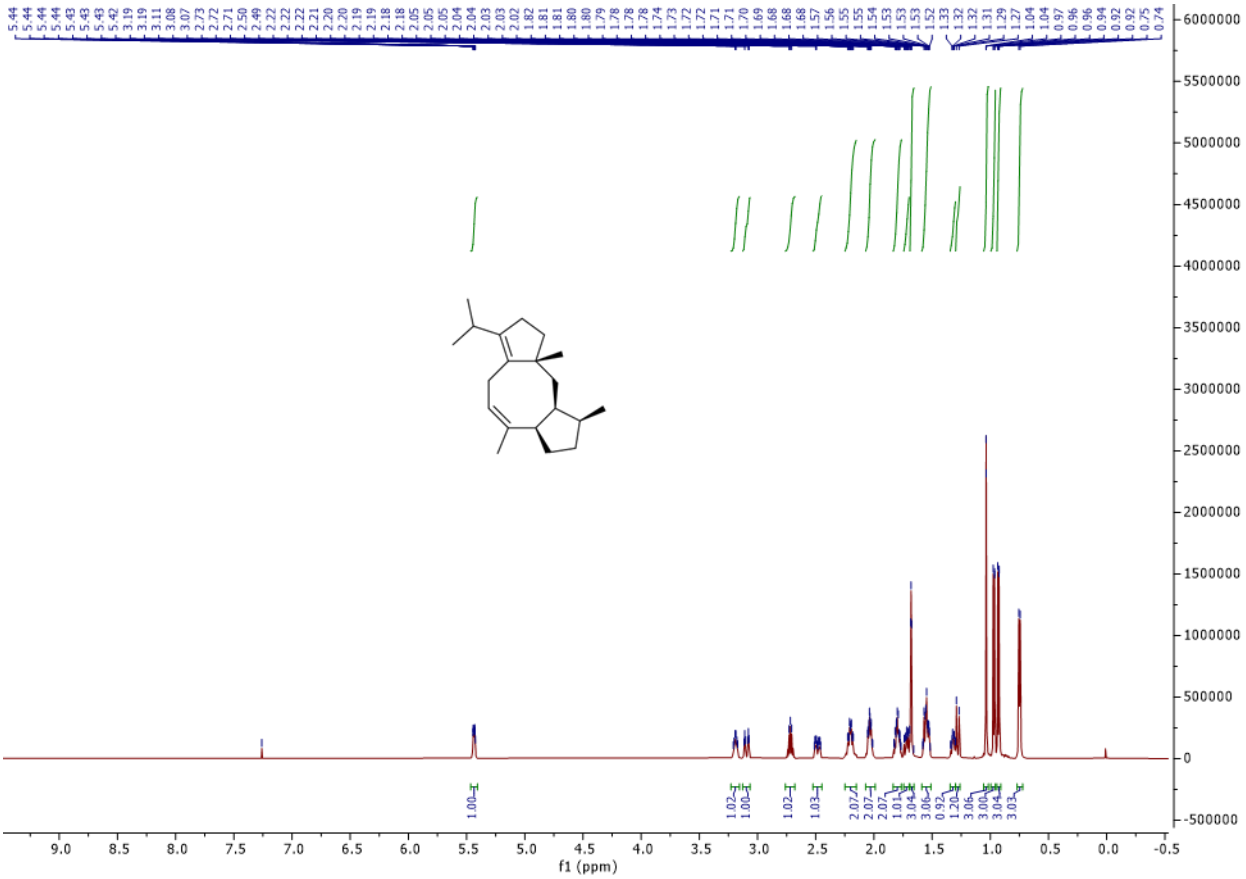

Supplementary Fig. 126. ^{1}H NMR spectrum of (+)-2*S*,3*S*,6*R*,7*Z*,10*Z*,11*R*-cyclooctat-7(8),10(14)-diene (**16**) in $CDCl_3$ (600 MHz).

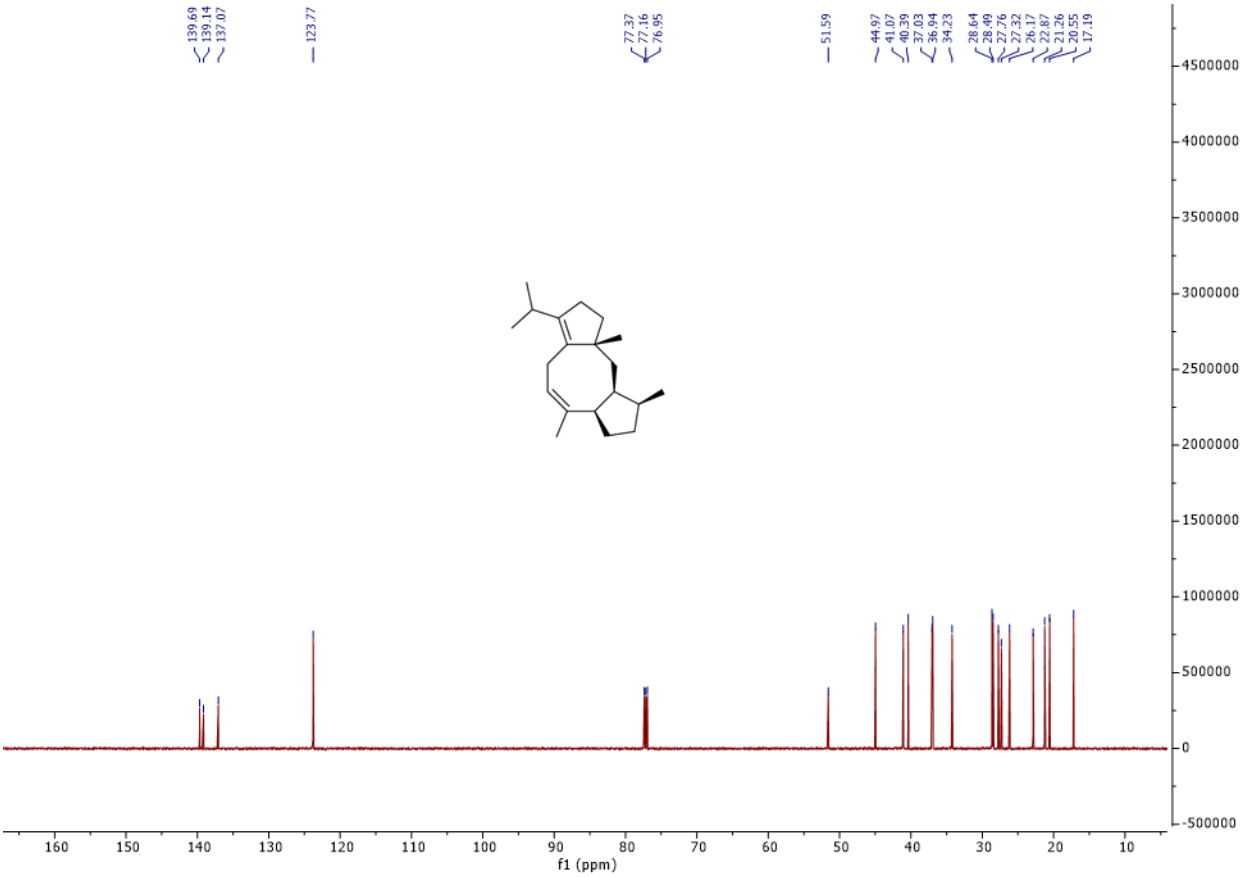

Supplementary Fig. 127. ^{13}C NMR spectrum of (+)-2*S*,3*S*,6*R*,7*Z*,10*Z*,11*R*-cyclooctat-7(8),10(14)-diene (**16**) in $CDCl_3$ (151 MHz).

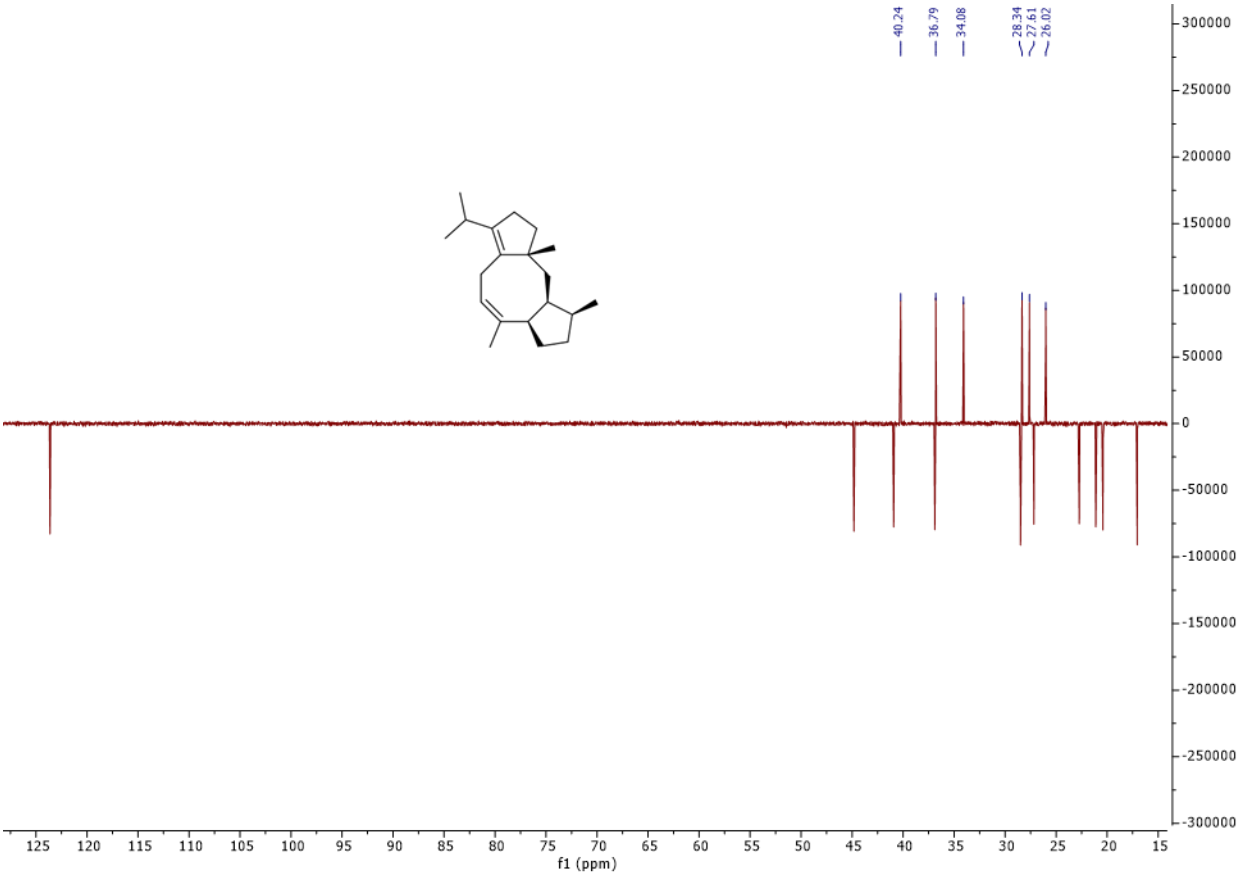

Supplementary Fig. 128. DEPT 135 spectrum of (+)-2*S*,3*S*,6*R*,7*Z*,10*Z*,11*R*-cyclooctat-7(8),10(14)-diene (**16**) in $CDCl_3$ (151 MHz).

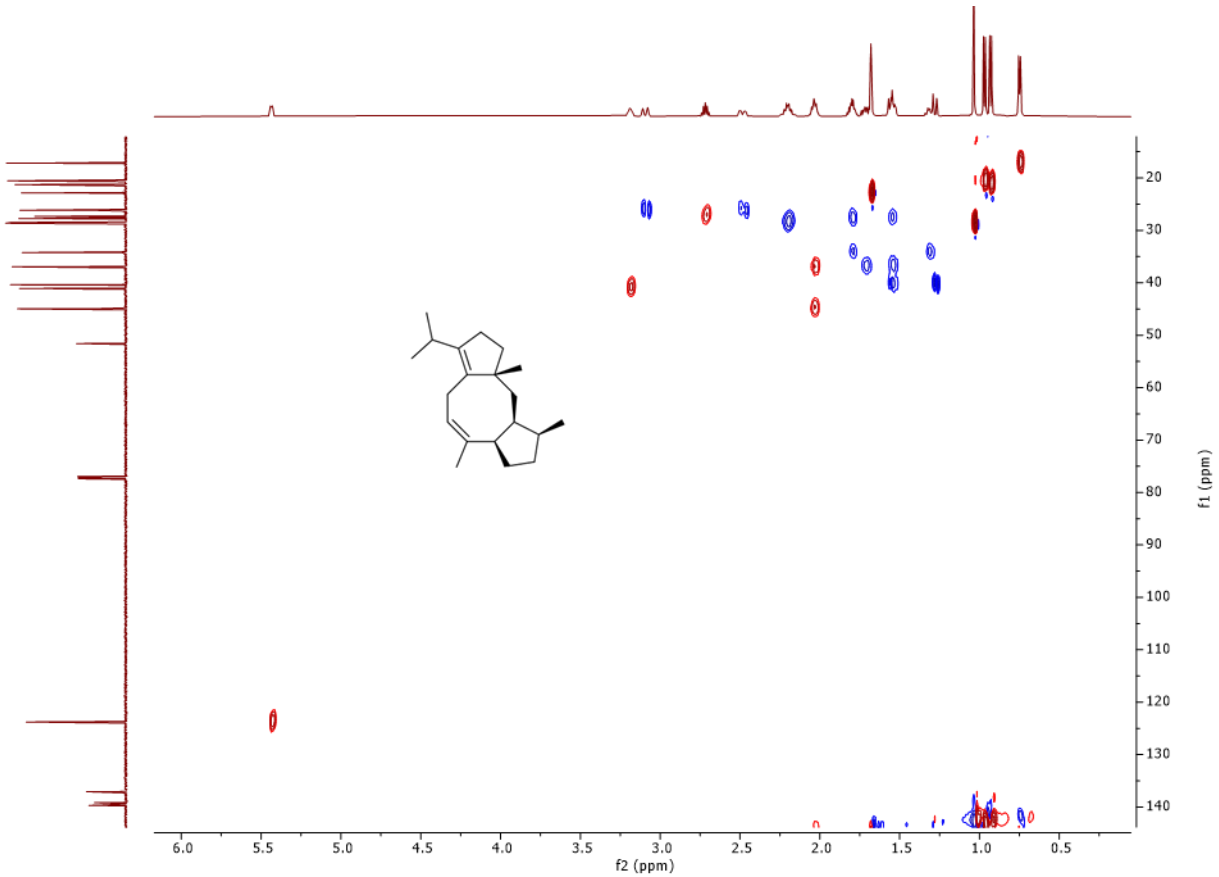

Supplementary Fig. 129. HSQC spectrum of (+)-2*S*,3*S*,6*R*,7*Z*,10*Z*,11*R*-cyclooctat-7(8),10(14)-diene (**16**) in $CDCl_3$.

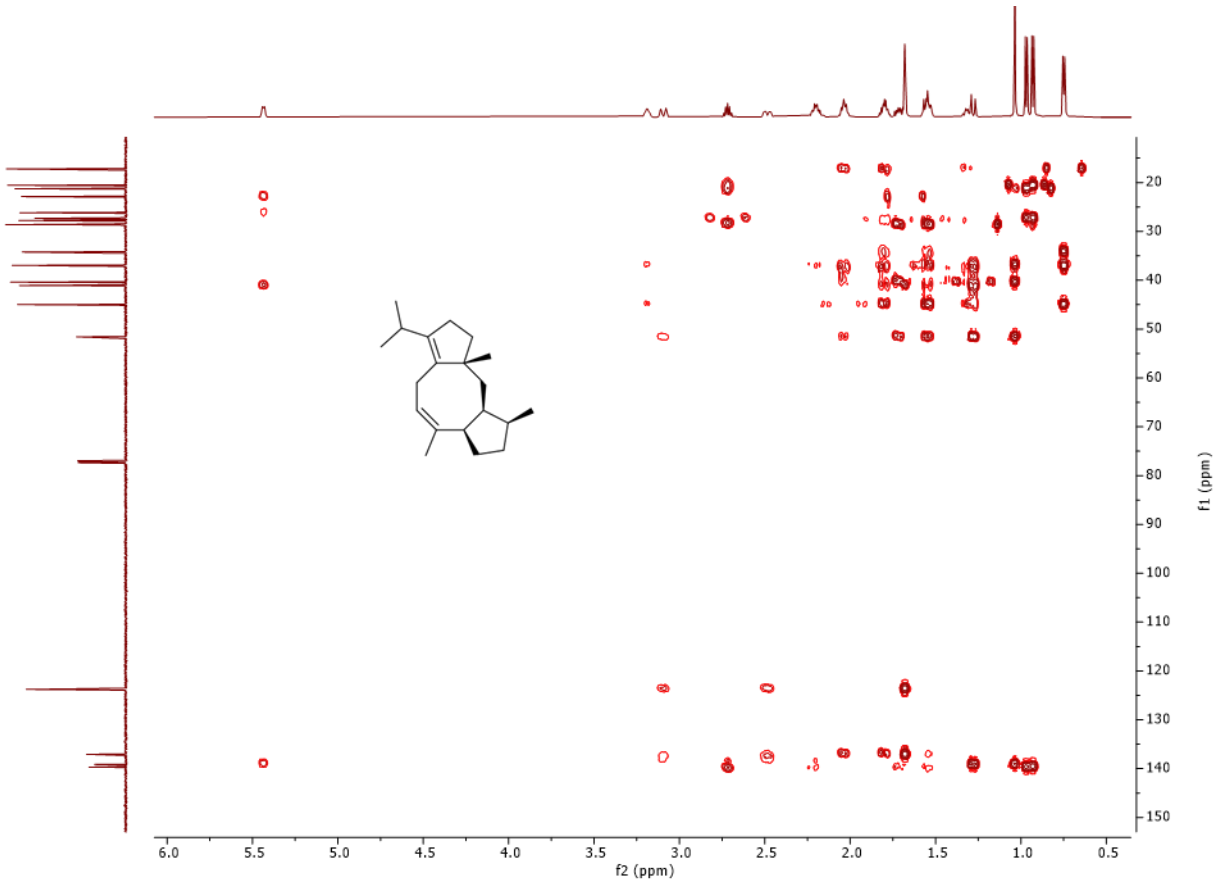

Supplementary Fig. 130. HMBC spectrum of (+)-2*S*,3*S*,6*R*,7*Z*,10*Z*,11*R*-cyclooctat-7(8),10(14)-diene (**16**) in $CDCl_3$ (151 MHz).

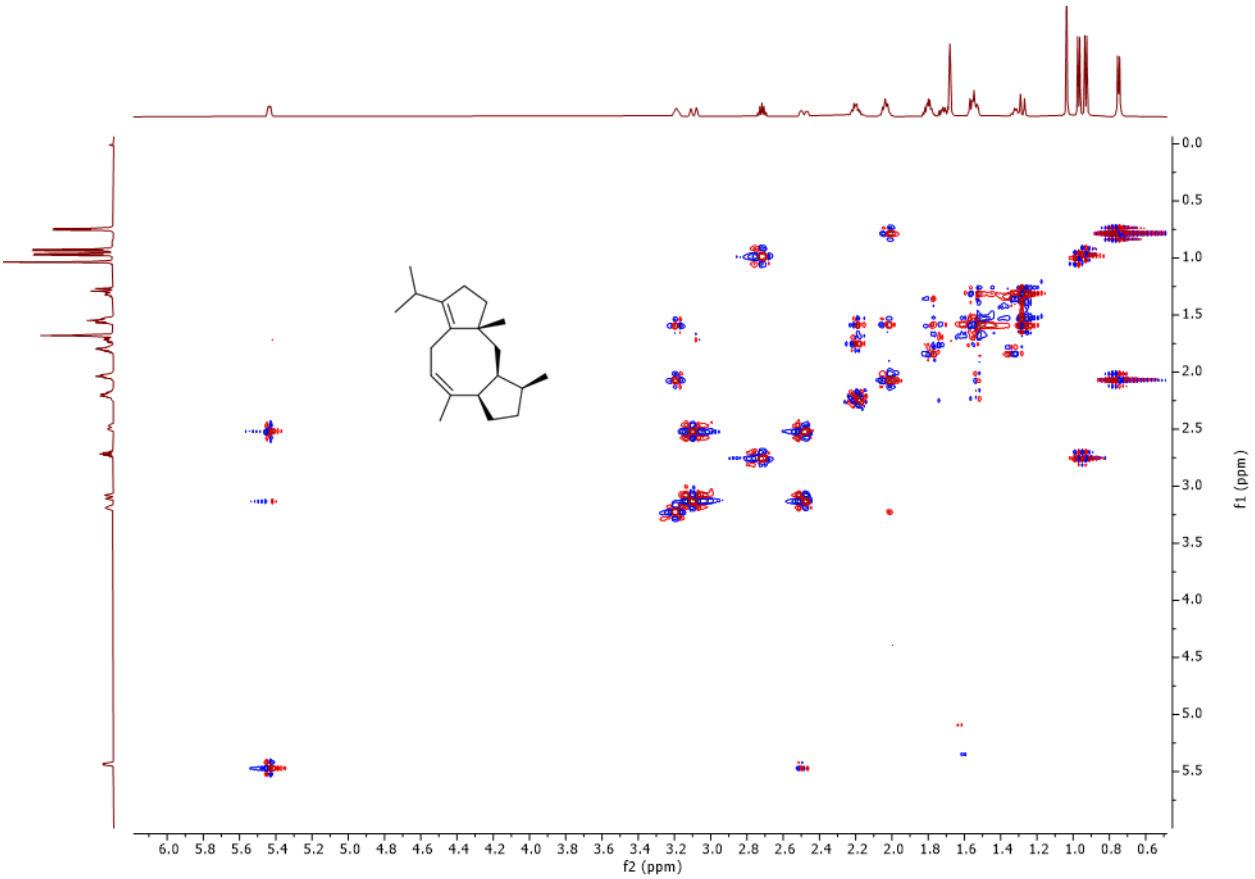

Supplementary Fig. 131. COSY spectrum of (+)-2*S*,3*S*,6*R*,7*Z*,10*Z*,11*R*-cyclooctat-7(8),10(14)-diene (**16**) in $CDCl_3$.

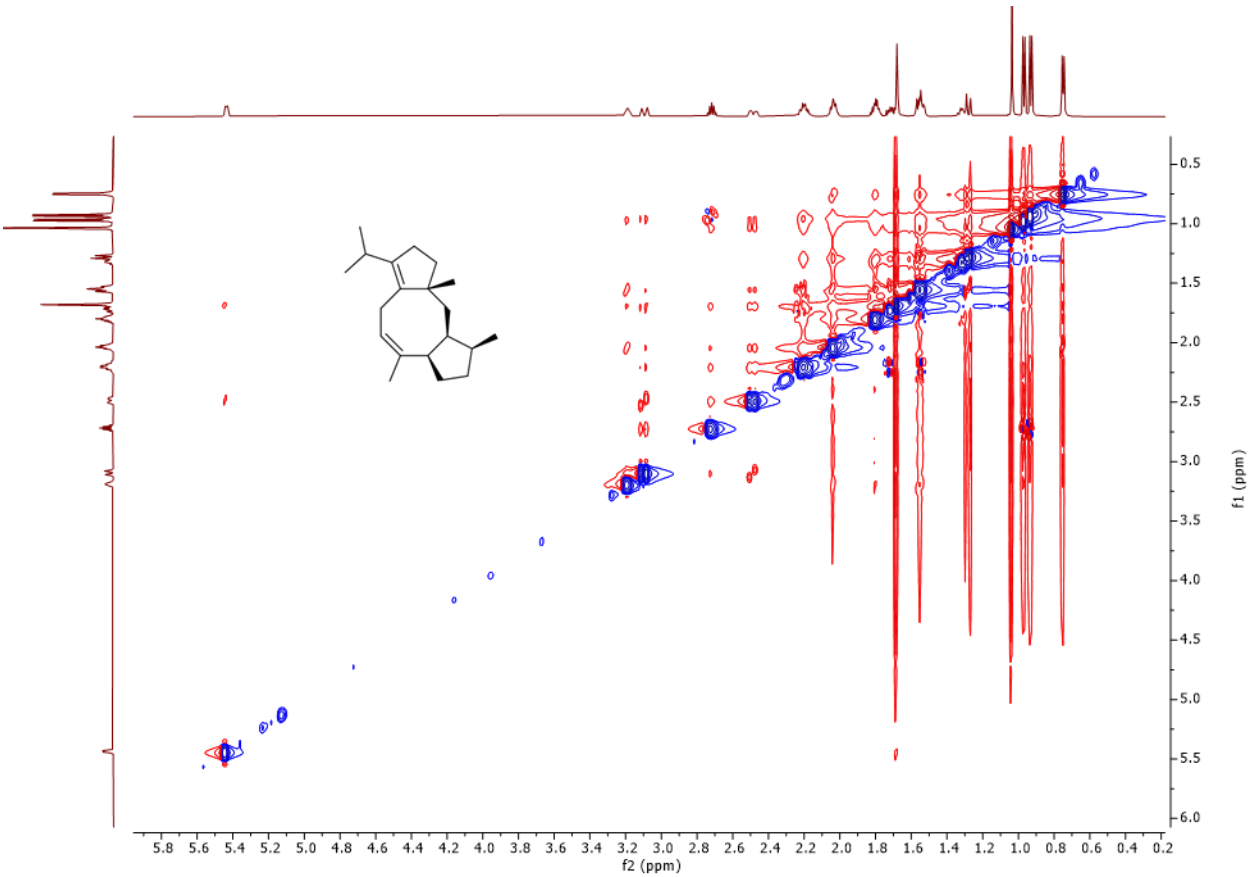

Supplementary Fig. 132. NOESY spectrum of (+)-2*S*,3*S*,6*R*,7*Z*,10*Z*,11*R*-cyclooctat-7(8),10(14)-diene (**16**) in $CDCl_3$ (151 MHz).

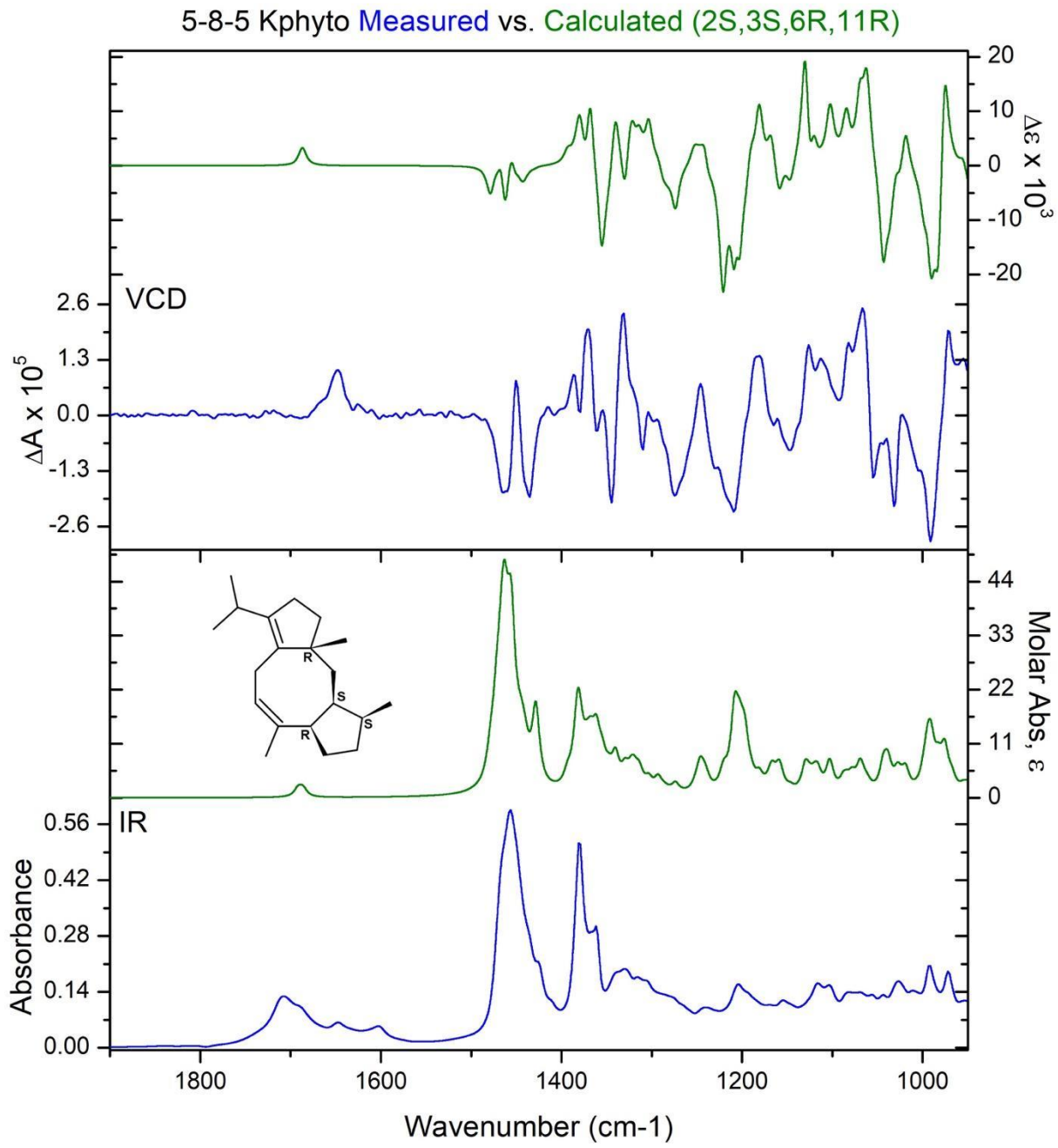

Supplementary Fig. 133. DFT calculated (green) and experimental (blue) VCD and IR spectra of (+)-2*S*,3*S*,6*R*,7*Z*,10*Z*,11*R*-cyclooctat-7(8),10(14)-diene (**16**) supporting the absolute configuration as 2*S*,3*S*,6*R*,11*R*.

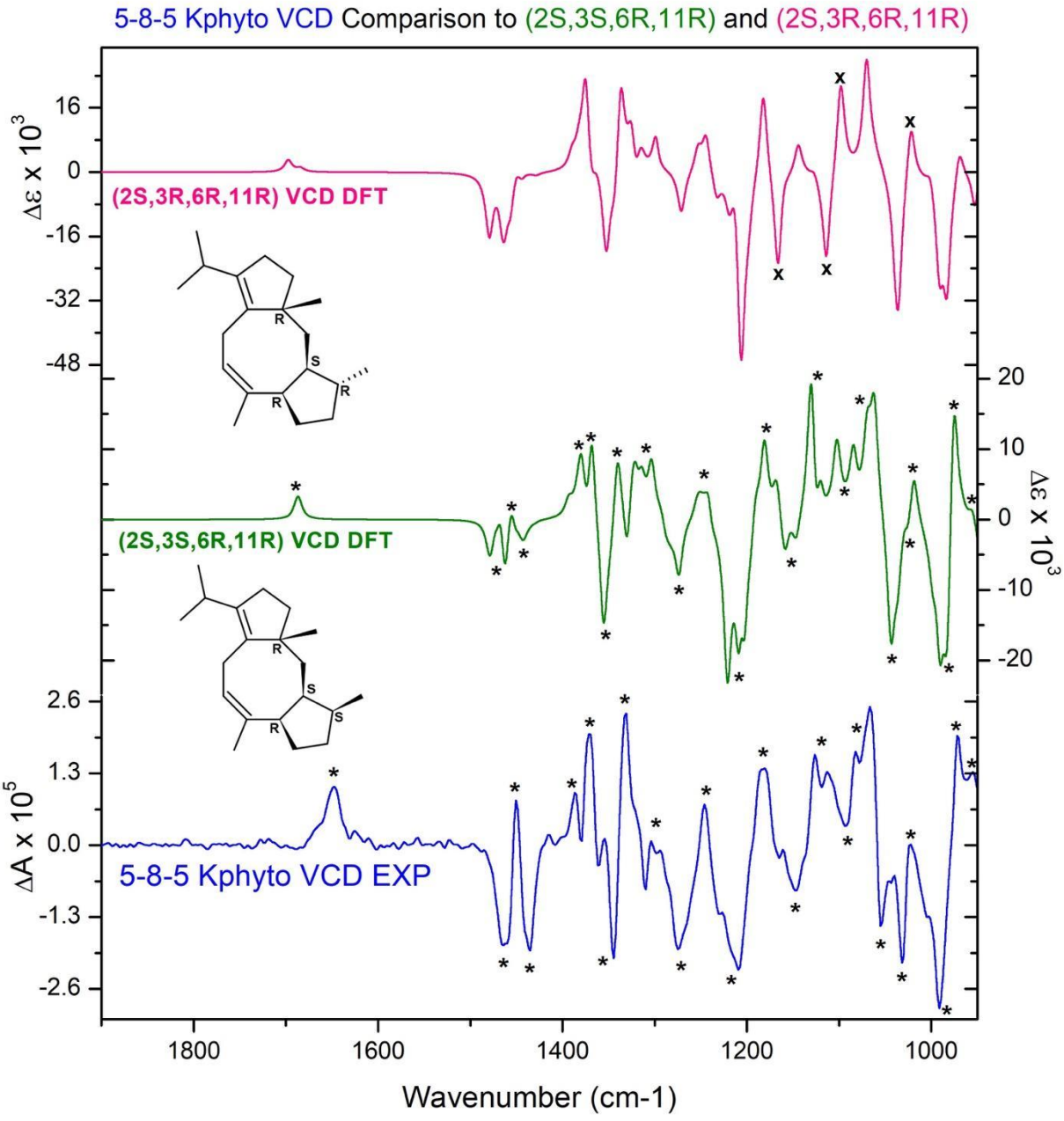

Supplementary Fig. 134. DFT calculated (pink and green) and experimental (blue) VCD and IR spectra of (+)-2*S*,3*S*,6*R*,7*Z*,10*Z*,11*R*-cyclooctat-7(8),10(14)-diene (**16**) supporting the absolute configuration as 2*S*,3*S*,6*R*,11*R*.

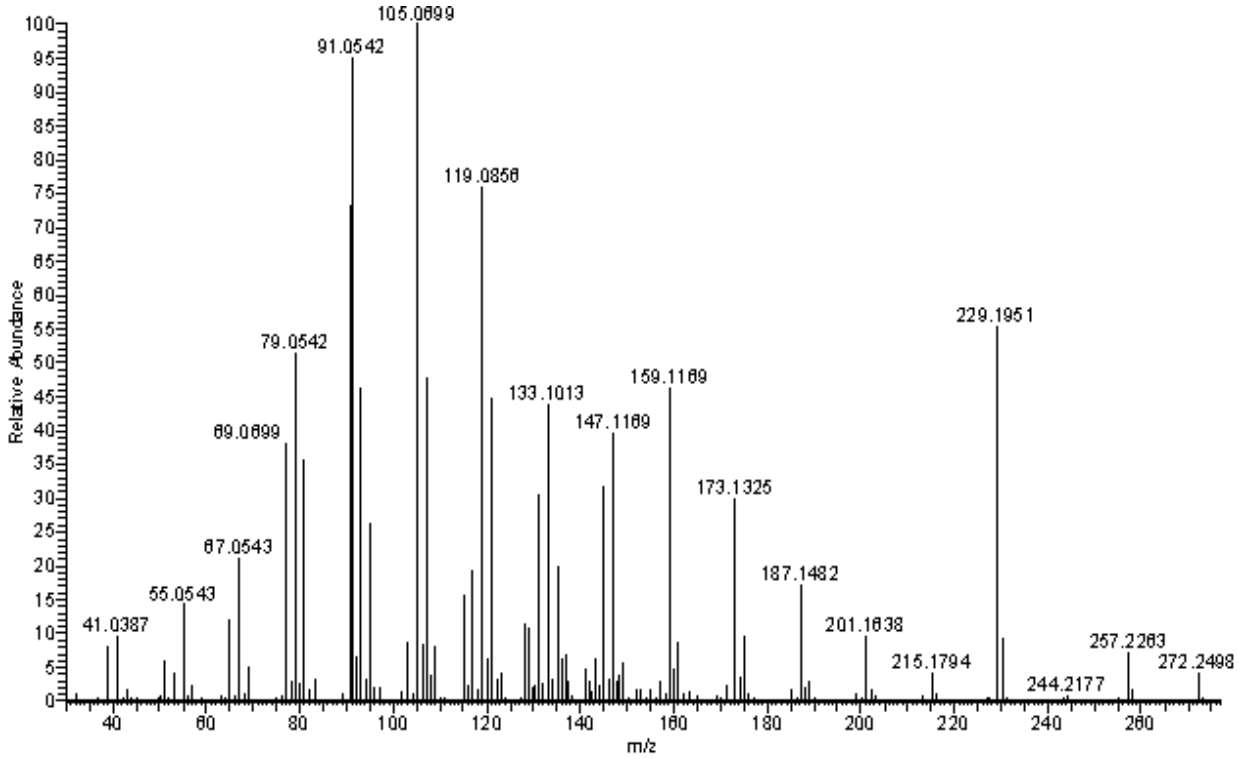

Supplementary Fig. 135. EIMS of (–)-2*R*,3*S*,6*R*,7*Z*,10*Z*,11*S*-cyclooctat-7(8),10(14)-diene (**17**). The fragmentation matched the literature[14].

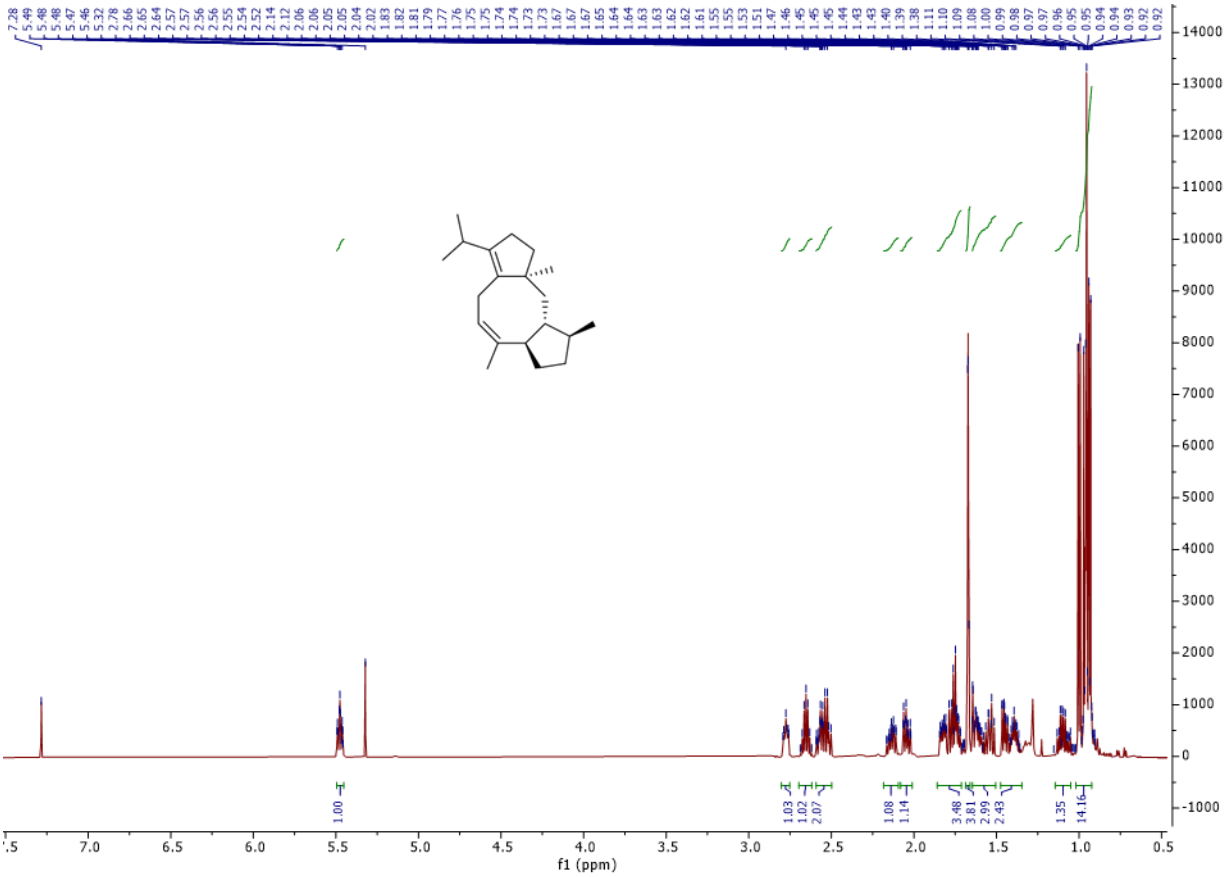

Supplementary Fig. 136. ^{1}H NMR spectrum of (–)-2*R*,3*S*,6*R*,7*Z*,10*Z*,11*S*-cyclooctat-7(8),10(14)-diene (**17**) in $CDCl_3$ (600 MHz).

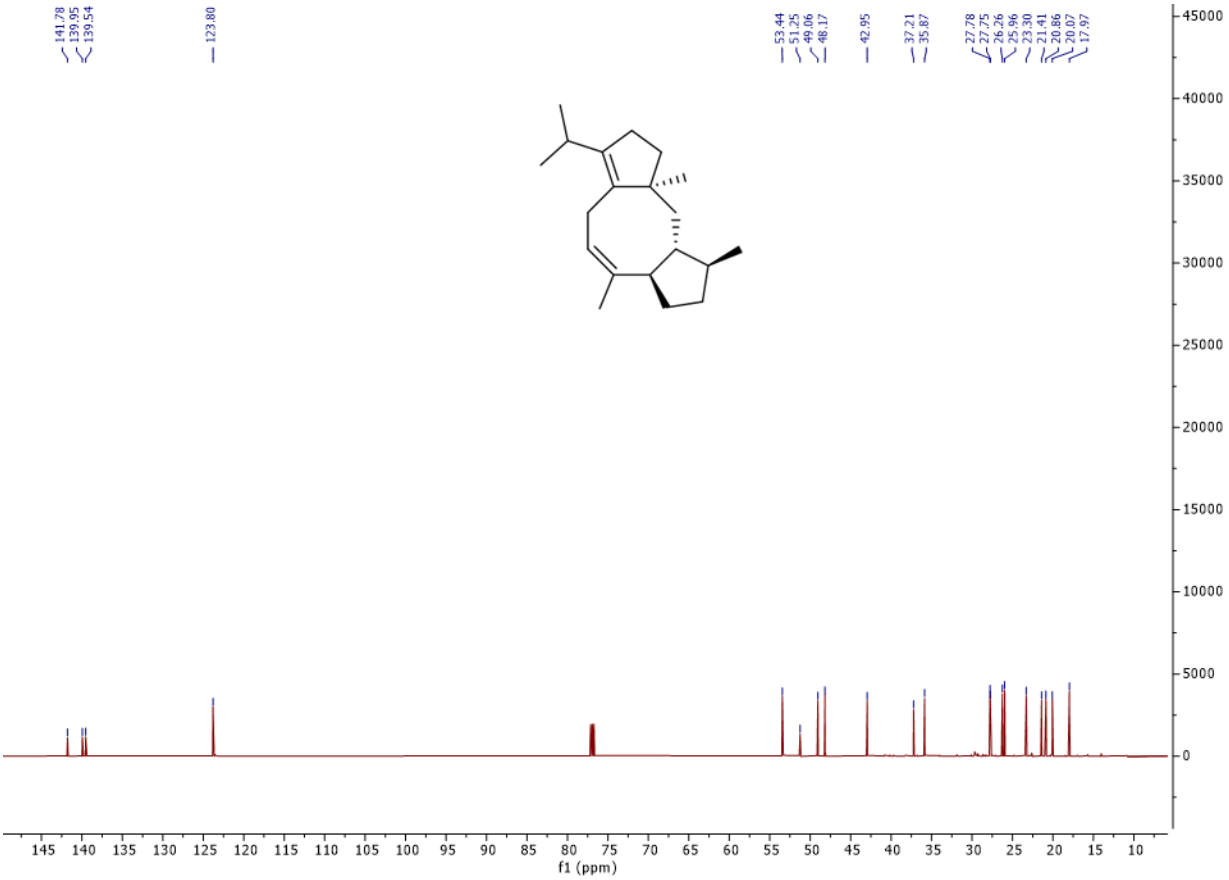

Supplementary Fig. 137. ^{13}C NMR spectrum of (–)-2*R*,3*S*,6*R*,7*Z*,10*Z*,11*S*-cyclooctat-7(8),10(14)-diene (**17**) in $CDCl_3$ (151 MHz).

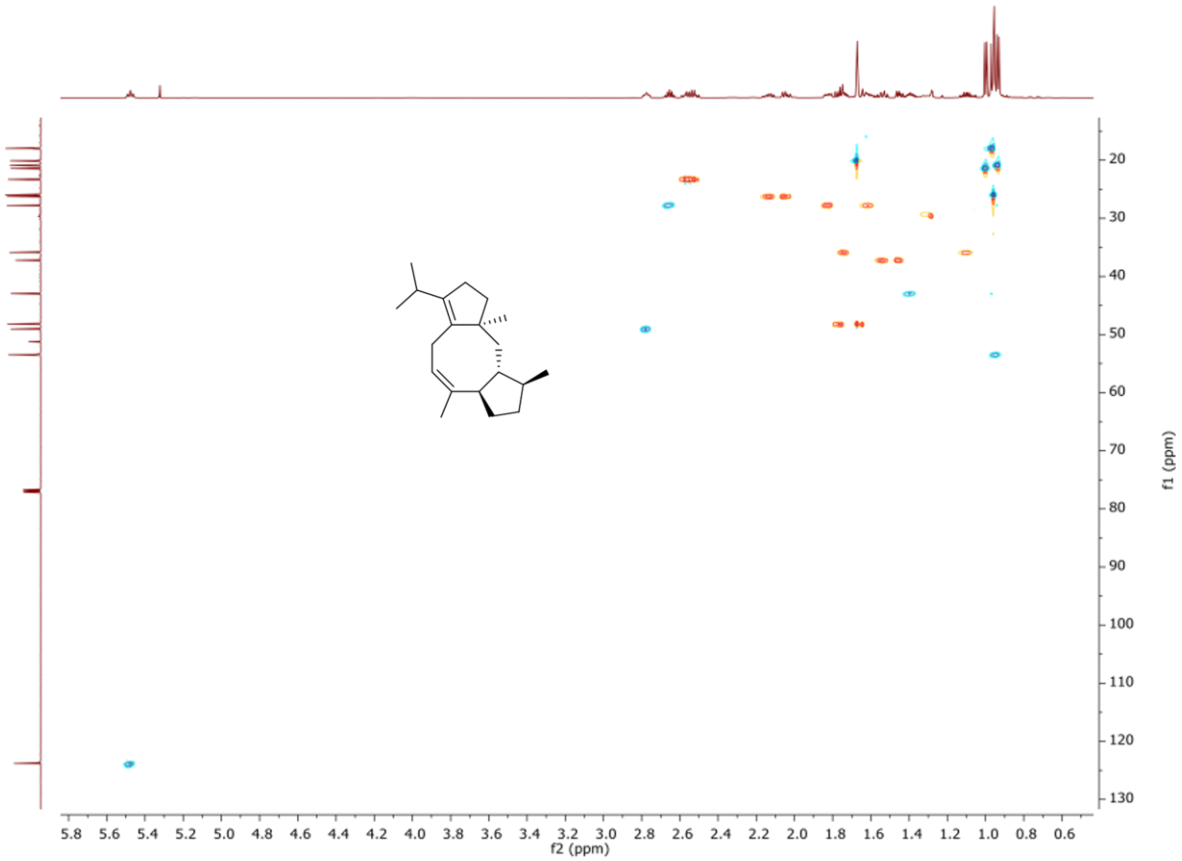

Supplementary Fig. 138. HSQC spectrum of (–)-2*R*,3*S*,6*R*,7*Z*,10*Z*,11*S*-cyclooctat-7(8),10(14)-diene (**17**) in $CDCl_3$.

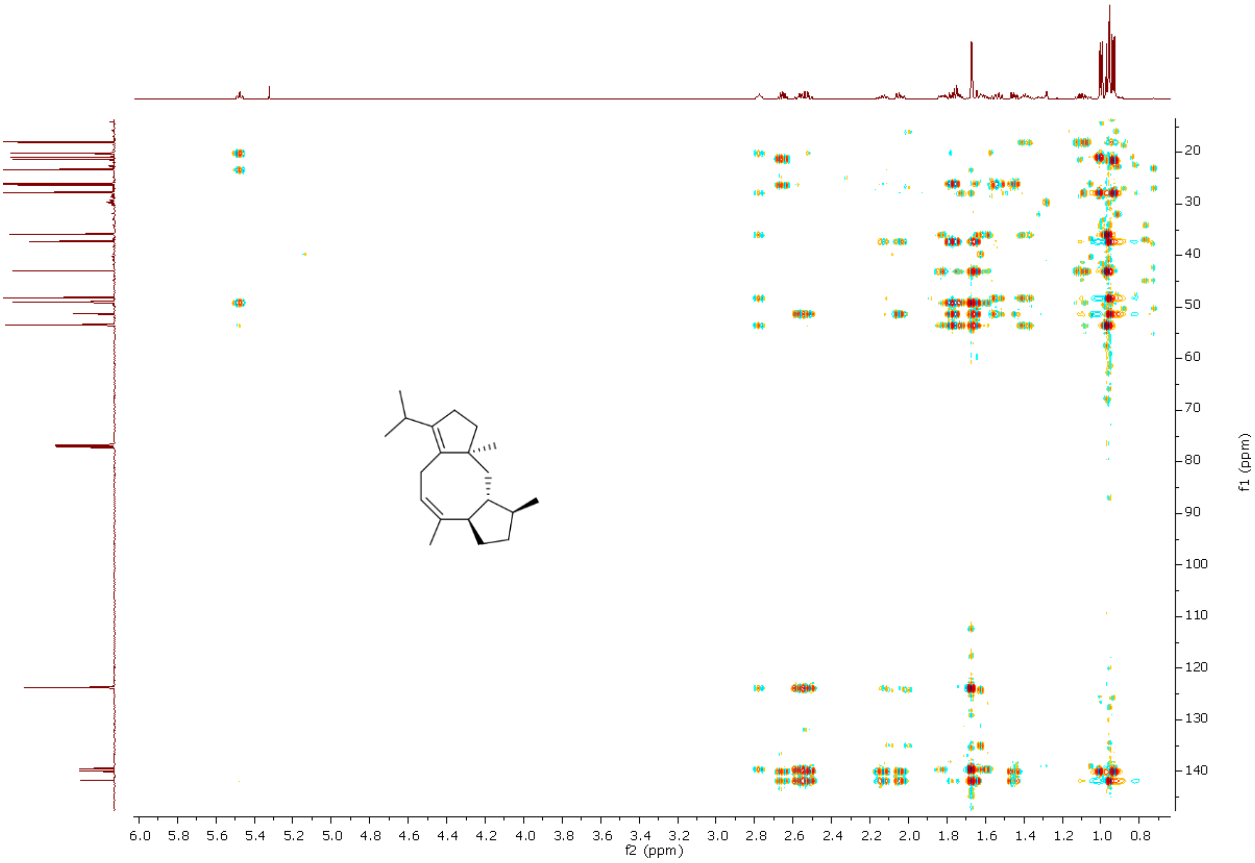

Supplementary Fig. 139. HMBC spectrum of (–)-2*R*,3*S*,6*R*,7*Z*,10*Z*,11*S*-cyclooctat-7(8),10(14)-diene (**17**) in $CDCl_3$ (151 MHz).

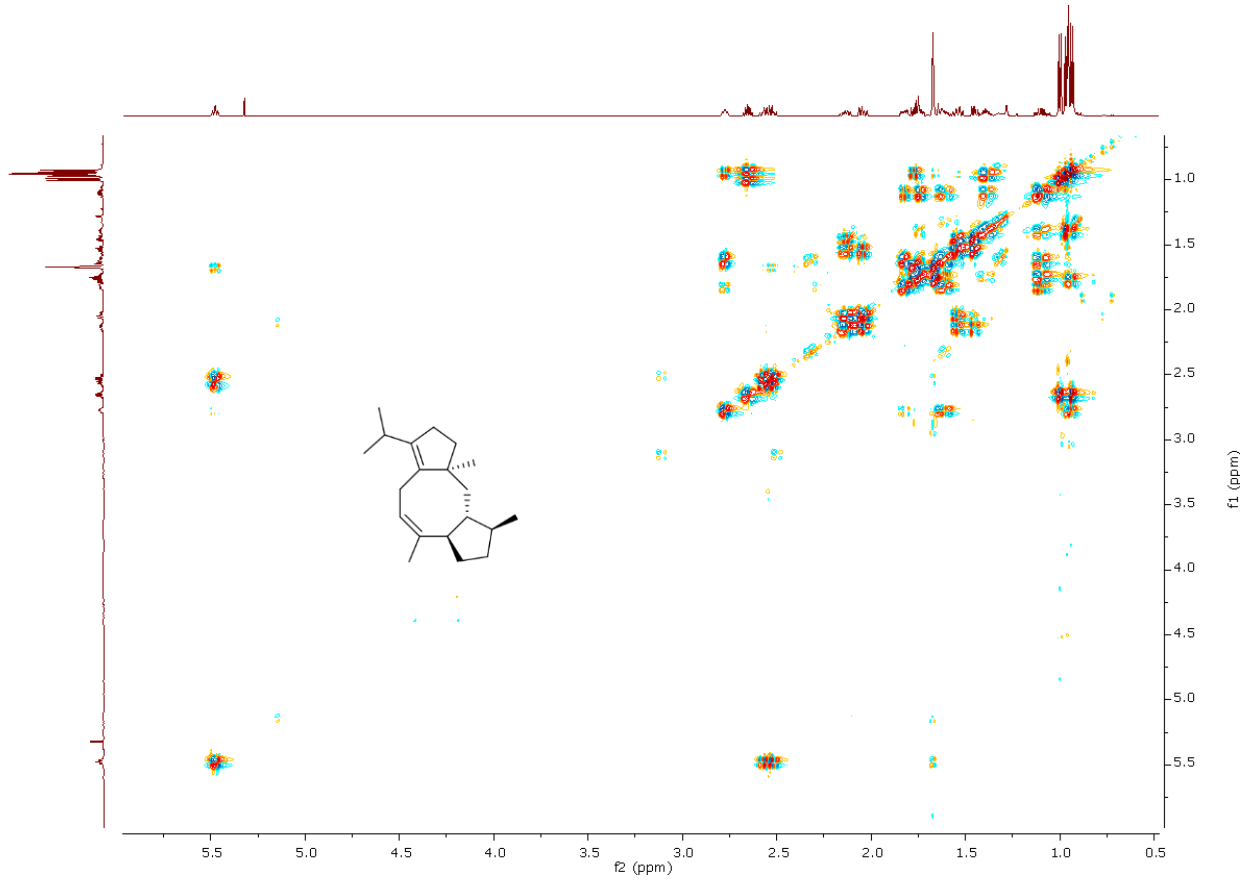

Supplementary Fig. 140. COSY spectrum of (–)-2*R*,3*S*,6*R*,7*Z*,10*Z*,11*S*-cyclooctat-7(8),10(14)-diene (**17**) in $CDCl_3$.

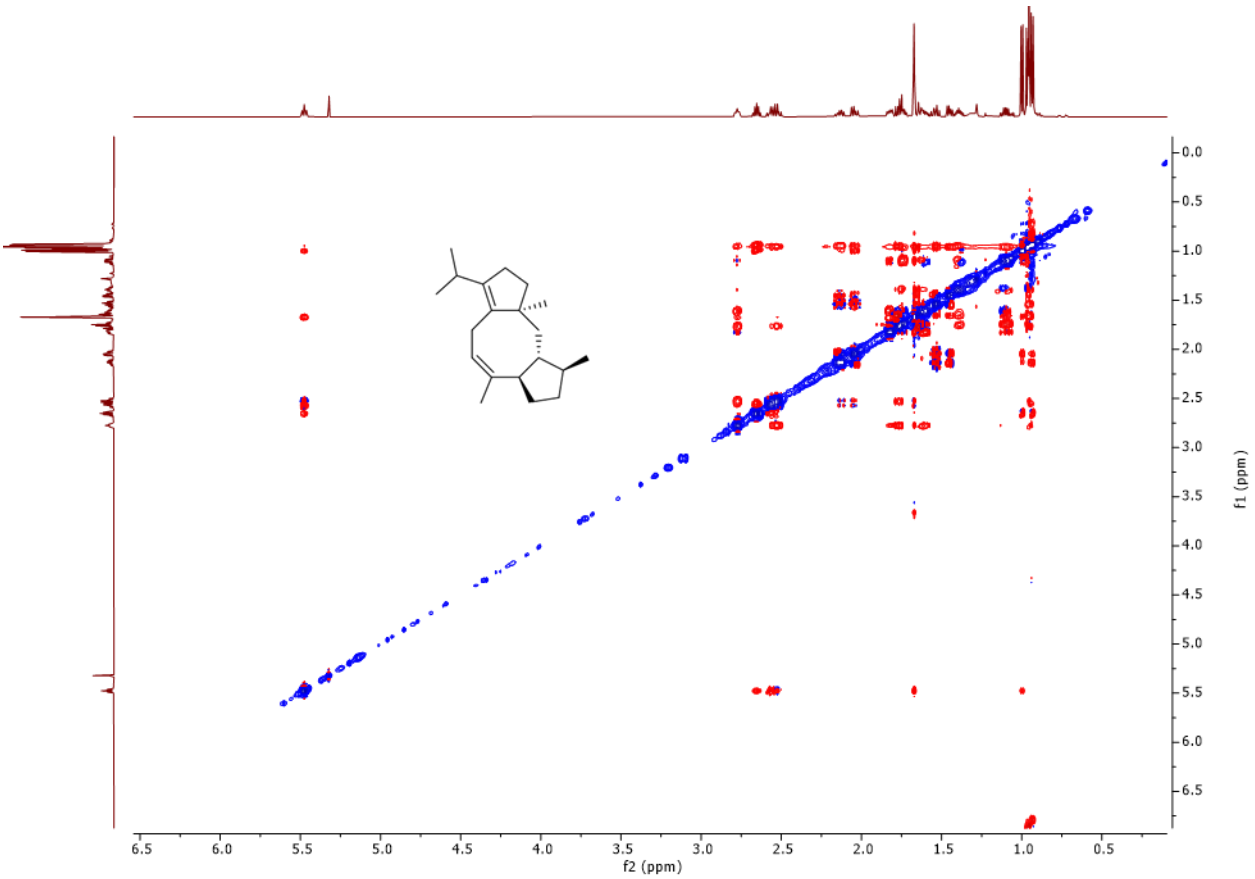

Supplementary Fig. 141. NOESY spectrum of (–)-2*R*,3*S*,6*R*,7*Z*,10*Z*,11*S*-cyclooctat-7(8),10(14)-diene (**17**) in $CDCl_3$ (800 MHz).

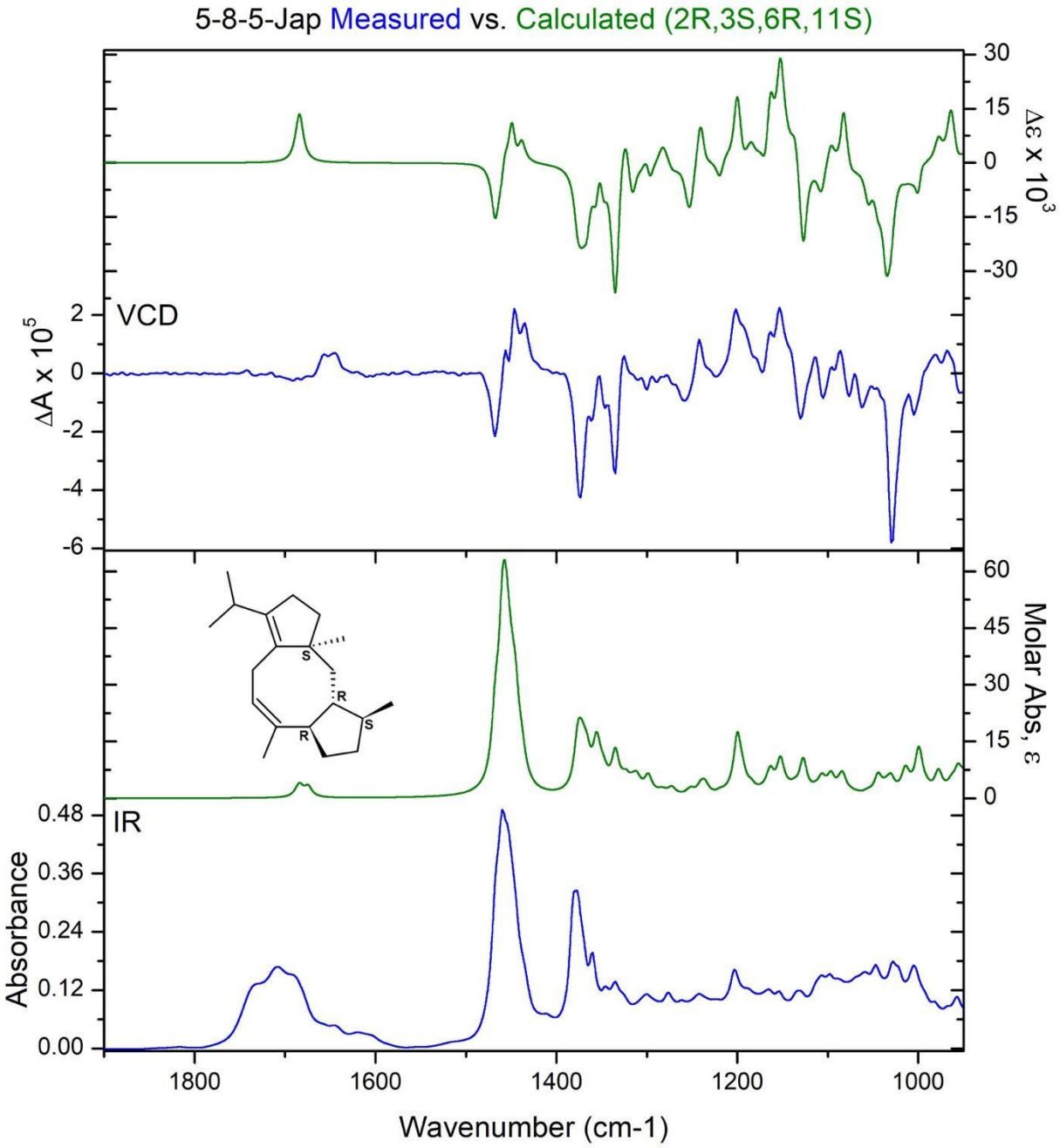

Supplementary Fig. 142. DFT calculated (green) and experimental (blue) VCD and IR spectra of (–)-2*R*,3*S*,6*R*,7*Z*,10*Z*,11*S*-cyclooctat-7(8),10(14)-diene (**17**) supporting the absolute configuration as 2*R*,3*S*,6*R*,11*S*.

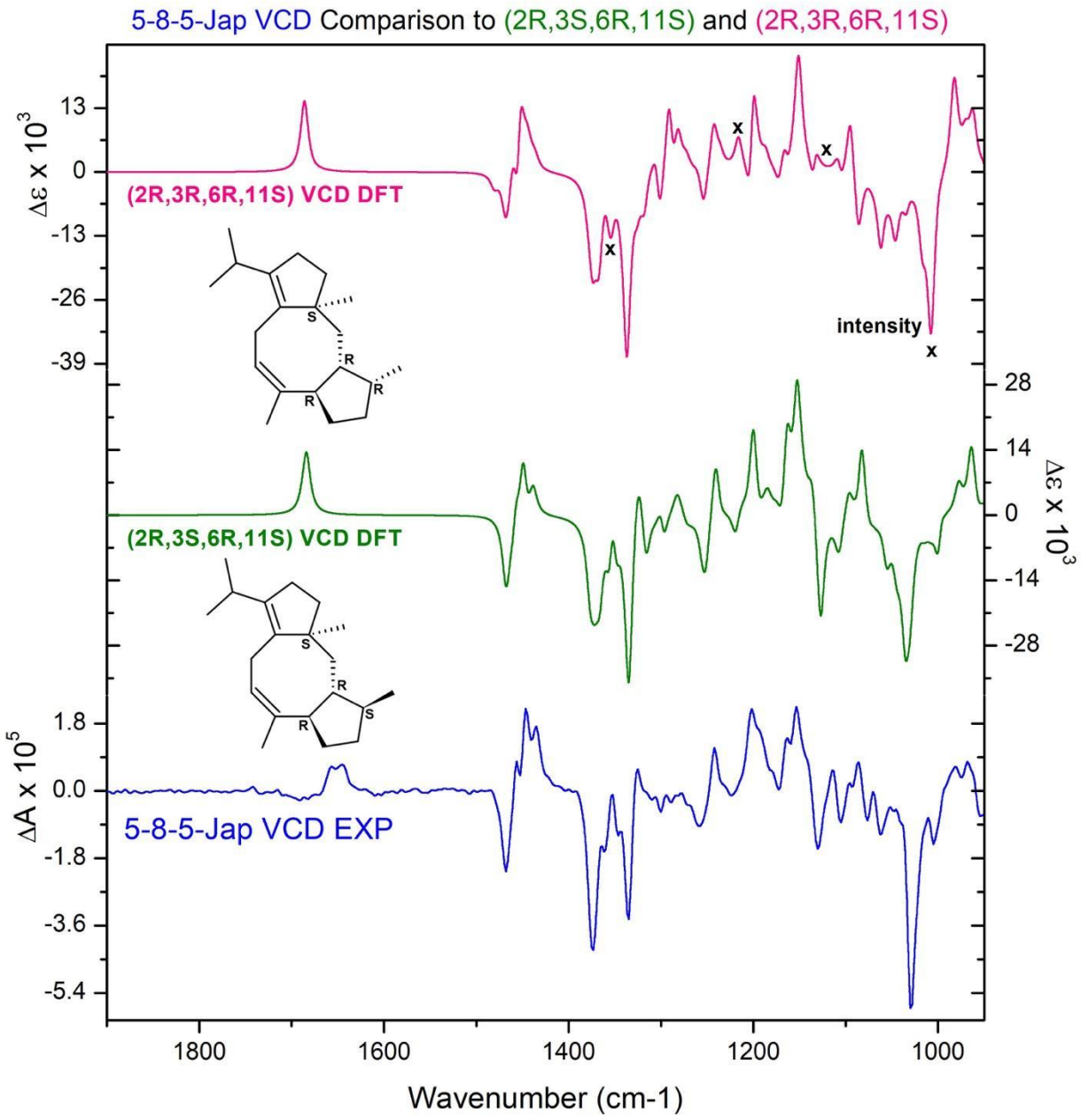

Supplementary Fig. 143. DFT calculated (pink and green) and experimental (blue) VCD and IR spectra of (–)-2*R*,3*S*,6*R*,7*Z*,10*Z*,11*S*-cyclooctat-7(8),10(14)-diene (**17**) supporting the absolute configuration as 2*R*,3*S*,6*R*,11*S*.

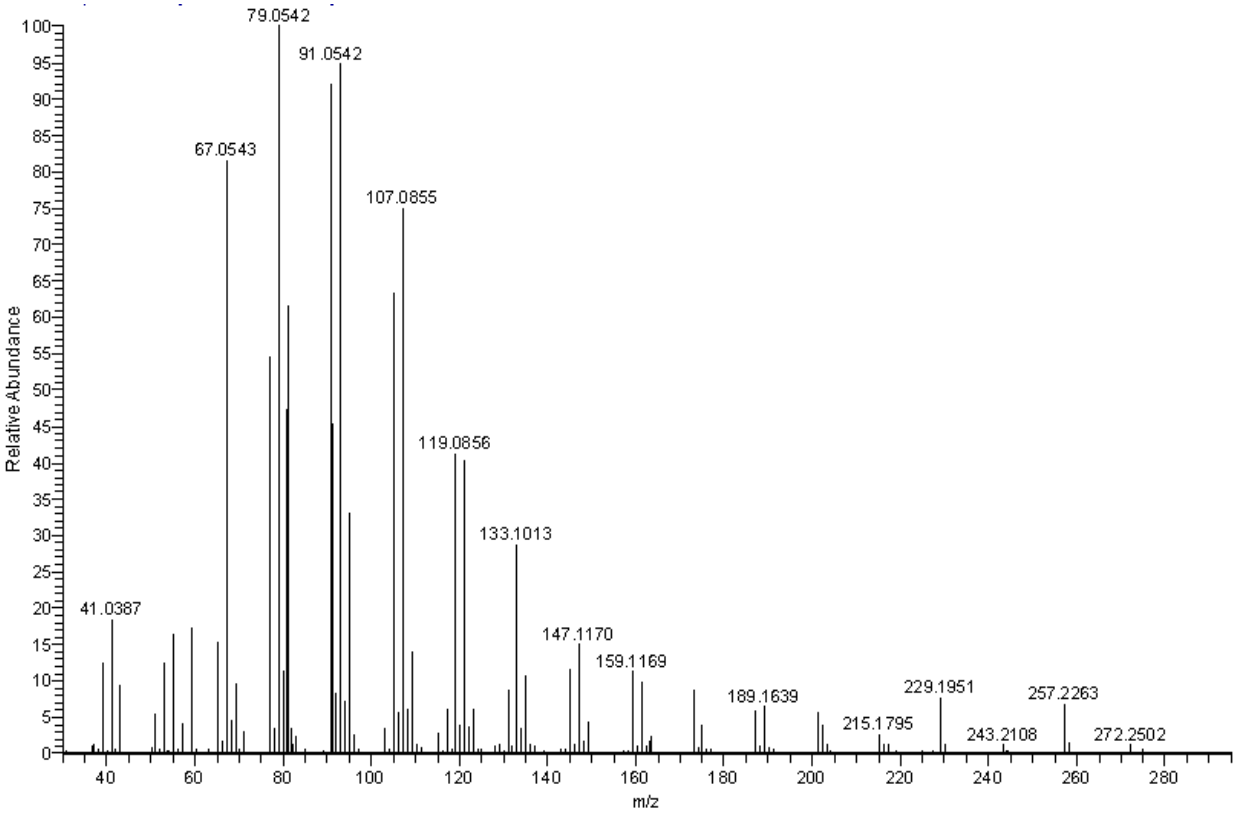

Supplementary Fig. 144. EIMS of monoprenyl-β-curcumene (**18**).

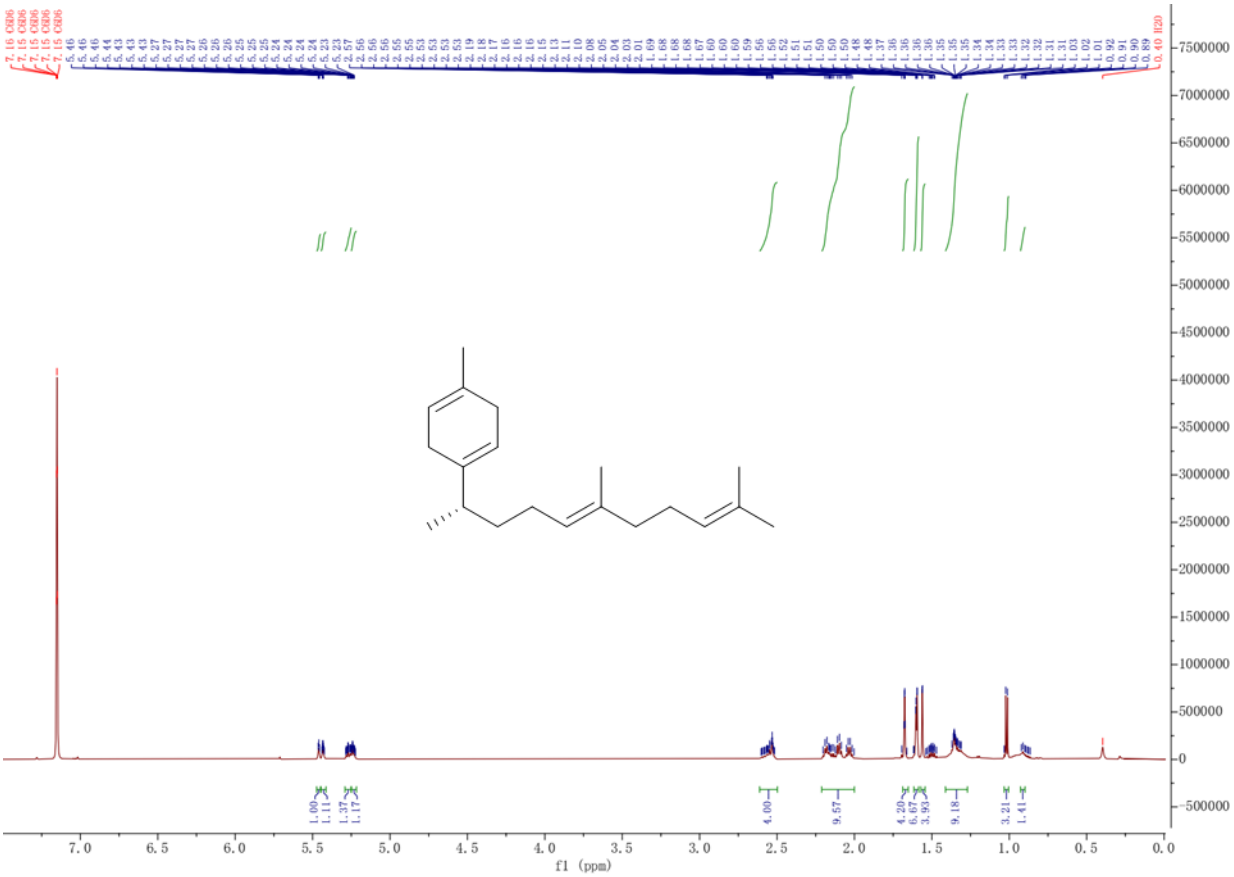

Supplementary Fig. 145. ^{1}H NMR spectrum of monoprenyl-β-curcumene (**18**) in C_6D_6 (600 MHz).

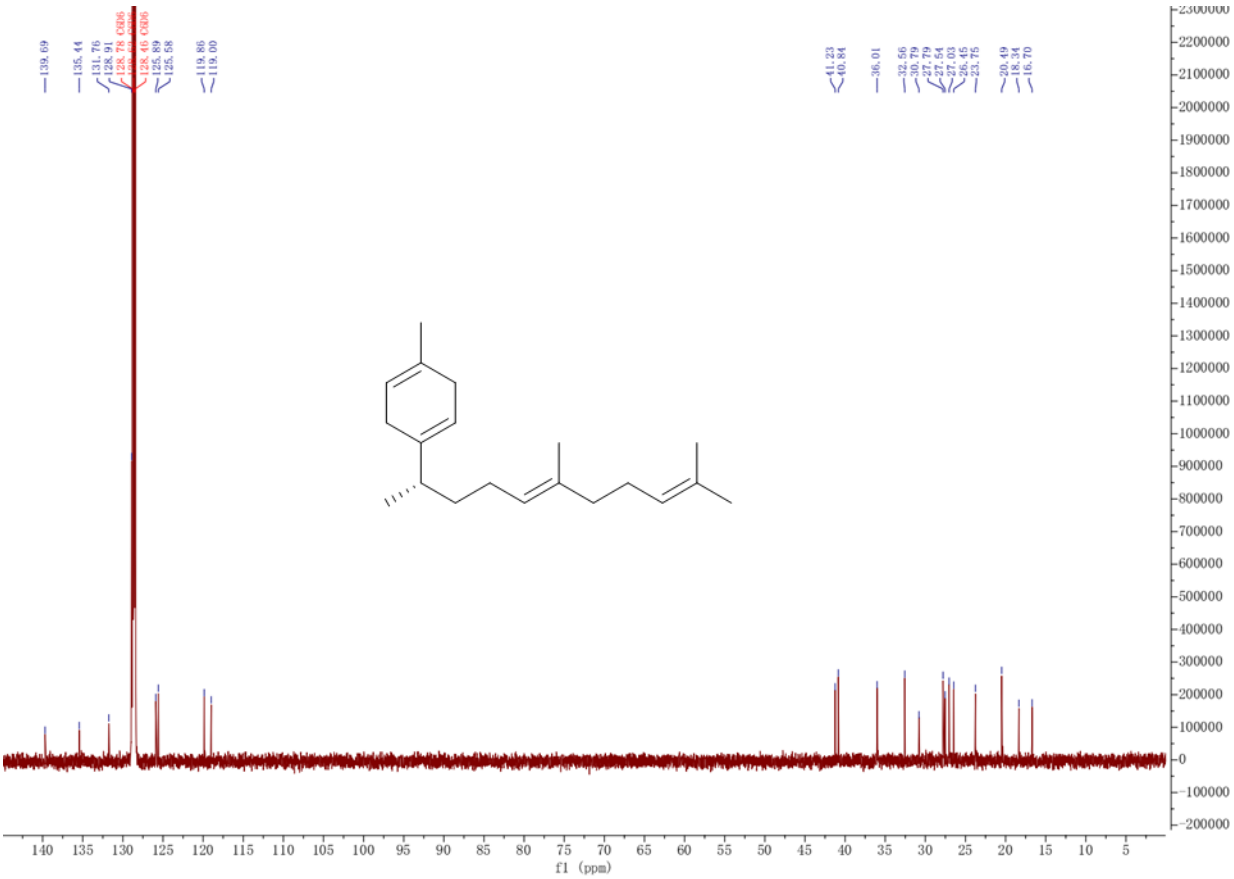

Supplementary Fig. 146. ^{13}C NMR spectrum of monoprenyl-β-curcumene (**18**) in C_6D_6 (151 MHz).

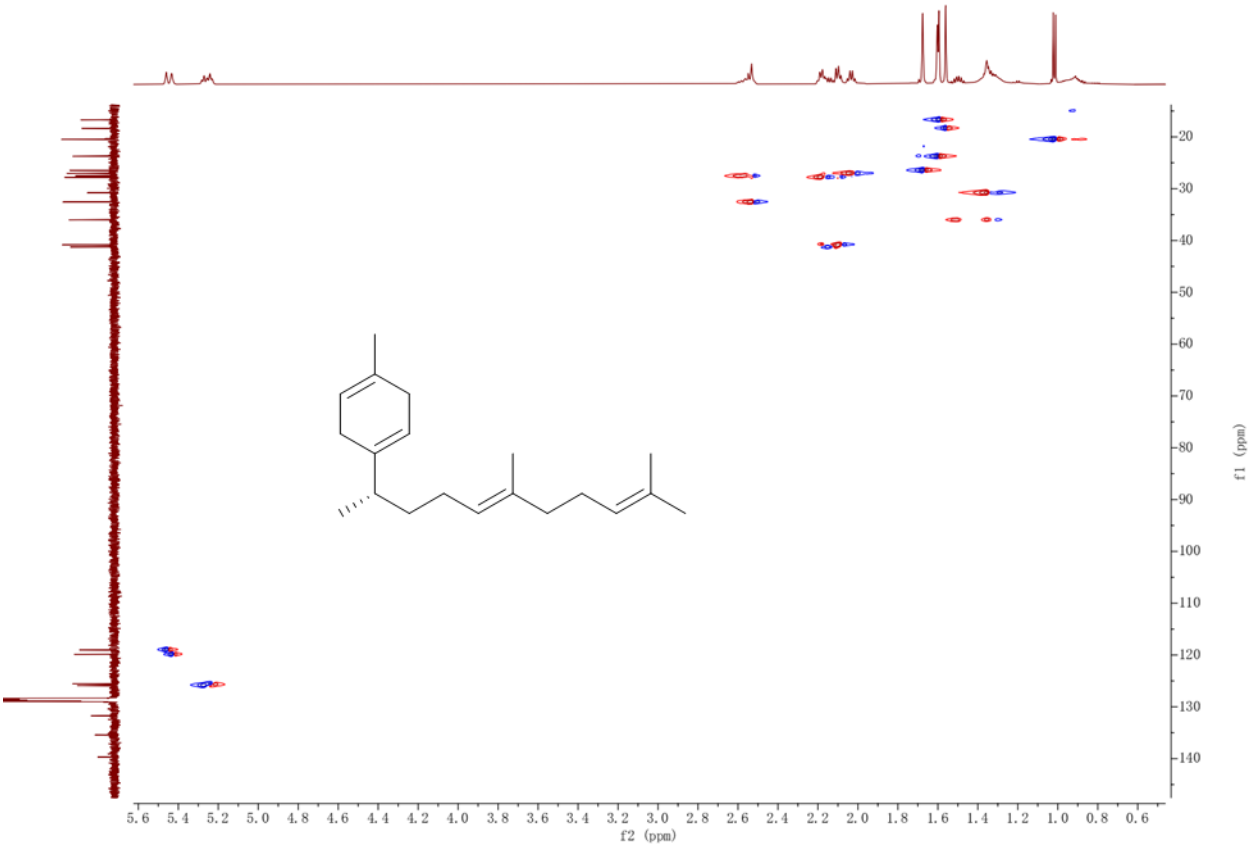

Supplementary Fig. 147. HSQC spectrum of monoprenyl-β-curcumene (**18**) in C_6D_6.

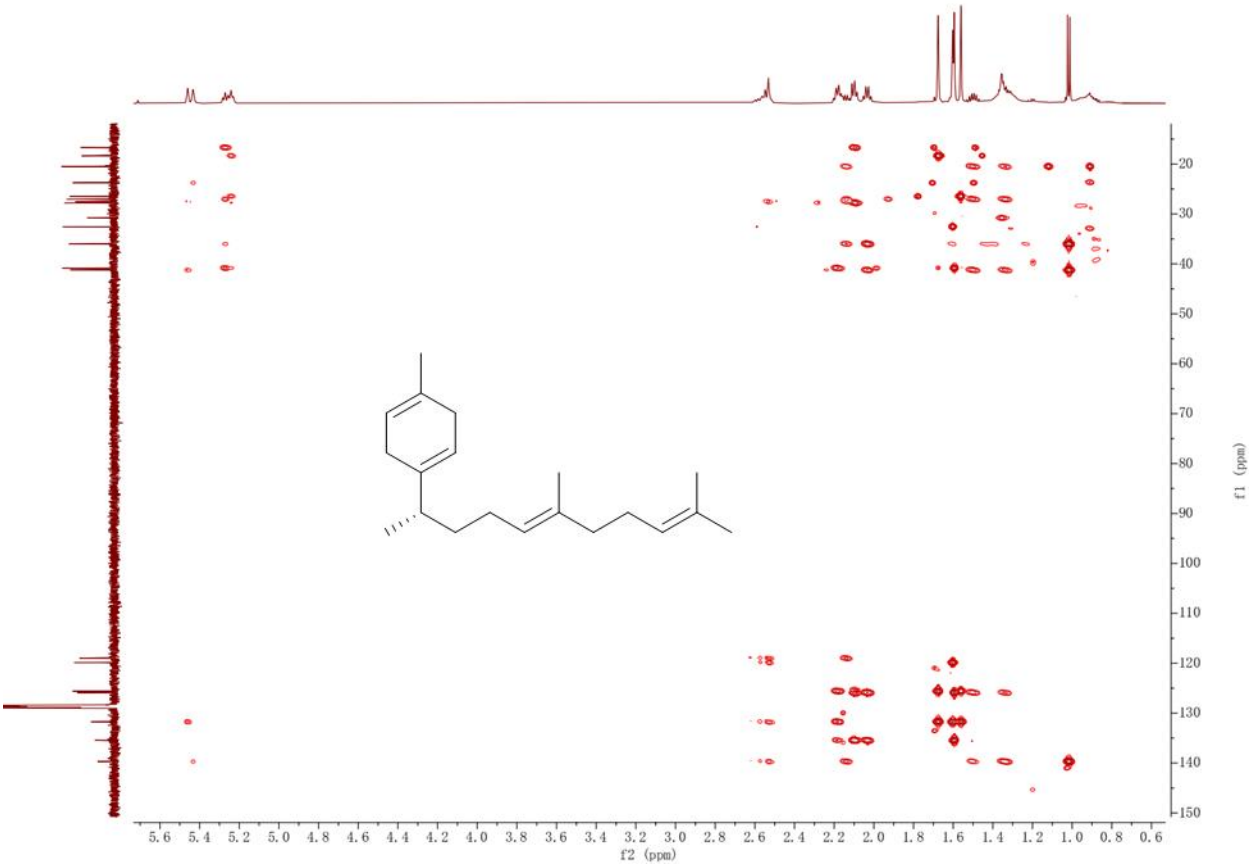

Supplementary Fig. 148. HMBC spectrum of monoprenyl-β-curcumene (**18**) in C_6D_6.

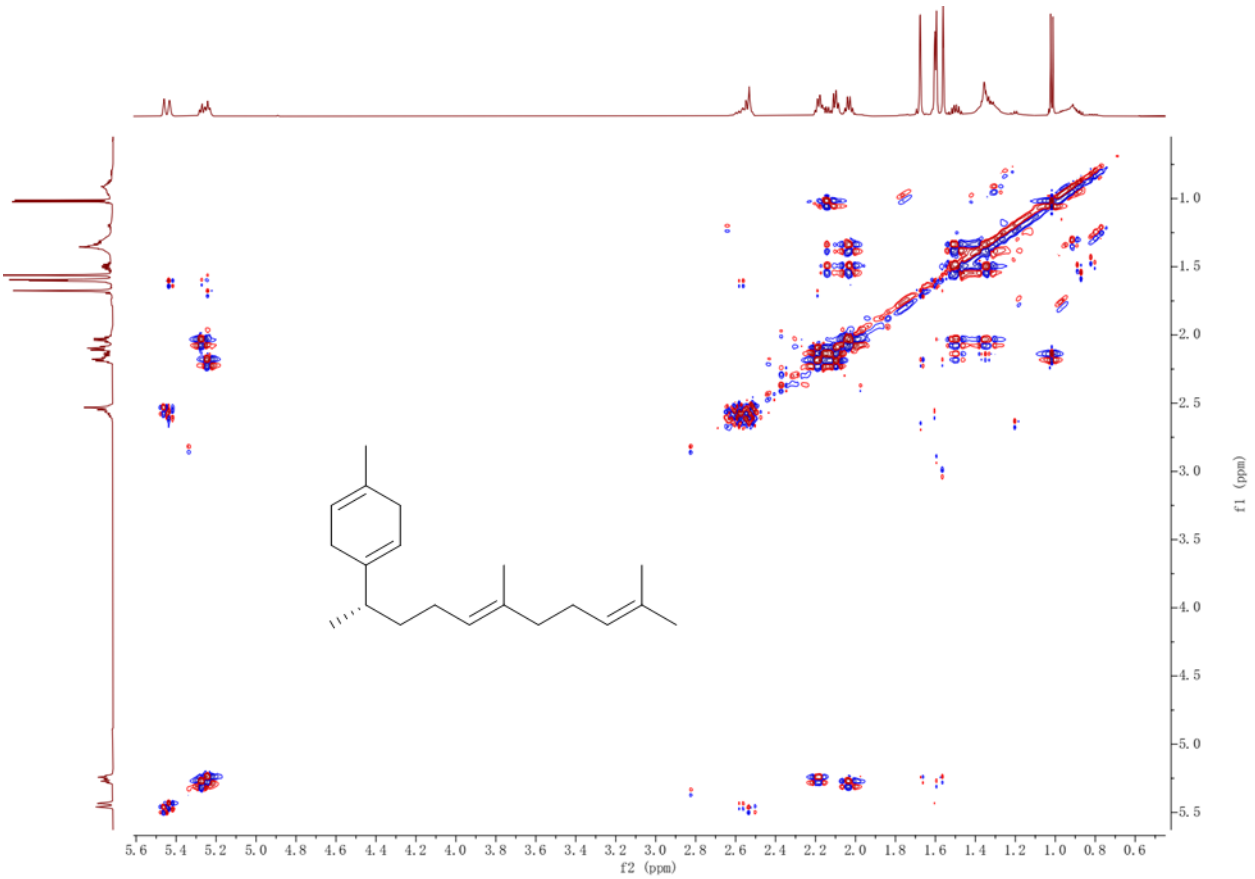

Supplementary Fig. 149. COSY spectrum of monoprenyl-β-curcumene (**18**) in C_6D_6.

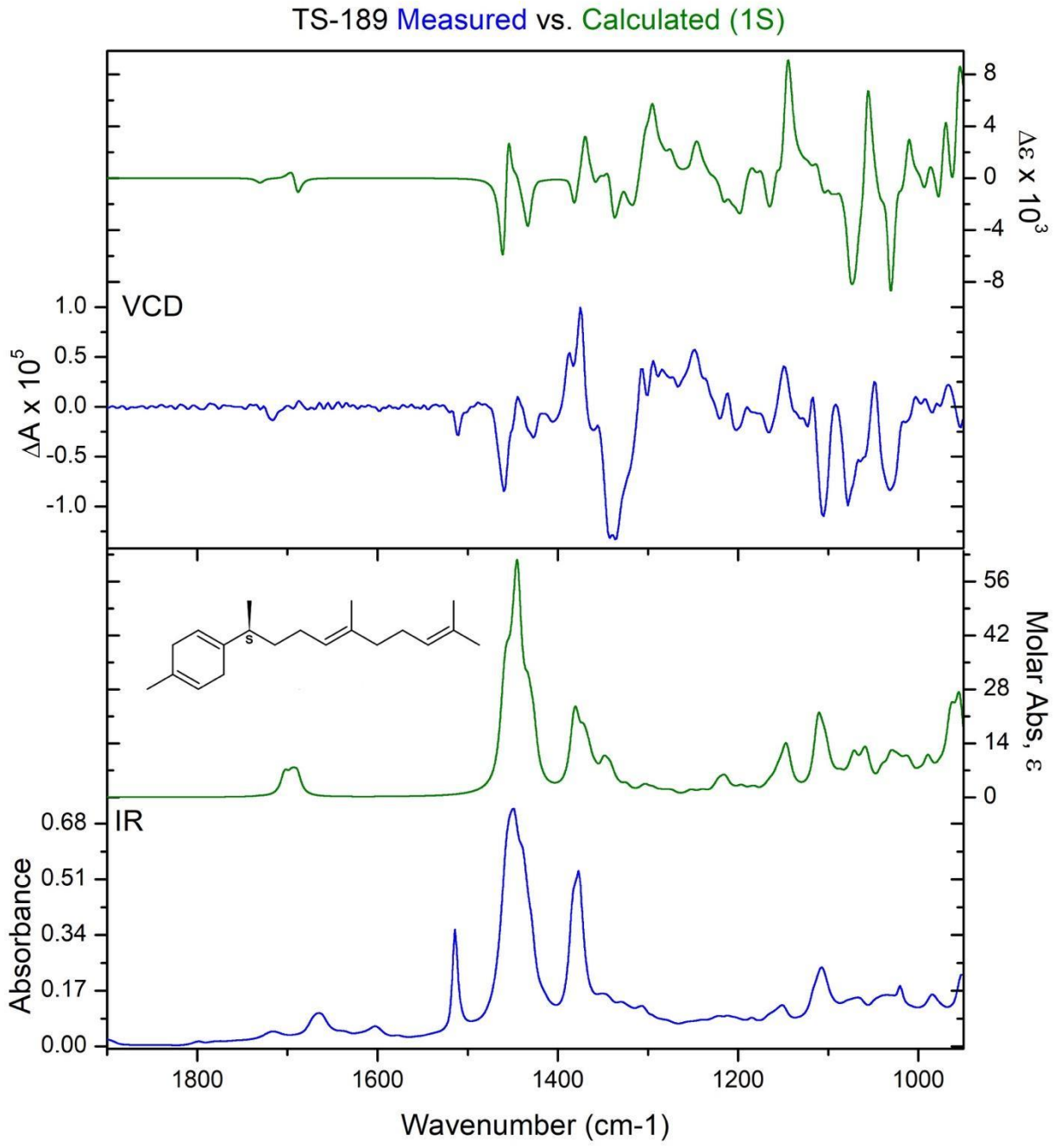

Supplementary Fig. 150. DFT calculated (pink and green) and experimental (blue) VCD and IR spectra of monoprenyl-β-curcumene (**18**).

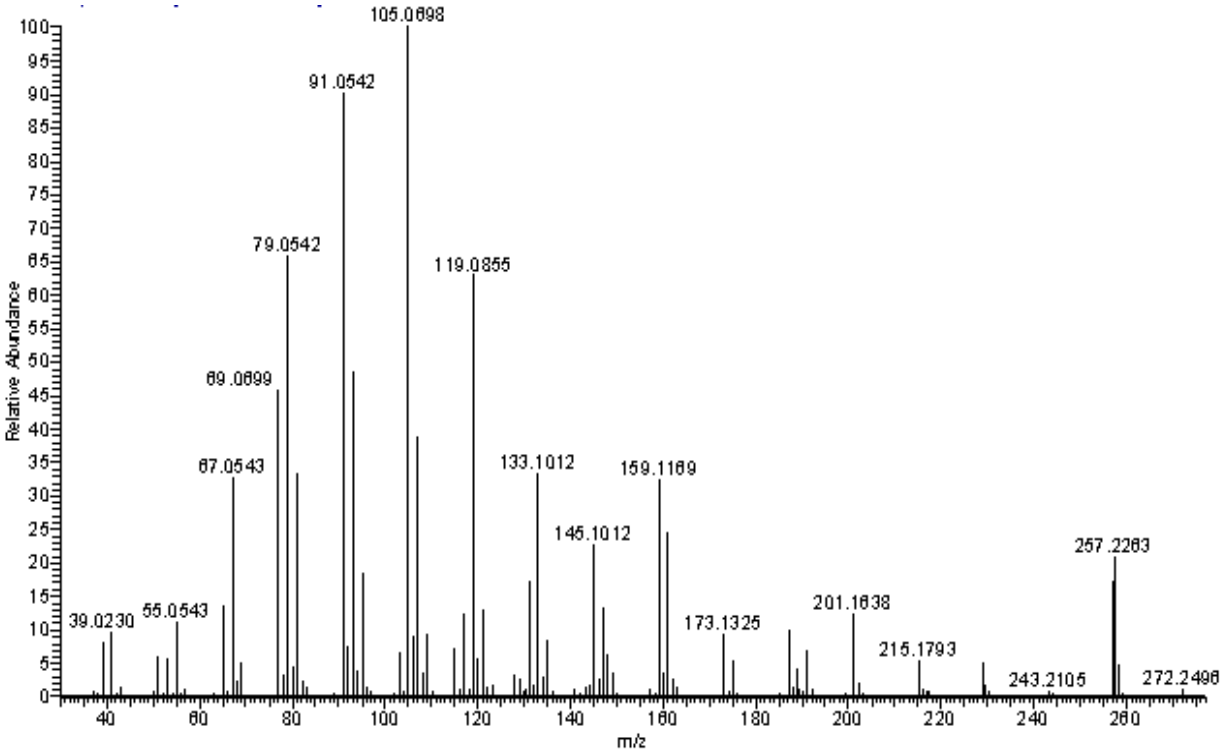

Supplementary Fig. 151. EIMS of benditerpetriene (**19**). The fragmentation matched the literature[13].

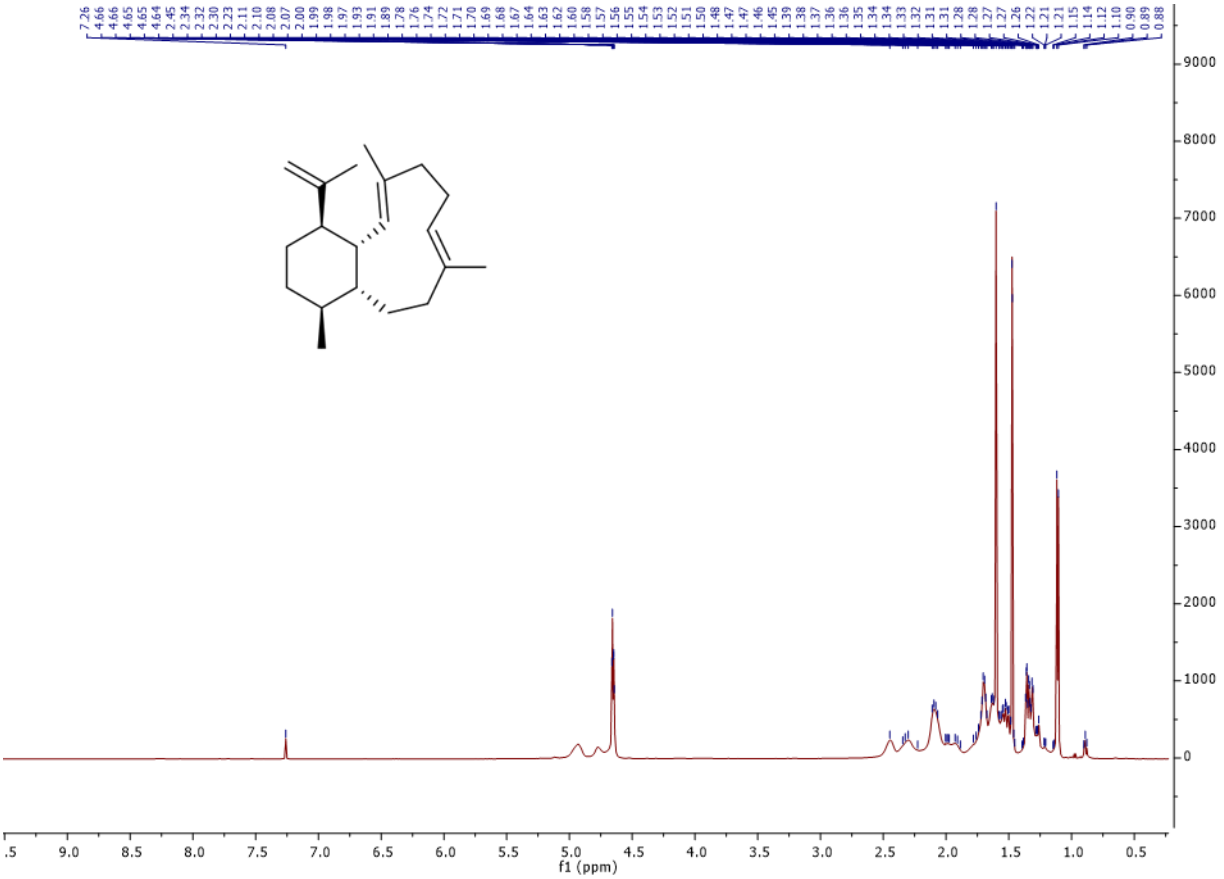

Supplementary Fig. 152. ^{1}H NMR spectrum of benditerpetriene (**19**) in $CDCl_3$ (600 MHz).

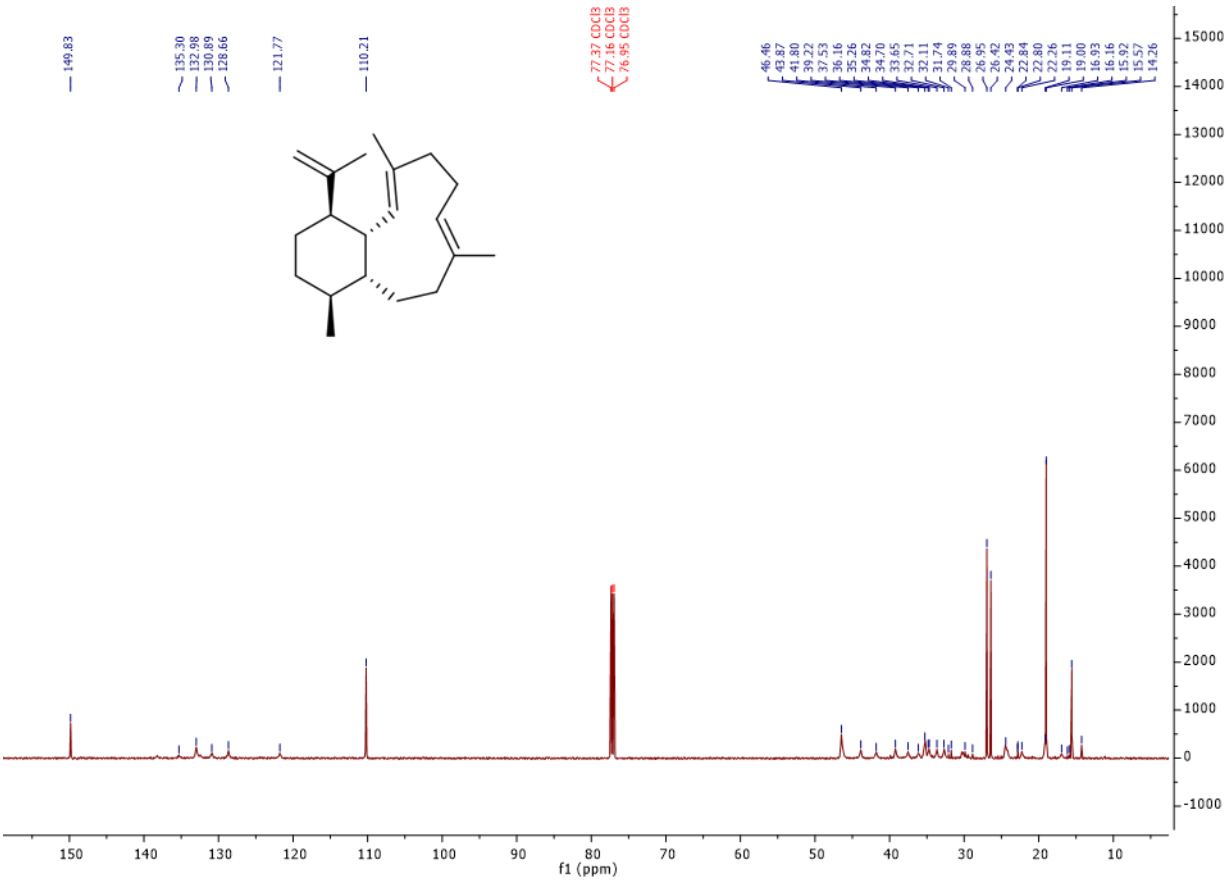

Supplementary Fig. 153. ^{13}C NMR spectrum of benditerpetriene (**19**) in $CDCl_3$ (151 MHz).

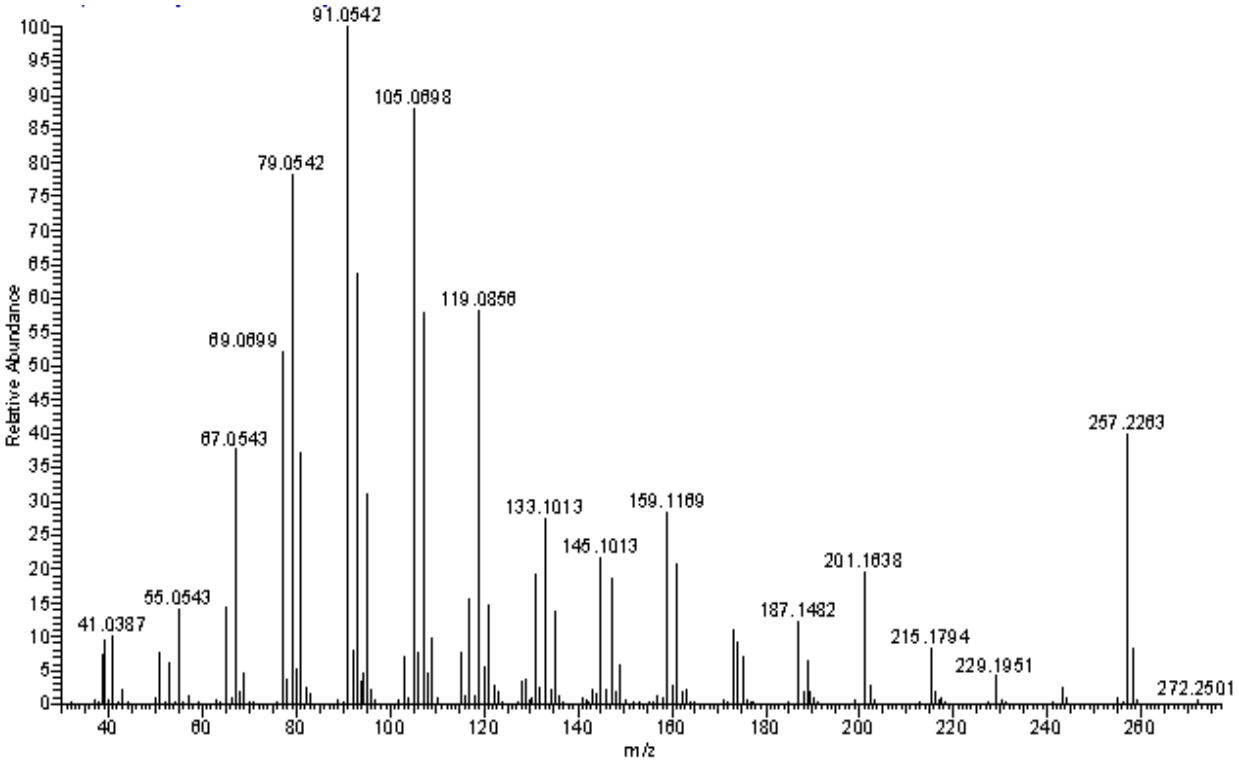

Supplementary Fig. 154. EIMS of prehydropyrene (**20**).

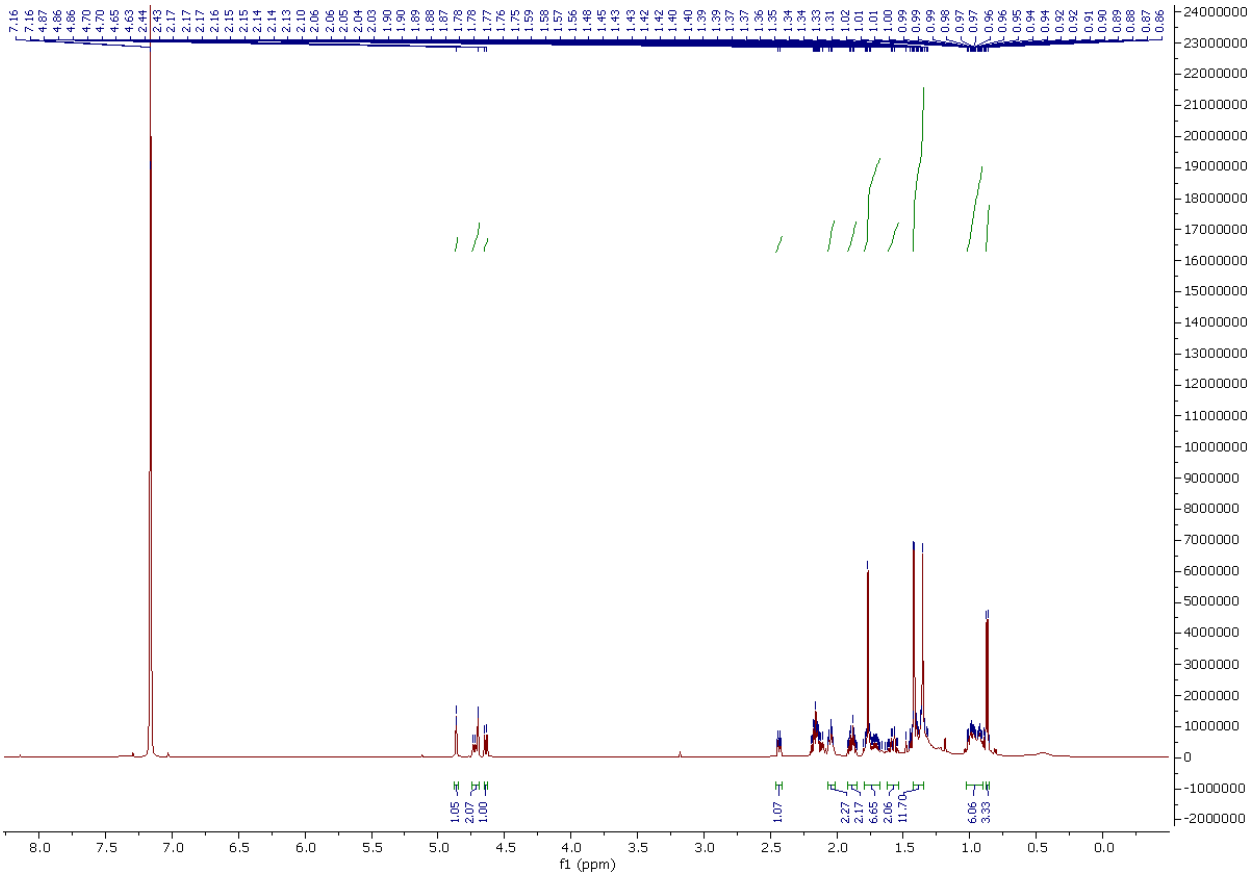

Supplementary Fig. 155. ^{1}H NMR spectrum of prehydropyrene (**20**) in C_6D_6 (600 MHz).

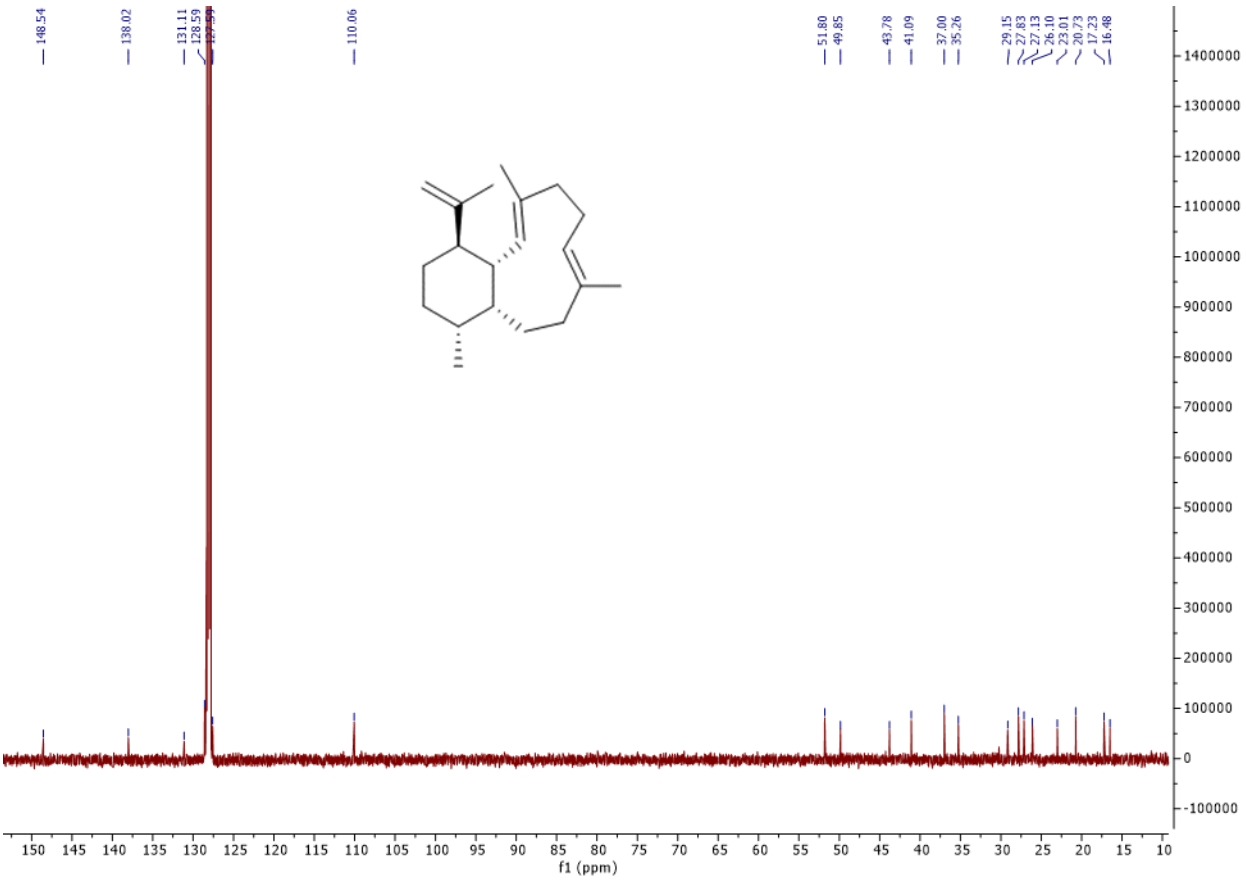

Supplementary Fig. 156. ^{13}C NMR spectrum of prehydropyrene (**20**) in C_6D_6 (151 MHz).

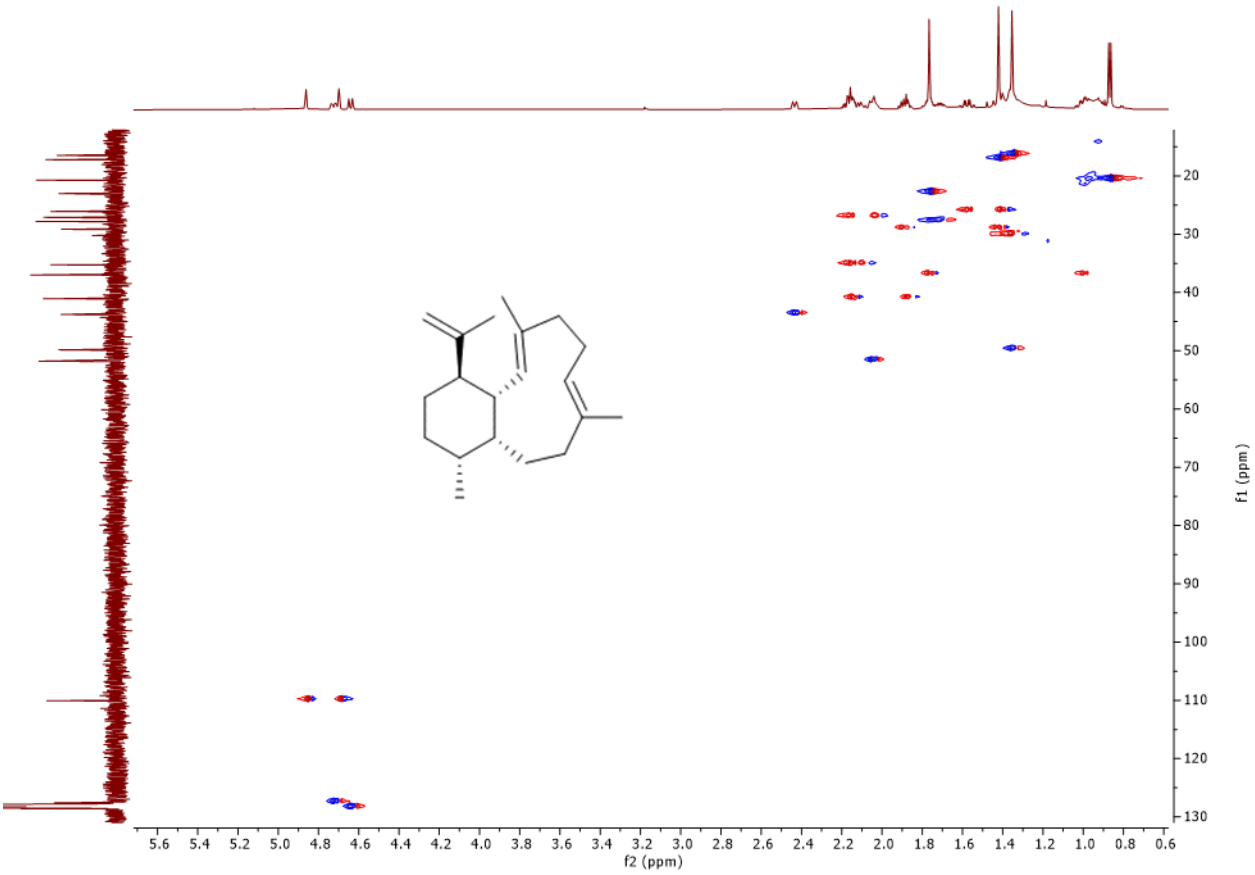

Supplementary Fig. 157. HSQC spectrum of prehydropyrene (**20**) in C_6D_6 (151 MHz).

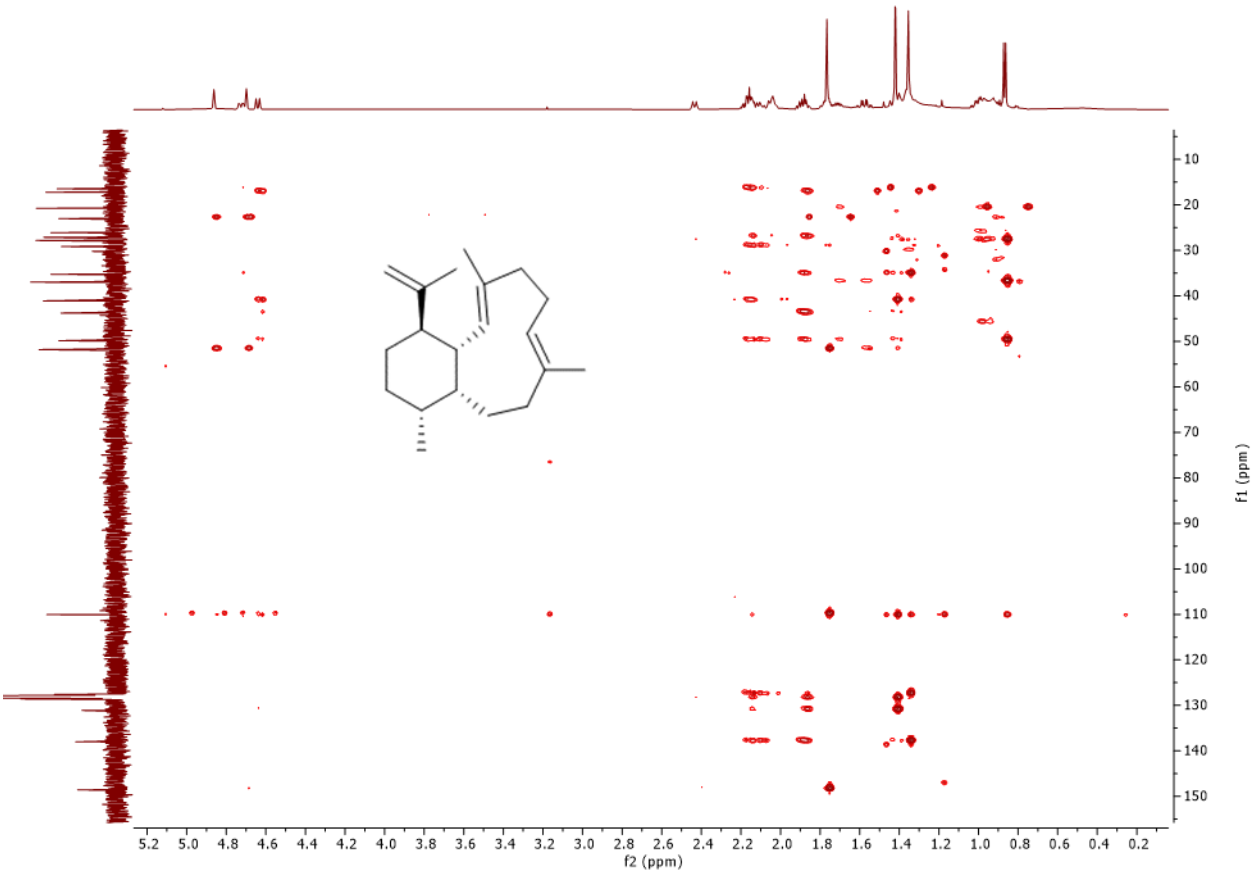

Supplementary Fig. 158. HMBC spectrum of prehydropyrene (**20**) in C_6D_6 (151 MHz).

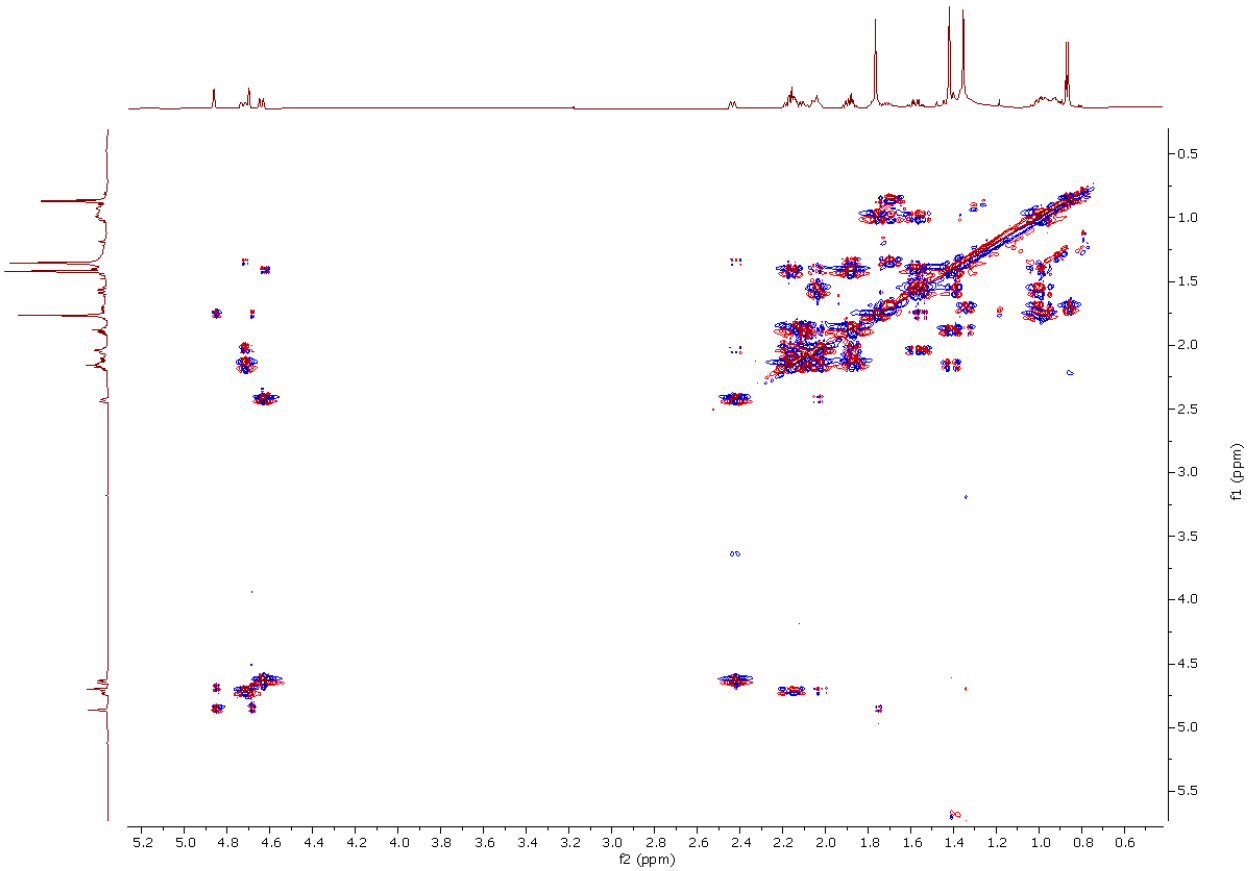

Supplementary Fig. 159. COSY spectrum of prehydropyrene (**20**) in C_6D_6 (151 MHz).

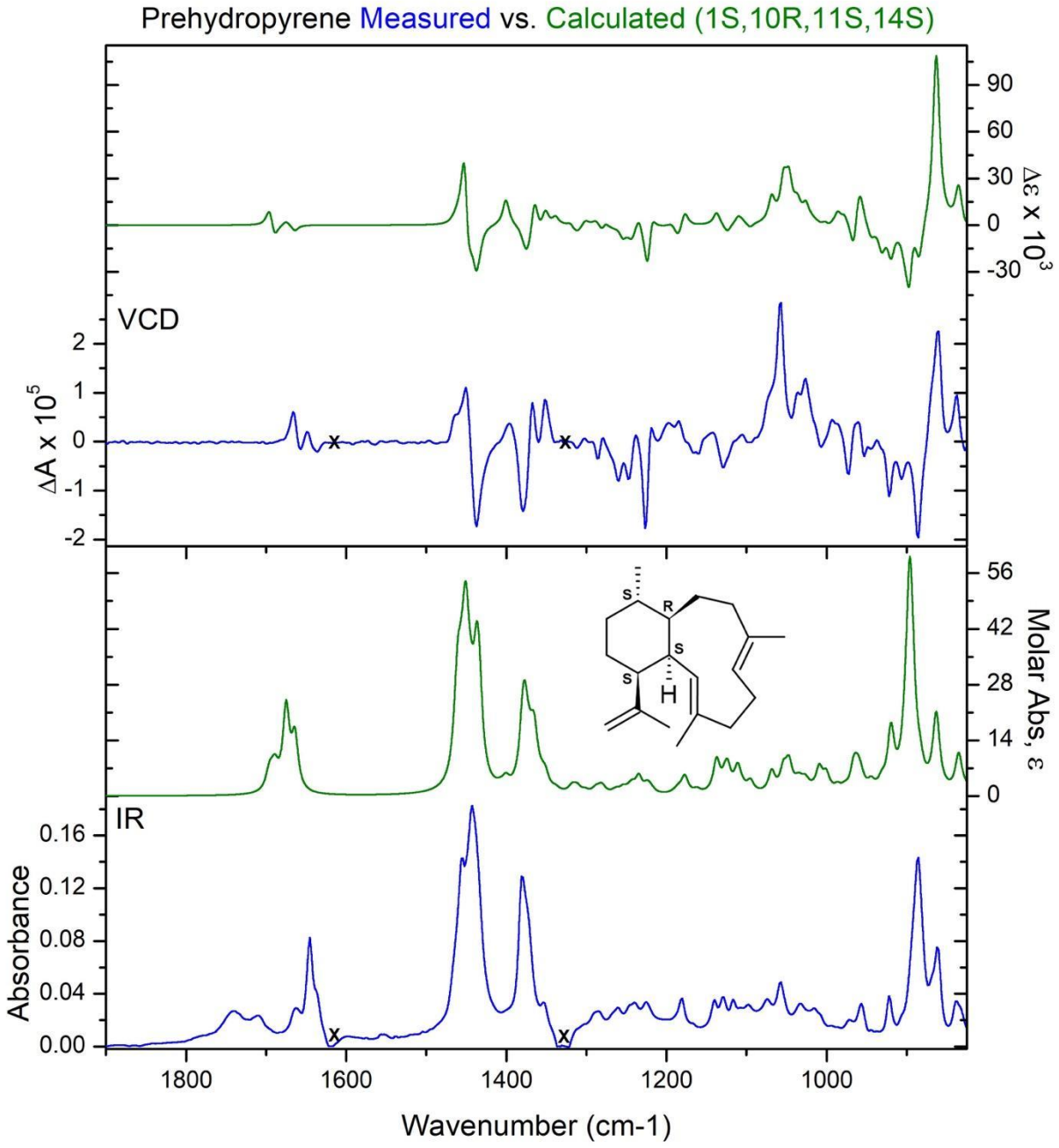

Supplementary Fig. 160. DFT calculated (green) and experimental (blue) VCD and IR spectra of prehydropyrene (**20**) measured in C_6D_6 due to instability of **20** in $CDCl_3$ "X" marks placed over the measured IR and VCD spectra were regions that were zeroed out due to strong absorption of C_6D_6 to limit any interference with visual or CompareVOA analysis.

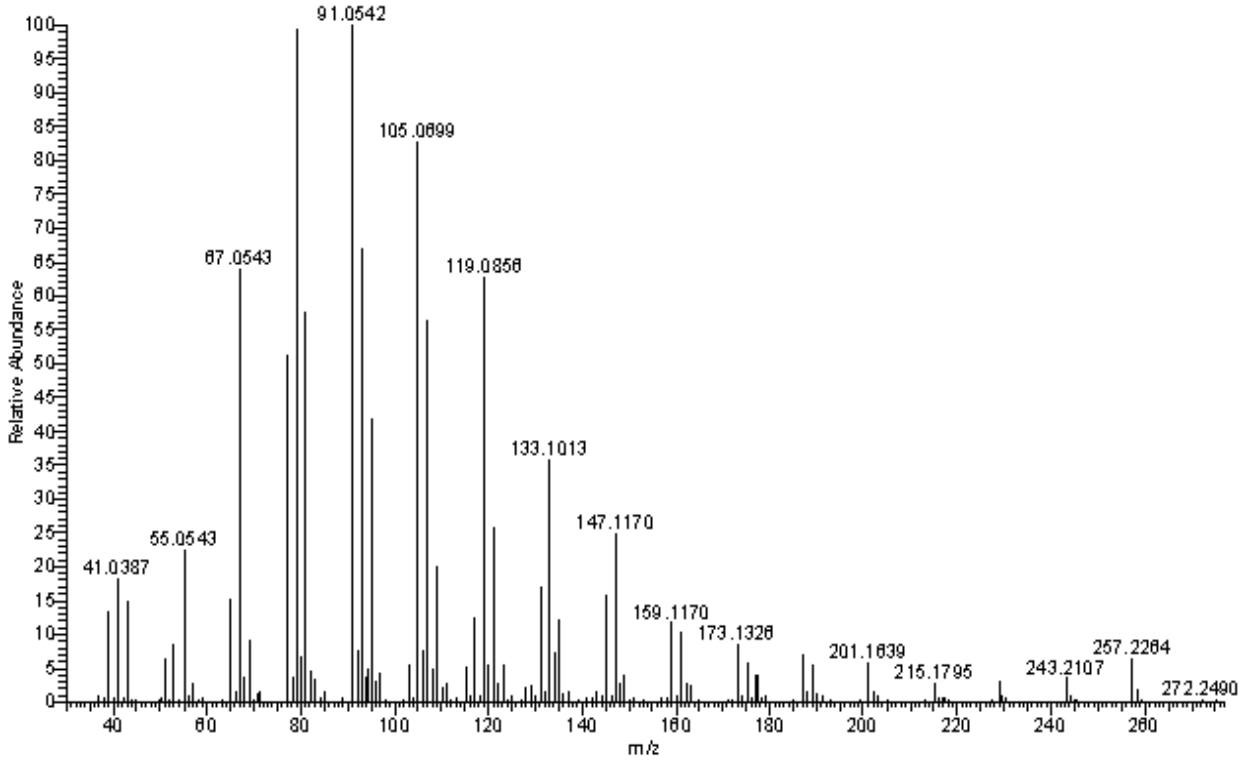

Supplementary Fig. 161. EIMS of micromonocyclol (**21**). The fragmentation and retention index (RI = 2085) matched the literature (RI =2075)[15].

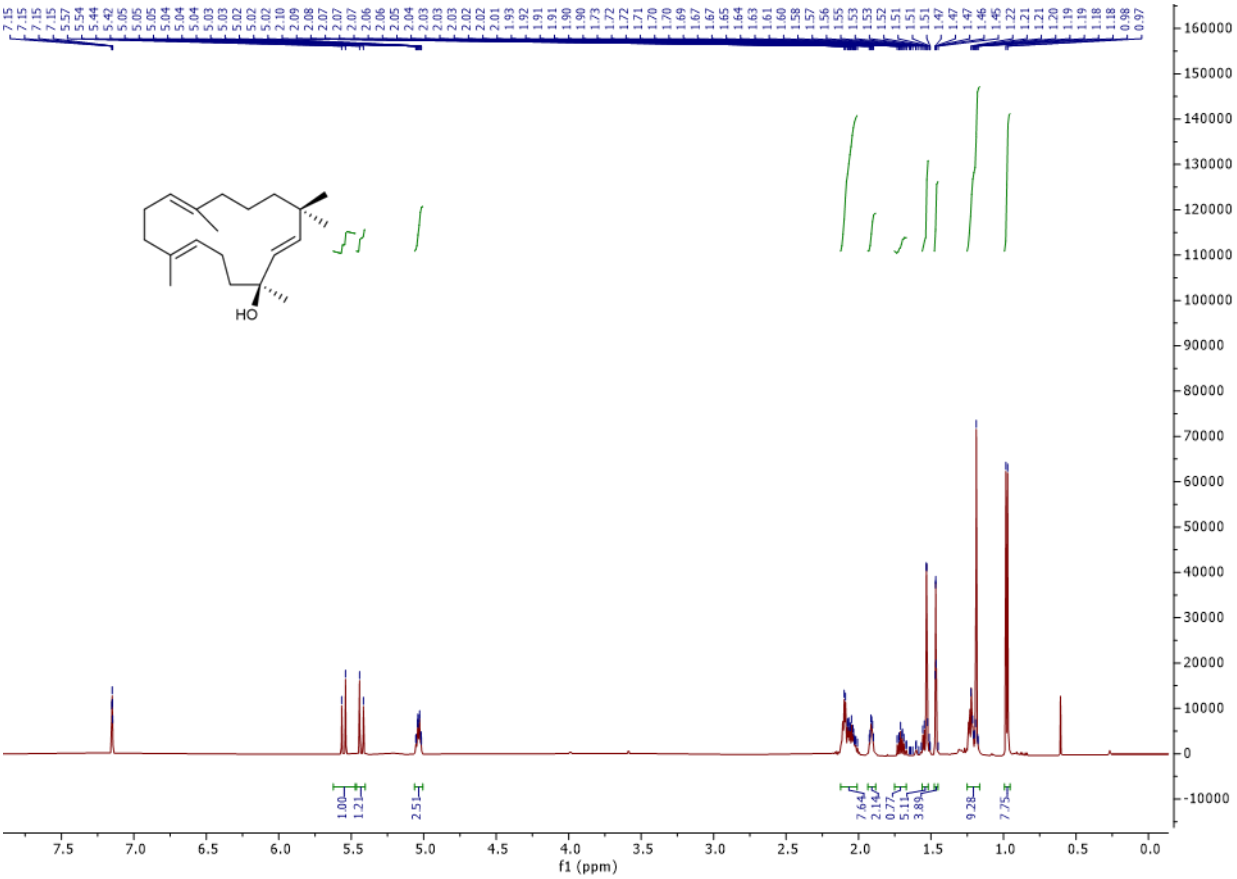

Supplementary Fig. 162. ^{1}H NMR spectrum of micromonocyclol (**21**) in C_6D_6 (600 MHz).

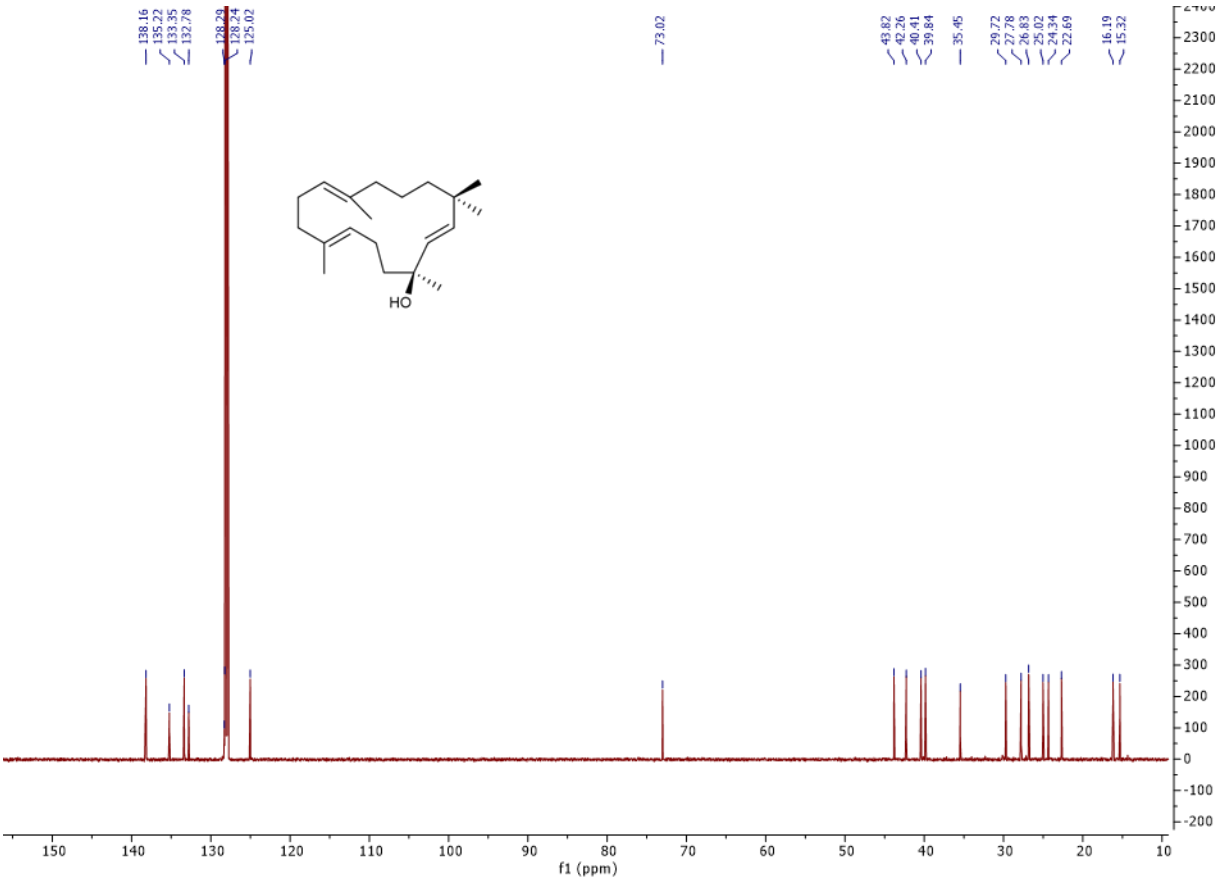

Supplementary Fig. 163. ^{13}C NMR spectrum of micromonocyclol (**21**) in C_6D_6 (151 MHz).

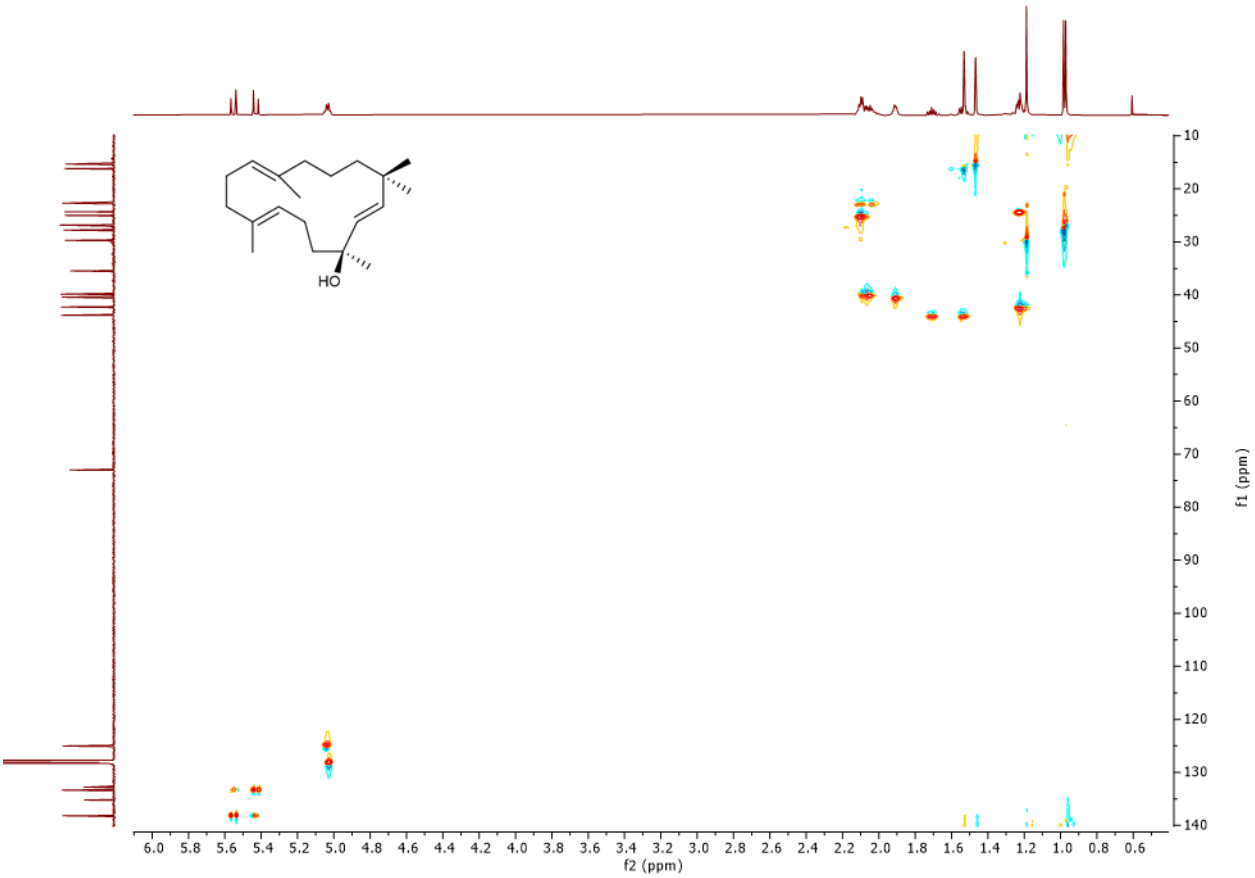

Supplementary Fig. 164. HSQC spectrum of micromonocyclol (**21**) in C_6D_6.

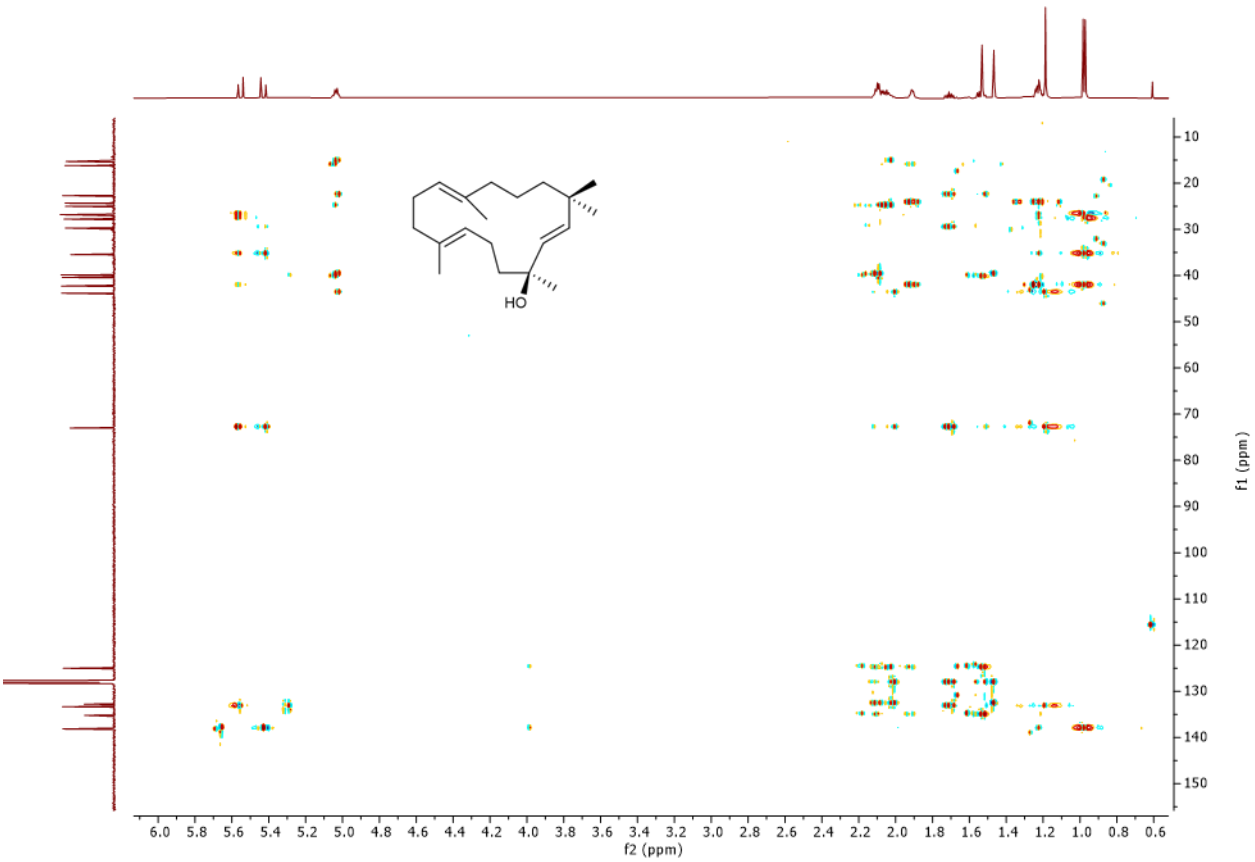

Supplementary Fig. 165. HMBC spectrum of micromonocyclol (**21**) in C_6D_6.

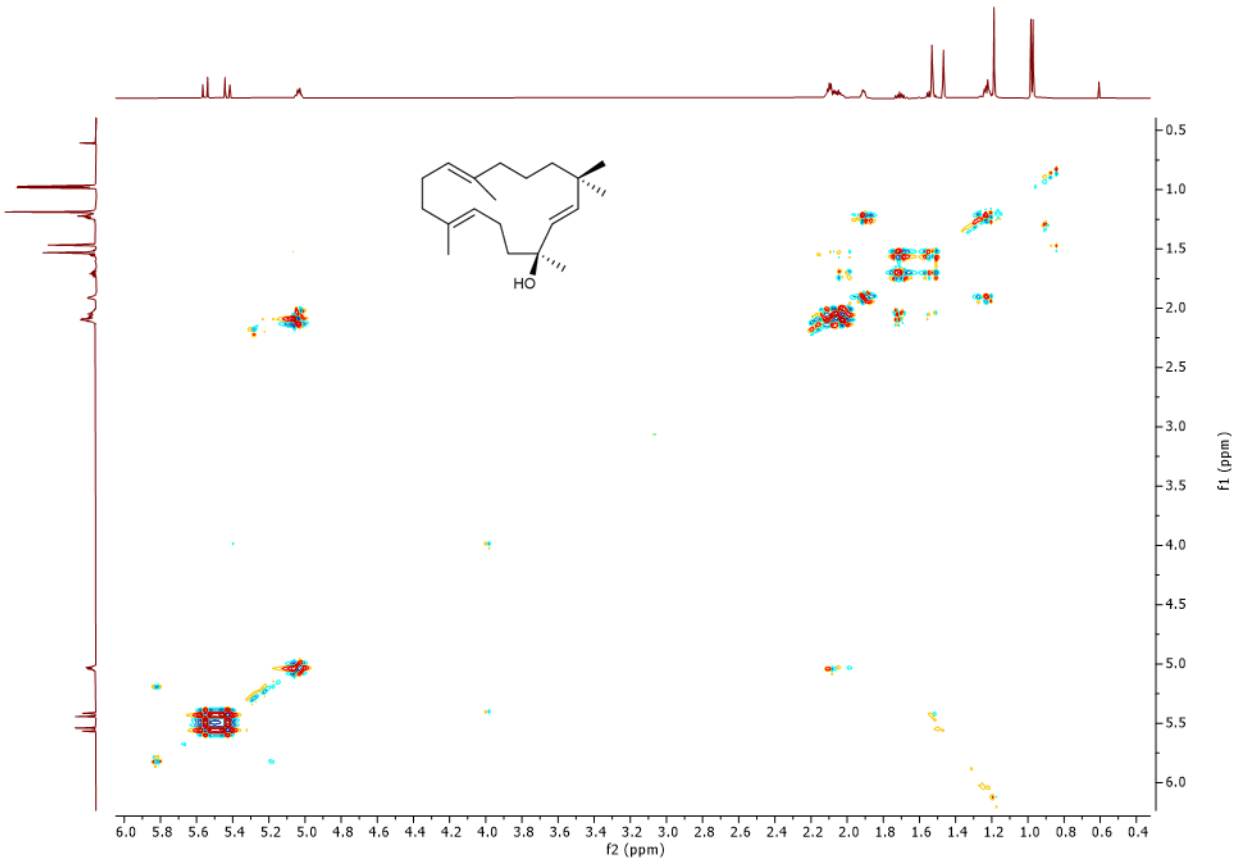

Supplementary Fig. 166. COSY spectrum of micromonocyclol (**21**) in C_6D_6.

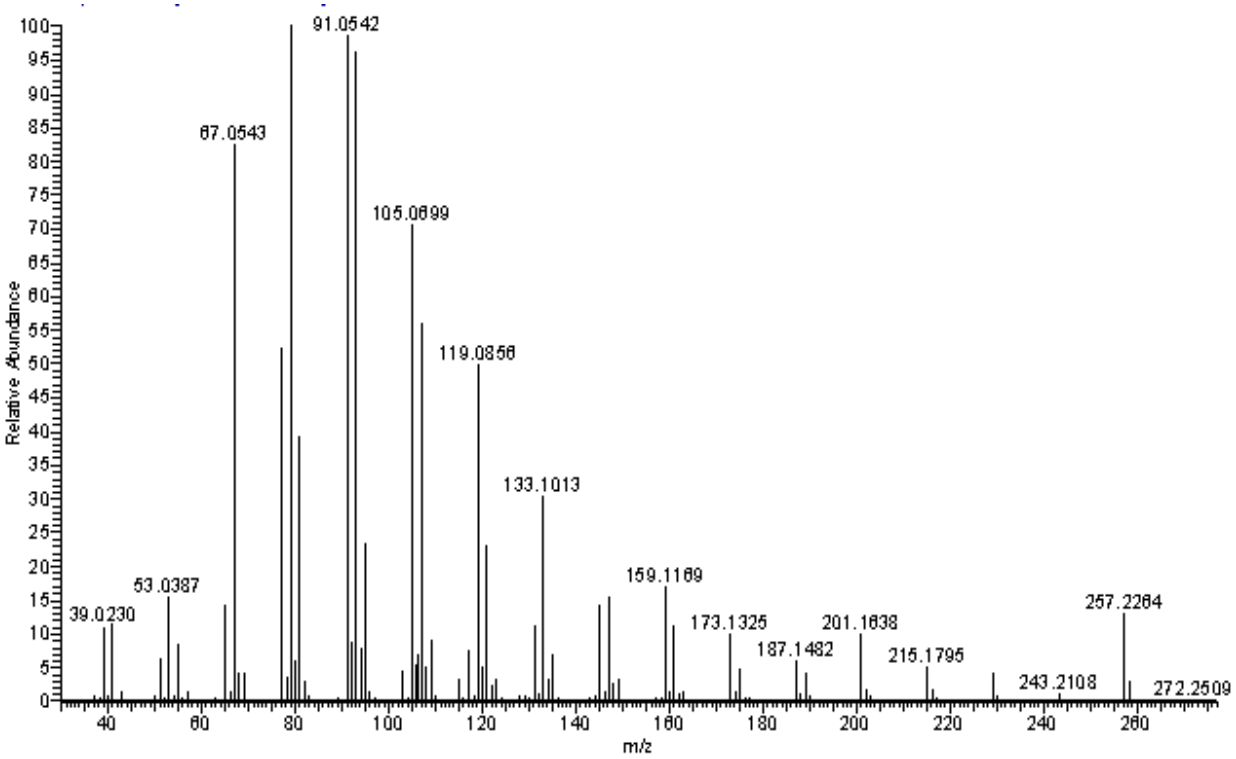

Supplementary Fig. 167. EIMS of cembrene A (**22**). The fragmentation and retention index (RI = 1989) matched the literature (RI =1948)[27].

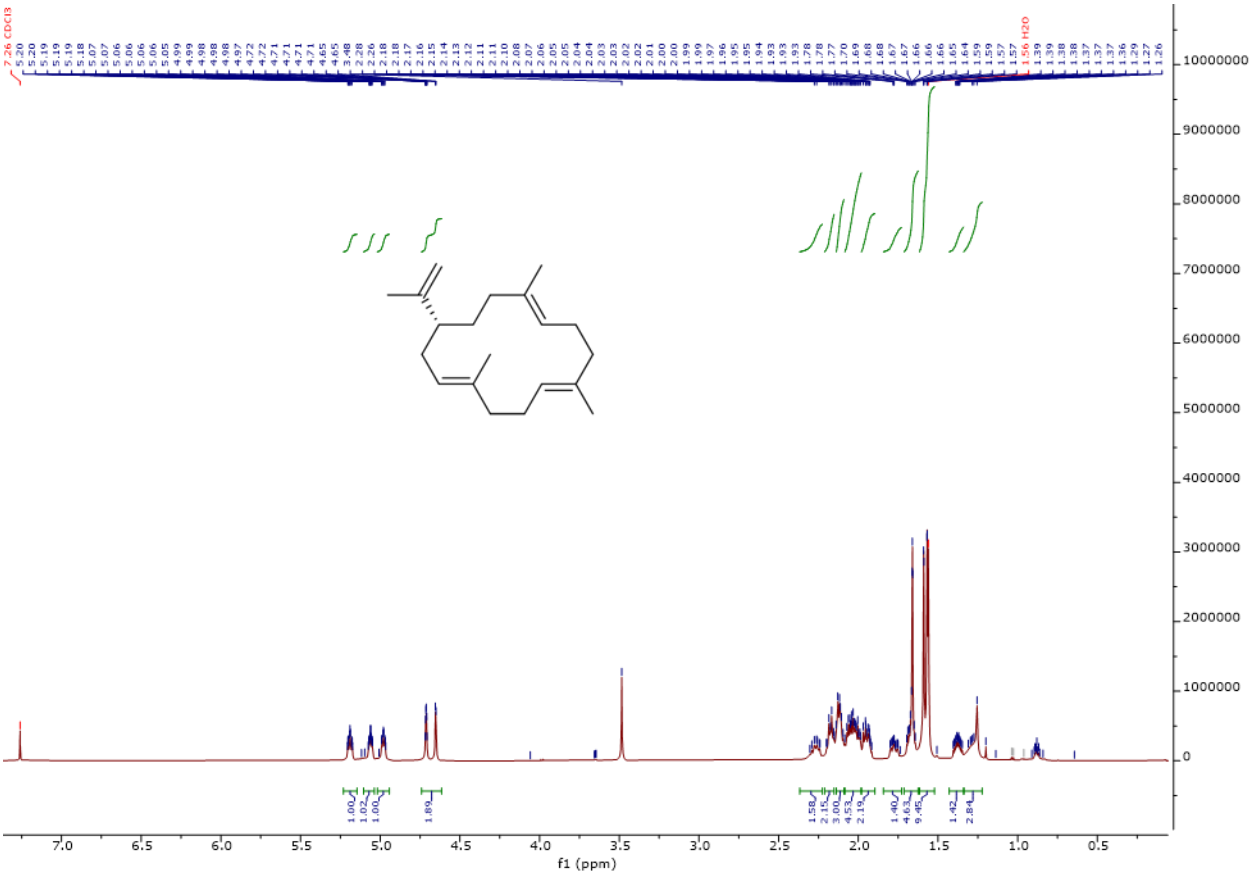

Supplementary Fig. 168. ^{1}H NMR spectrum of cembrene A (**22**) in $CDCl_3$ (600 MHz).

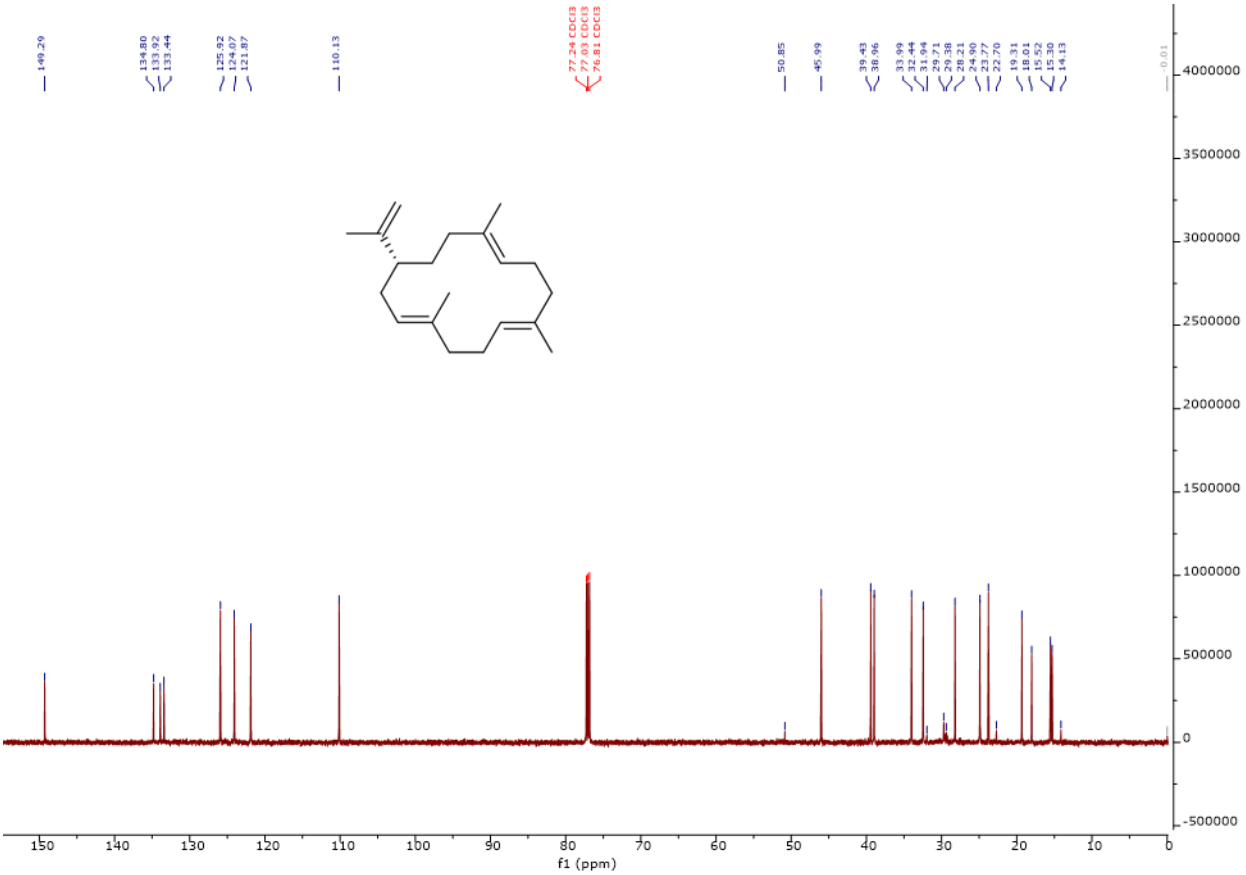

Supplementary Fig. 169. ^{13}C NMR spectrum of cembrene A (**22**) in $CDCl_3$ (151 MHz).

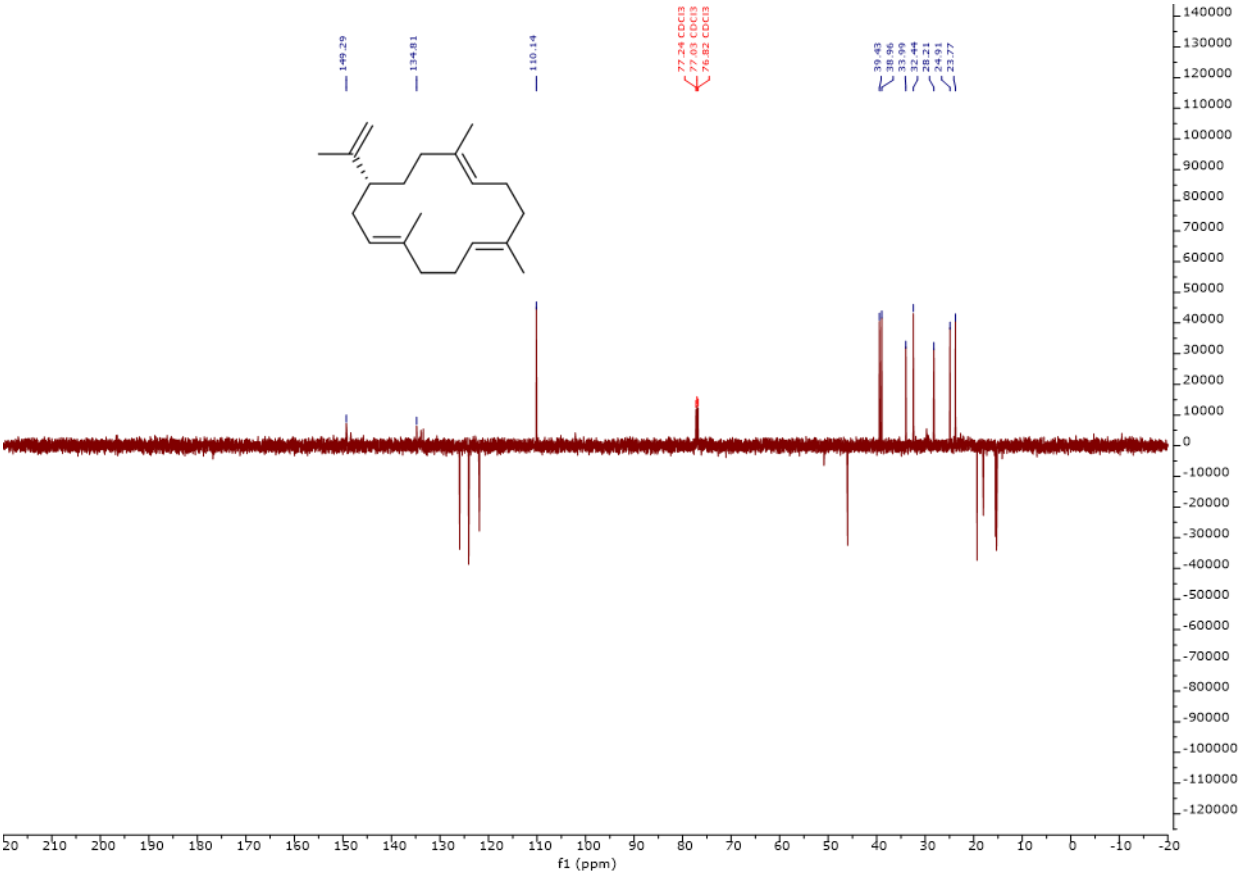

Supplementary Fig. 170. DEPT 135 spectrum of cembrene A (**22**) in $CDCl_3$ (151 MHz).

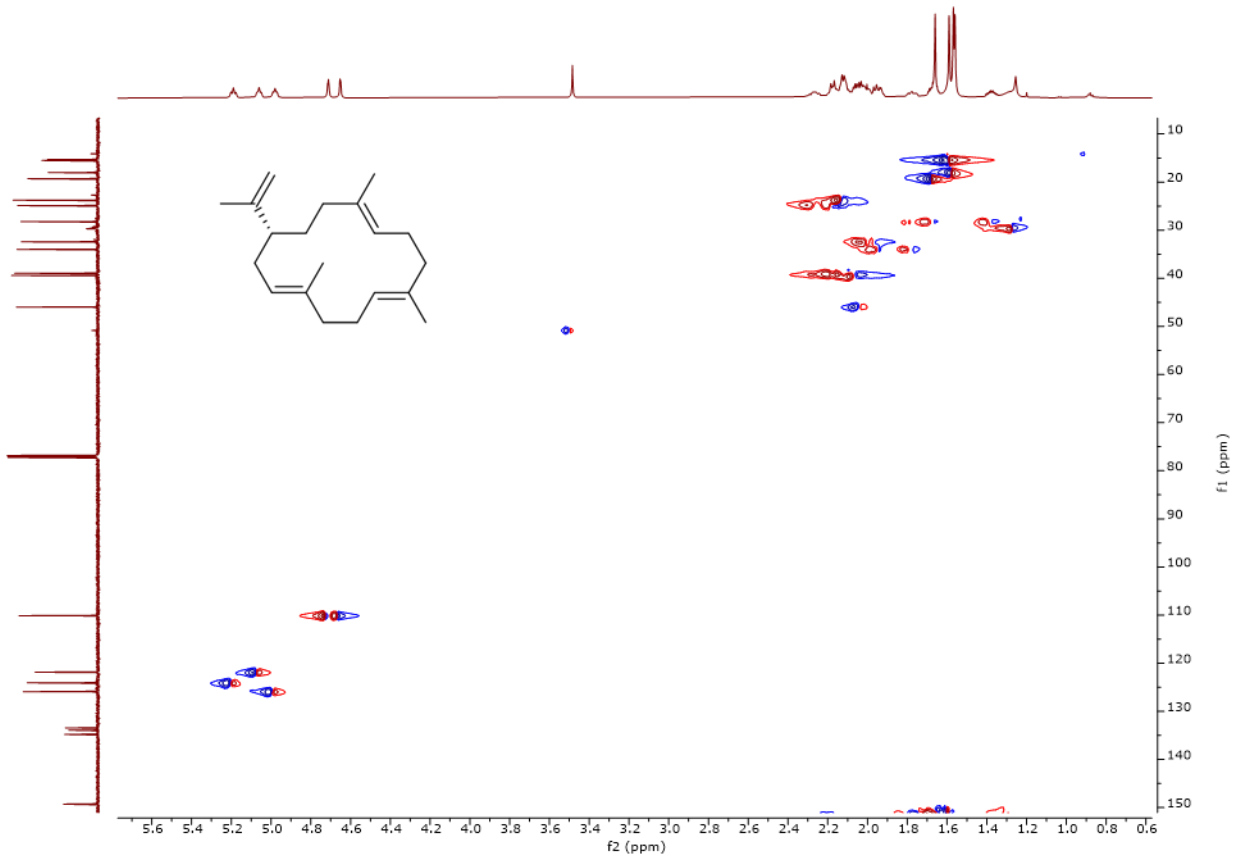

Supplementary Fig. 171. HSQC spectrum of cembrene A (**22**) in $CDCl_3$.

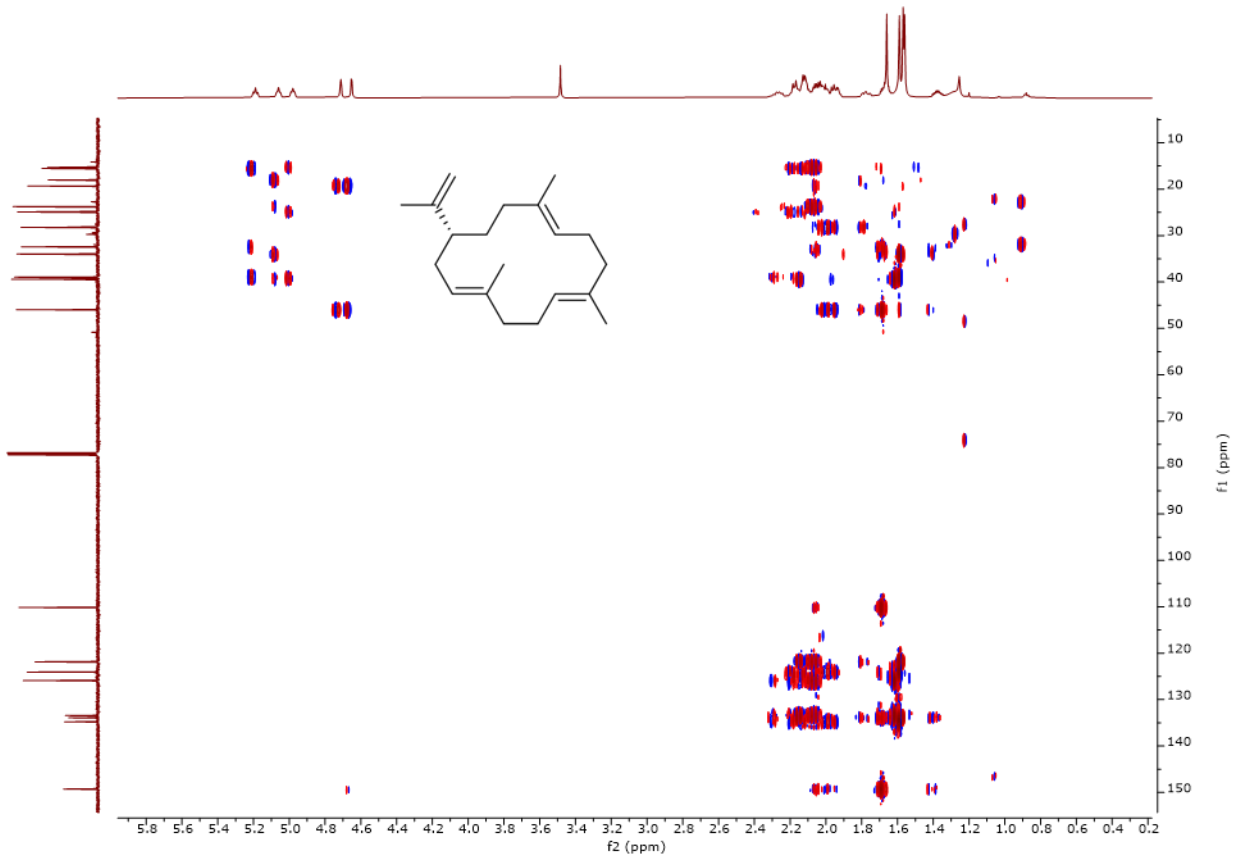

Supplementary Fig. 172. HMBC spectrum of cembrene A (**22**) in $CDCl_3$.

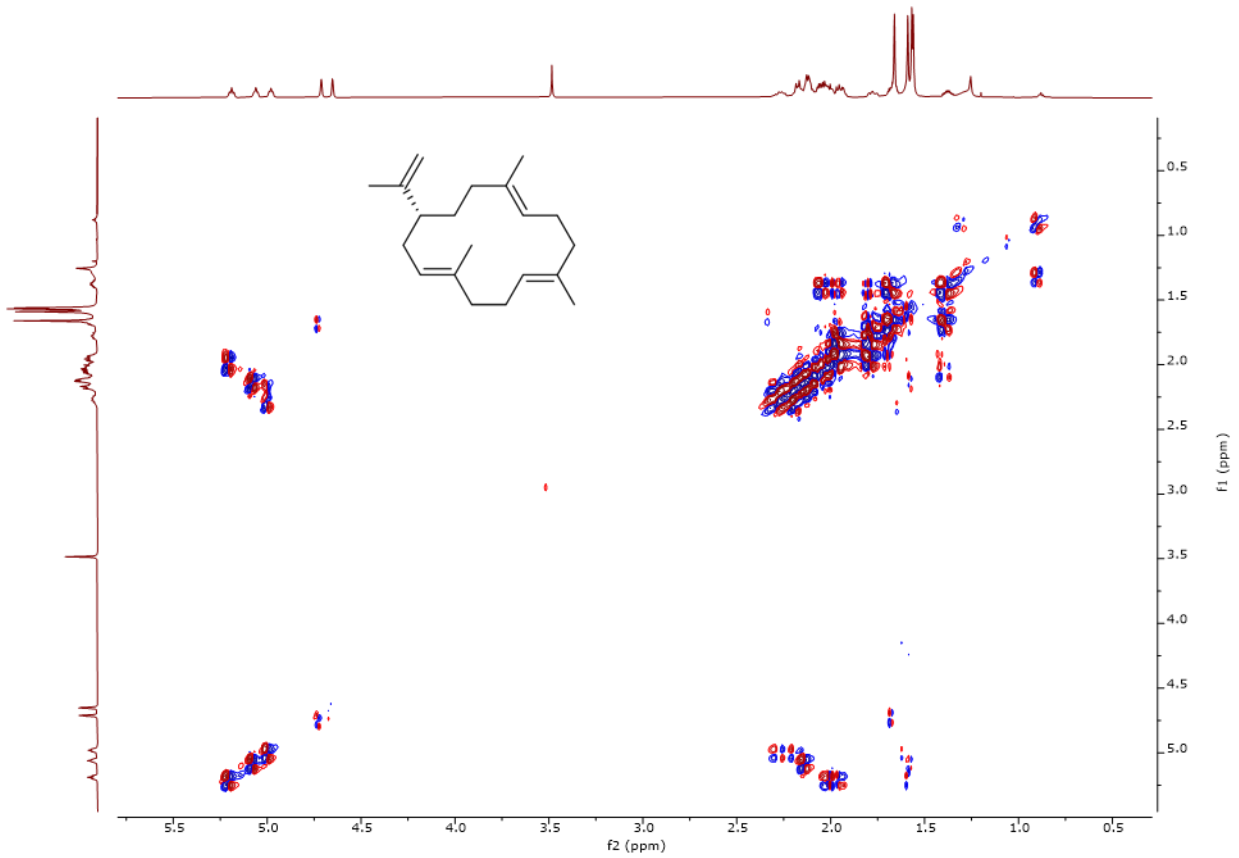

Supplementary Fig. 173. COSY spectrum of cembrene A (**22**) in $CDCl_3$ (600 MHz).

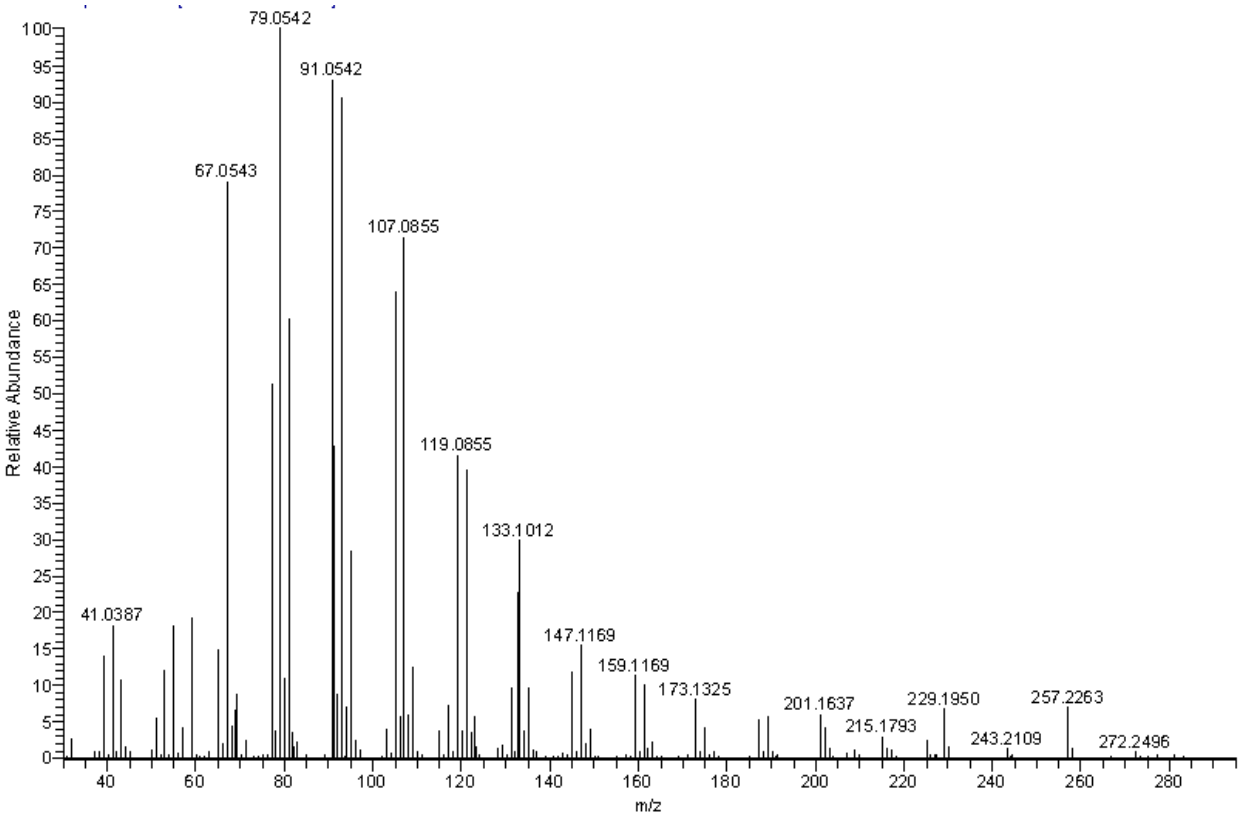

Supplementary Fig. 174. EIMS of (*S*)-nephthenol (**23**). The fragmentation matched the literature[18].

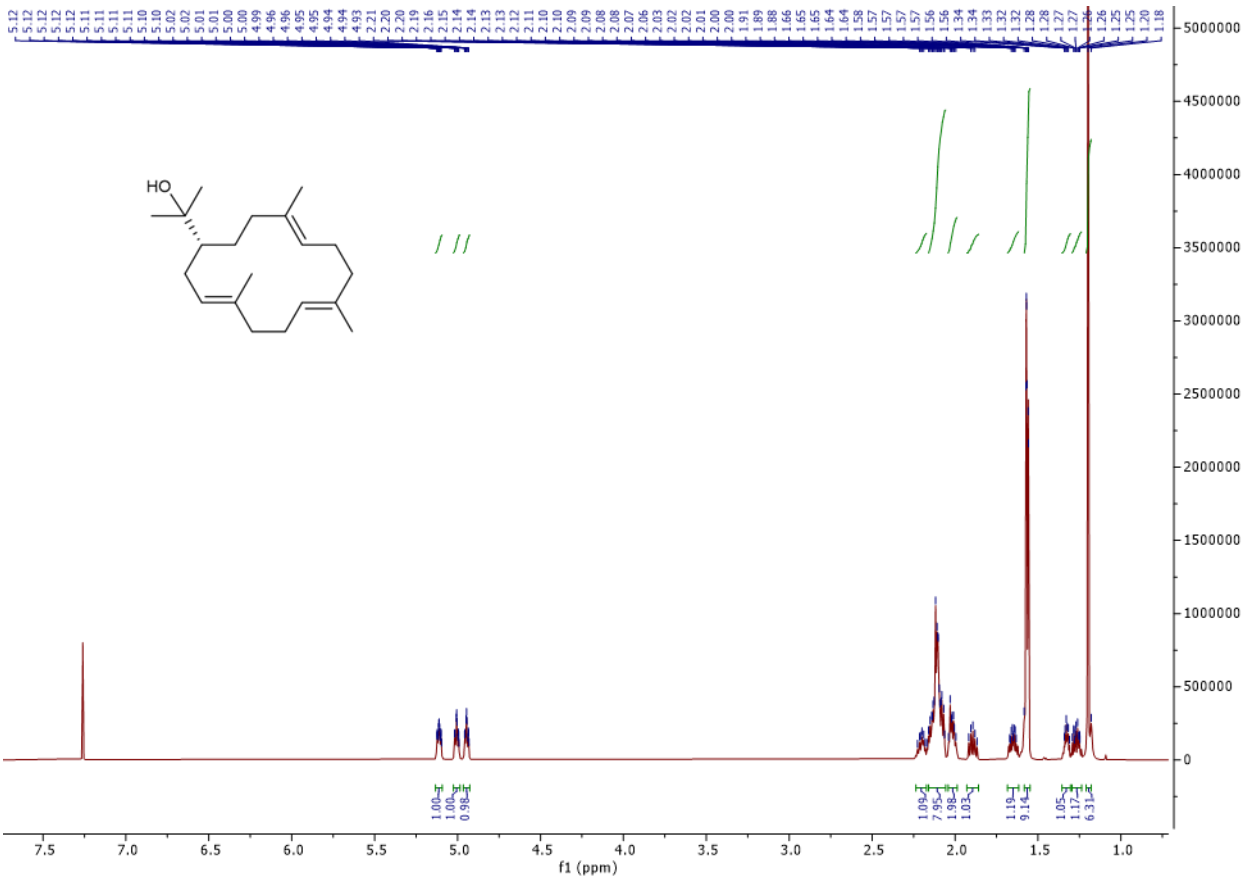

Supplementary Fig. 175. ^{1}H NMR spectrum of (*S*)-nephthenol (**23**) in $CDCl_3$ (600 MHz).

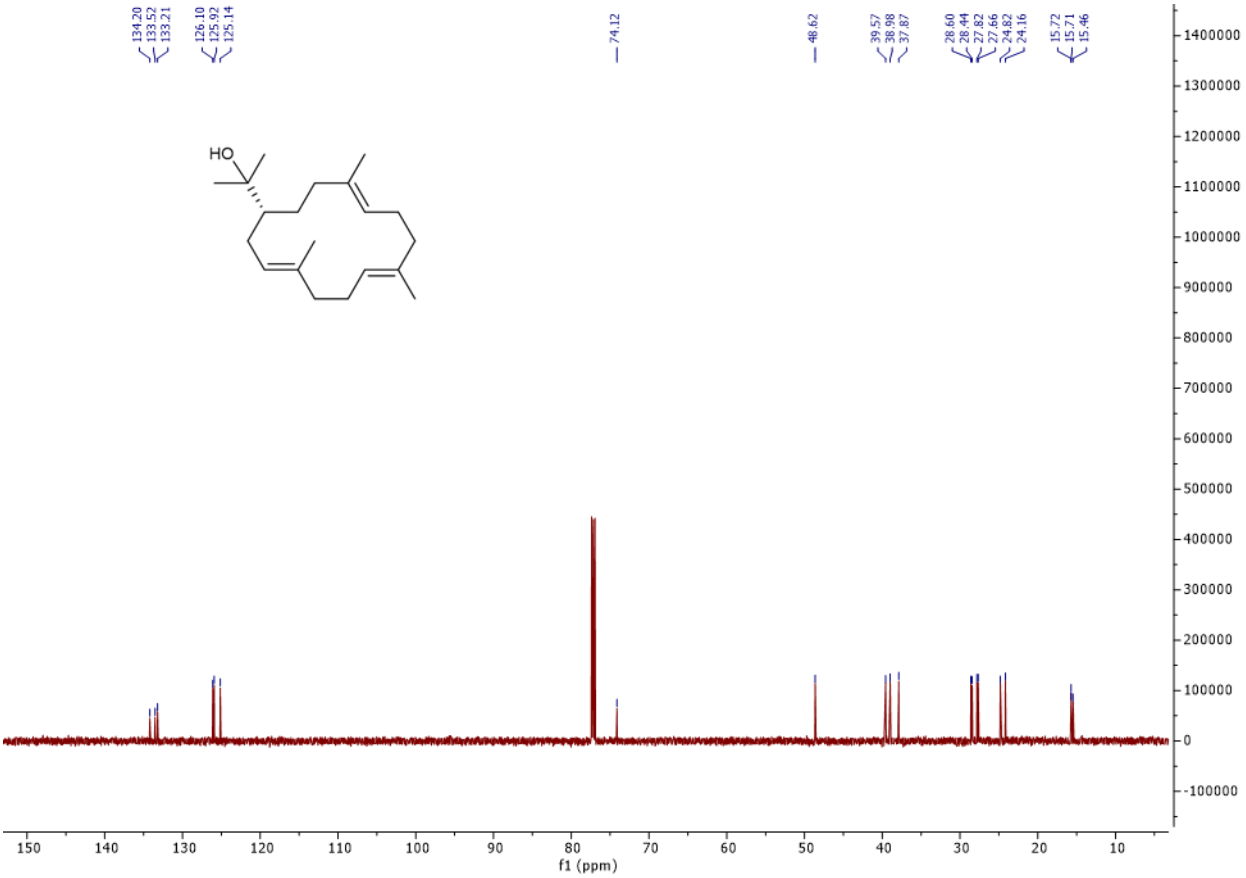

Supplementary Fig. 176. ^{13}C NMR spectrum of (*S*)-nephthenol (**23**) in $CDCl_3$ (151 MHz).

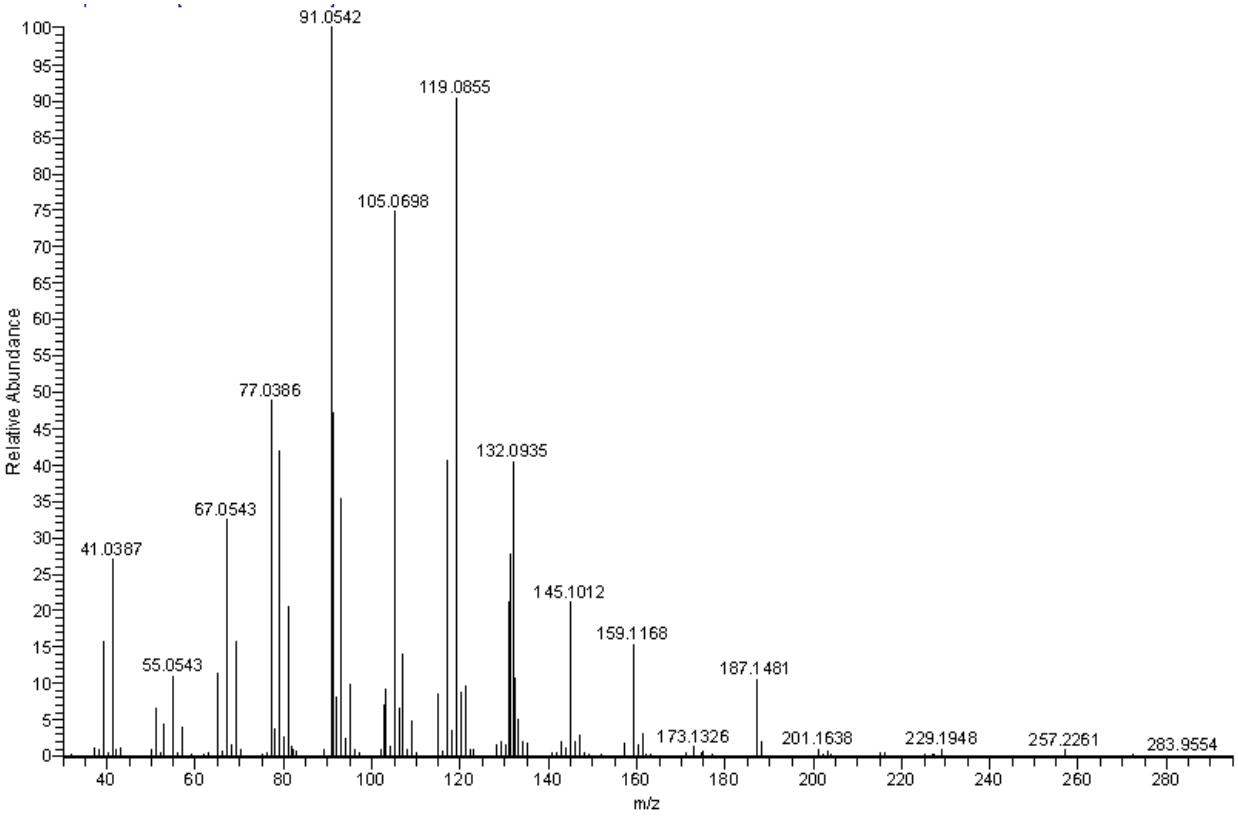

Supplementary Fig. 177. EIMS of isocembrene C (**24**). The fragmentation matched the literature[18].

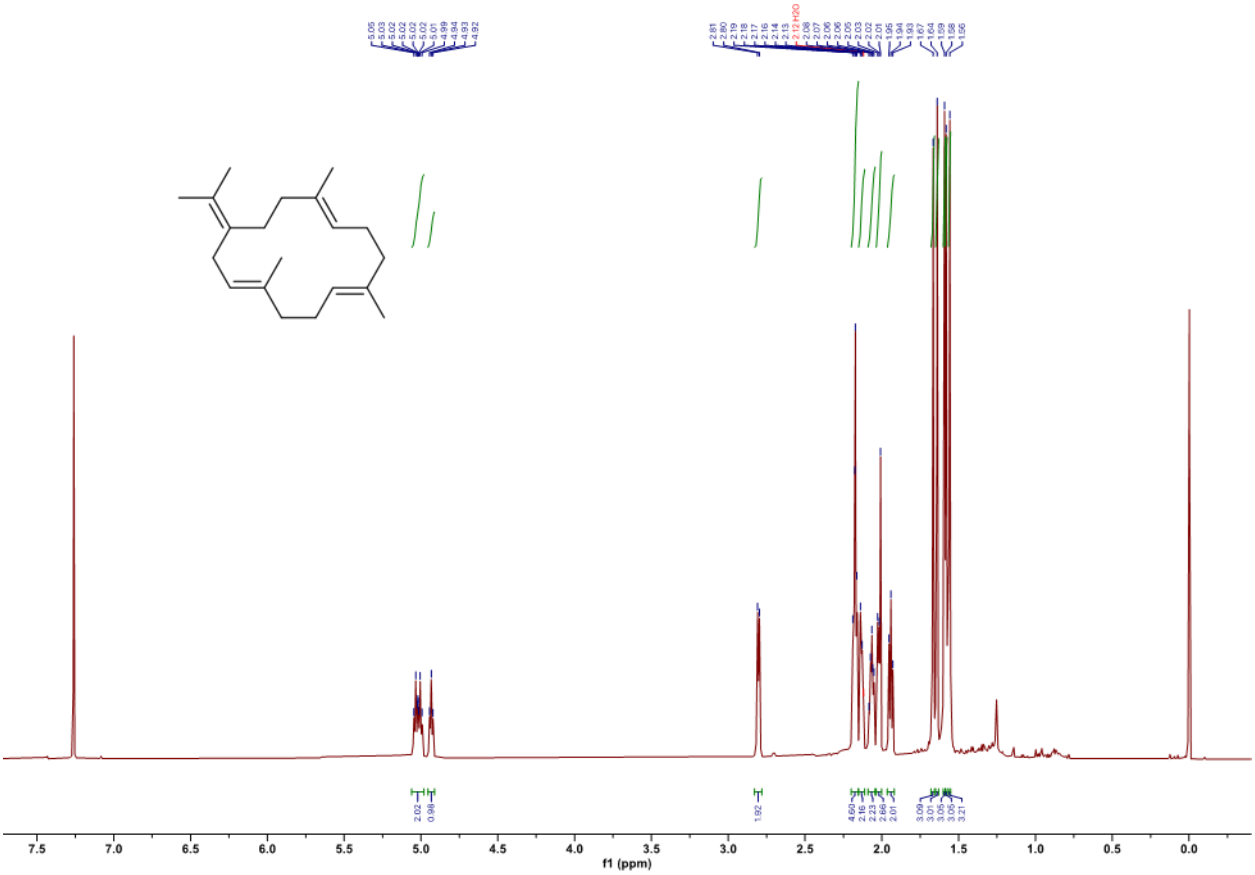

Supplementary Fig. 178. ^{1}H NMR spectrum of isocembrene C (**24**) in $CDCl_3$ (600 MHz).

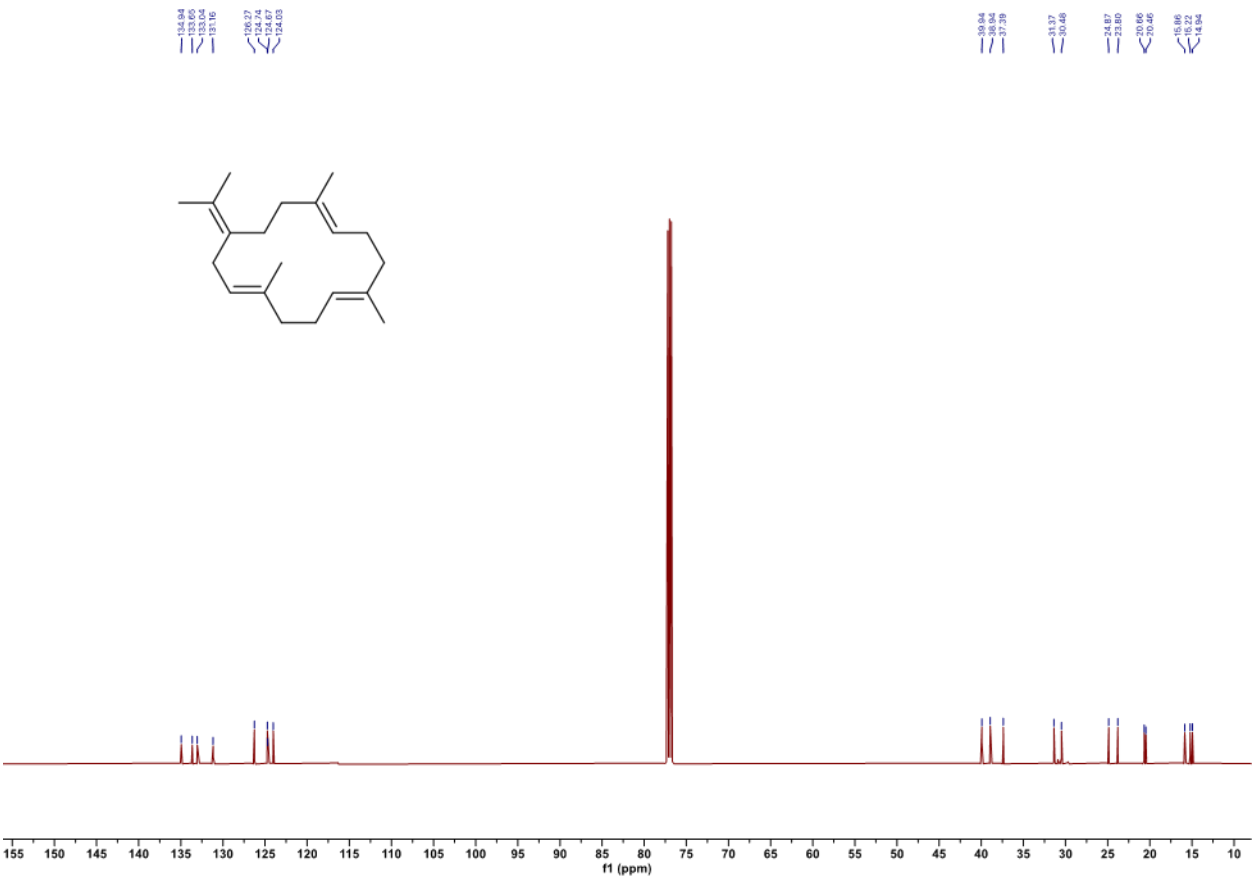

Supplementary Fig. 179. ^{13}C NMR spectrum of isocembrene C (**24**) in $CDCl_3$ (151 MHz).

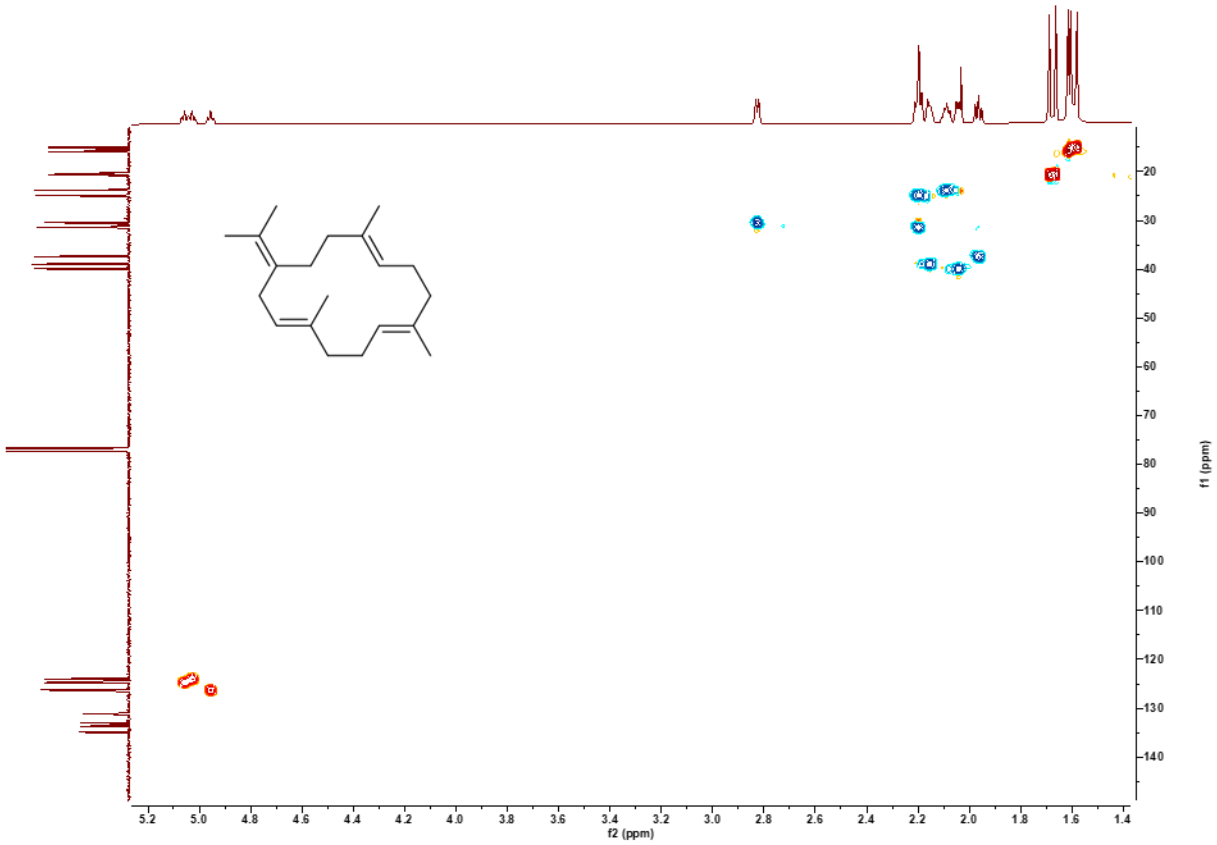

Supplementary Fig. 180. HSQC spectrum of isocembrene C (**24**) in $CDCl_3$.

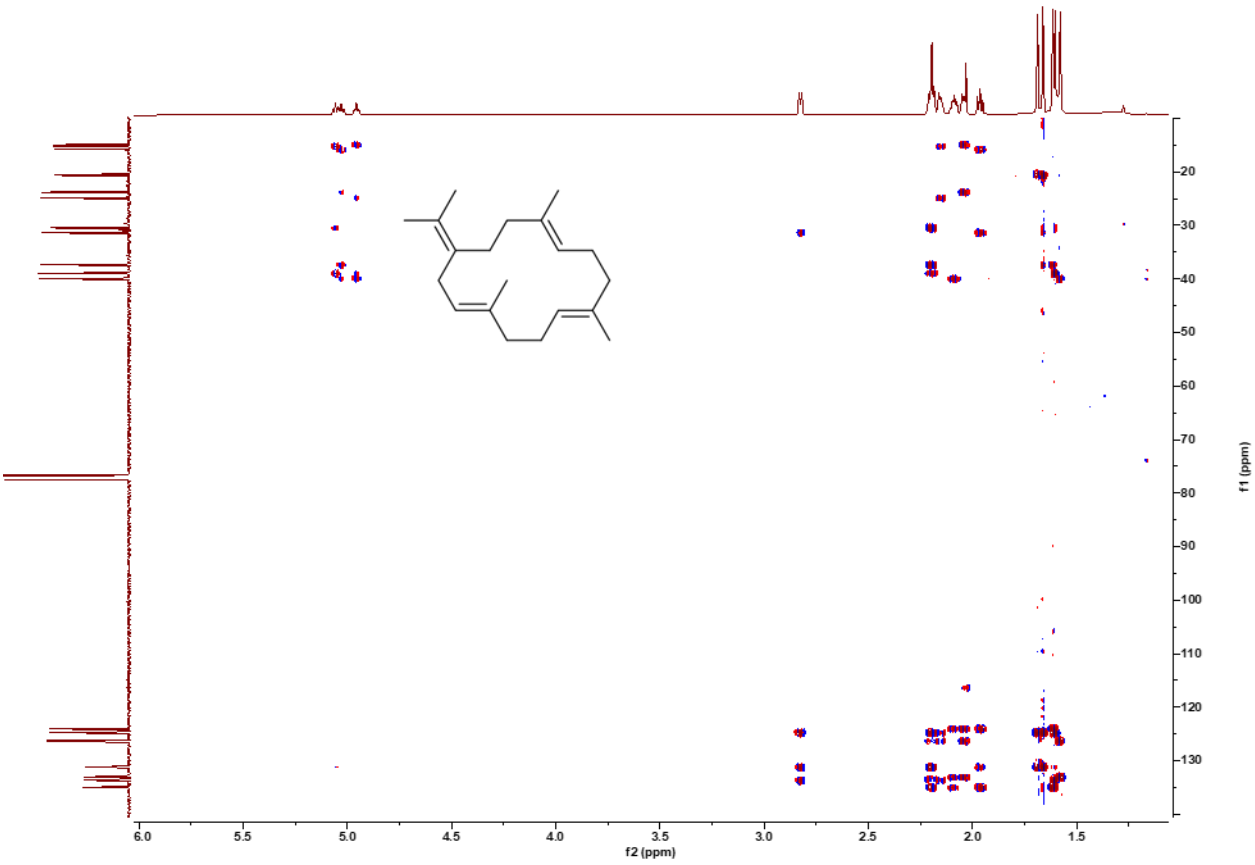

Supplementary Fig. 181. HMBC spectrum of isocembrene C (**24**) in $CDCl_3$.

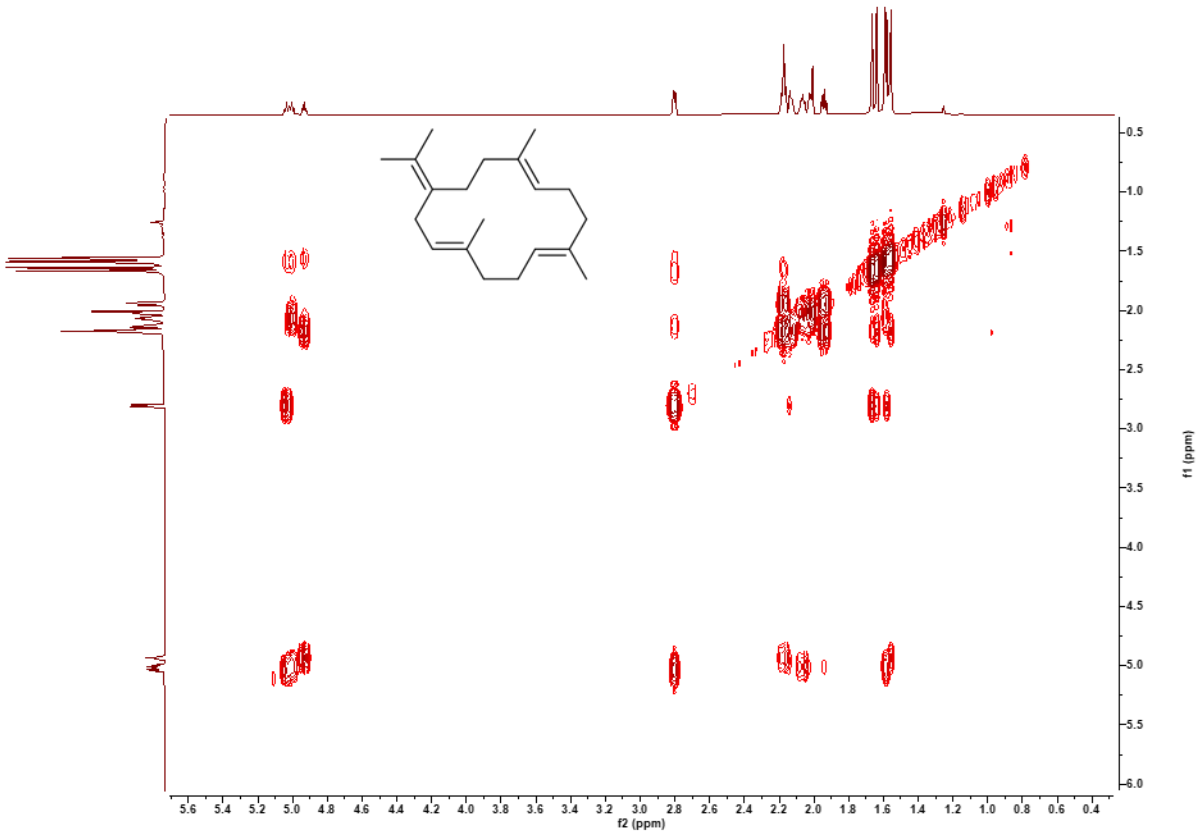

Supplementary Fig. 182. COSY spectrum of isocembrene C (**24**) in $CDCl_3$ (600 MHz).

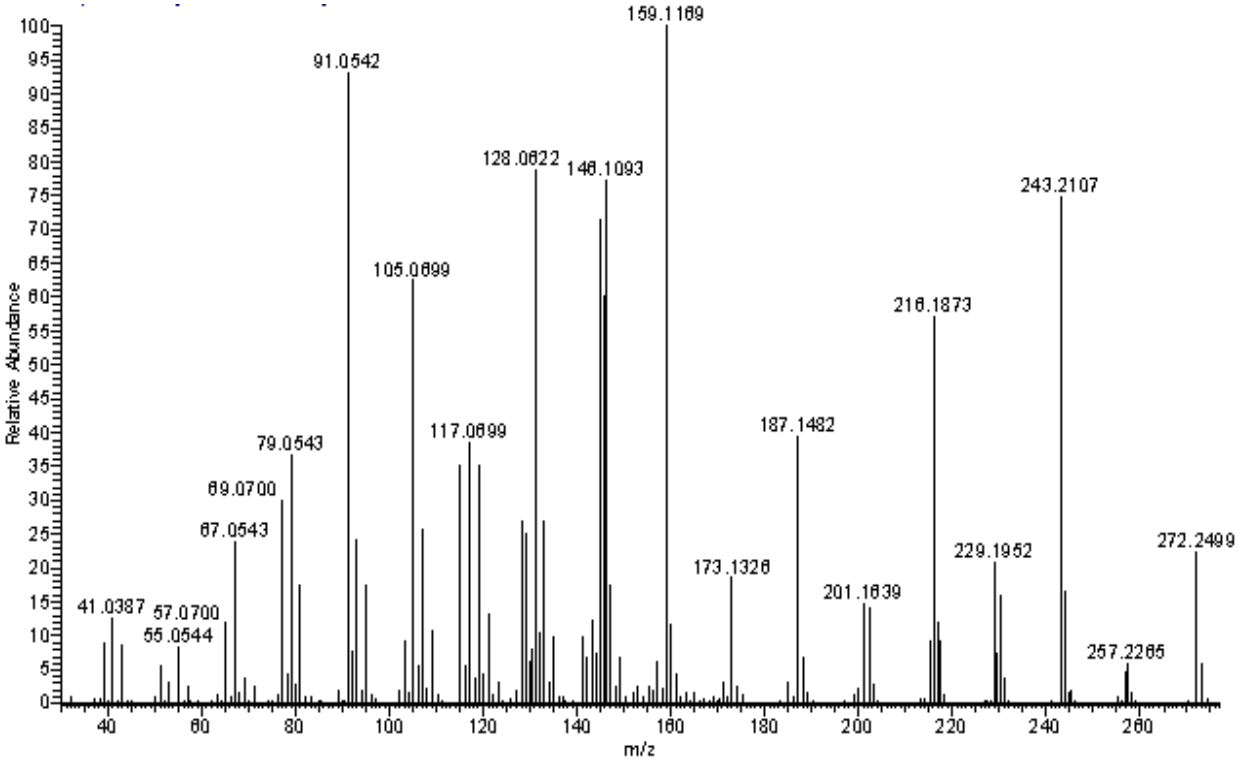

Supplementary Fig. 183. EIMS of spiroviolene (**25**). The fragmentation and retention index (RI = 1727) matched the literature (RI = 1724)[19].

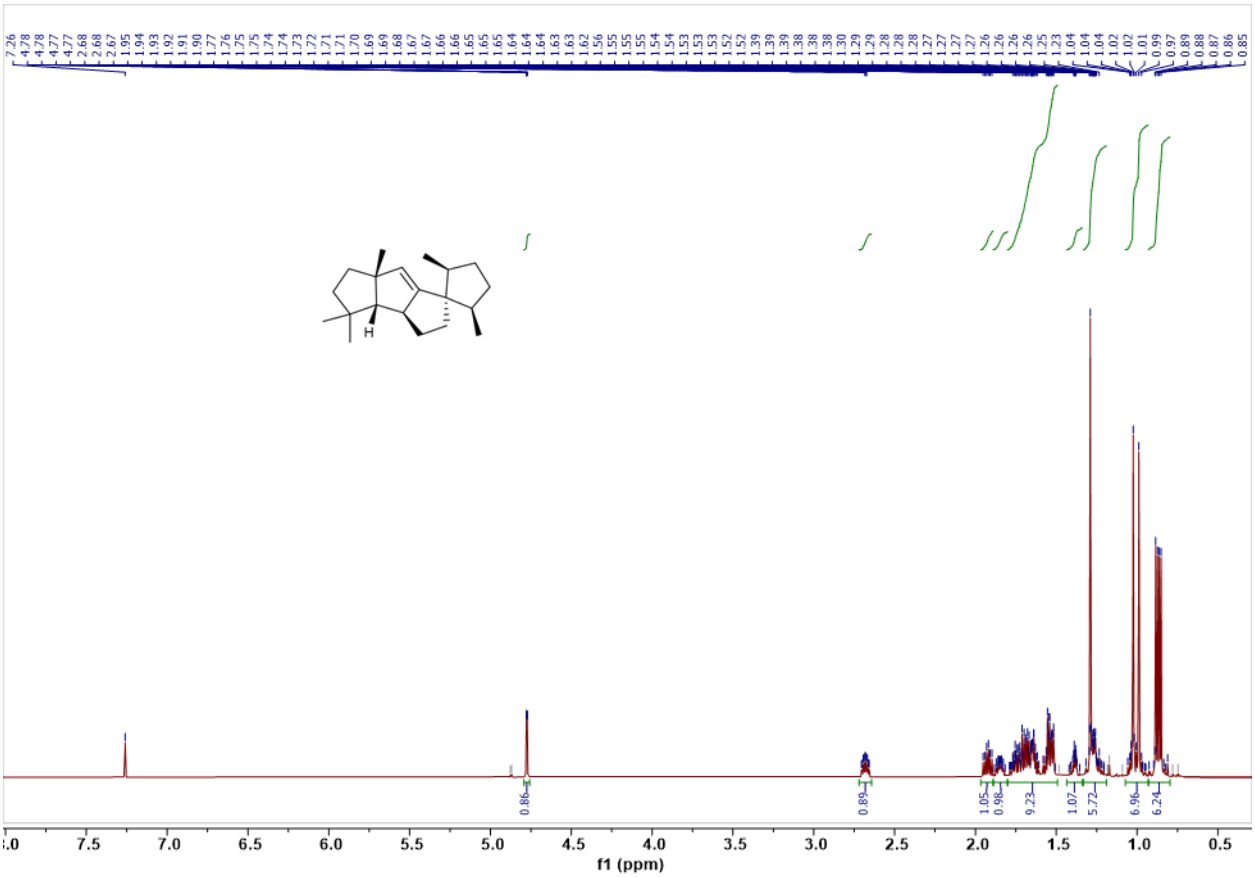

Supplementary Fig. 184. ^{1}H NMR spectrum of spiroviolene (**25**) in $CDCl_3$ (600 MHz).

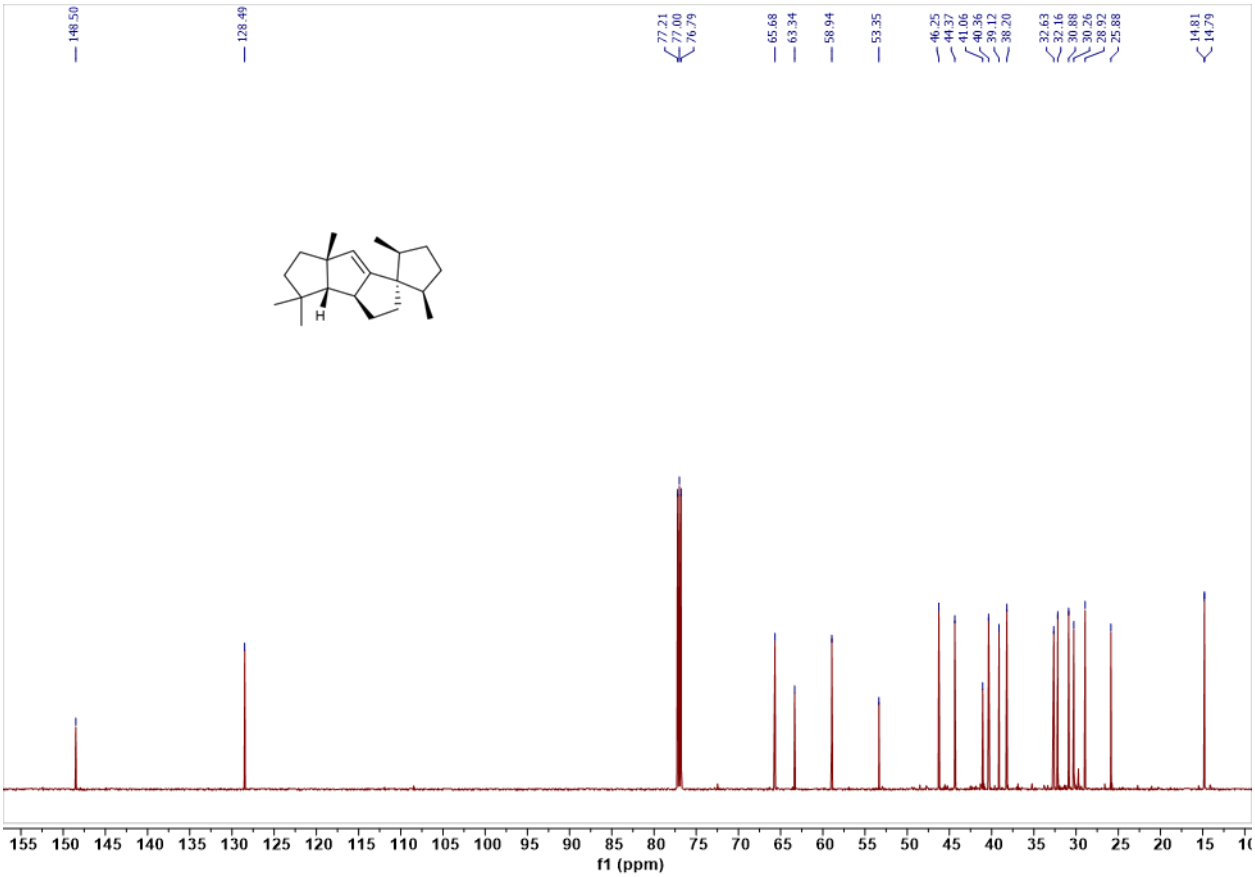

Supplementary Fig. 185. ^{13}C NMR spectrum of spiroviolene (**25**) in $CDCl_3$ (151 MHz).

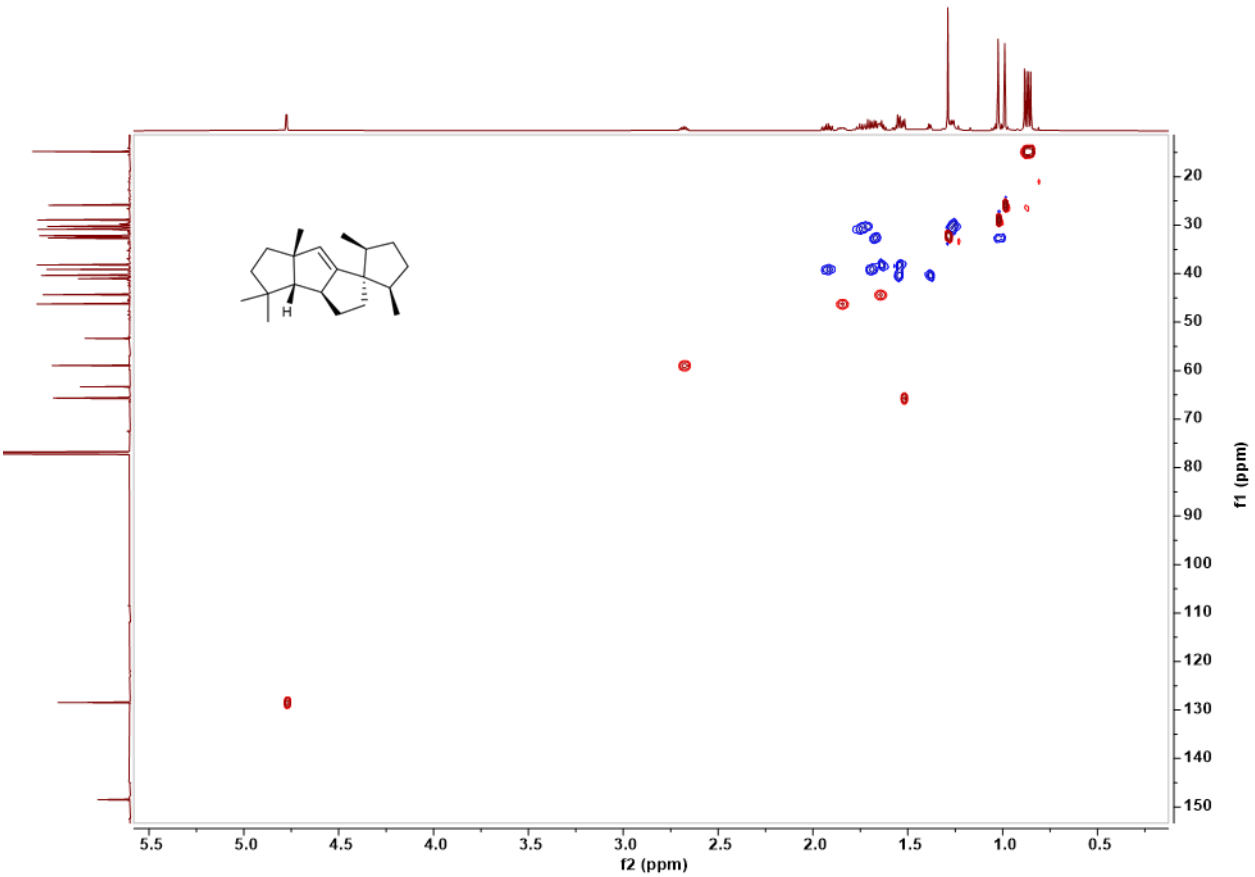

Supplementary Fig. 186. HSQC spectrum of spiroviolene (**25**) in $CDCl_3$.

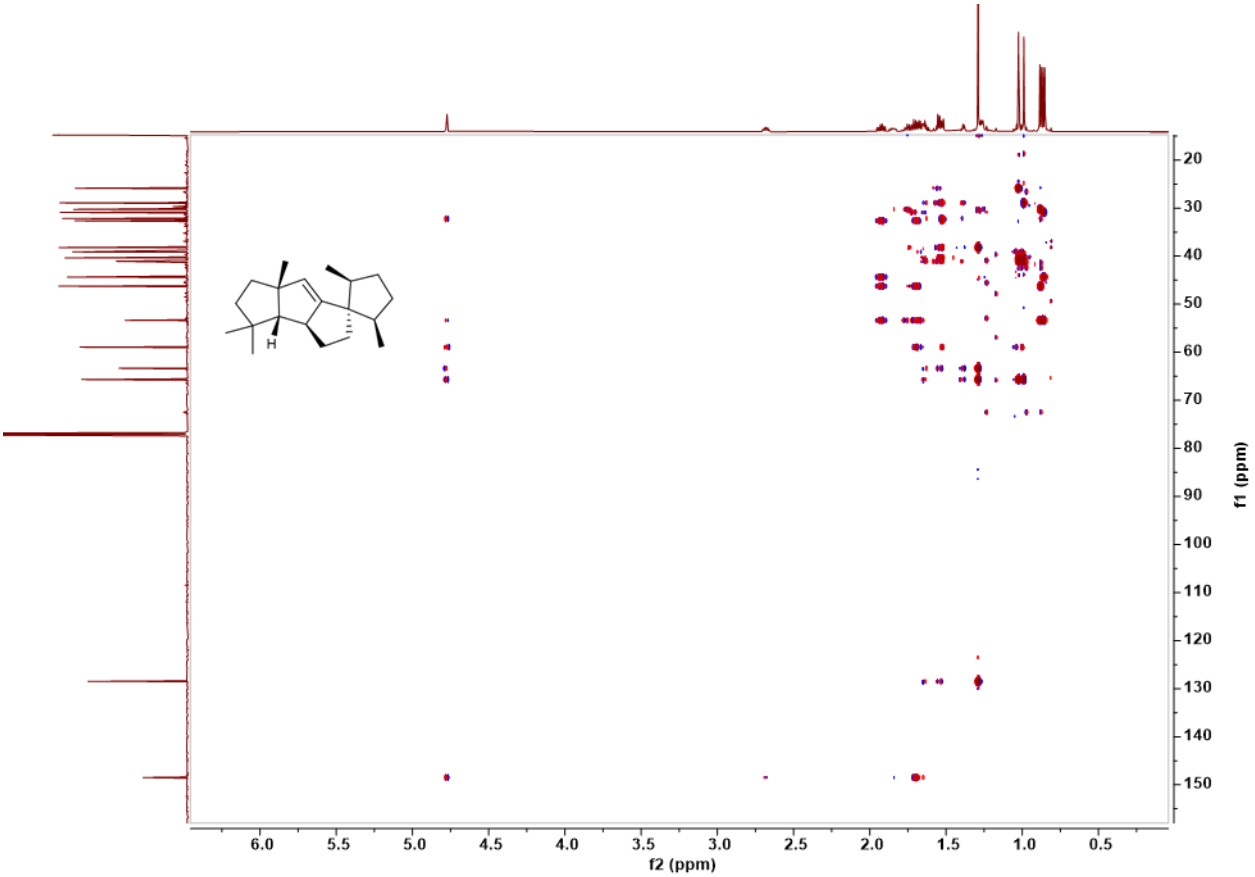

Supplementary Fig. 187. HMBC spectrum of spiroviolene (**25**) in $CDCl_3$ (600 MHz).

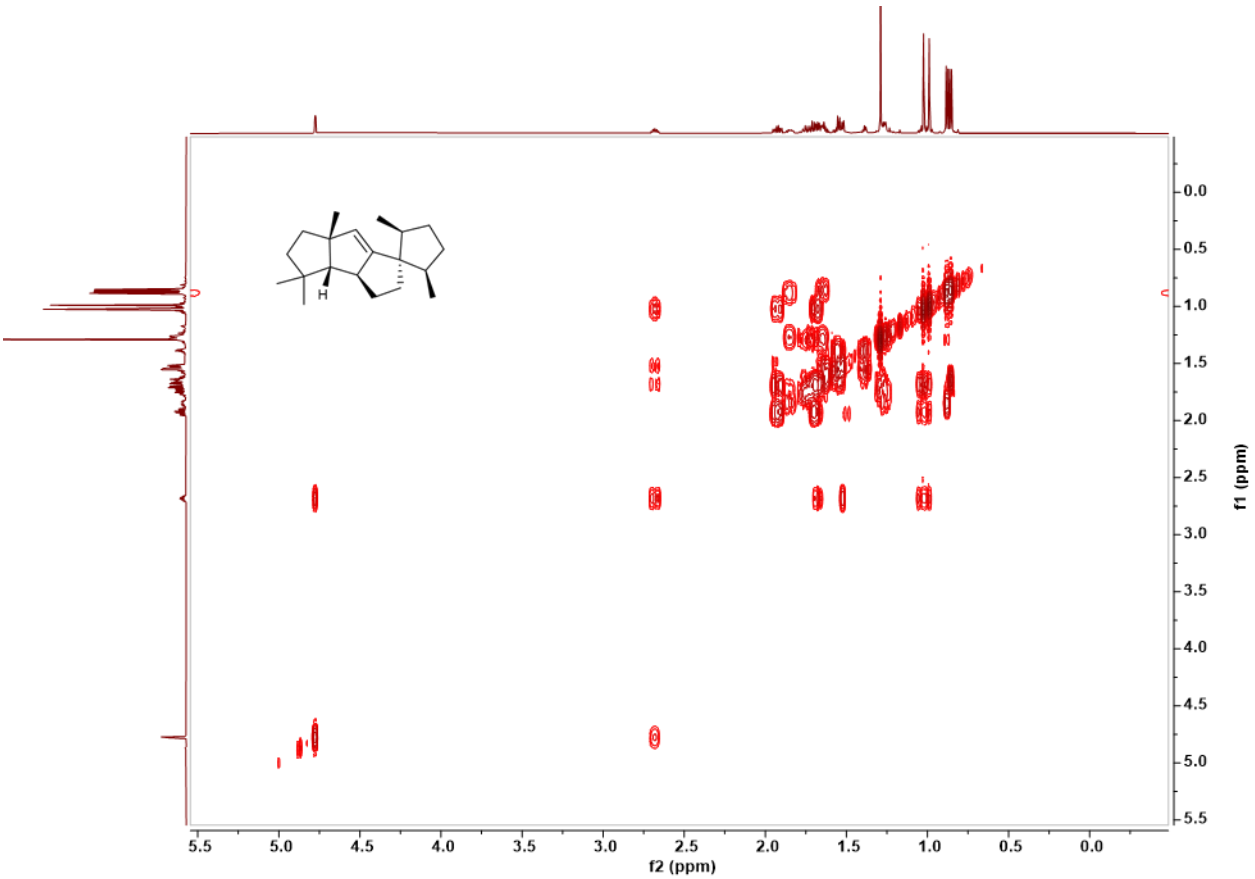

Supplementary Fig. 188. COSY spectrum of spiroviolene (**25**) in $CDCl_3$.

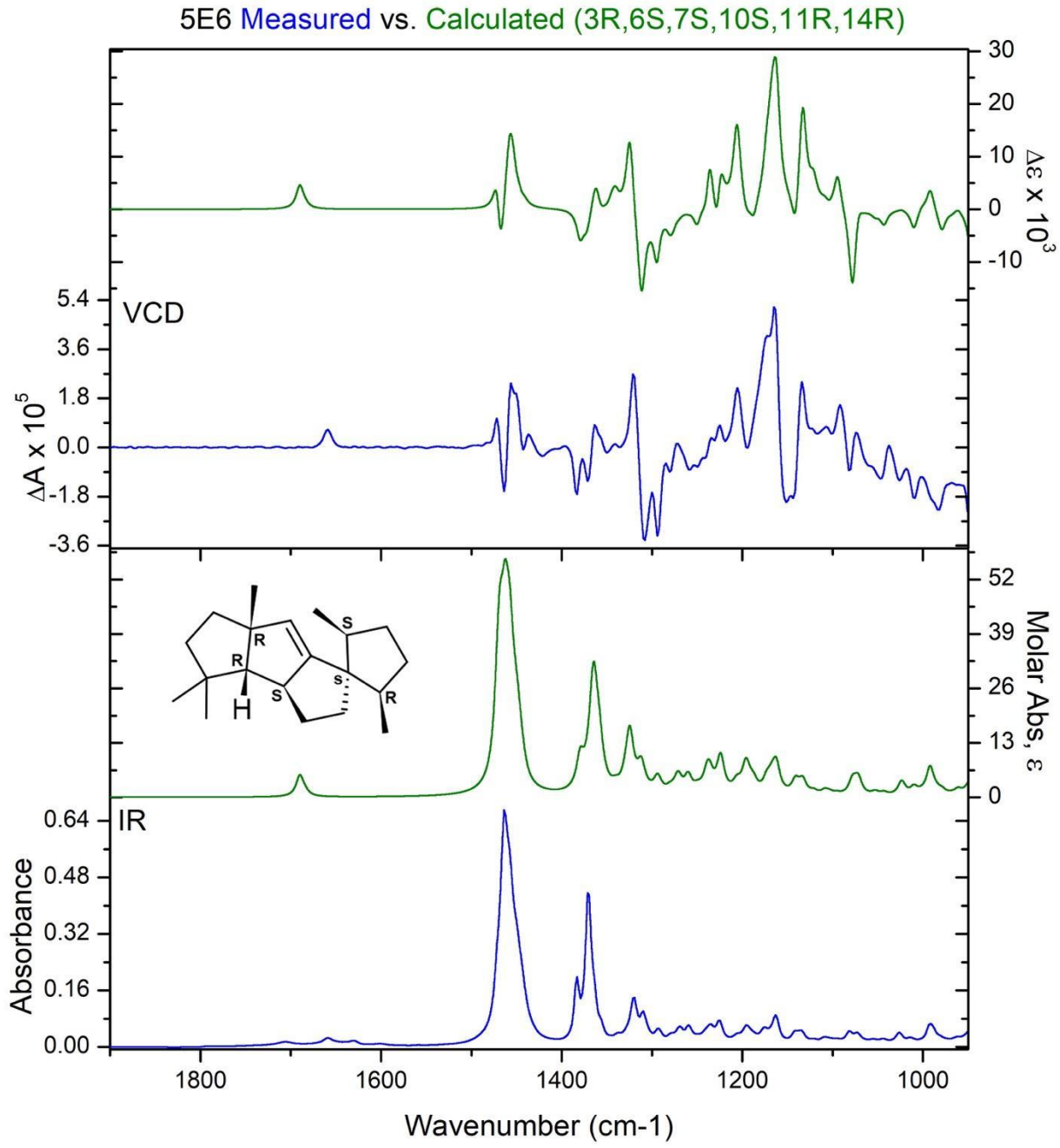

Supplementary Fig. 189. DFT calculated (green) and experimental (blue) VCD and IR spectra of spiroviolene (**25**).

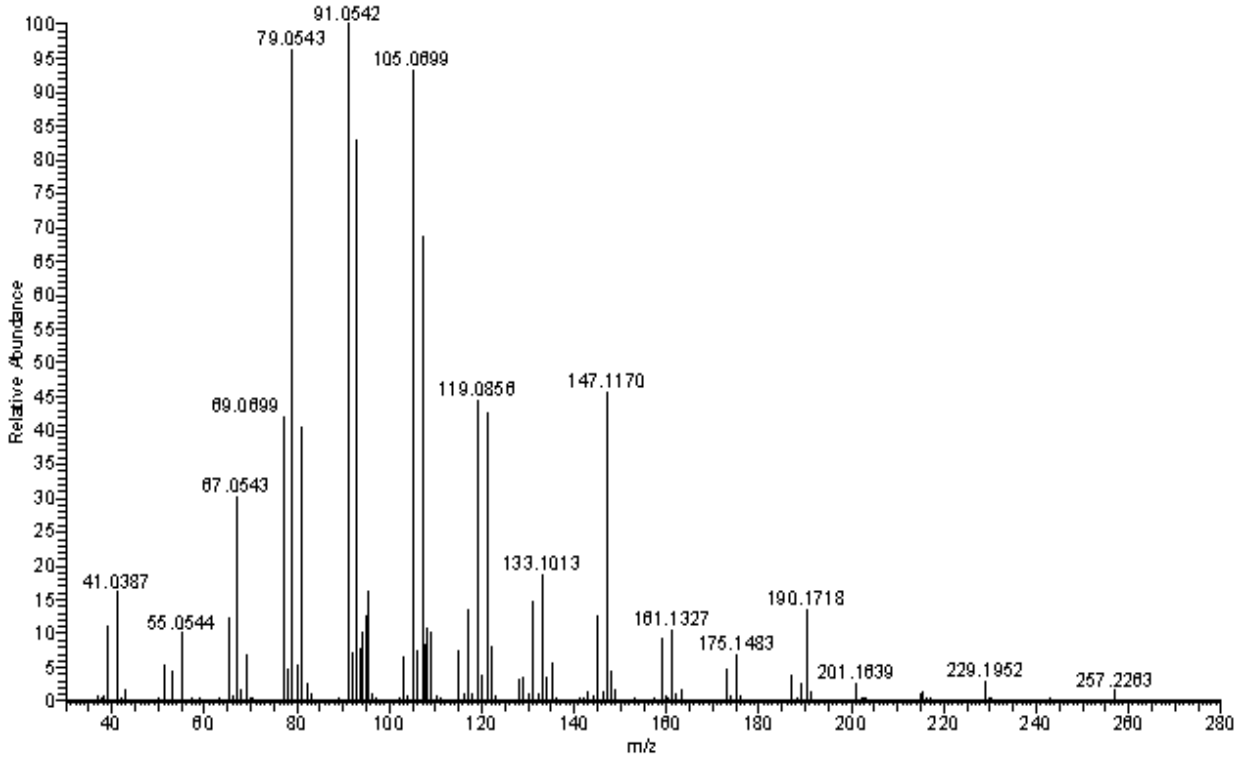

Supplementary Fig. 190. EIMS of spata-13,17-diene (**26**). The fragmentation matched the literature[28].

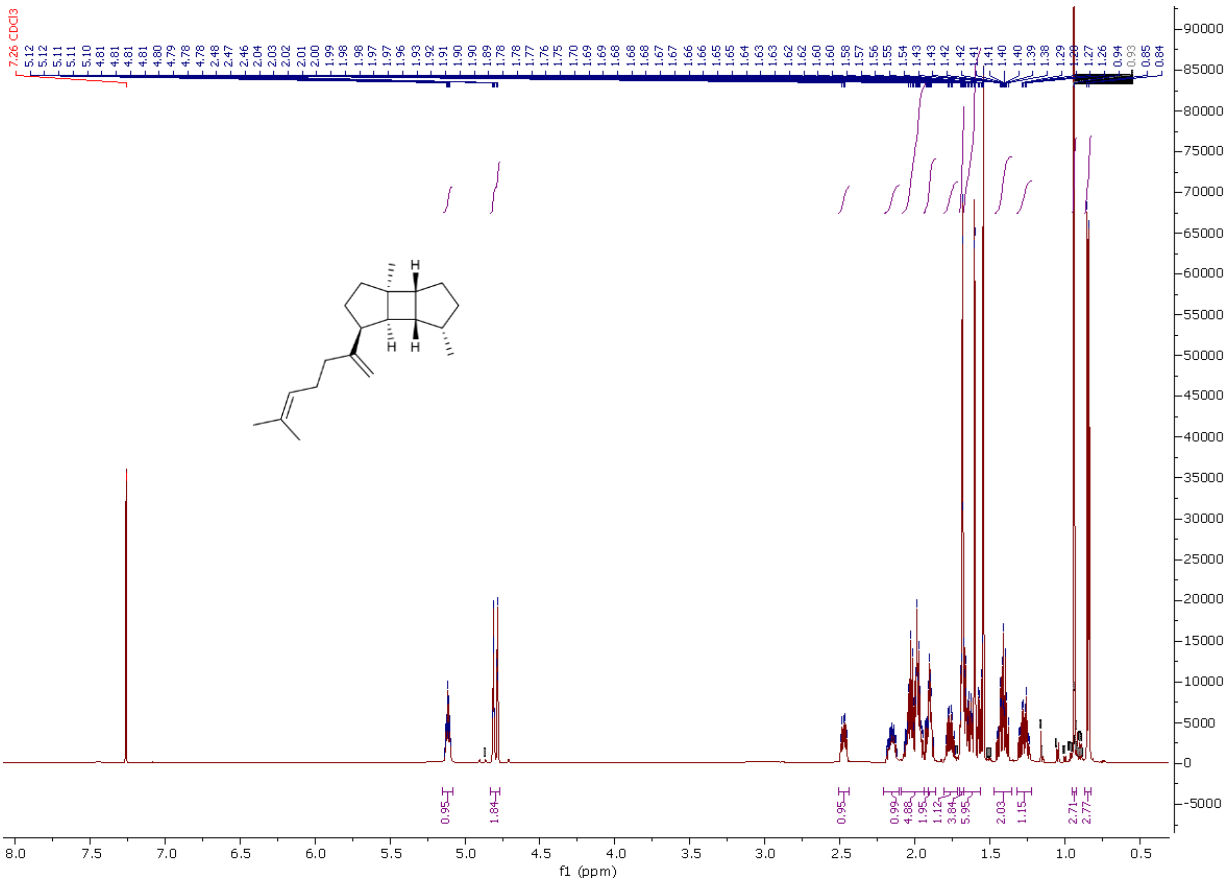

Supplementary Fig. 191. ^{1}H NMR spectrum of spata-13,17-diene (**26**) in $CDCl_3$ (600 MHz).

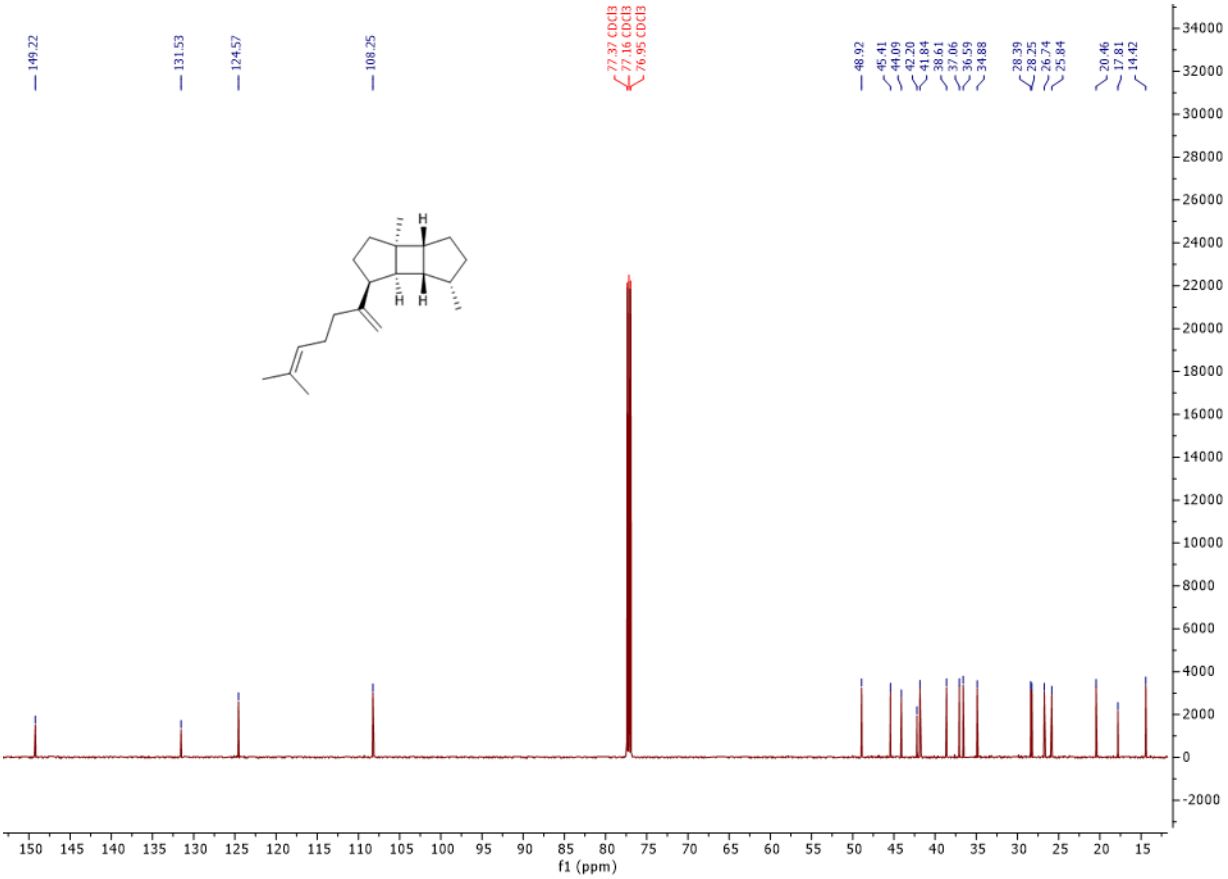

Supplementary Fig. 192. ^{13}C NMR spectrum of spata-13,17-diene (**26**) in $CDCl_3$ (151 MHz).

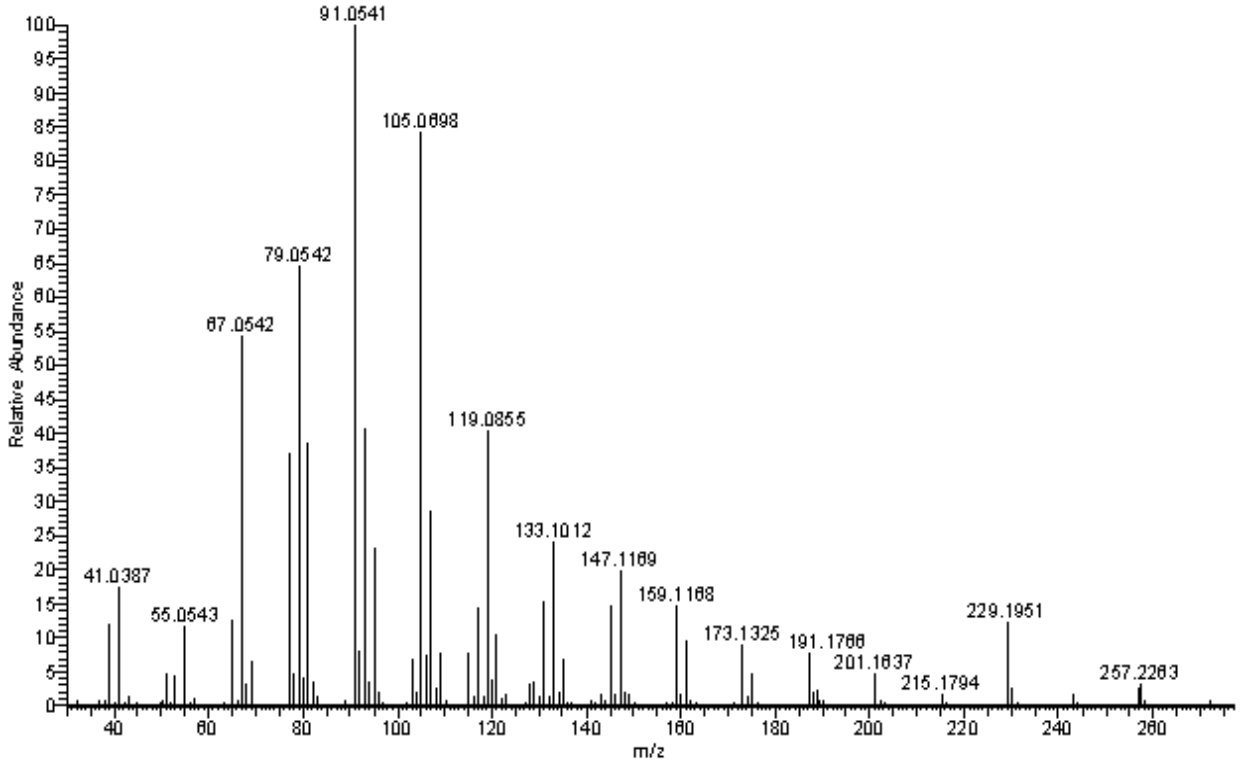

Supplementary Fig. 193. EIMS of cneorubin Y (**27**).

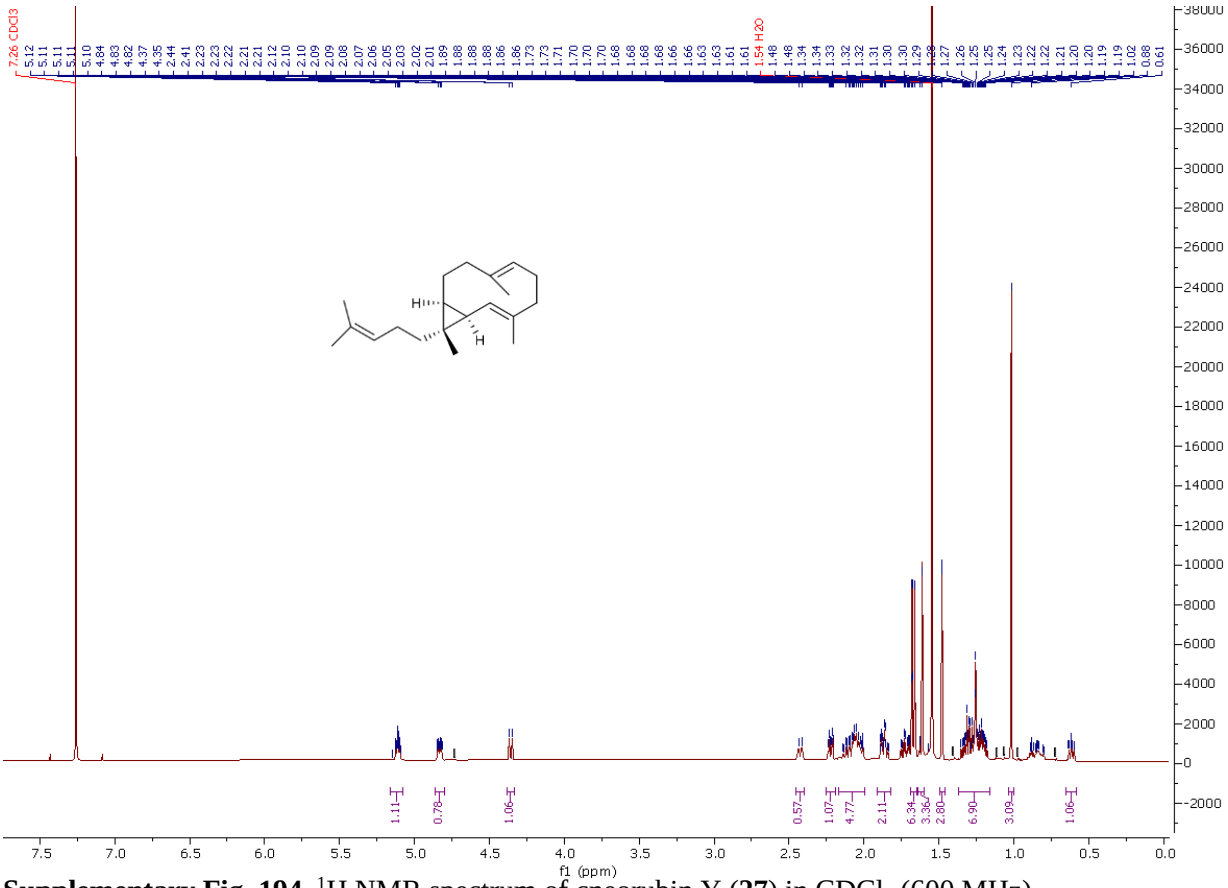

Supplementary Fig. 194. ^{1}H NMR spectrum of cneorubin Y (**27**) in $CDCl_3$ (600 MHz).

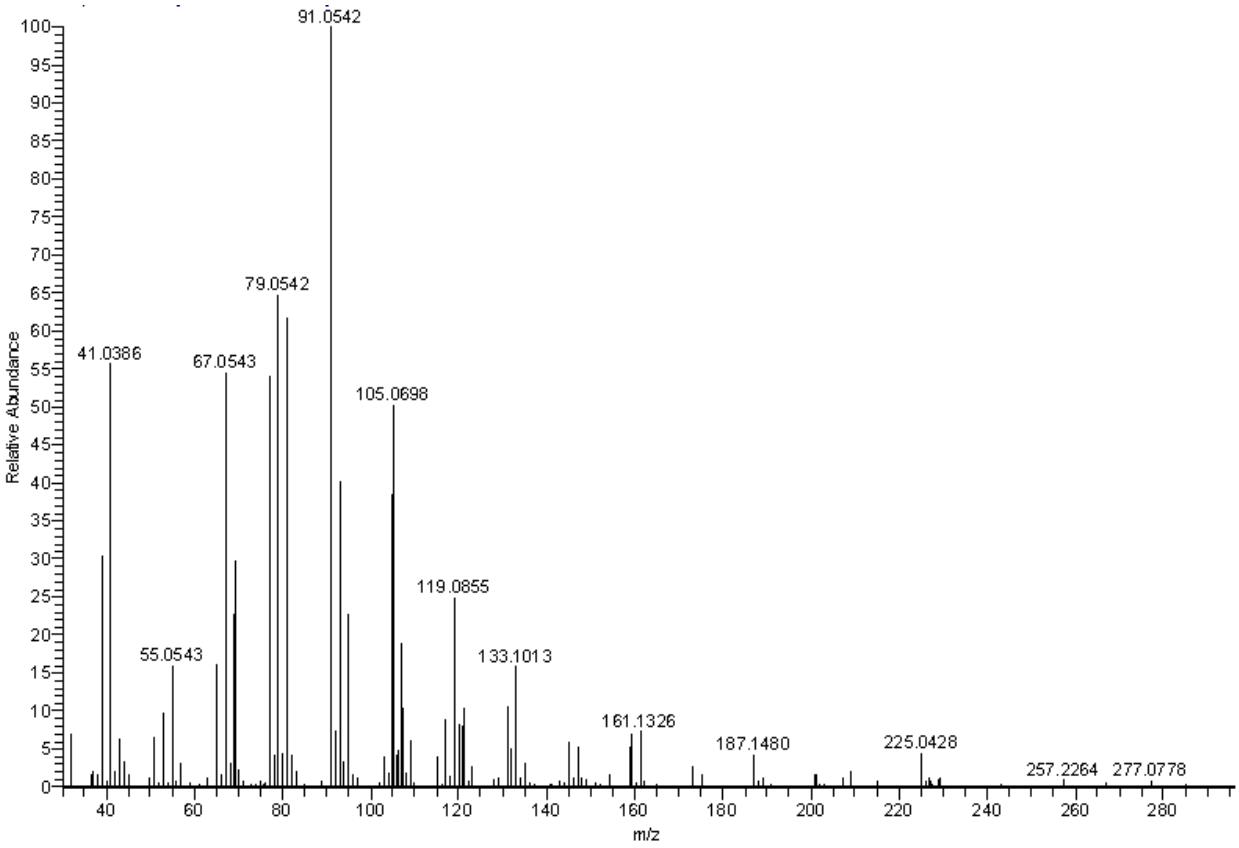

Supplementary Fig. 195. EIMS of β-springene (**28**). The fragmentation and retention index (RI = 1924) matched the literature (RI = 1918)[29].

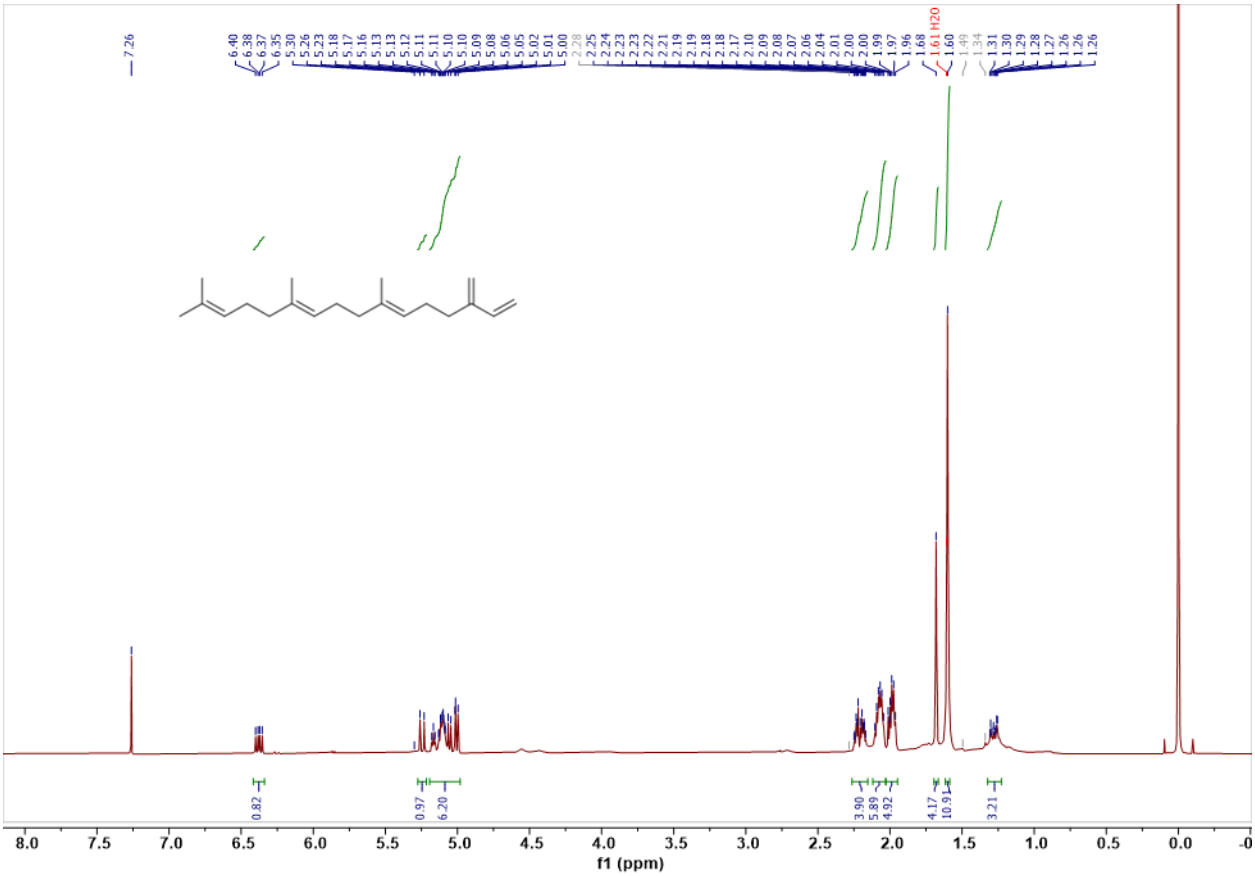

Supplementary Fig. 196. ^{1}H NMR spectrum of β-springene (**28**) in $CDCl_3$ (600 MHz).

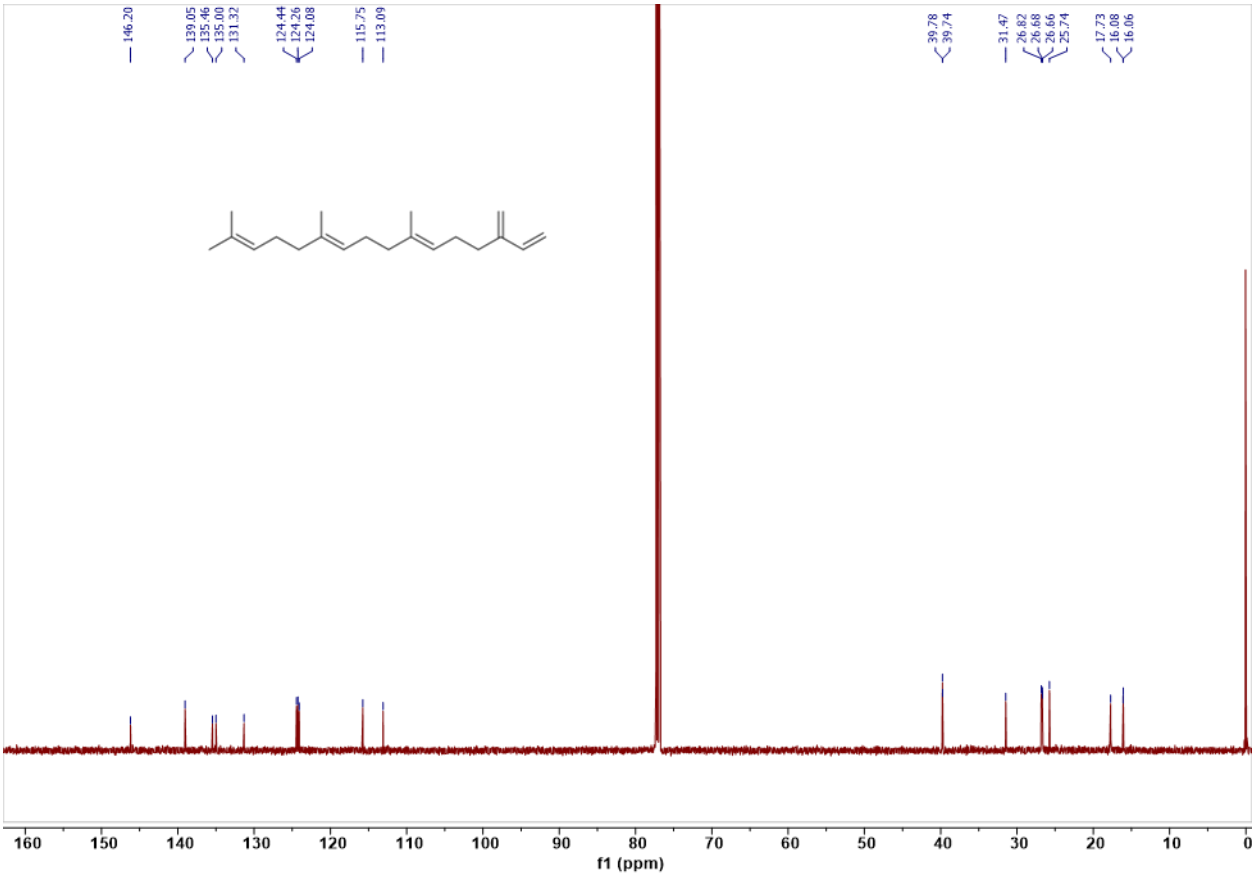

Supplementary Fig. 197. ^{13}C NMR spectrum of β-springene (**28**) in $CDCl_3$ (151 MHz).

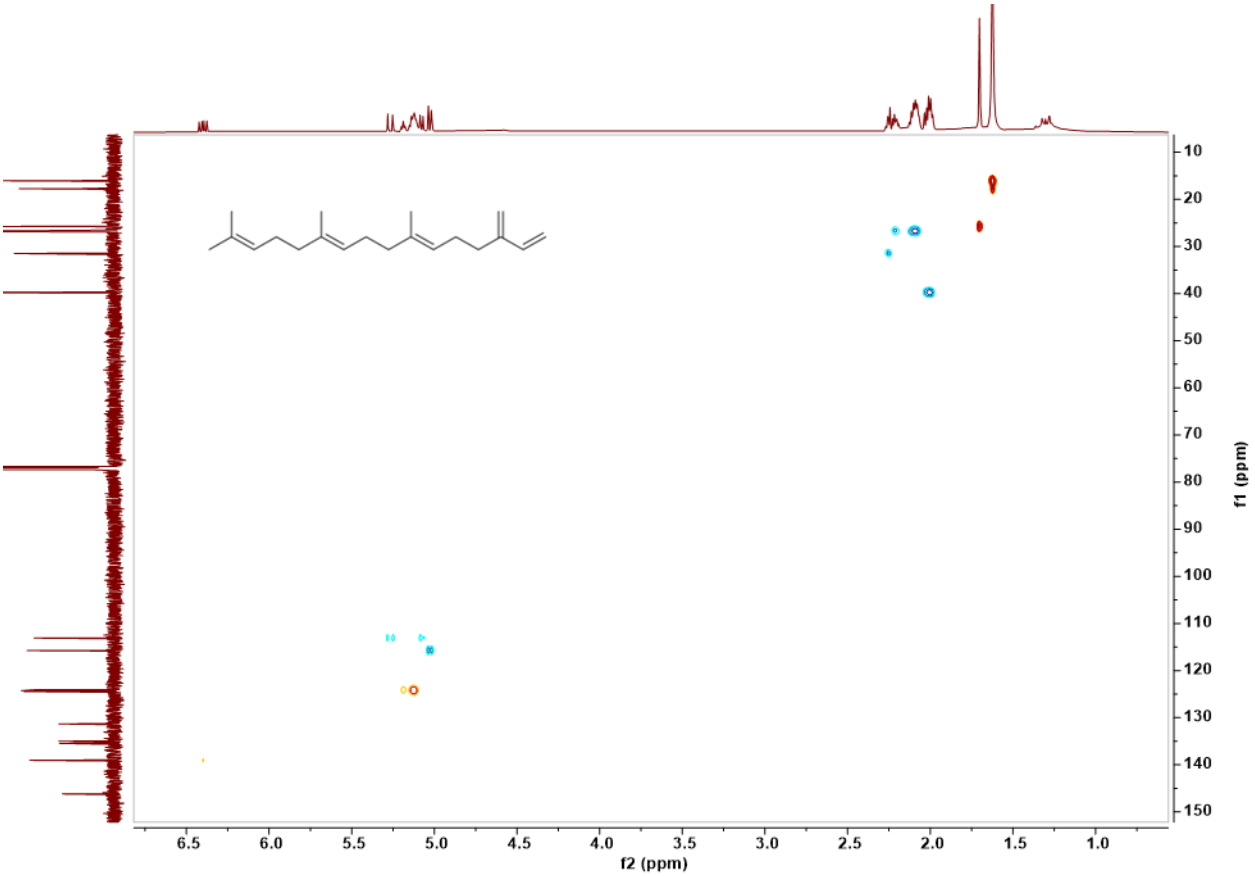

Supplementary Fig. 198. HSQC spectrum of β-springene (**28**) in $CDCl_3$.

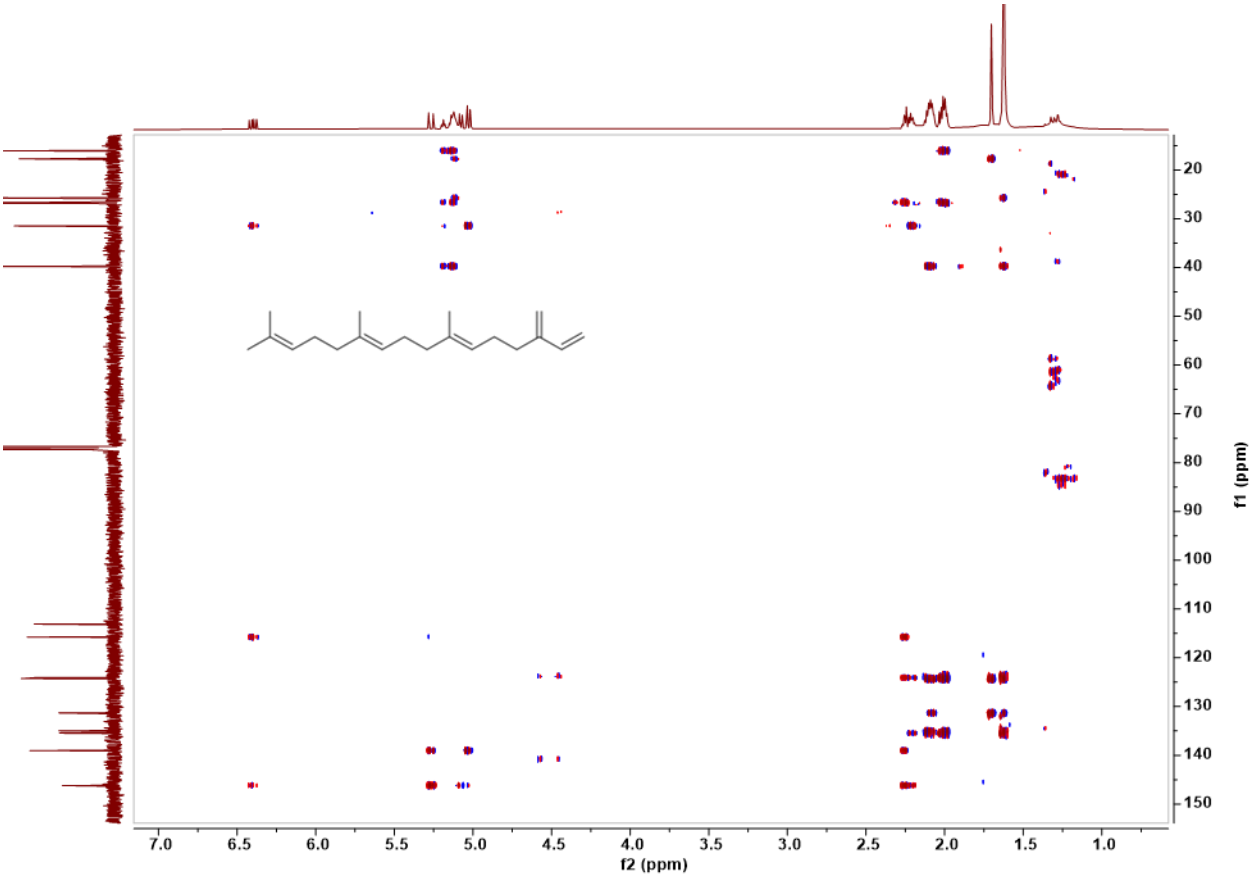

Supplementary Fig. 199. HMBC spectrum of β-springene (**28**) in $CDCl_3$.

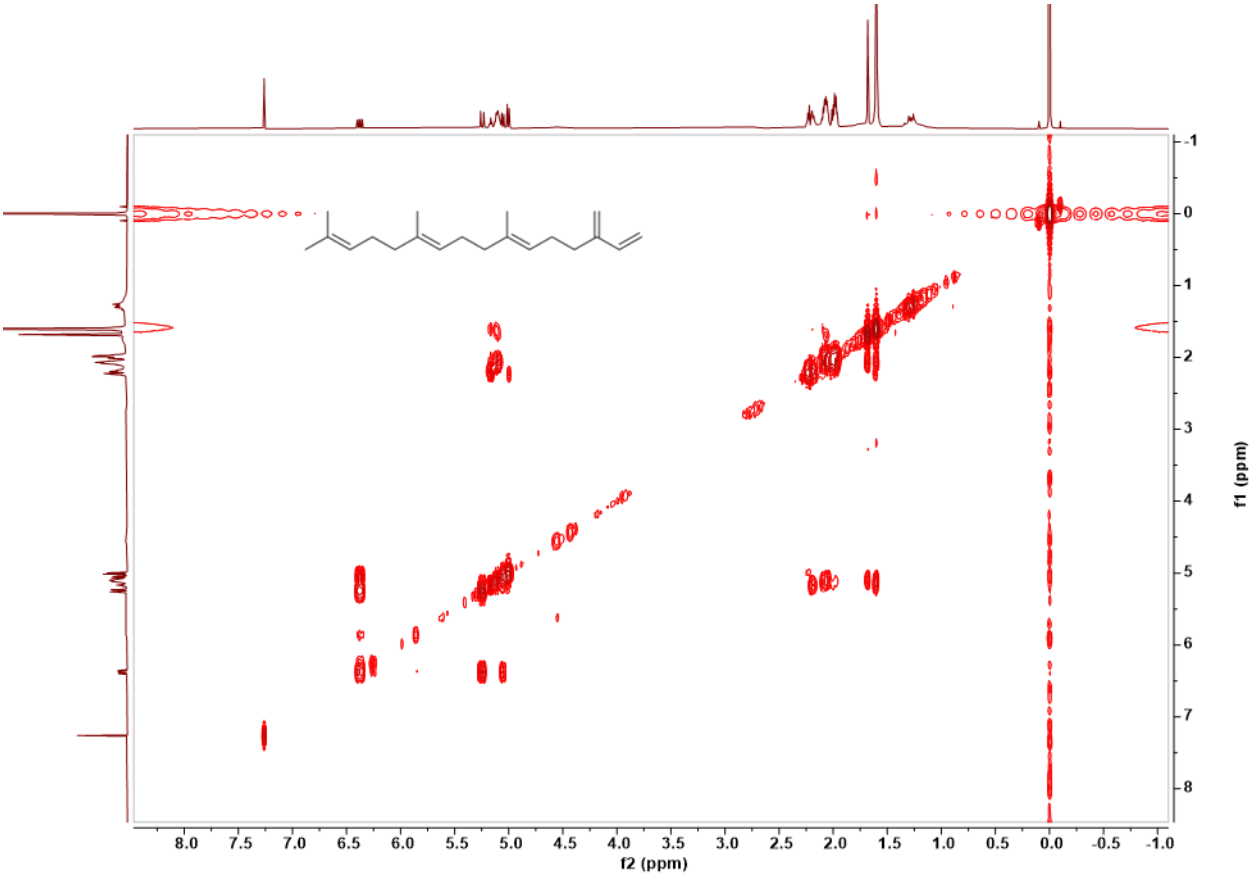

Supplementary Fig. 200. COSY spectrum of β-springene (**28**) in $CDCl_3$.

Supplementary Fig. 201. SDS-PAGE of nickel-affinity chromatography purified TSs. TiqS (40.8 kDa), SalS (38.6 kDa), PeyS (37.6 kDa), *Salk*S (38.3 kDa), *Od*VS (38.3 kDa) and *N*Bnd4 (40.9 kDa). "Mark" signifies Color Prestained Protein Standard Ladder (NEB).

Supplementary references

1. Frisch, M. J., Trucks, G. W., Schlegel, H. B., Scuseria, G. E., Robb, M. A., Cheeseman, J. R., Scalmani, G., Barone, V., Mennucci, B., Petersson, G. A., et al. *Gaussian 09 Citation | Gaussian.com*. https://gaussian.com/g09citation/ (accessed 2024-08-23). Gaussian 09, Revision D.01, (2013).
2. He, Y., Bo, W., Dukor, R. K., Nafie, L. A. Determination of absolute configuration of chiral molecules using vibrational optical activity: a review. *Appl. Spectrosc.* **65**, 699–723 (2011).
3. Polavarapu, P. L., Covington, C. L. Comparison of experimental and calculated chiroptical spectra for chiral molecular structure determination. *Chirality*, **26**, 539–552 (2014).
4. Xia, Y., Li, K., Li, J., Wang, T., Gu, L., Xun, L. T5 Exonuclease-dependent assembly offers a low-cost method for efficient cloning and site-directed mutagenesis. *Nucleic Acids Res.*, **47**, e15 (2019).
5. Kruger, N. J. The Bradford Method For Protein Quantitation. In *The Protein Protocols Handbook*, Walker, J. M., Ed., Humana Press: Totowa, NJ, pp 17–24 (2009).
6. Qin, B., Matsuda, Y., Mori, T., Okada, M., Quan, Z., Mitsuhashi, T., Wakimoto, T., Abe, I. An unusual chimeric diterpene synthase from *Emericella variecolor* and its functional conversion into a sesterterpene synthase by domain swapping. *Angew. Chem. Int. Ed.* **55**, 1658–1661 (2016).
7. Jackson, C. B., Pattenden, G. Total synthesis of verticillene, the putative biogenetic precursor of the taxane alkaloids. *Tet. Lett.* **26**, 3393–3396 (1985) .
8. Tungcharoen, P., Wattanapiromsakul, C., Tansakul, P., Nakamura, S., Matsuda, H., Tewtrakul, S. Anti-inflammatory isopimarane diterpenoids from *Kaempferia galanga*. *Phytother. Res.* **34**, 612–623 (2020).
9. Li, Z., Jiang, Y., Zhang, X., Chang, Y., Li, S., Zhang, X., Zheng, S., Geng, C., Men, P., Ma, L., Yang, Y., Gao, Z., Tang, Y.-J., Li, S. Fragrant venezuelaenes A and B with A 5–5–6–7 tetracyclic skeleton: discovery, biosynthesis, and mechanisms of central catalysts. *ACS Catal.* **10**, 5846–5851 (2020).
10. Li, Z., Zhang, L., Xu, K., Jiang, Y., Du, J., Zhang, X., Meng, L.-H., Wu, Q., Du, L., Li, X., Hu, Y., Xie, Z., Jiang, X., Tang, Y.-J., Wu, R., Guo, R.-T., Li, S. Molecular insights into the catalytic promiscuity of a bacterial diterpene synthase. *Nat Commun.* **14**, 4001 (2023).
11. Ioannou, E., Quesada, A., Rahman, M. M., Gibbons, S., Vagias, C., Roussis, V. Dolabellanes with antibacterial activity from the brown alga *Dilophus spiralis*. *J. Nat. Prod.* **74**, 213–222 (2011).
12. Yamada, Y., Arima, S., Nagamitsu, T., Johmoto, K., Uekusa, H., Eguchi, T., Shin-ya, K., Cane, D. E., Ikeda, H. Novel terpenes generated by heterologous expression of bacterial terpene synthase genes in an engineered streptomyces Host. *J. Antibiot.* **68**, 385–394 (2015).
13. Xu, B., Tantillo, D. J., Rudolf, J. D. Mechanistic insights into the formation of the 6,10-bicyclic eunicellane skeleton by the bacterial diterpene synthase Bnd4. *Angew. Chem. Int. Ed.* **60**, 23159–23163 (2021).
14. Rinkel, J., Rabe, P., Chen, X., Köllner, T. G., Chen, F., Dickschat, J. S. Mechanisms of the diterpene cyclases β-pinacene synthase from *Dictyostelium discoideum* and hydropyrene synthase from *Streptomyces clavuligerus*. *Chem. Eur. J.* **23**, 10501–10505 (2017).
15. Rinkel, J., Dickschat, J. S. Characterization of micromonocyclol synthase from the marine actinomycete *Micromonospora marina*. *Org. Lett.* **21**, 9442–9445 (2019).
16. Mattern, D. L., Scott, W. D., McDaniel, C. A., Weldon, P. J., Graves, D. E. Cembrene A and a congeneric ketone isolated from the paracloacal glands of the Chinese alligator (*Alligator sinensis*). *J. Nat. Prod.* **60**, 828–831 (1997).
17. Xu, H., Dickschat, J. S. Turning a sesquiterpene synthase into a di- and sesterterpene synthase. *ACS Catal.* **13**, 12723–12729 (2023).

18. Meguro, A., Tomita, T., Nishiyama, M., Kuzuyama, T. Identification and characterization of bacterial diterpene cyclases that synthesize the cembrane skeleton. *ChemBioChem*. **14**, 316–321 (2013).
19. Rabe, P., Rinkel, J., Dolja, E., Schmitz, T., Nubbemeyer, B., Luu, T. H., Dickschat, J. S. Mechanistic investigations of two bacterial diterpene cyclases: spiroviolene synthase and tsukubadiene synthase. *Angew. Chem. Int. Ed.* **56**, 2776–2779 (2017).
20. Xu, B., Li, Z., Alsup, T. A., Ehrenberger, M. A., Rudolf, J. D. Bacterial diterpene synthases prenylate small molecules. *ACS Catal.* **11**, 5906–5915 (2021).
21. Burger, B. V., le Roux, M., Spies, H. S. C., Truter, V., Bigalke, R. C. Mammalian pheromone studies - III. (e,e)-7,11,15-trimethyl-3-methylenehexadeca-1,6,10,14-tetraene, a new diterpene analogue of β-farnesene from the dorsal gland of the springbok, *Antidorcas marsupialis*. *Tet. Lett.* **19**, 5221–5224 (1978).
22. Li, Z.; Xu, B., Kojasoy, V., Ortega, T., Adpressa, D. A., Ning, W., Wei, X., Liu, J., Tantillo, D. J., Loesgen, S., Rudolf, J. D. First *trans*-eunicellane terpene synthase in bacteria. *Chem*. **9**, 698–708 (2023).
23. Tamura, K., Stecher, G., Kumar, S. MEGA11: Molecular Evolutionary Genetics Analysis Version 11. *Mol. Biol. Evol.* **38**, 3022–3027 (2021).
24. Letunic, I., Bork, P. Interactive Tree of Life (iTOL) v6: recent updates to the phylogenetic tree display and annotation tool. *Nucl. Acids Res.* **52**, W78–W82 (2024).
25. Rinkel, J., Steiner, S. T., Bian, G., Chen, R., Liu, T., Dickschat, J. S. A family of related fungal and bacterial di- and sesterterpenes: studies on fusaterpenol and variediene. *ChemBioChem.* **21**, 486–491 (2020).
26. Macchioni, F., Cioni, P. L., Flamini, G., Morelli, I., Maccioni, S., Ansaldi, M. Chemical composition of essential oils from needles, branches and cones of *Pinus pinea*, *P. halepensis*, *P. pinaster* and *P. nigra* from central Italy. *Flavour Frag. J.* **18**, 139–143 (2003).
27. Sparkman, O. D. Identification of essential oil components by gas chromatography/quadrupole mass spectroscopy Robert P. Adams. *J. Am. Soc. Mass Spectrom.* **16**, 1902–1903 (2005).
28. Rinkel, J., Lauterbach, L., Dickschat, J. S. Spata-13,17-diene synthase-an enzyme with sesqui-, di-, and sesterterpene synthase activity from *Streptomyces xinghaiensis*. *Angew. Chem. Int. Ed.* **56**, 16385–16389 (2017).
29. Heinrich, G., Pfeifhofer, H. W., Stabentheiner, E., Sawidis, T. Glandular hairs of *Sigesbeckia jorullensis* Kunth (Asteraceae): morphology, histochemistry and composition of essential oil. *Annals Botany*. **89**, 459–469 (2002).